REPUBLIQUE DU CAMEROUN
PAIX-TRAVAIL-PATRIE
****
UNIVERSITE DE YAOUNDE I
****
FACULTE DES SCIENCES
****
BP 812 Yaoundé

REPUBLIC OF CAMEROON
PEACE-WORK-FATHERLAND
****
THE UNIVERSITY OF YAOUNDE I
****
FACULTY OF SCIENCE
****
PO. Box 812 Yaounde

DEPARTEMENT DE CHIMIE ORGANIQUE
DEPARTMENT OF ORGANIC CHEMISTRY

Spécialité : Substances Naturelles
****
Speciality : Natural Products
****

Chemical Investigations and Evaluation of Antisamonella Properties of a Cameroonian Medicinal Plant: *Detarium microcarpum* Guill. et Perr. (Caesalpiniaceae).

Thesis

Presented and defended publicly for the fulfilment of the award of the degree of Doctorat/PhD.

By

FEUDJOU FOUATIO William

Registration number: 08T0165
Master in Organic Chemistry

Under the supervision of

NKENGFACK Augustin E.,
(Professor)

Year 2020/2021

REPUBLIQUE DU CAMEROUN
Paix-Travail-Patrie
****
UNIVERSITÉ DE YAOUNDÉ I
****
FACULTE DES SCIENCES
****

REPUBLIC OF CAMEROON
Peace-Work-Fatherland
****
THE UNIVERSITY OF YAOUNDE I
****
FACULTY OF SCIENCE
****

DEPARTEMENT DE CHIMIE ORGANIQUE
DEPARTMENT OF ORGANIC CHEMISTRY

ATTESTATION DE CORRECTION DE MEMOIRE DE THESE DE DOCTORAT/*Ph.D* DE MONSIEUR FEUDJOU FOUATIO WILLIAM

Titre de thèse: CHEMICAL INVESTIGATIONS AND EVALUATION OF ANTISALMONELLA PROPERTIES OF A CAMEROONIAN MEDICINAL PLANT: *DETARIUM MICROCARPUM* GUILL. ET PERR. (CAESALPINIACEAE)

Nous soussignés, enseignants ci-dessous nommés, membres du jury de soutenance de thèse de Doctorat/*Ph.D* de Monsieur **FEUDJOU FOUATIO William**, Matricule **08T0165**, attestons que ce candidat a bel et bien pris en compte dans la mouture finale de sa thèse, toutes corrections et recommandations qui lui ont été faites au cours de sa soutenance en date du 05 Mai 2021.

En foi de quoi, la présente attestation de correction lui est délivrée pour servir et valoir ce que de droit.

Fait à Yaoundé, le .....

Le Jury :

Le Président :
WANDJI Jean, *Professeur*

Le rapporteur :
NKENGFACK Augustin Ephrem, *Professeur*

Les membres

PENLAP NINTCHOM Véronique épouse BENG, *Professeur*

LENTA NDJAKOU Bruno, *Professeur*

FOTSO WABO Ghislain, *Maître de Conférences*

UNIVERSITÉ DE YAOUNDÉ I **Faculté des Sciences** Division de la Programmation et du Suivi des Activités Académiques		THE UNIVERSITY OF YAOUNDE I **Faculty of Science** Division of Programming and Follow-up Of Academic Affaires
LISTE DES ENSEIGNANTS PERMANENTS		**LIST OF PERMANENT TEACHING STAFF**

OFFICIAL LIST OF LECTURERS OF THE FACULTY OF SCIENCE

ACADEMIC YEAR 2020/2021

(*by Department and by Grade*)

LAST UPDATED: May 10, 2021

ADMINISTRATION

Dean: TCHOUANKEU Jean- Claude, Associate Professor

Vice Dean in Charge of Academic Affairs: ATCHADE Alex de Théodore, Associate Professor

Vice Dean in Charge of Student Affairs: AJEAGAH Gideon AGHAINDUM, Professor

Vice Dean in Charge of Research and Cooperation: ABOSSOLO Monique, Associate Professor

Head of Administrative and Financial Division: NDOYE FOE Marie C. F., Associate Professor

Head of Academic Affairs division, Keeping of Terms and Research: MBAZE MEVA'A Luc Léonard, Professor

1- DEPARTMENT OF BIOCHIMISTRY (BCH) (38)			
N°	**NAME AND SURNAME**	**GRADE**	**OBSERVATIONS**
1	BIGOGA DIAGA Jude	Professor	In service
2	FEKAM BOYOM Fabrice	Professor	In service
3	FOKOU Elie	Professor	In service
4	KANSCI Germain	Professor	In service
5	MBACHAM FON Wilfried	Professor	In service
6	MOUNDIPA FEWOU Paul	Professor	**Head of Department**
7	NINTCHOM PENLAP V. épse BENG	Professor	In service
8	OBEN Julius ENYONG	Professor	In service
9	ACHU Merci BIH	Associate Professor	In service
10	ATOGHO Barbara Mma	Associate Professor	In service
11	AZANTSA KINGUE GABIN BORIS	Associate Professor	In service

12	BELINGA née NDOYE FOE M. C. F.	Associate Professor	**Chief DAF / FS**
13	BOUDJEKO Thaddée	Associate Professor	In service
14	DJUIDJE NGOUNOUE Marcelline	Associate Professor	In service
15	EFFA NNOMO Pierre	Associate Professor	In service
16	NANA Louise épouse WAKAM	Associate Professor	In service
17	NGONDI Judith Laure	Associate Professor	In service
18	NGUEFACK Julienne	Associate Professor	In service
19	NJAYOU Frédéric Nico	Associate Professor	In service
20	MOFOR née TEUGWA Clotilde	Associate Professor	**Insp. Serv. MINESUP**
21	TCHANA KOUATCHOUA Angèle	Associate Professor	In service
22	AKINDEH MBUH NJI	Senior Lecturer	In service
23	BEBOY EDZENGUELE Sara N.	Senior Lecturer	In service
24	DAKOLE DABOY Charles	Senior Lecturer	In service
25	DJUIKWO NKONGA Ruth Viviane	Senior Lecturer	In service
26	DONGMO LEKAGNE Joseph Blaise	Senior Lecturer	In service
27	FONKOUA Martin	Senior Lecturer	In service
28	BEBEE Fadimatou	Senior Lecturer	In service
29	KOTUE KAPTUE Charles	Senior Lecturer	In service
30	LUNGA Paul KEILAH	Senior Lecturer	In service
31	MANANGA Marlyse Joséphine	Senior Lecturer	In service
32	MBONG ANGIE M. Mary Anne	Senior Lecturer	In service
33	PECHANGOU NSANGOU Sylvain	Senior Lecturer	In service
34	Palmer MASUMBE NETONGO	Senior Lecturer	In service
35	MBOUCHE FANMOE Marceline J.	Assist. Lecturer	In service
36	OWONA AYISSI Vincent Brice	Assist. Lecturer	In service
37	WILFRIED ANGIE Abia	Assist. Lecturer	In service
2- DEPARTMENT OF ANIMAL BIOLOGY AND PHYSIOLOGY (A. B. P.) (48)			
1	AJEAGAH Gideon AGHAINDUM	Professor	**Vice Dean/DSSE**
2	BILONG BILONG Charles-Félix	Professor	**Head of Department**
3	DIMO Théophile	Professor	In service
4	DJIETO LORDON Champlain	Professor	In service
5	ESSOMBA née NTSAMA MBALA	Professor	**Vice dean/FMSB/UYI**
6	FOMENA Abraham	Professor	In service
7	KAMTCHOUING Pierre	Professor	In service
8	NJAMEN Dieudonné	Professor	In service
9	NJIOKOU Flobert	Professor	In service
10	NOLA Moïse	Professor	In service
11	TAN Paul VERNYUY	Professor	In service
12	TCHUEM TCHUENTE Louis Albert	Professor	**Insp. Serv. Coord. Progr. in HEALTH**
13	ZEBAZE TOGOUET Serge Hubert	Professor	In service
14	BILANDA Danielle Claude	Associate Professor	In service
15	DJIOGUE Séfirin	Associate Professor	In service
16	DZEUFIET DJOMENI Paul Désiré	Associate Professor	In service
17	JATSA BOUKENG Hermine épse M.	Associate Professor	In service
18	KEKEUNOU Sévilor	Associate Professor	In service
19	MEGNEKOU Rosette	Associate Professor	In service
20	MONY Ruth épse NTONE	Associate Professor	In service

21	NGUEGUIM TSOFACK Florence	Associate Professor	In service
22	TOMBI Jeannette	Associate Professor	In service
23	ALENE Désirée Chantal	Senior Lecturer	In service
26	ATSAMO Albert Donatien	Senior Lecturer	In service
27	BELLET EDIMO Oscar Roger	Senior Lecturer	In service
28	DONFACK Mireille	Senior Lecturer	In service
29	ETEME ENAMA Serge	Senior Lecturer	In service
30	GOUNOUE KAMKUMO Raceline	Senior Lecturer	In service
31	KANDEDA KAVAYE Antoine	Senior Lecturer	In service
32	LEKEUFACK FOLEFACK Guy B.	Senior Lecturer	In service
33	MAHOB Raymond Joseph	Senior Lecturer	In service
34	MBENOUN MASSE Paul Serge	Senior Lecturer	In service
35	MOUNGANG LucianeMarlyse	Senior Lecturer	In service
36	MVEYO NDANKEU Yves Patrick	Senior Lecturer	In service
37	NGOUATEU KENFACK Omer Bébé	Senior Lecturer	In service
38	NGUEMBOK	Senior Lecturer	In service
39	NJUA Clarisse Yafi	Senior Lecturer	**Chief of Division/UBA**
40	NOAH EWOTI Olive Vivien	Senior Lecturer	In service
41	TADU Zephyrin	Senior Lecturer	In service
42	TAMSA ARFAO Antoine	Senior Lecturer	In service
43	YEDE	Senior Lecturer	In service
44	BASSOCK BAYIHA Etienne Didier	Assist. Lecturer	In service
45	ESSAMA MBIDA Désirée Sandrine	Assist. Lecturer	In service
46	KOGA MANG DOBARA	Assist. Lecturer	In service
47	LEME BANOCK Lucie	Assist. Lecturer	In service
48	YOUNOUSSA LAME	Assist. Lecturer	In service
3- DEPARTMENT OF PLANT BIOLOGY AND PHYSIOLOGY (P. B. P.) (33)			
1	AMBANG Zachée	Professor	**Chief of Division/UYII**
2	BELL Joseph Martin	Professor	In service
3	DJOCGOUE Pierre François	Professor	In service
4	MOSSEBO Dominique Claude	Professor	In service
5	YOUMBI Emmanuel	Professor	**Head of Department**
6	ZAPFACK Louis	Professor	In service
7	ANGONI Hyacinthe	Associate Professor	In service
8	BIYE Elvire Hortense	Associate Professor	In service
9	KENGNE NOUMSI Ives Magloire	Associate Professor	In service
10	MALA Armand William	Associate Professor	In service
11	MBARGA BINDZI Marie Alain	Associate Professor	**CT/ MINESUP**
12	MBOLO Marie	Associate Professor	In service
13	NDONGO BEKOLO	Associate Professor	**CE/MINRESI**
14	NGODO MELINGUI Jean Baptiste	Associate Professor	In service
15	NGONKEU MAGAPTCHE Eddy L.	Associate Professor	In service
16	TSOATA Esaïe	Associate Professor	In service
17	TONFACK Libert Brice	Associate Professor	In service
18	DJEUANI Astride Carole	Senior Lecturer	In service
19	GOMANDJE Christelle	Senior Lecturer	In service
20	MAFFO MAFFO Nicole Liliane	Senior Lecturer	In service
21	MAHBOU SOMO TOUKAM G.	Senior Lecturer	In service

22	NGALLE Hermine BILLE	Senior Lecturer	In service
23	NGOUO Lucas Vincent	Senior Lecturer	In service
24	NNANGA MEBENGA Ruth Laure	Senior Lecturer	In service
25	NOUKEU KOUAKAM Armelle	Senior Lecturer	In service
26	ONANA JEAN MICHEL	Senior Lecturer	In service
27	GODSWILL NTSOMBAH N.	Assist. Lecturer	In service
28	KABELONG BANAHO Louis-P.-R.	Assist. Lecturer	In service
29	KONO Léon Dieudonné	Assist. Lecturer	In service
30	LIBALAH Moses BAKONCK	Assist. Lecturer	In service
31	LIKENG-LI-NGUE Benoit C	Assist. Lecturer	In service
32	TAEDOUNG Evariste Hermann	Assist. Lecturer	In service
33	TEMEGNE NONO Carine	Assist. Lecturer	In service
4- DEPARTMENT OF INORGANIC CHEMISTRY (I. C.) (35)			
1	AGWARA ONDOH Moïse	Professor	**Head of Department**
2	ELIMBI Antoine	Professor	In service
3	Florence UFI CHINJE épouse MELO	Professor	**Rector Univ. Ngaoundere**
4	GHOGOMU Paul MINGO	Professor	**Ministre Chargé de Miss. P.R.**
5	NANSEU Njiki Charles Péguy	Professor	In service
6	NDIFON Peter TEKE	Professor	**C.T. MINRESI**
7	NGOMO Horace MANGA	Professor	**Vice Chancellor/U.B**.
8	NDIKONTAR Maurice KOR	Professor	**Vice-Dean Un. Bamenda**
9	NENWA Justin	Professor	In service
10	NGAMENI Emmanuel	Professor	**Dean F.S. U.Ds**
11	BABALE née DJAM DOUDOU	Associate Professor	**Chargée Mission P.R.**
12	DJOUFAC WOUMFO Emmanuel	Associate Professor	In service
13	KAMGANG YOUBI Georges	Associate Professor	In service
14	KEMMEGNE MBOUGUEM Jean C.	Associate Professor	In service
15	KONG SAKEO	Associate Professor	In service
16	NDI NSAMI Julius	Associate Professor	In service
17	NJIOMOU C. épse DJANGANG	Associate Professor	In service
18	NJOYA Dayirou	Associate Professor	In service
19	YOUNANG Elie	Associate Professor	In service
20	ACAYANKA Elie	Senior Lecturer	In service
21	BELIBI BELIBI Placide Désiré	Senior Lecturer	**CS/ ENS Bertoua**
22	CHEUMANI YONA Arnaud M.	Senior Lecturer	In service
23	EMADACK Alphonse	Senior Lecturer	In service
24	KENNE DEDZO GUSTAVE	Senior Lecturer	In service
25	KOUOTOU DAOUDA	Senior Lecturer	In service
26	MAKON Thomas Beauregard	Senior Lecturer	In service
27	MBEY Jean Aime	Senior Lecturer	In service
28	NCHIMI NONO KATIA	Senior Lecturer	In service
29	NEBA nee NDOSIRI Bridget N.	Senior Lecturer	**CT/ MINFEM**
30	NYAMEN Linda Dyorisse	Senior Lecturer	In service
31	PABOUDAM GBAMBIE A.	Senior Lecturer	In service
32	TCHAKOUTE KOUAMO Hervé	Senior Lecturer	In service
33	NJANKWA NJABONG N. Eric	Assist. Lecturer	In service
34	PATOUOSSA ISSOFA	Assist. Lecturer	In service

35	SIEWE Jean Mermoz	Assist. Lecturer	In service
5- DEPARTMENT OF ORGANIC CHIMISTRY (O. C.) (35)			
1	DONGO Etienne	Professor	**Vice Dean/CSA/ *F. SED***
2	GHOGOMU TIH Robert Ralph	Professor	**Director B. A. I Foumban**
3	NGOUELA Silvère Augustin	Professor	**Head of Department UDs**
4	NKENGFACK Augustin Ephrem	Professor	**Head of Department**
5	NYASSE Barthélemy	Professor	In service
6	PEGNYEMB Dieudonné Emmanuel	Professor	**Director/MINESUP**
7	WANDJI Jean	Professor	In service
8	Alex de Théodore ATCHADE	Associate Professor	**Vice-Dean/CAA**
9	EYONG Kenneth OBEN	Associate Professor	In service
10	FOLEFOC Gabriel NGOSONG	Associate Professor	In service
11	FOTSO WABO Ghislain	Associate Professor	In service
12	KEUMEDJIO Félix	Associate Professor	In service
13	KEUMOGNE Marguerite	Associate Professor	In service
14	KOUAM Jacques	Associate Professor	In service
15	MBAZOA née DJAMA Céline	Associate Professor	In service
16	MKOUNGA Pierre	Associate Professor	In service
17	NOTE LOUGBOT Olivier Placide	Associate Professor	**Chief Service/MINESUP**
18	NGO MBING Joséphine	Associate Professor	**Sous/Direct. MINERESI**
19	NGONO BIKOBO Dominique Serge	Associate Professor	**Chargé d'Études Ass. n°3/MINESUP**
20	NOUNGOUE TCHAMO Diderot	Associate Professor	In service
21	TABOPDA KUATE Turibio	Associate Professor	In service
22	TCHOUANKEU Jean-Claude	Associate Professor	**Dean/FS/ UY1**
23	TIH née NGO BILONG E. Anastasie	Associate Professor	In service
24	YANKEP Emmanuel	Associate Professor	In service
25	MVOT AKAK Carine	Associate Professor	In service
26	AMBASSA Pantaléon	Associate Professor	In service
27	TAGATSING FOTSING Maurice	Associate Professor	In service
28	ZONDENDEGOUMBA Ernestine	Associate Professor	In service
29	KAMTO Eutrophe Le Doux	Senior Lecturer	In service
30	NGNINTEDO Dominique	Senior Lecturer	In service
31	NGOMO Orléans	Senior Lecturer	In service
32	OUAHOUO WACHE Blandine M.	Senior Lecturer	In service
33	SIELINOU TEDJON Valérie	Senior Lecturer	In service
34	MESSI Angélique Nicolas	Assist. Lecturer	In service
35	TSEMEUGNE Joseph	Assist. Lecturer	In service
36	TCHAMGOUE Joseph	Assist. Lecturer	In service
37	TSAFACK Maurice	Assist. Lecturer	In service
38	TSAMO Armelle	Assist. Lecturer	In service
39	NONO Eric Carly	Assist. Lecturer	In service
6- DEPARTMENT OF COMPUTER SCIENCE (C. S.) (25)			
1	ATSA ETOUNDI Roger	Professor	**Chief Div.MINESUP**
2	FOUDA NDJODO Marcel Laurent	Professor	**Head of Dpt HTTC/Chief IGA. MINESUP**
3	NDOUNDAM Réné	Associate Professor	In service
4	AMINOU Halidou	Senior Lecturer	**Head of Department**

5	DJAM Xaviera YOUH - KIMBI	Senior Lecturer	In service
6	EBELE Serge Alain	Senior Lecturer	In service
7	KOUOKAM KOUOKAM E. A.	Senior Lecturer	In service
8	MELATAGIA YONTA Paulin	Senior Lecturer	In service
9	MOTO MPONG Serge Alain	Senior Lecturer	In service
10	TAPAMO Hyppolite	Senior Lecturer	In service
11	ABESSOLO ALO'O Gislain	Senior Lecturer	In service
12	MONTHE DJIADEU Valery M.	Senior Lecturer	In service
13	OLLE OLLE Daniel Claude Delort	Senior Lecturer	**C/D Enset. Ebolowa**
14	TINDO Gilbert	Senior Lecturer	In service
15	TSOPZE Norbert	Senior Lecturer	In service
16	WAKU KOUAMOU Jules	Senior Lecturer	In service
17	BAYEM Jacques Narcisse	Assist. Lecturer	In service
18	DOMGA KOMGUEM Rodrigue	Assist. Lecturer	In service
19	EKODECK Stéphane Gaël Raymond	Assist. Lecturer	In service
20	HAMZA Adamou	Assist. Lecturer	In service
21	JIOMEKONG AZANZI Fidel	Assist. Lecturer	In service
22	MAKEMBE. S. Oswald	Assist. Lecturer	In service
23	MESSI NGUELE Thomas	Assist. Lecturer	In service
24	MEYEMDOU Nadège Sylvianne	Assist. Lecturer	In service
25	NKONDOCK. MI. BAHANACK.N.	Assist. Lecturer	In service
7- DEPARTMENT OF MATHEMATICS (MAT) (30)			
1	EMVUDU WONO Yves S.	Professor	**CD Info/Inspecteur MINESUP**
2	AYISSI Raoult Domingo	Associate Professor	**Head of Department**
3	NKUIMI JUGNIA Célestin	Associate Professor	In service
4	NOUNDJEU Pierre	Associate Professor	**Chief serv. certif. prog.**
5	MBEHOU Mohamed	Associate Professor	In service
6	TCHAPNDA NJABO Sophonie B.	Associate Professor	**Director/AIMS Rwanda**
7	AGHOUKENG JIOFACK Jean G.	Senior Lecturer	**Chief Cell MINPLAMAT**
8	CHENDJOU Gilbert	Senior Lecturer	In service
9	DJIADEU NGAHA Michel	Senior Lecturer	In service
10	DOUANLA YONTA Herman	Senior Lecturer	In service
11	FOMEKONG Christophe	Senior Lecturer	In service
12	KIANPI Maurice	Senior Lecturer	In service
13	KIKI Maxime Armand	Senior Lecturer	In service
14	MBAKOP Guy Merlin	Senior Lecturer	In service
15	MBANG Joseph	Senior Lecturer	In service
16	MBELE BIDIMA Martin Ledoux	Senior Lecturer	In service
17	MENGUE MENGUE David Joe	Senior Lecturer	In service
18	NGUEFACK Bernard	Senior Lecturer	In service
19	NIMPA PEFOUNKEU Romain	Senior Lecturer	In service
20	POLA DOUNDOU Emmanuel	Senior Lecturer	In service
21	TAKAM SOH Patrice	Senior Lecturer	In service
22	TCHANGANG Roger Duclos	Senior Lecturer	In service
23	TCHOUNDJA Edgar Landry	Senior Lecturer	In service
24	TETSADJIO TCHILEPECK M. E.	Senior Lecturer	In service
25	TIAYA TSAGUE N. Anne-Marie	Senior Lecturer	In service

26	MBIAKOP Hilaire George	Assist. Lecturer	In service
27	BITYE MVONDO Esther Claudine	Assist. Lecturer	In service
28	MBATAKOU Salomon Joseph	Assist. Lecturer	In service
29	MEFENZA NOUNTU Thiery	Assist. Lecturer	In service
30	TCHEUTIA Daniel Duviol	Assist. Lecturer	In service
8- DEPARTMENT OF MICROBIOLOGY (MIB) (18)			
1	ESSIA NGANG Jean Justin	Professor	**Head of Department**
2	BOYOMO ONANA	Associate Professor	In service
3	NWAGA Dieudonné M.	Associate Professor	In service
4	NYEGUE Maximilienne Ascension	Associate Professor	In service
5	RIWOM Sara Honorine	Associate Professor	In service
6	SADO KAMDEM Sylvain Leroy	Associate Professor	In service
7	ASSAM ASSAM Jean Paul	Senior Lecturer	In service
8	BODA Maurice	Senior Lecturer	In service
9	BOUGNOM Blaise Pascal	Senior Lecturer	In service
10	ESSONO OBOUGOU Germain G.	Senior Lecturer	In service
11	NJIKI BIKOÏ Jacky	Senior Lecturer	In service
12	TCHIKOUA Roger	Senior Lecturer	In service
13	ESSONO Damien Marie	Assist. Lecturer	In service
14	LAMYE Glory MOH	Assist. Lecturer	In service
15	MEYIN A EBONG Solange	Assist. Lecturer	In service
16	NKOUDOU ZE Nardis	Assist. Lecturer	In service
17	SAKE NGANE Carole Stéphanie	Assist. Lecturer	In service
18	TOBOLBAÏ Richard	Assist. Lecturer	In service
9- DEPARTMENT OF PHYSICS (PHY) (42)			
1	BEN-BOLIE Germain Hubert	Professor	In service
2	ESSIMBI ZOBO Bernard	Professor	In service
3	EKOBENA FOUDA Henri Paul	Associate Professor	**Chief of Division. UN**
4	KOFANE Timoléon Crépin	Professor	In service
5	NANA ENGO Serge Guy	Professor	In service
6	NDJAKA Jean Marie Bienvenu	Professor	**Head of Department**
7	NOUAYOU Robert	Professor	In service
8	NJANDJOCK NOUCK Philippe	Professor	**Under Director/ MINRESI**
9	PEMHA Elkana	Professor	In service
10	TABOD Charles TABOD	Professor	**Dean Univ. Bda**
11	TCHAWOUA Clément	Professor	In service
12	WOAFO Paul	Professor	In service
13	BIYA MOTTO Frédéric	Associate Professor	**G. D./HYDRO Mekin**
14	BODO Bertrand	Associate Professor	In service
15	DJUIDJE KENMOE épouse A.	Associate Professor	In service
16	EYEBE FOUDA Jean sire	Associate Professor	In service
17	FEWO Serge Ibraïd	Associate Professor	In service
18	HONA Jacques	Associate Professor	In service
19	MBANE BIOUELE César	Associate Professor	In service
20	NANA NBENDJO Blaise	Associate Professor	In service
21	NDOP Joseph	Associate Professor	In service
22	SAIDOU	Associate Professor	**MINRESI**

23	SIEWE SIEWE Martin	Associate Professor	In service
24	SIMO Elie	Associate Professor	In service
25	VONDOU Derbetini Appolinaire	Associate Professor	In service
26	WAKATA née BEYA Annie	Associate Professor	**Under Dir./ MINESUP**
27	ZEKENG Serge Sylvain	Associate Professor	In service
28	ABDOURAHIMI	Senior Lecturer	In service
29	EDONGUE HERVAIS	Senior Lecturer	In service
30	ENYEGUE A NYAM épse BELINGA	Senior Lecturer	In service
31	FOUEDJIO David	Senior Lecturer	**Chief of Cell MINADER**
32	MBINACK Clément	Senior Lecturer	In service
33	MBONO SAMBA Yves Christian U.	Senior Lecturer	In service
34	MELI'I Joelle Larissa	Senior Lecturer	In service
35	MVOGO ALAIN	Senior Lecturer	In service
38	OBOUNOU Marcel	Senior Lecturer	**DA/U. Int. Etat/Sangma.**
39	WOULACHE Rosalie Laure	Senior Lecturer	In service
40	AYISSI EYEBE Guy François V.	Assist. Lecturer	In service
41	CHAMANI Roméo	Assist. Lecturer	In service
42	TEYOU NGOUPOU Ariel	Assist. Lecturer	In service
10- DEPARTMENT OF EARTH SCIENCES (E. S.) (43)			
1	BITOM Dieudonné	Professor	**Dean/FASA/UDs**
2	FOUATEU Rose épse YONGUE	Professor	In service
3	KAMGANG Pierre	Professor	In service
4	NDJIGUI Paul Désiré	Professor	**Head of Department**
5	NDAM NGOUPAYOU Jules-Remy	Professor	In service
6	NGOS III Simon	Professor	**DAAC/Uma**
7	NKOUMBOU Charles	Professor	In service
8	NZENTI Jean-Paul	Professor	In service
9	ABOSSOLO née ANGUE Monique	Associate Professor	**Vice-Dean/DRC**
10	GHOGOMU Richard TANWI	Associate Professor	**CD/Uma**
11	MOUNDI Amidou	Associate Professor	**CT/ MINIMDT**
12	NGUEUTCHOUA Gabriel	Associate Professor	**CEA/MINRESI**
13	NJILAH Isaac KONFOR	Associate Professor	In service
14	ONANA Vincent Laurent	Associate Professor	**Chief serv. Mater. Maint**.
15	BISSO Dieudonné	Associate Professor	**Director/Project Barrage Memve'ele**
16	EKOMANE Emile	Associate Professor	In service
17	GANNO Sylvestre	Associate Professor	In service
18	NYECK Bruno	Associate Professor	In service
19	TCHOUANKOUE Jean-Pierre	Associate Professor	In service
20	TEMDJIM Robert	Associate Professor	In service
21	YENE ATANGANA Joseph Q.	Associate Professor	**Chief Div. /MINTP**
22	ZO'O ZAME Philémon	Associate Professor	**G. D./ART**
23	ANABA ONANA Achille Basile	Senior Lecturer	In service
24	BEKOA Etienne	Senior Lecturer	In service
25	ELISE SABABA	Senior Lecturer	In service
26	ESSONO Jean	Senior Lecturer	In service
27	EYONG JOHN TAKEM	Senior Lecturer	In service
28	FUH Calistus Gentry	Senior Lecturer	**Sec. D'Etat/MINMIDT**

29	LAMILEN BILLA Daniel	Senior Lecturer	In service
30	MBESSE CECILE OLIVE	Senior Lecturer	In service
31	MBIDA YEM	Senior Lecturer	In service
32	METANG Victor	Senior Lecturer	In service
33	MINYEM Dieudonné-Lucien	Senior Lecturer	**CD/Uma**
34	NGO BELNOUN Rose Noël	Senior Lecturer	In service
35	NGO BIDJECK Louise Marie	Senior Lecturer	In service
36	NOMO NEGUE Emmanuel	Senior Lecturer	In service
37	NTSAMA ATANGANA Jacqueline	Senior Lecturer	In service
38	TCHAKOUNTE J. épse NOUMBEM	Senior Lecturer	**Chief of cell/MINRESI**
39	TCHAPTCHET TCHATO De P.	Senior Lecturer	In service
40	TEHNA Nathanaël	Senior Lecturer	In service
41	TEMGA Jean Pierre	Senior Lecturer	In service
42	FEUMBA Roger	Assist. Lecturer	In service
43	MBANGA NYOBE Jules	Assist. Lecturer	In service

Classification of teaching staff at the faculty of Science of the University of Yaoundé 1

NUMBER OF LECTURERS					
Department	**Professor**	**Associate Professor**	**Senior Lecturer**	**Assist. Lecturer**	**Total**
BCH	9 (1)	13 (09)	14 (06)	3 (2)	**39 (18)**
A. B. P.	13 (1)	09 (06)	19 (05)	05 (2)	**46 (14)**
P. B. P.	06 (0)	11 (02)	9 (06)	07 (01)	**33 (9)**
I. C.	10 (1)	09 (02)	12 (02)	03 (0)	**34 (5)**
O. C.	7 (0)	19 (06)	09 (03)	05 (01)	**40 (10)**
C. S.	2 (0)	1 (0)	13 (01)	09 (01)	**25 (2)**
MAT	1 (0)	5 (0)	19 (01)	05 (02)	**30 (3)**
MIB	1 (0)	5 (02)	06 (01)	06 (02)	**18 (5)**
PHY	12 (0)	15 (02)	10 (03)	03 (0)	**40 (5)**
E. S.	8 (1)	14 (01)	19 (05)	02 (0)	**43 (7)**
Total	**69 (4)**	**99 (28)**	**130 (33)**	**45 (10)**	**348 (78)**

A total of: **348 (78)** including:
Professors **69 (4)**
Associate Professors **101 (30)**
Senior Lecturers **130 (33)**
Assist. Lecturers **48 (11)**

( ) = Number of women **75**

The Dean of the Faculty of Science
Prof. TCHOUANKEU Jean-Claude

DEDICACES

I dedicate this thesis:

- To my wife **KAMLO Michelle**
- To all my children.

ACKNOWLEDGEMENTS

The research work that is the subject of this dissertation was carried out at the Laboratory of Analytical Organic Chemistry (LACOSA) of the University of Yaoundé I, under the supervision of Prof. NKENGFACK A. E. (Head of the Department of Organic Chemistry). I would like to express my deep gratitude to all those who, from near or far, have been able to grant me their assistance, at the same time showing their attachment to me. I think in particular:

- To God the Creator, for the grace and blessings he never ceases to grant me;
- To the German Academic Exchange Service (DAAD), for having fully funded this work through the YaBiNaPA project;
- To Prof. NKENGFACK A. E. who accepted me into his research team, proposed this subject to me and who, with all his multiple occupations, directed this work rigorously to the end. I would like to express to him here all my gratitude and my deep admiration;
- To Professors LENTA N. B. and SEWALD N., for having not only accepted me into the YaBiNaPA project, but also for all the facilities set up for our research work. I would like to express to them here all my gratitude;
- To Prof. MKOUNGA P. for his availability, help and advice at the right time.
- To Dr FREEZE M. for facilitating the analysis of our compounds in Germany during the first four years of the YaBiNaPA project and to whom I express all my gratitude;
- To all the lecturers in the Department of Organic Chemistry for their determination to provide all the students in the Department with quality training;
- To Prof. MVOT AKAK C., Prof. BANKEU K. J. J. and Dr. SIELINOU T. V., for their invaluable help and support during the write up of articles and the thesis manuscripts resulting from this work. I express my sincere thanksto them;
- To my team-mates Mr MBOCK M. A. and Mr PAGNA M. I. J. for the team spirit and camaraderie they have shown during our work;
- To my elders in the laboratory, particularly Drs OUAHOUO B. M., TSAMO A., TSAFACF M., TSEMEGNE J., NONO E. C., DEMANGOU B., FOUOTSA H., MAFO F. M. A., TSANA G. R., NANGMO K. P., GOMPE B. E. G., TSOPMEJIO J. P., ABDOU J. P., MFIFEN M. A., to whom I am grateful for having agreed to supervise me on the bench and have provided me with tireless advice in carrying out this work. May they find here the expression of my sincere gratitude;
- To all my comrades in the YaBiNaPA project for the warm and fraternal welcome as well as the spirit of solidarity they have shown towards me;

- To all my colleagues at the IMPM, more particularly those of the phytochemistry laboratory for their constant encouragement;
- To my laboratory mattes: Mss and Mrs DJOMKAM E., TCHAPO E. C., JOUWA T. N., TAIZOUMBE K., TOKO G. E., TSAMO F. L., MBARGA P., KAMTCHOUM L., KOUCHELE B., DONFACK M. and others, with whom I spent strong and unforgettable moments during the preparation of this thesis;
- To my father FOUATIO A. whose main concern was my success in life;
- To my mother KENFACK C. for her advices and encouragements;
- To my late grandfather FOTIE A. for his multiple wise advices;
- To my uncle TETANG V. for his multiple advices and for my education;
- To my aunt TEFO épse NOUMEDEM Madeleine for her multiple advices and encouragements for my education;
- To my parent's in-law dad NGUEMDJOUO R. and mum NJOMO A. for their moral, material and financial support during the preparation of this thesis;
- To my uncle DONGMO G. and his wife NONGNI S. for all their material support and encouragement;
- To my brothers and sisters: TETANG A., DONGHO D., FOUATIO S. T., FOFIE R., TETANG U. V., FOUATIO F. SONKENG F. G., for their constant encouragement;
- To my brothers and sisters'in-law MEGIP B. A., TCHIPKAP O., CHENDA C. J., KAMLEU L., NGUEMJOUO T. S.;
- To the great KONFO and FEUDJOU families for their love and encouragement.
- To all my family in-laws for their encouragement;
- To all those who have not been mentioned and who from near or far; facilitated the realization of this thesis.

TABLE OF CONTENTS

LIST OF ABBREVIATIONS

ALT (I U /L)…….	alanine aminotransferase (international units per liter)
(-)…….	no comment on taxon status
ALP (I U /L)……..	alkaline phosphatase (international units per liter)
AST (I U /L)……..	Aspartate aminotransferase (international units per liter)
ATP……	Attached Proton Test
CC……..	Column Chromatography
COSY…….	Correlation Spectroscopy
d……..	Doublet
DCM.....	Dichloromethane
dd……	Doublet of doublet
DEPT……..	Distortionless Enhancement by Polarization Tranfer
dt…….	Doublet of triplet
EI……	Electronic Impact
ESI……..	Electrospray Ionization
ESITOF……...	Electrospray Ionization Time-Of-Flight
EtOAc…….	Ethyl Acetate
g.....	gram
GBIF.....	**G**lobal **B**iodiversity **I**nformation **F**acility
GRIN.....	**G**ermplasm **R**esources **I**nformation **N**etwork (United States Department of Agriculture)
HE……...	Hamatoxylin Eosin
Hex……..	Hexane
HIV…….	Human immunodeficiency virus
HMBC……	Heteronuclear Multiple Bond Connectivity
HPLC……..	High Performance Liquid Chromatography
HR-ESIMS…….	High Resolution Electrospray Ionization Mass Spectrometry
HSQC……..	Heteronuclear Single Quantum Coherence
Hz……	Hertz
ILDIS.....	**I**nternational **L**egume **D**atabase & **I**nformation **S**ervice (Université de Reading)
IPNI.....	**I**nternational **P**lant **N**ame **I**ndex (Kew Botanical Garden (Grande-Bretagne), Harward Herbaria (Etats-Unis), Australian National Herbarium (Canberra, Australie)).
IR……	Infra-Red
***J* ……..**	Coupling constant
MIC	Minimum Inhibitory Concentrations
m. p.....	Melting point
m. w.....	molecular weight
m……..	Multiplet
MeOH……..	Methanol

MHz.....	Mégahertz
mL.....	milliliter
mm.....	millimeter
MS……...	Mass Spectrometry
***n*-BuOH……...**	*n*- butanol
nm.....	nanometer
NMR……	Nuclear Magnetic Resonance
NOE.....	Nuclear Overhauser Effect
NOESY……	Nuclear Overhauser Effect Spectroscopy
ppm……..	Part per million
q.....	Quartet or quadruplet
Ref……...	References
ROESY……	Rotating frame Overhauser Effect Spectroscopy
S.	Salmonella
s……...	Singlet
t……	Triplet
TLC……	Thin Layer Chromatography
TMS.....	Tetramethylsilane
UV……...	Ultra Violet
W_3TROPICOS.....	Missouri Botanical Garden (United States).
δ.....	chemical shift scale
ε.....	Extinction coefficient
λ_{max}……	Maximum wavelength
μ g.....	microgram
μ m.....	Micrometer

LIST OF TABLES

LIST OF FIGURES

LIST OF SCHEMES

ABSTRACT

Typhoid fever is a disease caused by a microbe of the specie *Salmonella enterica*. It causes a lot of damage in the world. The remedy used to treat this disease is ciprofloxacin. But these salmonellas have developed forms of resistance to these remedies, hence the need to seek new therapeutic agents. The use of plants in traditional medecine suggest that they contain bioactive molecules that can be used in the treatment of this disease.

This thesis reports the phytochemical investigation of a cameroonian medicinal plant: *Detarium microcarpum Guill*. Perr. (Caesalpiniaceae) and the antisalmonella assay of the hydroethanolic extracts, fractions and some isolated compounds. Twenty-five compounds were obtained from the procedures described in this work, and eighteen were fully characterized among which three new derivatives. The method used for the isolation of the compounds was mainly column chromatography. Structure elucidation was achieved mainly by NMR spectroscopy including IR spectroscopy, mass spectrometry and 1D and 2D-NMR (COSY, HMQC, HMBC and NOESY).

A bio-guided investigation of the methanolic and hydroethanolic extracts of the fruits of *D. microcarpum* led to the isolation and the characterization of ten compounds while the hydroethanolic extracts of root bark and root wood afforded eight compounds. They belong to six classes of natural substances and were classified as follows:

- Three diterpenoids: one of the clerodane type known as (4a*R*, 5*S*, 6*R*, 8a*R*) 5-(carboxymethyl)-5,6,8a-trimethyl-3,4,4a,5,6,7,8,8a-octahydronaphthalene-1-carboxylic acid **118** and two of the labdane type, including a new one to which the trivial name microcarpin **116** was assigned and another known as rhinocerotinoic acid **117**,
- One new cyanogenic derivative to which we assigned the name Microcarposide **114**,
- One new ceramide to which the trivial name microcarpamide **115** has been assigned,
- One xanthone : 1,7-dihydroxy-6-methylxanthone **129**,
- Two flavonoids: luteolin **131** and epicatechin **132,**
- Five pentacyclic triterpenes: ursolic acid **123**, alphitolic acid **121**, betulinic acid **120**, 3α, 24α-dihydroxylup-20 (29) -en-28-oic acid **122** and lupeol **119** all known,
- Four phytosterols: *β*-sitosterol **128** and its 3-*O*-*β*-*D*-glucopyranoside derivative **125**, stigmasterol **127** and its 3-*O*-*β*-*D*-glucopyranoside derivative **126** and the mixture of *β*-sitosterol and stigmasterol **124**,
- One phenolic compound: methyl gallate **130**.

Crystallographic data of acid (4aR, 5S, 6R, 8aR)-5-(carboxymethyl)-5,6,8a-trimethyl-3,4,4a, 5,6,7,8,8a-octahydronaphthalene-1-carboxylic and microcarpine are presented here for the first time. Rhinocerotonoic acid has been transformed to its hydroxylated derivative with the aim of studying its structure activity relationship. Microcarposide, rhinocerotinoic acid and microcarpamide exhibited moderate antisalmonella activity *in vitro* against three strains namely *S. typhi, S. enteritidis* and *S. typhimurium* with a MIC values of 62.5, 31.25, and 31.25 μg/mL, respectively. The results of *in vitro* and *in vivo* tests on the same *Salmonella* strains with a MIC value of 1.95 μg/mL, in addition to the low acute and subacute toxicity of the hydro-ethanolic root-bark extract obtained, allowed us to perform a pre-formulation of a phyto-drug in the form of a syrup, to be used for the treatment of typhoid fever.

Key words: *Detarium microcarpum*, antisalmonella activities, *S. typhi, S. Enteritidis*, *S. typhimurium*, pre-formulation.

RESUME

La fièvre typhoïde est une maladie causée par des microbes des espèces des *Salmonella enterica*. Elle cause de nombreux dégâts dans le monde. Le remède utilisé pour traiter cette maladie est la ciprofloxacine. Mais ces salmonelles ont développé à l'égard de ces remèdes des formes de résistance, d'où la nécessité de chercher de nouvelles cibles thérapeutiques. L'utilisation des plantes en médecine traditionnelle laisse penser qu'elles contiendraient de molécules bioactives pouvant servir dans le traitement de cette maladie.

C'est ainsi que cette thèse rapporte les résultats des investigations phytochimiques faites sur *Detarium microcarpum* Guill. Perr., une plante médicinale camerounaise de la famille des Caesalpiniaceae, et les activités antisalmonelle des extraits, fractions et de certains des composés isolés. Vingt-cinq métabolites secondaires ont été isolés à l'aide des méthodes usuelles de séparation et dix-huit ont été entièrement caractérisés parmi lesquels trois dérivés nouveaux. Les structures de ces composés ont été élucidées à l'aide des techniques spectroscopiques modernes telles la spectroscopie IR, la spectrométrie de masse et la RMN 1D et 2D (COSY, HMQC, HMBC, NOESY).

L'investigation phytochimique par la méthode bio-guidée des extraits méthanolique et hydroethanolique des fruits de *D. microcarpum* ont conduit à l'isolement et à la caractérisation de dix composés, tandis que les extraits hydroethanoliques des écorces et du bois des racines ont conduit à huit composés. Ces composés appartiennent à six classes de substances naturelles et ont été classés comme suit :

• Trois diterpénoïdes : parmi lesquels, un du type clérodane l'acide (4a*R*,5*S*,6*R*,8a*R*) 5-(carboxyméthyl)-5,6,8a-triméthyl-3,4,4a,5,6,7,8,8a-octahydronaphtalène-1-carboxylique **118** et deux du type labdane, dont un dérivé nouveau auquel le nom trivial de microcarpine **116** lui a été attribué et un autre appelé acide rhinocérotinoïque **117** isolé pour la première fois de cette espèce,

• Un dérivé cyanogénique desmoside nouveau, auquel nous avons attribué le nom de Microcarposide **114**,

• Une céramide nouvelle auquel le nom trivial de microcarpamide **115** lui a été attribué,

• Une xanthone : 1,7-dihydroxy-6-méthylxanthone **129**,

• Deux flavonoïdes : la lutéoline **131** et l'épicatéchine **132**,

• Cinq triterpènes pentacycliques : acide ursolique **123**, acide alphitolique **121**, acide bétulinique **120**, l'acide 3*β*,23*β*-dihydroxylup-20(29)-en-28-oïque **122** et lupéol **119** tous connus,

• Cinq phytostérols : le *β*-sitostérol **128** et son dérivé 3-*O*-*β*-*D*-glucopyranoside **125**, le stigmastérol **127** et son dérivé 3-*O*-*β*-*D*-glucopyranoside **126** et le mélange du *β*-sitostérol et du stigmastérol **124**,

• Un composé phénolique : le gallate de méthyle 130.

Les données critallographiques de l'acide (4a*R*,5*S*,6*R*,8a*R*)-5-(carboxymethyl)-5,6,8a-trimethyl-3,4,4a,5,6,7,8,8a-octahydronaphthalene-1-carboxylique et du microcarpine sont présentées pour la première fois. L'acide rhinocérotonoique a été transformée en son dérivé hydroxylé dans le but potentialiser son activité. Le microcarposide, l'acide rhinocerotinoic et le microcarpamide ont exhibé une activité antisalmonelle modérée *in vitro* contre trois souches à savoir *S. typhi, S. enteritidis* and *S. typhimurium* avec des valeurs de concentration minimale inhibitrice (CMI) de 62.5, 31.25, and 31.25 μg/mL, respectivement. Les résultats de tests *in vitro* et *in vivo* sur les mêmes souches de salmonelles avec une valeur de CMI de 1.95 μg/mL, associé à la faible toxicité aigue et subaigue de l'extrait hydro-éthanolique des écorces des racines obtenues, nous ont permis d'effectuer un essai de pré-formulation d'un phytomédicament sous forme d'un sirop, devant être utilisé pour le traitement de la fièvre typhoïde.

Mots clés : *Detarium microcarpum*, activités antisalmonelles, *S. typhi*, *S. Enteritidis*, *S. typhimurium*, pré-formulation.

GENERAL INTRODUCTION

GENERAL INTRODUCTION

Typhoid fever is a bacterial enteric infection that continues to cause a considerable burden to about 5.5 billion people living in low- and middle-income countries (LMICs). Central Africa more precisely the Cameroon, was predicted to experience the highest incidence of typhoid, followed by certain countries in Central, South, and Southeast Asia (Antillon *et al*., 2017). Investigators from the US Centers for Disease Control and Prevention estimated that there are about 21.6 million typhoid cases annually, with the annual incidence varying from 100 to 1000 cases per 100,000 populations (Antillon *et al*., 2017). This disease still remains an important global health problem with an estimated 16 million cases leading to 600,000 deaths yearly (Date et *al*., 2014), mainly occurring in developing countries due to poor hygiene (WHO, 2018). Typhoid fever is caused by *Salmonella enterica* serovar *typhi* and *para-typhi*, pathogens specific only to humans (Song *et al*, 2010). In response to an outbreak of typhoid fever in 2010, the World Health Organization (WHO) approved ciprofloxacin as the drug of choice for its treatment in all age groups, except in pregnant women, for inpatients as well as outpatients (WHO, 2011). But, an increasing rate of the development of resistance to conventional used antibiotics such as ciprofloxacin, remains a preoccupation for researchers, and has led to the search for new drugs more effective, affordable and readily available as therapeutic agents (Li *et al*., 2018).

One approach consists of targeting key enzymes that are associated with the disease process. *In vitro* studies showed that some plant extracts are active against antibiotic resistant *S. typhi* clinical isolates (Doughar *et al*., 2007). The significance of natural products in health care is supported by the WHO which reported that about 80% of the world's population still relies on traditional medicines for healthcare in general (WHO, 2018), and in certain African countries, up to 90% of the population still relies exclusively on plants as a source of medicines (WHO, 2019). Despite the constant development of synthetic pharmaceutical chemistry, including combinatorial chemistry and microbial fermentation, the pharmaceutical industry has realized that plants represent a huge reservoir of active substances. Natural compounds and their analogs represent over 50% of all drugs in clinical use (Baladrin *et al.*, 1993). It is also estimated that 74% of the most important drugs contain active ingredients from plants (Arvigo *et al.*, 1993). Plants are unique chemical factories, capable of synthesizing unlimited numbers of highly complex and unusual chemical substances whose structures could escape the imagination (Kayser *et al*., 2003).

Hence, the research around the world has turned to natural plants for ethno-medical purposes with the aim of rationalizing their use in one hand, and promoting traditional medicine, on the other hand. This practice also aims to obtain the active extracts or fractions that can go into the manufacture for new, more effective and less toxic phytodrugs. One of such novel source is the use of natural antimicrobial compounds such as plant-derived products (spices, essential oils, extracts or the consumption of herbal teas alone or in combination with antibiotics) (Oyewole *et al*., 2012). Herbal teas contain biologically active chemical substances (secondary metabolites) such as; polyphenols (flavonoids, phenylpropanoids, rosmarinic acid, catechins, tannins, polyketides), and terpenoids (mono-, di- and sesquiterpenes, iridoids, saponins) which synergistically act together thereby enhancing their activity (Malongane *et al*., 2017). These secondary metabolites are multitarget agents modulating the activity of proteins, nucleic acids and biomembranes in a less specific way in cells of animals (Wink, 2015).

Many plant species are used in Cameroonian traditional medicine to treat infectious diseases, and several interesting openings have originated for further inquiry following *in vitro* and *in vivo* antimicrobial activity evaluation (Kuete *et al*., 2010). Among these plants used, *Detarium microcarpum*, is a small tree or shrub that occurs in the tropical zone of Africa (Kouyaté & van Damme, 2006). Moreover, the ethnopharmacological uses, specifically for treatment against typhoid, inflammation and the close connection between inflammatory/infectious diseases (Aquino *et al*, 1992) led us to chemically investigate and evaluate the antibacterial properties of this plant.

To the best of our knowledge, phytochemical and pharmacological investigations have not been reported on the Cameroonian species. The widespread uses of this plant in traditional medicine for the treatment of several ailments, its great antimicrobial potential and the availability of literature justified our choice. The aim of this work was the chemical investigations and evaluation of antisalmonella properties of *Detarium microcarpum* Guill. et Perr. (Caesalpiniaceae), based on the bio-guided process and to chemically investigate the active fractions of the selected plant extracts. More specifically:

- To prepare the plant extracts and assess their antisolmonella activities;
- To characterize their secondary metabolites;
- To pre-formulate a phytodrug from the extract or the most active fraction.

This work is divided into three chapters. The first chapter deals with the literature review which concern the botanical and ethnobotanical aspect, the previous phytochemical and pharmacological studies. The second chapter is related to the presentation and discussion of the

results from our personal work. In the third chapter entitled experimental part, will be presented the material and method used to obtained the results.

CHAPTER I:

LITERATURE REVIEW

I.1. OVERVIEW ON SALMONELLOSIS

Human pathogenic bacteria are the cause of multiple infectious diseases, especially in developing countries, and are still wreaking havoc. Among these pathogenic bacteria, those of the genus *Salmonella*, which cause salmonellosis, are one of the leading causes of long hospitalizations and treatments. Salmonellosis covers two main types of infection including typhoid and paratyphoid fevers and non-typhic (or non-typhoid) salmonellosis (Ramkumar *et al*, 2012).

I.1.1. Overview on typhoid fever

I.1.1.1. Definition

Typhoid fever, also known as typhoid, is an acute, highly infectious and a common worldwide bacterial disease, caused by the bacterium *S. enterica*, *S. typhi* (Giannella, 1996). The term "enteric fever" is a collective term that refers to typhoid and paratyphoid (Parry and Beeching, 2009).

I.1.1.2. Different types of *Salmonella* species

Salmonella spp. are Gram-negative flagellated non-capsulated, non-sporulating, facultative anaerobic bacillus bacteria that can cause food- and waterborne gastroenteritis and typhoid fever in humans (Ramkumar *et al*, 2012). Since 2004, the genus *Salmonella* is known to have three species including *Salmonella enterica*, *S. bongori* and *S. subterranean* (Preeti *et al*, 2012). The main species is *S. enterica*, which itself comprises six subspecies divided into several serovars including *dublin*, *enteritidis*, *infantis*, *paratyphi*, *typhi*, *typhimurium*, *virchow*, etc (Preeti *et al*, 2012). They can also cause non typhoid salmonellosis. *Salmonella* that are strictly adapted to humans including *S. typhi*, *S. paratyphi* A, *S. paratyphi* B and certain strains of *S. paratyphi* C, cause typhoid and paratyphoid fevers (Pennec and Garré, 2003). *S. typhi* infects only humans while *S. paratyphi* A and *S. paratyphi* B infects both humans and other animals (Pilly, 1992). *S. typhimurium* induces systemic infection in mice and just a localized gastroenteritis in humans. However, certain species of *S. typhimurium* can cause systemic infections in humans (Wilkins and Roberts, 1988). The infection dose of *Salmonella* is not well defined and varies widely, but for humans, a dose of 10^4 CFU has been considered for *S. typhi*; this dose is higher for other serotypes (Bryan, 1977).

Salmonella can be responsible for bacteremia, a short-lasting bacteremia during the early stage of the pathogenesis rather. This bacteremia is short lasting because the bacteria are rapidly captured and killed by phagocytes. *S. typhimurium* and sometimes *S. enteritidis* are exceptions because they can lead to systemic infections, notably where phagocytosis abnormality exists

(sickle cell) (Berk, 2008). These salmonellae multiply in the lamina propria and provoke diarrhea by the production of toxin, just like in cholera, and by the induction of inflammation mediators, which modify the transport of electrolyte and liquid through the mucous (De Jong et al., 2012). Virulence factors are coded by the genes present on the chromosome (*S. typhi*), explaining the gravity of the infection, or by genes present on the chromosome and plasmid (e.g. *S. typhimurium*), explaining why for the same serovar, a strain can be more pathogenic than the other (Pennec and Garré, 2003).

I.1.1.3. Transmission of *Salmonella*

Typhoid is a common worldwide bacterial disease transmitted by the ingestion of food or water contaminated with the feces of an infected person, which contain the bacterium *S. enterica*, *S. typhi* (Giannella, 1996). The bacteria which causes typhoid fever may be spread through poor hygiene habits and public sanitation conditions, and sometimes by flying insects feeding on feces. The bacterium grows best at 37°C, corresponding to human body temperature. A person may become an asymptomatic carrier of typhoid fever, suffering no symptoms, but capable of infecting others. According to the CDC, approximately 5% of people who contract typhoid continue to carry the disease after they recover (NYT, 1938).

I.1.1.4. Physiopathology of typhoid fever

After ingestion, the typhic bacilli adhere to the enterocytes and the lymphoid follicles (M cells of Peyer's plaques); they are internalized by the actin-dependent system. They access the lamina propria and they are phagocytosed by the macrophages in which they multiply and join the mesenteric nodes. Some bacilli enter the blood flow; most of them are destroyed in the lymph nodes. Their lysis releases the endotoxin, which will permeate the nerve endings of the abdominal neurovegetative system, creating intestinal lesions, which are then invaded by the *Salmonella* eliminated in the bile. The endotoxin diffuses throughout the body and binds to the diencephalic nerve centers and to other organs, including the myocardium (Damilola *et al*, 2015).

I.1.1.5. Diagnosis of typhoid fever

Diagnosis is made by any blood, bone marrow, urine or stool cultures and with the Widal test (demonstration of *Salmonella* antibodies against antigens O-somatic and H-flagellar). In epidemics and less wealthy countries, after excluding malaria, dysentery or pneumonia, a therapeutic trial time with chloramphenicol is generally undertaken while awaiting the results of Widal test and cultures of the blood and stool (Ryan and Ray, 2004). The Widal test is time

consuming and oftentimes when diagnosis is reached, it is too late to start an antibiotic regimen (Parry and Beeching, 2009).

I.1.1.6. Bacterial cultures, serology and PCR

The common tests for *Salmonella* include blood cultures, co-cultures, the principle of Widal and Félix's serodiagnosis and PCR.

- Blood cultures: they are positive in 90% of cases in the first week, 75% in the second week and only 40% in the third week. 10 mL of blood for adults and 5 mL for children should be inoculated, as the number of bacteria in the blood is generally low. The inoculation is carried out in a Castaneda bottle (Meier *et al*., 2019).

- Co-cultures: they are positive in the second week (between 40 and 80% of cases). It is necessary to inoculate on selective medium such as *Salmonella* - *Shigella* medium (SS medium), taking into account the presence of many other bacteria in the stool (Chen et al., 2014).

- The principle of Widal and Félix's serodiagnosis: it is the search for agglutinins O and H. Agglutinins O are positive on day 8 to 10, agglutinins H on day 10-12. They are therefore present in the second septenary. A level ≥ 1/200 for agglutinins O and H is usually used as a limit for the positivity of the test. Several serodiagnostics are necessary to monitor the development of agglutinins. The agglutinins O disappear in 2 to 3 months. The agglutinins H persist for several years (Agbenu *et al*., 2010). Widal's serodiagnosis has low sensitivity and low specificity when practiced routinely. The reference technique is agglutination in a tube and not on a plate, as it is practiced routinely (Zorgani and Ziglam *et al*., 2014).

- PCR: it is used for early diagnosis while recommending the use of the Widal and Félix test when there is a suspected diagnosis and eliminating it as a screening test. The PCR amplification test of cultures from blood samples performs better than routine blood cultures to diagnose persistent typhoid fever (Mackay *et al*., 2002).

I.1.1.7. Treatment of typhoid fever

The treatment of typhoid fever and paratyphoid fevers is based on antibiotics with strong intracellular penetration, especially intra macrophage.

The availability of generic fluoroquinolones, which initially had preserved activity in many parts of the world, permitted a treatment option in primary care settings, and this group of antibiotics soon became the standard of care for typhoid among teenagers and adults (Rowe *et al*., 1987). Where resistance is uncommon, the treatment of choice is a fluoroquinolone such as ciprofloxacin (Parry and Beeching, 2009; Effa *et al*., 2011). Otherwise, a third-generation

cephalosporin such as ceftriaxone or cefotaxime is the first choice (Soe and O., 1987; Wallace *et al*., 1993). Cefixime is a suitable oral alternative (Bhutta *et al*., 1994; Cao *et al*., 1999). Typhoid fever in most cases is not fatal. Antibiotics, such as ampicillin, chloramphenicol, trimethoprim-sulfamethoxazole, amoxicillin and ciprofloxacin, have been commonly used to treat typhoid fever in developed countries. Prompt treatment of the disease with antibiotics reduces the case-fatality rate to approximately 1%. When untreated, typhoid fever persists for three weeks to a month. Death occurs in between 10% and 30% of untreated cases. In some communities, however, case fatality rates may reach as high as 47% (Dutta *et al*., 2001). The guidelines for drug treatment of typhoid fever is summarized in Table 2.

Table I : Guidelines for drug treatment of typhoid (Abhishek and Vinod, 2012)

Antibiotic	Daily dose	Route[1]	Dose/ day	Duration
Typhoid fever				
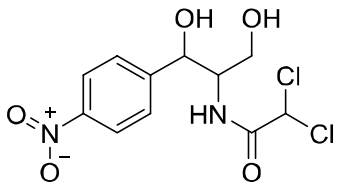 Chloramphenicol (**1**)	50–75 mg/kg	p.o./i.m./i.v[2].	4	14 days
Sulfamethooxazole 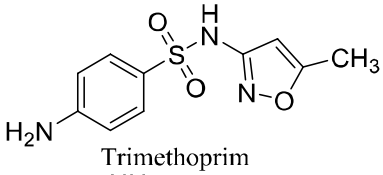 Trimethoprim 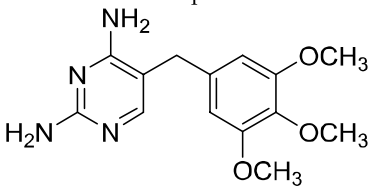 Co-trimoxazole (**2**)	Trimethoprim, 6.5–10 mg/kg Sulfamethoxazole, 40 mg/kg	p.o./i.m./i.v.	2 or 3	14 days
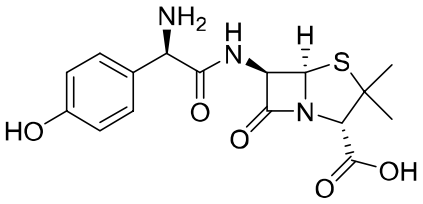 Amoxicillin (**3**)	75–100 mg/kg	p.o./i.m./i.v.	3	14 days

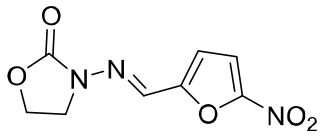 Furazolidone (**4**)	7.5 mg/kg	p.o.	4	14 days
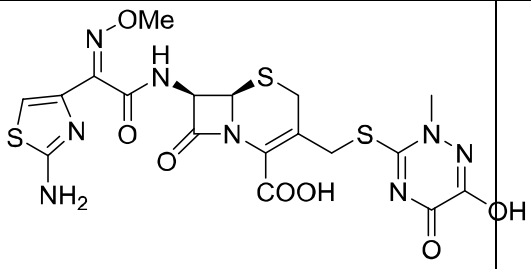 Ceftriaxone (**5**)	50–60 mg/kg	i.m./i.v.	2	7–14 days
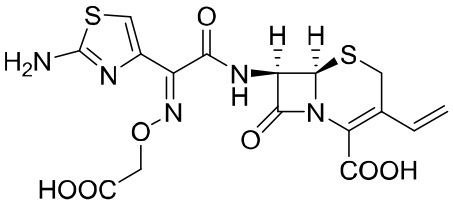 Cefixime (**6**)	20 mg/kg	p.o.	2	7–14 days
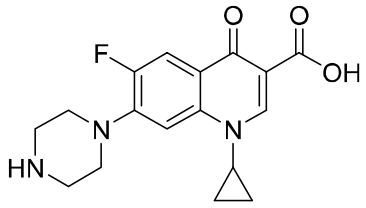 Ciprofloxacin (**7**)	0.5–1 g	p.o./i.v.	2	7–14 days
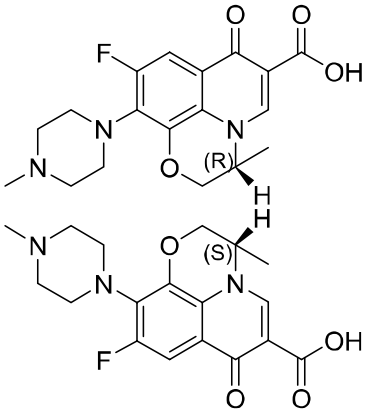 Ofloxacin (**8**)	800 mg	p.o./i.v.	2	7–14 days
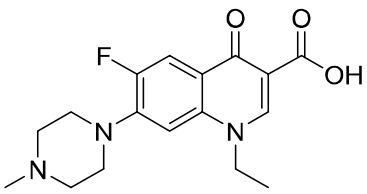	800 mg	p.o./i.v.	2	7–14 days

Pefloxacin (**9**)				
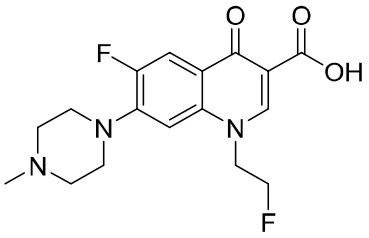 Fleroxacin (**10**)	400 mg	p.o./i.v.	1	7–14 days
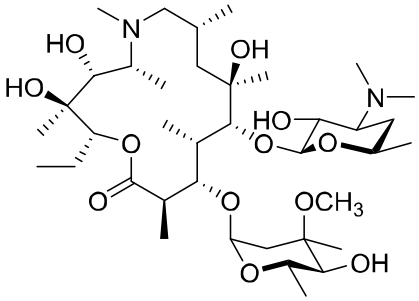 Azithromycin3 (**11**)	500 mg	p.o.	1	7 days
Treatment of typhoid carriers				
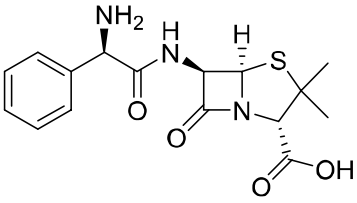 Ampicillin (**12**) or amoxicillin (**3**)	100 mg/kg		3 or 4	3 months[4]
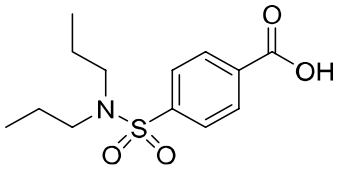 With probenecid (**13**)	30 mg/kg			
Co-trimoxazole (**2**)	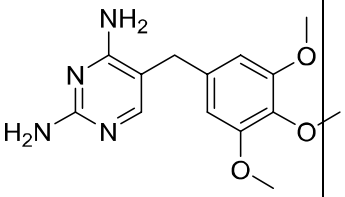 Trimethoprim (**14**), 6.5–10 mg/kg 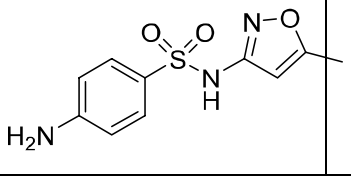	p.o./i.v.	2	3 months

	Sulfamethoxazole (**15**), 40 mg/kg			
Ciprofloxacin (**7**)	1500 mg	p.o.	2	28 days

[1]Oral therapy is satisfactory in most patients; parenteral therapy is generally reserved for severely ill patients.

[2]The oral route is preferred; there are reports of lower blood levels of chloramphenicol in patients given parenteral therapy.

[3]Azithromycin has been shown to be effective in mild-to-moderate disease, but there is currently no evidence for its efficacy in severe typhoid.

[4]The duration of treatment can be reduced if parenteral therapy is given (e.g. intravenous ampicillin 8-hourly for 2 weeks).

I.1.1.8. Resistance of *Salmonella* to commercial antibiotics

In the late 1980s and early 1990s, the emergence of *S. typhi* isolates resistant to first-line drugs including oral amoxicillin, chloramphenicol, and cotrimoxazole, so-called multidrug-resistant *S typhi* (MDRST), was associated with significantly higher rates of complications and mortality (Bhutta *et al*., 1994). The emergence of nalidixic acid-resistant *S. typhi* (NARST) isolates from parts of South and Southeast Asia (Parry, 2004), followed by clinical and laboratory fluoroquinolone resistance, has now created a specter of highly resistant strains of *S typhi* that requires treatment with a diminishing range of alternative antibiotics (Britto *et al*., 2018) . Resistance to ampicillin, chloramphenicol, trimethoprim-sulfamethoxazole and streptomycin is now common, and these agents have not been used as first-line treatment now for almost 20 years. Typhoid that is resistant to these agents is known as multidrug-resistant typhoid (Effa *et al*., 2011). Ciprofloxacin resistance is an increasing problem, especially in the Indian subcontinent and Southeast Asia. Many centers are therefore moving away from using ciprofloxacin as first-line for treating suspected typhoid originating in South America, India, Pakistan, Bangladesh, Thailand or Vietnam. For these patients, the recommended first-line treatment is ceftriaxone. It has also been suggested that azithromycin is better at treating typhoid in resistant populations than both fluoroquinolone drugs and ceftriaxone (Effa *et al*., 2011). Azithromycin significantly reduces relapse rates as compared to ceftriaxone.

There is a separate problem with laboratory testing for reduced susceptibility to ciprofloxacin. Current recommendations are that isolates should be tested simultaneously against ciprofloxacin (CIP) and against nalidixic acid (NAL), and that isolates that are sensitive to both CIP and NAL should be reported as "sensitive to ciprofloxacin", but that isolates testing sensitive to CIP but not to NAL should be reported as "reduced sensitivity to ciprofloxacin" (Fang *et al*., 2019). However, an analysis of 271 isolates showed that around 18% of isolates with a reduced

susceptibility to ciprofloxacin (MIC 0.125-1.0 mg/l) would not be picked up by this method (Rahman *et al*., 2014). It is not certain how this problem can be solved, because most laboratories around the world (including the West) are dependent on disk testing and cannot test for MICs.

I.1.1.9. Prevention of typhoid fever

Prevention of typhoid is based on vaccination and access to clean water. There are currently three types of approved vaccines:

- typhoid conjugate vaccines (TyVAC), which are Typbar-TyVAC ® and PedaTyph™;
- Vi polysaccharide vaccines, non-conjugated ViPS;
- live attenuated vaccines Ty21a.

The ViPS and Ty21a vaccines have been recommended by WHO since 2008 to combat typhoid fever in endemic and epidemic areas (WHO, 2019). The Typbar-TyVAC ® vaccine was approved for the first time in 2013 (Qamar *et al*., 2020). The following table 2 summarizes the characteristics of typhoid vaccines.

Table II : Summary on the characteristics of typhoid vaccines

Vaccines	Typhar-TyVAC ®	ViPS	Ty21a
Composition	25 μg of purified Vi capsular polysaccharide, conjugated with tetanus toxoid	25 μg of purified Vi capsular polysaccharide	2 to 6×109 CFU of Ty2a (attenuated Ty2 strain of *S. typhi*)
Route of administration and dosage	IM 1 dose	IM/SC 1 dose	Oral 3 doses (4 in the USA and Canada) administered every other day
Presentation	Liquid	Liquid	Gastro-resistant capsules
Recommended age	Adults and children $\geq$ 6 months to $\leq$ 45 years of age	Adults and children $\geq$ 2 years of age	Adults and children over 6 years of age

Currently, the TyVAC is to be preferred at all ages because of its better immunological properties, its ability to be used in young children and the longer duration of protection (up to 5 years and more). The WHO recommends that the introduction of TyVAC should be a priority in countries with the highest burden of typhoid fever or with high levels of antibiotic-resistant to *S. typhi* (Data *et al*., 2020). WHO recommends the vaccination in response to a confirmed typhoid fever outbreak. However, in a humanitarian emergency, priority should be given to the provision of clean water and the promotion of sanitation and hygiene.

Please insert a sentence here that will link typhoid to the study of a plant. It is very important to do so. Don’t forget to take information from sources that you will cite at the end.

At the time of therapeutic combinations comprising an antibiotic, information on the level of resistance is essential, because the WHO recommends new anti-typhoid treatment strategies when the resistance rate is high at more than 20% (Data *et al*., 2020). At this stage, faced with resistance to active molecules (antibiotics) by samonella, the discovery and development of new anti-typhoid therapies becomes a necessity. In this regard, medicinal plants in general, and *Detarium microcarpum* Guill. Perr. belonging to the Caesalpiniaceae families, used in traditional medicine for the treatment of typhoid fever in particular, are likely to constitute an alternative solution.

I.2. OVERVIEW ON THE FAMILY CAESALPINIACEAE

Caesalpiniaceae constitute a subfamily of Leguminosae consisting of about 150 genera and 2800 species including the genus *Detarium* (Hutchinson, 1964). The subfamily occurs exclusively in the tropics (Spichiger *et al*. 2002). It occurs mainly in South America, tropical Africa and South East Asia (Van Damme, 1993). This subfamily is composed of trees, shrubs and very rarely grasses, and consisting of about 162 genera, including 88 in Africa (Van Damme 1993, Spichiger *et al* 2002). The Detarieae tribe contains approximately 82 genera including *Detarium* (Mabberley 1981, Tucker 2002).

According to the latest classification system (APG II, 2003), these species are distributed in three subfamilies: Caesalpinioideae, Mimosoideae and Faboideae. Phylogeny is shown in Figure below.

Division…….……..	Angiospermae
Class……	Eudicot
Subclass……..……..	Core-Eudicot
Super-order……..……..	Rosid
Sub-ordre……	Eurosid I
Order……	Fabales
Family……..	Fabaceae
Sub-family…….	Caesalpinioideae
	Mimosoideae
	Faboideae (Papilionoideae)

Figure 1 : Taxonomy of the subfamily Caesalpinioideae (APG II, 2003)

I.3. BOTANICAL DESCRIPTION OF *DETARIUM* GENUS

I.3.1. Overview on the genus *Detarium*

The genus *Detarium* belongs to the Caesalpiniaceae family, subfamily Faboideae, tribe Detarieae.

The table below presents some species of the genus *Detarium.*

Table III : Taxes listed for the genus *Detarium* in databases

Databases	Species of the genus *Detarium*	Status/Comments
GRIN	*D. microcarpum* Guill. et Perr.	accepted
	D. senegalense J.F. Gmel.	accepted
	D. macrocarpum Harms.	unrevised
	D. hedelotianum Baill.	unrevised
IPNI	*D. microcarpum* Guill. et Perr	Syn. : *D. senegalense* J.F.Gmel
	D. senegalense Gmel.	accepted
	D. macrocarpum Harms.	accepted
	D. beurmannianum Schweinf.,ex C.Muell.	-
	D. chevalieri Harms	-
	D. heudelotianum Baill.	Syn. : *D. senegalense* J.F. Gmel.
	D. letestui Pellegr	-
	D. zeylanicum Thwaites.	reclasse : *Crudia zeylanica* benth.
W^{3}TROPICOS	*D. microcarpum* Guill. et Perr.	-
	D. senegalense J.F. Gmel.	-
	D. macrocarpum Harms.	-
	D. beurmannianum Schweinf.,ex C.Muell.	-
	D. chevalieri Harms.	-
	D. heudelotianum	-
	D. lestetui Pellegr	reclassifies: sindoropsis letestui Pell.
	D. zeylannicum Thwaites	-
GBIF	*D. microcarpum* Guill. et Perr.	accepted; syn. malapplique : D. senegalense J. Gmel.
	D.senegalense J.F. Gmel	accepted; syn. Clair :D. heudelotianum Baillon

	D. macrocarpum Harms.	accepted
	D. letestui	Attempt of taxonomic repositioning
	D. senegalensis J.F. Gmel.	Attempt of taxonomic repositioning
ILDIS	*D. microcarpum* Guill. et Perr.	accepted; syn, mal applique : *D. senegalense* J. Gmelin
	D. senegalense J.F. Gmel.	accepted; syn, clair : *D. heudelotianum* Baillon
	D. macrocarpum Harms.	accepted
	D. beurmannianum Schweinf.	Provisiore
	D. heudelotianum Baillon	Syn. : *D. senegalense* J. F. Gmel.
	D. senegalense Sensu Auct.	Badly applied
	D. zeylanicum Thwaites	reclassifies: *Crudia zeylanica* (Thwaites) benth.

(-): no comments on the status of the genus.

I.3.2. Description of plants of the genus *Detarium*

The genus *Detarium* was described for the first time in 1789 by DE JUSSIEU (*Detarium* juss; Genera *Plantarum*). He described it as a genus of trees of alternate leaves, which are imparipinnate or paripinnate. Leaves are pinnate or bipinnate, rarely single or unifoliate (Mabberley, 1981; Cavin, 2007). Leaflets are alternate or opaque, not very prominent, with 15-30 pairs of secondary veins intersecting at the edge of the lamina. A petal of the flower has 4 sepals and 8-10 prominent stamens creamy white. Flower petal, form of four sepals with ten short stamens alternate. The genera *Detarium* are species of straight-bodied fruit trees about 10 m in height. The drupes are orbicular with floury pulp and hard seed; they are ovoid or globose more or less flattened, 2 to 8 cm in diameter, containing a large central core surrounded by a floury pulp and very fibrous (Watson and Dallwitz, 1993). *Detarium*, of African origin, is characterized by large drupaceous fruits, subdivided, indehiscent, flattened and globose with a hard epicarp, and small hermaphrodite flowers (Aubréville, 1950; Keay, 1989; Watson and Dallwitz, 1993).

I.4. OVERVIEW ON *D. MICROCARPUM*

I.4.1. Botanical description

Detarium microcarpum is called in French “Petit Detar” (Malgras, 1992). It is also called "Konkhéhi" in Foufouldé and "Nbop" in Dii, which are local languages in the Adamaoua region of Cameroon. This species is a fruit tree up to 10 m high, as shown in figure 2 below.

Figure 2 : *Detarium microcarpum* species in savannah (personnal source).

The specie is recognizable by its rounded leaflets at the extremities, composed of 7 to 9 leaflets (7-11 * 3.5-5) cm, with an apex and a disc of respectively, emargatized and crenulate forms (Keay, 1989). The flowers of the specie are grouped in auxiliary panicles of 15 to 25 cm long and of 6 to 10 cm wide, as shown in figure 3 below. Its sweet and edible fruits, are ovoid or globose, 2.5 to 5 cm in diameter, to enclose in an endocarp, which is surrounded by a juicy mesocarp sometimes fibrous and protected externally by an epicarp. The bark of the trunk is smooth in young trees then becomes scaly in adults. These bark have red slices (Kerharo and Adam, 1974; Arbonnier, 2000).

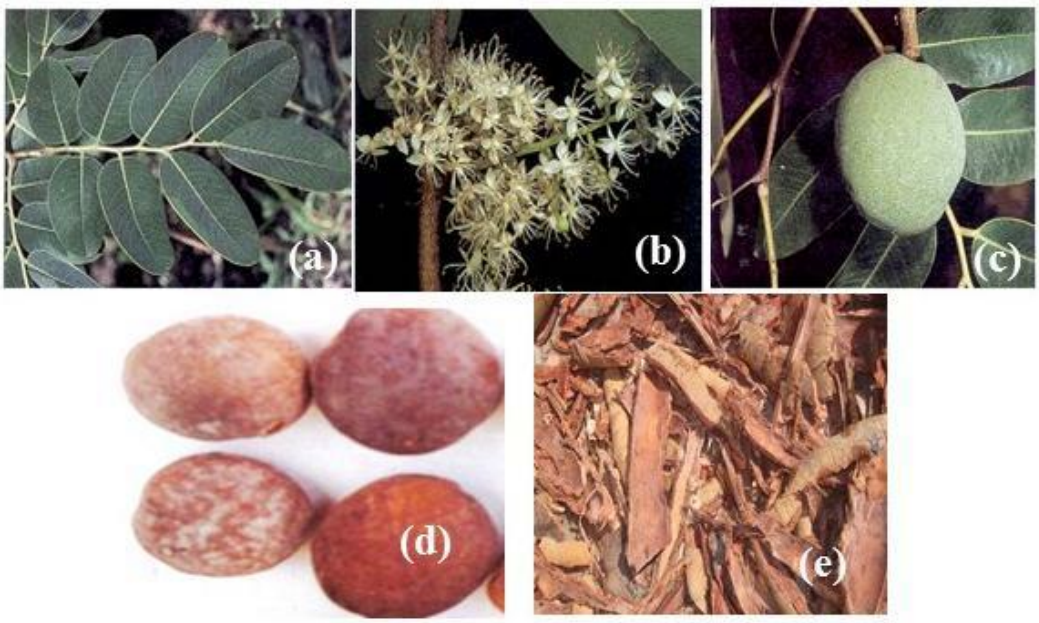

Figure 3 : (a)-leaves (b)-flowers (c)-fruits in maturity (Cavine, 2007) (d)-mature fruits (e)-stem bark. (Kouyate 2005)

D. microcarpum blooms during the period from July to November and the ripening of the fruit takes place in January.

I.4.2. Geographical distribution of *D. microcarpum*

D. microcarpum grows exclusively in the tropical zone of Africa. In Cameroon, it is found in the Far North, North and Adamaoua regions (Mouraba *et al*., 2017; Agbo *et al*., 2019). The map below shows black spots that represent their habitat.

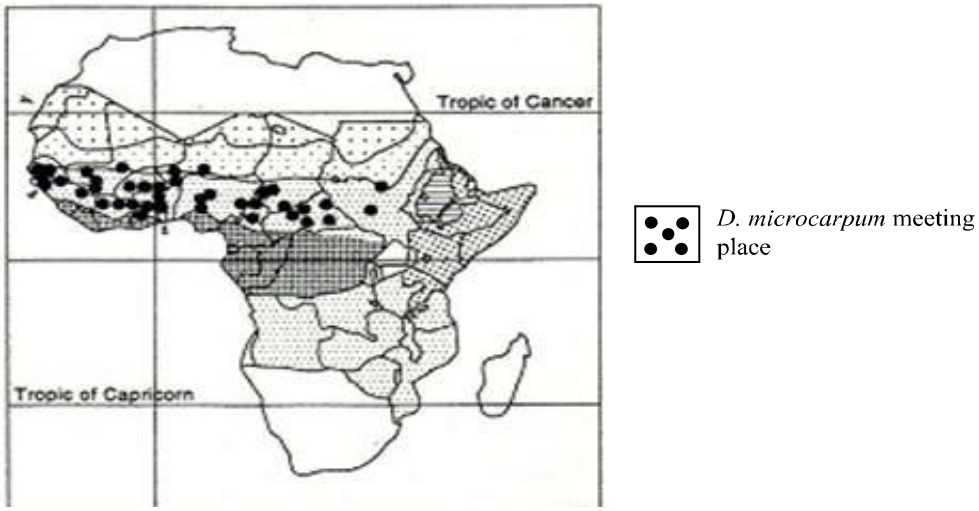

Figure 4 : Distribution map of *D. microcarpum* (Agbo *et al*., 2019)

I.5. USES OF *D. MICROCARPUM*

I.5.1. Economic uses

This species is used in diet, agriculture, livestock, domestic work and traditional pharmacopoeia. The fruits of this plant are much more solicited by the populations of the tropical zone. These fruits, rich in vitamin C, are also a source of vegetable protein and dietary sugars. Investigations related to the use of this plant are recorded in the table 4 below.

Table IV : Dietary, agricultural, veterinary and domestic uses of *D. microcarpum* Guill.and Perr. (Kerharo and Adam, 1962, Kerharo and Adam, 1974, Berhaut, 1975, Malgras, 1992, Burkill, 1995, Lajide *et al*, 1995, Arbonnier, 2002).

Organ	Property/use	Ethnic groups or countries
Fruit	The ripe fruits are sweet and rich in vitamin C. It is consumed fresh or in confectionery.	Sudan-Guinean region, Upper Volta, Nigeria, Sudan.
	The fruit pulp is used as a substitute for sugar.	Sudan
	Fruits are also used as feed for livestock.	West Africa.
Seed	Cooked seeds are used in making breads and pastries; they are equally used as a thickening agent in soups.	West Africa.

Flower	Has a sweet smell and are much appreciated by bees and cattle.	Unspecified
leaves	They are consumed as vegetables.	Sudan
	They are used in livestock feeding.	West Africa.
Wood	The wood is easy to work and particularly resistant to insects and water; it is therefore a good wood for carpentry and handicrafts.	Sudan
	It is forbidden to use it as firewood when cooking a remedy, because that would remove its effectiveness.	Mali
Resinous gum of bark	It is used to keep insects away from houses and clothes	Nigeria
Root	When heated, the root has a pleasant fragrance and is used as a perfume by women.	Dinka of Senegal

I.5.2. Uses in folk medicine

D. microcarpum is a tree of great importance in tropical Africa. It is used in folk medicine for the treatment of many diseases and is a part of several local pharmacopoeias (Burkill, 1995). The therapeutic uses of the various organs of this plant are depicted in table 5 below.

Table V : Main uses of *D. microcarpum* Guill. and Perr. in traditional medicine (Kerharo and Adam, 1962, Kerharo and Adam, 1974, Berhaut, 1975, Aquino *et al*., 1991, Malgras, 1992, Burkill, 1995, Arbonnier, 2002).

Organ	Properties / Uses	Preparation and method of administration	Ethnic group or country
Fruit	They are used for the treatment of vertigo, meningitis and in many magico-religious practices.	Unspecified	West Africa
Leaves	Leaves are used the treatment of diarrhea and dysentery; they are	Unspecified	Nigeria, Mali

	also used as a dressing for wounds.		
	They are involved in the treatment of leprosy, hemorrhoids, syphilis, gonorrhea, and amenorrhoea	Decoction, in association with other plants	Mali
	It is used in the treatment of paralysis	Bath and fumigation of boiled leafy roots	Mali
Leafy twig	It is used in treating asthenia and meningitis, to calm cramps, and to ease deliveries	Decoction	Mali
Stem Bark	It has application in the treatment of simple diarrhea and bloody diarrhea	Boiled bark, administered per os	Unspecified
	It is used in the treatment of dysentery and as a dressing for wounds	Unspecified	Nigeria
	It is also used in the treatment of hemorrhoids and gonorrhea	Unspecified	Foula and Fulani Toucouleur in Senegal
	It is a treatment for amibiasis and rheumatism	Unspecified	Niger
	It is used for its astringent properties	Unspecified	Unspecified
	When combined with other plants, it is used to heal mental illnesses and enteralgia ; it also has diuretic properties.	Unspecified	Unspecified
	It has anti-inflammatory and diuretic properties	Infusion	Senegal
	It is used in the treatment of red itching, stomach pain and typhoid	Unspecified	Foufouldé and Dii in Cameroon

Roots	It is indicated in handling stomach upset and intestinal problems, especially against dysentery diarrhea. It is also used as a diuretic	Decoction	Foula and Fulani Toucouleur in Senegal
	It is also indicated for the treatment of tuberculosis, smallpox, schistosomiasis and itching	Unspecified	Unspecified
	It is used in the treatment of syphilis	Decoction consumed per os	Senegal
	It is used to handle paralysis	Bath and fumigation of roots and boiled leaves	Mali
	It is used to treat epilepsy	Ash of the bark	Unspecified
	It is used for medico-magic treatment of mental illnesses	Used in combination with other plants	Cayor et Ferlo in Senegal
Different organs	It is used for diarrhea, dysentery, infant diarrhea, hemorrhoids, leprosy, syphilis, gonorrhea, rheumatism, impotence, infertility, fungal infections and biliary diseases	Unspecified	Senegal
	It is used against dysentery and syphilis	Unspecified	Igbo du Nigeria
Root	It is used to manage stomach upset and intestinal problems, especially against dysentery diarrhea. It is also used as a diuretic	Decoction	Foula and Fulani Toucouleur in Senegal
Root (fresh or dried)	It is used to heal typhoid fever	Bath with it twice daily for five days, also inhale the steam twice daily for five day	Niger

These numerous uses in traditional pharmacopoeias are at the origin of the pharmacological and chemical investigations of *D. microcarpum*.

I.6. PREVIOUS PHARMACOLOGICAL AND CHEMICAL STUDIES OF *D. MICROCARPUM*

I.6.1. Pharmacological investigations

Secondary metabolites isolated from *D. microcarpum* have been reported to display several pharmacological properties.

Coumarin (**5)** isolated from the bark (Ikhiri, K. and Ilagouma, 1995) has anti-oedematous properties. It is indicated in cases of lymphoedema of the upper limb after radiosurgical treatment of breast cancer. With regard to coumarin derivatives, some of them have pharmacological activities, mainly anticoagulant. The best known are dicoumarol and esculoside, both venotonic and vasoprotective (Hostettmann, 1997, Bruneton, 1999).

Catechin (**22**), epicatechin (**23**), catechin-7-Ogalloylester (**24**) and epicatechin-3-O-galloylester (**25**), isolated from bark (Aquino *et al*., 1991), while kaempferol-3-O-β-glucopyranoside (**26**) isolated from leaves (Lajide *et al*., 1995), have antioxidant properties (Bruneton, 1999). The anti-HIV-1 activity of the compounds **22** to **23** was evaluated on a cell line infected with the strain HIV-111B, and the compound 10 showed a high toxicity (Aquino *et al*., 1995).

Lupeol (**31**) and his derivative, lup-20(29)-èn-2α,3β-diol (**32)** isolated from the chloroform extract of the bark, exhibited different pharmacological activities: cytostatic antioxidant and anti-inflammatory. They also demonstrated *in vivo* a decreased risk of kidney stone formation (Hatake *et al*., 2006, Tolstikova *et al*., 2006).

A labdane-type diterpene, copalic acid (**38)** isolated from the bark of *D. microcarpum* showed a strong *in vitro* inhibition of the growth of certain bacteria including *Bacillus Subtilis*, *Staplylococus aureus* and *S. epidermis* (Tincusi *et al*., 2002). Tetranorditerpenes, 1-naphthalene acetic-7-oxo-1,2,3,4,4a,7,8,8a-octahydro-1,2,4a,5-tetramethyl acid (**39**) and 1-naphthalene acetic-5-carboxy-1,2,3,4,4a,7,8,8a-octahydro-1,2,4a-trimethyl acid (**40**), isolated from the chloroform extract of the bark of the same plant displayed growth inhibitory activities of yeasts *Candida albicans* and *Cryptococcus neoformans* (Hosose *et al*., 1999).

I.6.2. Previous chemical work

Given the medicinal importance of this plant in tropical Africa, several phytochemical studies have already been conducted on the leaves, bark and roots of *D. microcarpum*. They led

to the isolation and characterization of several families of compounds including carbohydrates, phenolic compounds, flavonoids, sterols, triterpenoids, diterpenoids and tetranorditerpenoids. The following table 6 below shows the different families of secondary metabolites isolated so far from this plant.

Table VI : Some isolated compounds of the species *D. microcarpum*

Structures	Name	Sources	References
Carbohydrates			
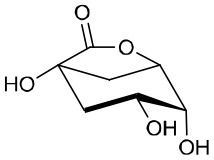	*L*-quino-1,5-lactone (**16**)	Bark	Abreu and Relva, 2002
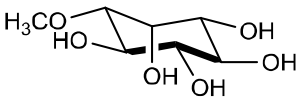	*D*-(-)-bornesitol (**17**)		
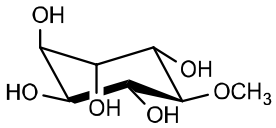	*D*-pinitol (**18**)		
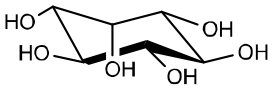	Myo-inositol (**19**)		
Phenolic compounds			
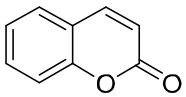	Coumarin (**20**)	Bark	Aquino *et al*., 1991
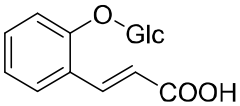	Melilotoside (**21**)		
Flavonoïds			
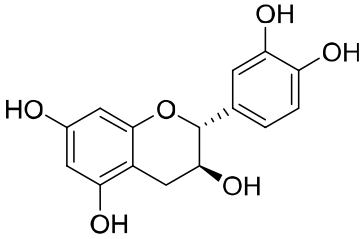	Catechin (**22**)	Bark	Aquino *et al*.,1991

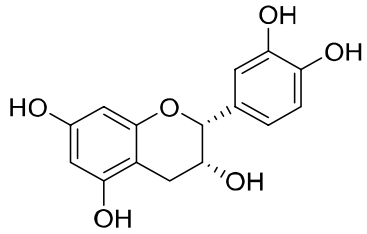	Epicatechin (**23**)		
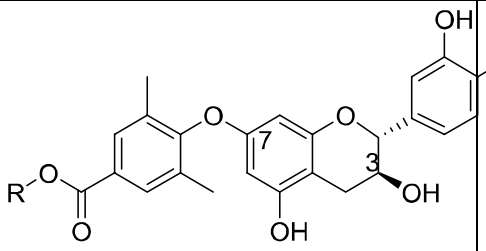	Cathechine-7-*O*-galloylester (**24**)		
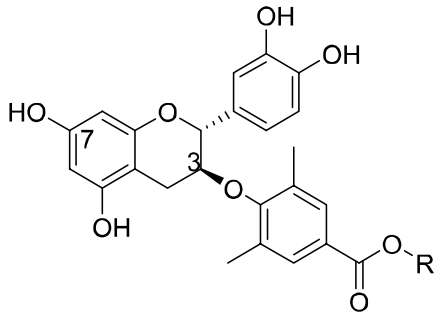	Epicatechin-3-*O*-galloylester (**25**)		
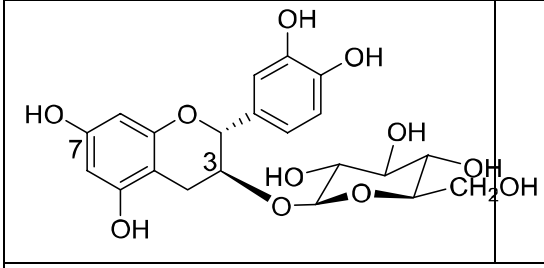	Kaempferol-3-*O*-*β*-glucopyranoside (**26**)		
Sterols et triterpenoids			
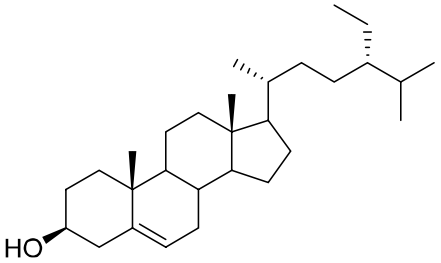	*β*-sitosterol (**27**)	Bark	Abreu *et al*., 1998
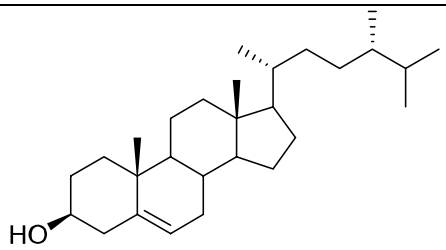	Campesterol (**28**)		

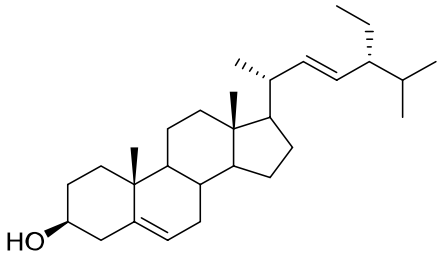	Stigmasterol (**29**)		
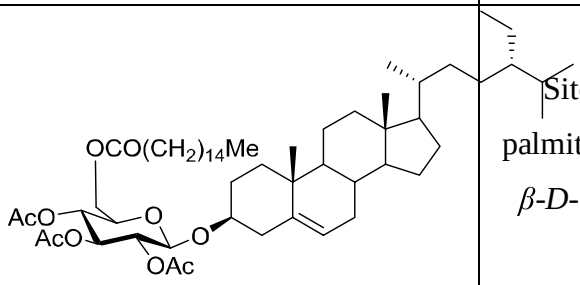	Sitosterol-3*β*-*O* -[6′-*O*-palmitoyl-2′,3′,4′-*O*-triacetyl-*β*-*D*-glucopyranoside] (**30**)	Bark	Abreu *et al*., 1998
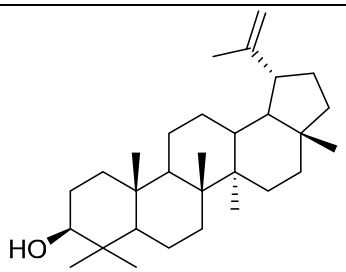	Lupeol (**31**)		Hatake *et al*., 2006
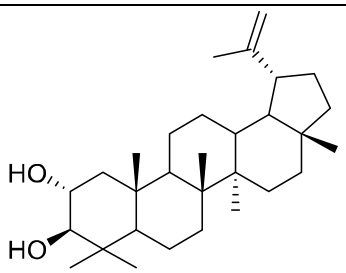	Lup-20(29)-en-2*α*,3*β*-diol (**32**)		Tolstikova *et al*., 2006
Diterpenoids and tetranorditerpenoids			
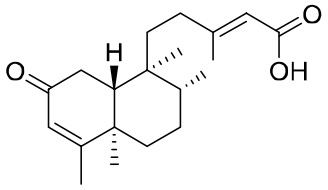	2-oxokolavenic acid or 2-oxo-3,13*E*-clerodiene-15-oic acid (**33**)	Leave and bark	Aquino *et al*., 1992
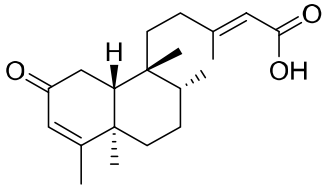	*Cis*-2-oxokolavenic acid (**34**)	Bark	Ikhiri and Llagouma, 1995
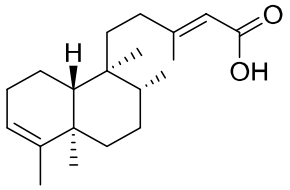	Kolavenic acid (**35**)	Leaves	Lajide *et al*., 1995

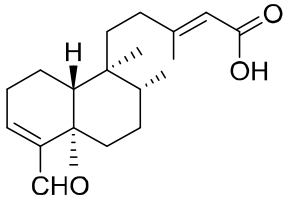	5-(5-formyl-1,2,3,4,4a,7,8,8a-octahydro-1,2,4a-trimethyle-1-naphtalenyle)-3-methyle-[1*S*-[1α(*E*),2β,4aβ,8aα] pent-2-enoic acid (**36**)		
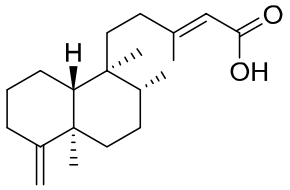	Ent-4(18)-13*E*-clerodien-15-oic acid (**37**)		
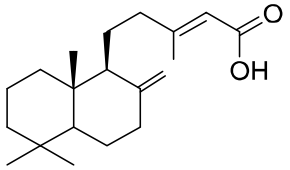	Copalic acid (**38**)	Bark	Ikhiri et Llagouma., 1995
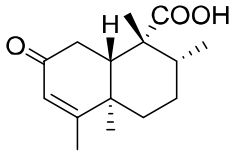	Naphtalene acetic-7-oxo-1,2,3,4,4a,7,8,8a-octahydro-1,2,4a,5-tetramethyl acid (**39**)		Aquino *et al*., 1992
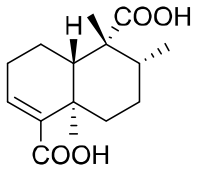	Naphtalene acetic-5-carboxyl-1,2,3,4,4a,7,8,8a-octahydro-1,2,4a-trimethyl acid (**40**)		

Due to the fact that among the isolated secondary metabolites the most abundant were the terpenoids, and more particularly diterpenoids, it seemed important to us to attach particular importance to this class of compounds. It is equally the type of secondary metabolites that we were looking for, because of their great anti-bacterial potential.

I.7. CHEMICAL STUDIES OF DITERPENOIDS

I.7.1. Overview on diterpenes and diterpenoids

The name diterpene refers to a class of naturally occurring compounds having a C-20 base backbone, derived from the condensation of four isoprenic units. They are found in the plant kingdom (Compositeae, Asteraceae, Verbenaceae, Meliaceae, and Fabaceae etc…) as well as in the animal kingdom (especially in certain insects), and fungi (Bruneton, 1993; Hanson, 2007). Diterpenes are made of carbons and hydrogens, while diterpenoids are oxidized diterpenes.

Diterpenes and diterpenoids have a large structural diversity that is highly dependent on their biogenesis. It is, moreover, based on biogenetic considerations that their classification have been established (Bruneton, 1993).

I.7.2. Biosynthesis of diterpenes and diterpenoids

The biogenetic precursor of diterpenes is geranylgeranyl pyrophosphate (GGPP) (**57**). GGPP results from the condensation of a C-15 unit, notably farnesyl pyrophosphate (FPP) (**55**) and a C-5 unit, isopentenyl pyrophosphate (IPP) (**50**). GGPP reacts under the influence of biocatalysts to leading to the different structural types of diterpenes that we will describe later. The biosynthesis of diterpenes and diterpenoids is subdivided into three main stages:

- Formation of the isopentenyl unit (isopentenylpyrophosphate);
- Condensation of isopentenyl units to give linear or acyclic diterpenes;
- Conversion of acyclic diterpenes to cyclic diterpenes.

I.7.2.1. Formation of the isopentenyl pyrophosphorus unit (IPP) (50)

IPP is formed by two different biogenetic pathways including the acetate-mevalonate pathway (which is the most widespread) and the phosphate-pyruvate triose pathway (Bruneton, 1993; Rohmer *et al*., 1996).

- **Formation of the IPP unit by acetate-mevalonate route**

It is done under enzymatic catalysis in several stages of which the first is a Claisen-type condensation of three molecules of Acetyl-Coenzyme A (**42**). The conversion of the latter into mevalonic acid (**45**) is done by a reduction in the carbonyl to alcohol by means of nicotinamide adenine dinucleotide phosphate (NADPH).

The mevalonic acid (**45**) obtained undergoes double phosphorylation in presence of mevalonate kinase and phosphomevalonate kinase, followed by decarboxylation to give isopentenyl pyrophosphate (IPP) (**50**). The latter is converted by enzymatic isomerization to dimethylallylpyrophosphate (DMAPP) (**51**). The sequence thus described is illustrated in scheme 1 (Bruneton, 1993).

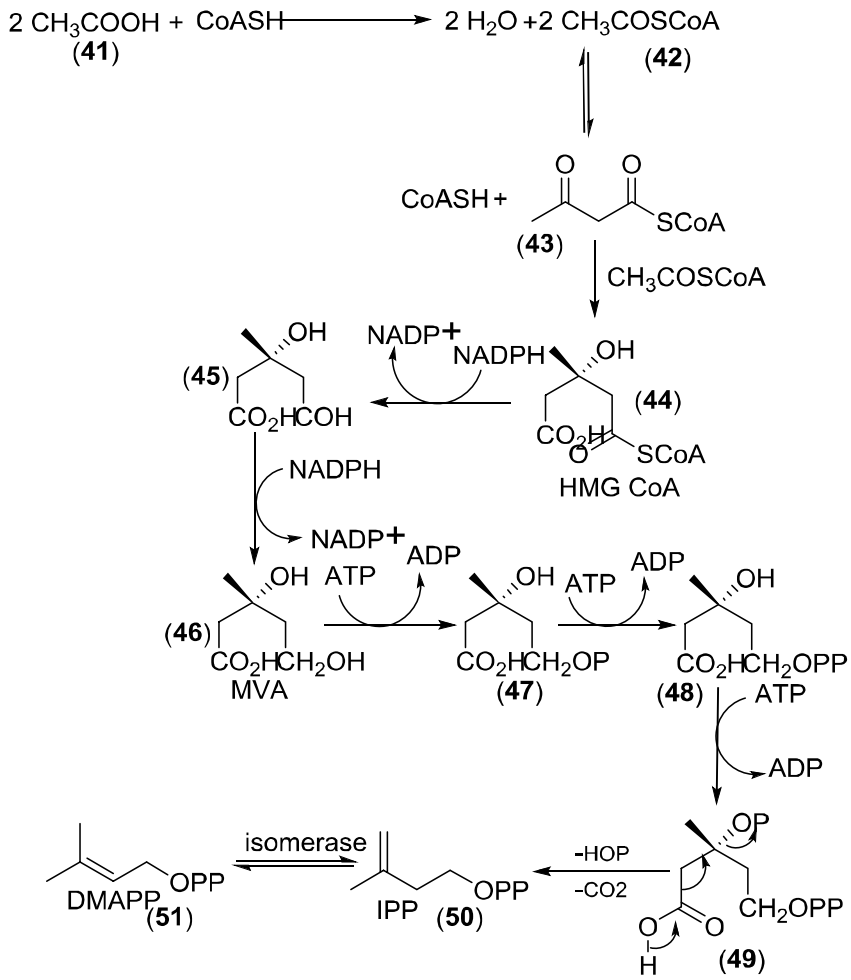

Scheme 1 : Biosynthesis of isopentenyl pyrophosphate by acetate-mevalonate route

- **Formation of the isopentenyl pyrophosphate unit by pyruvate triosephosphate**

This alternative route was developed by Rohmer *et al*., (1996). Studying the biosynthesis of terpenoids by isotopic labeling with ^{13}C, these authors suggested that IPP (**50**) was produced from 5-phosphate-1-deoxyxylulose **(54)**, formed by condensation of pyruvate **(53)** and 3-phosphate glyceraldehyde **(52)** (Scheme2).

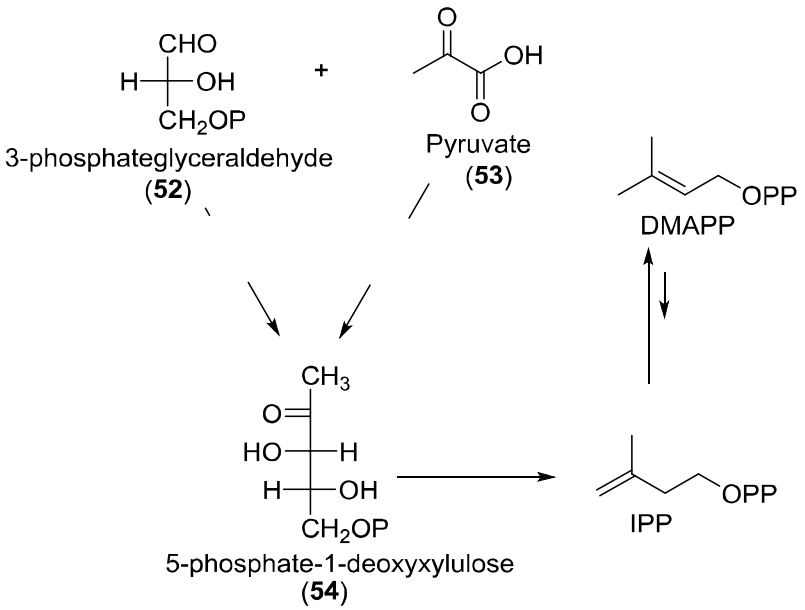

Scheme 2 : Biosynthesis of IPP by the triosephosphate-pyruvate route

The isopentenyl pyrophosphate thus obtained constitutes the starting point for the biosynthesis of the different classes of terpenes and terpenoids via the specific precursors. Indeed, all terpene compounds result from the condensation of a variable number of isoprenic units (Ruzicka, 1953). We will focus on the biosynthesis of geranylgeranyl pyrophosphate (GGPP) **(54)**, precursor of diterpenes.

I.7.2.2. Biosynthesis of geranylgeranyl pyrophosphate (54)

After the enzymatic isomerization of IPP **(50)** leading to DMAPP **(51)**, the two isomers will undergo head-to-tail condensation with elimination of the pyrophosphate group in DMAPP **36** to form the geranyl pyrophosphate (GPP) **(56)**, C-10 molecule, precursor of monoterpenes.

It is indeed a stereoselective addition of DMAPP on the double bond of IPP. The head-to-tail condensation of this C-10 compound with an IPP molecule lead to farnesyl pyrophosphate (FPP) **(55)**, a C-15 molecule precursor of sesquiterpenes, which in turn reacts with another molecule of IPP **(50)** to produce geranylgeranyl pyrophosphate (GGPP) **(57)**, a C-20 molecule precursor of diterpenes. These reactions are summarized in Scheme 3.

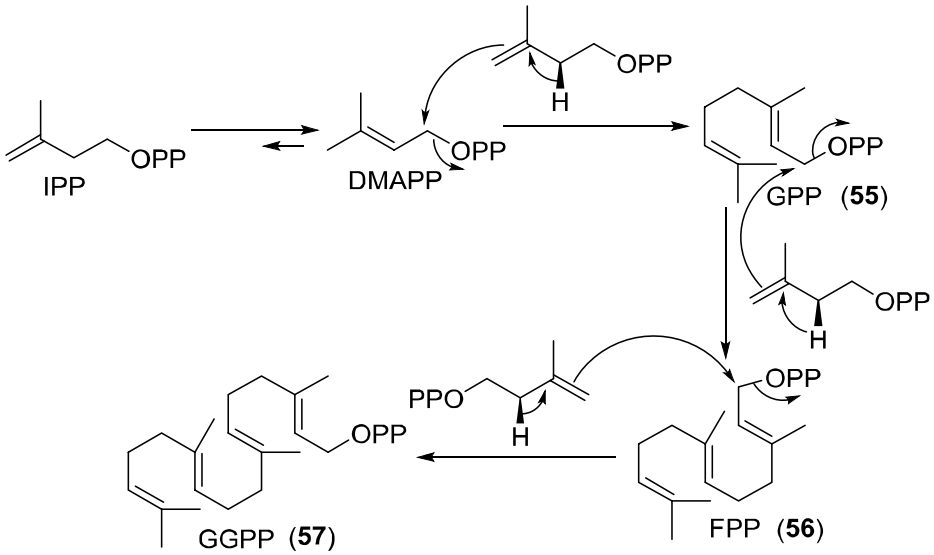

Scheme 3 : Biosynthesis of GGPP from IPP

The GGPP **(57)** thus formed can cyclize, rearrange or not and lead to the various diterpene skeletons.

I.7.2.3. Formation of cyclic diterpenes (Bruneton, 1993)

The different structural types of cyclic diterpenes are derived from the metabolism of (2*E*,6*E*,10*E*) geranylgeranyl pyrophosphate (GGPP) **(57)**. The acquisition of each class is a function of the type of cyclization undergone by GGPP **(57)**. In fact, there are two main cyclization modes, which we will be designated by mode A and mode B (Torsell, 1997).

- Cyclization according to mode A

In this case, the cyclization is induced by the departure of the pyrophosphate group with the formation of a carbocation and the alkylation of a double bond by the latter. In most cases, the double bond of the terminal isopropylidene is alkylated. This is how a macrocyclic carbocation is formed, the stabilization of which leads to the formation of macrocyclic diterpenes. In fact, this carbocation is very reactive and can be stabilized either by elimination of a proton with the formation of compounds such as cembrenes **(60)**, or more often by intramolecular nucleophilic substitution leading to macrocyclic structures such as lathyrenes **(62)**, tiglans **(63)**, etc… (Scheme 4).

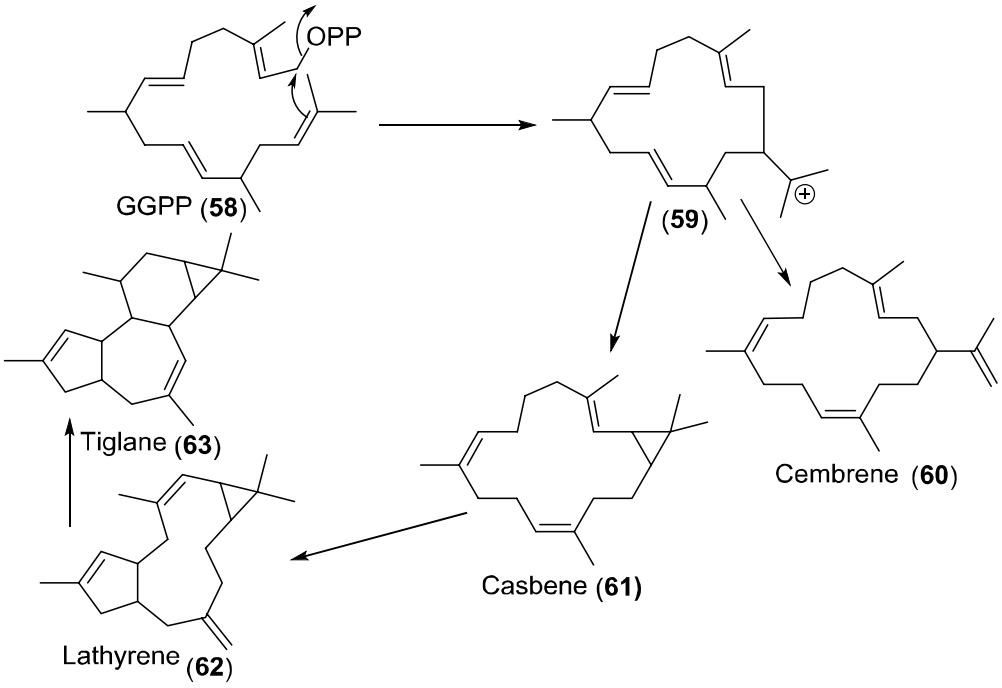

Scheme 4 : Some macrocyclic diterpenes

- Cyclization according to mode B

It is an acid-catalyzed cyclization of GGPP **(57)** leading to a substituted decahydronaphthalene. This type of cyclization generates two pairs of enantiomers (64-65 and 67-68) differ in the opposite configurations of carbons C-5, C-9 and C-10. Here, the orientation to one or other of the enantiomers depends on the conformation of GGPP **(57)** on the surface of the cyclization-catalyzing enzyme. The different types of orientation are illustrated in Scheme 5.

Chair - chair orientation «normal»

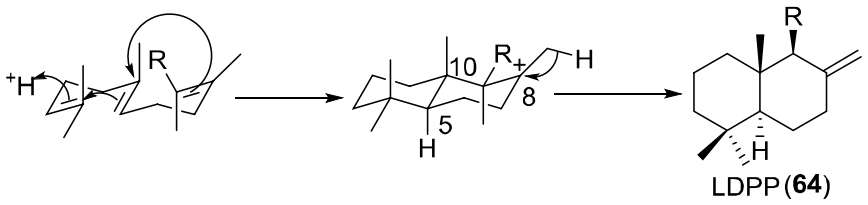

Chair – chair Orientation « antipodal »

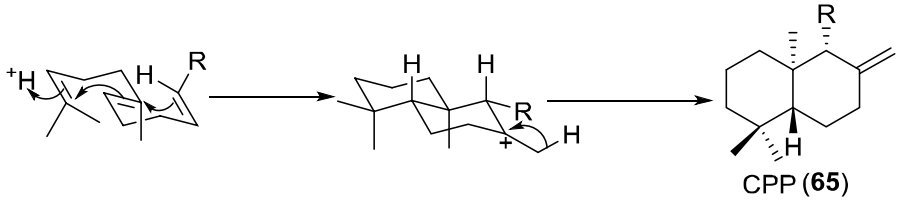

Chair – boat Orientation « normal »

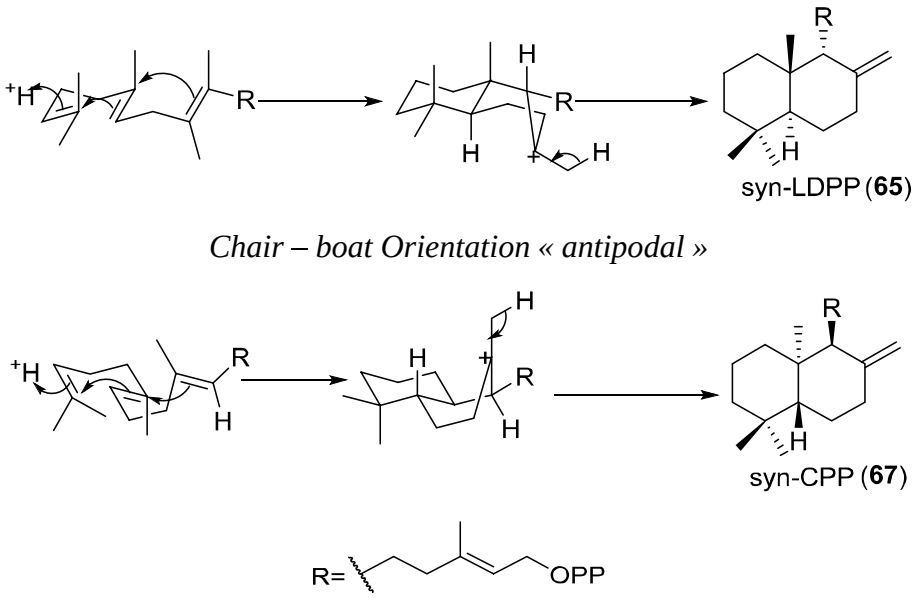

Scheme 5 : Orientation of intermediates 64 to 67

A large part of the bicyclic diterpenes comes from the pair of enantiomers **64** and **65** in which each leads to a particular series. Thus, labda-8-(17),13-dien-15-yl pyrophophate (LDPP) (**64**) produces the diterpenes of the so-called "normal" series while its antipode, copalyl pyrophosphate (CPP) (**65**) leads to the series called "enantio" or "ent". The hypothetical carbocations resulting from LDPP or from CPP can be stabilized by the elimination of a proton, by hydration or by rearrangement to lead to bicyclic diterpenes of the labdane (**68** and **69**) and clerodane (**70** and **71**) series. An illustration is presented in scheme 6.

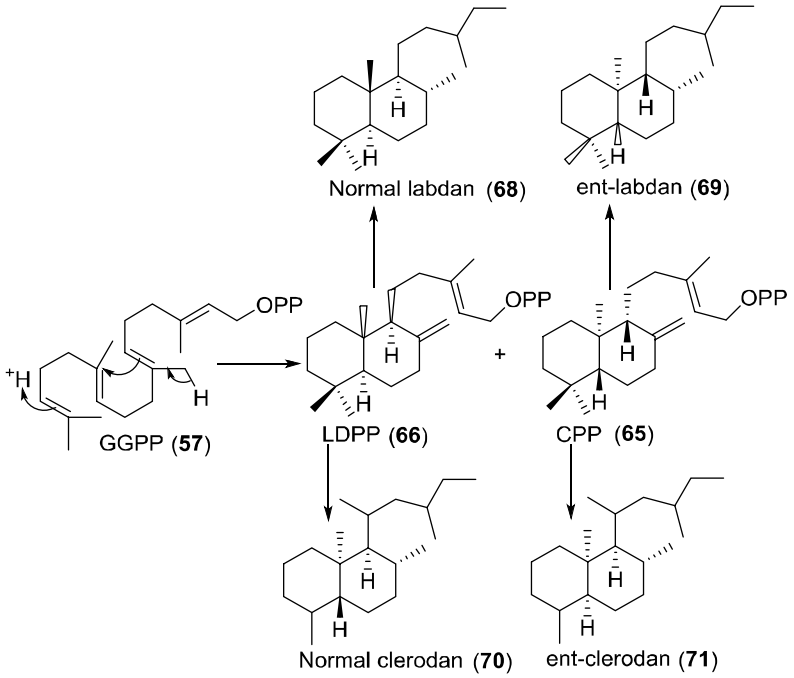

Scheme 6 : Basic skeletons of labdanes and clerodanes

After the cyclization of GGPP **(57)** according to mode B, the decaline system obtained can undergo several rearrangements leading to tricyclic, tetracyclic and pentacyclic triterpenes. This set of cyclization and rearrangement mechanisms explains the great structural diversity observed within the diterpenes.

I.7.3. The main structural types of diterpene

Diterpenes have several structural types closely related to their biogenesis. It is therefore reasonable to use these to classify them. There are essentially two groups of diterpenes, notably the acyclic and the cyclic (Manitto, 1981).

I.7.3.1. Acyclic diterpenoids

They are the least encountered. They are linear and can result from the condensation of two monoterpene units of:

- geranyl-linalol type such as compound **(72)** ((E)-5,14-dihydroxy-2,6,10,14-tetramethylhexadeca-2,6,15-triene-4,12-dione) isolated from *Croton salutaris* (Euphorbiaceae) (Itokawa *et al*., 1998);

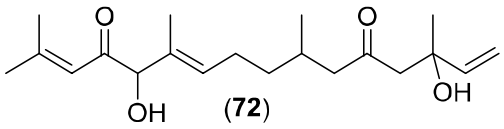

(**72**)

- a geranyl-geraniol derivative such as compound (**73**) isolated from *Diplostephium meyenii* (Asteraceae) (Bittner *et al*., 1991);

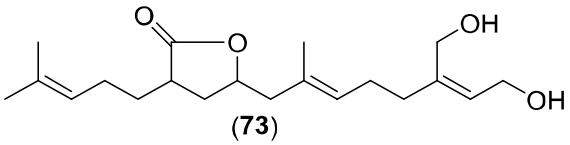

(**73**)

- a geranyl-nerol entity such as compound (**74**) isolated from *Siegesbeckia orientalis* (Compositeae) (Zdero *et al*., 1991).

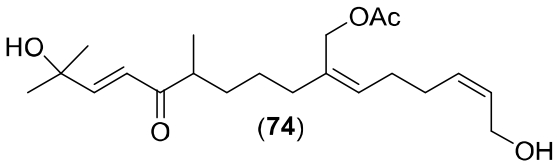

(**74**)

While some acyclic diterpenes contain in their structures an epoxide, such as zoapatol (**75**) isolated from one Compositeae, *Montana tomentosa* (Quijano *et al*., 1991), others such as conysaleucolide (**76**) isolated from another Compositaea, *Conysa hypoleuca* (Zdero *et al*., 1991), contains a terminal furan nucleus.

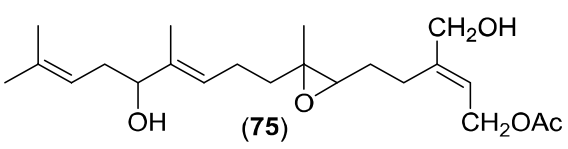

(**75**)

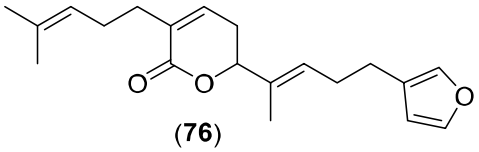

(**76**)

I.7.3.2 Cyclic diterpenoids

Considering their number and their great structural diversity, cyclic diterpenes constitute the most important group. This is how we distinguish bicyclic, tricyclic, tetracyclic, macrocyclic diterpenes with various structures.

I.7.3.2.1. Macrocyclic diterpenoids

They result from cyclization according to mode A described above. The main representatives of this class are cembrenes, casbene, lathyrenes, tiglans and taxanes. However, the most abundant are cembrenes and taxanes.

The main sources of cembrenes are marine organisms, particularly corals. This is the case for 2-hydroperoxysarcophine (**77**) isolated from *Lopophytum crasum* as well as crassocolide A (**78**) isolated *Sarcophyton crassocaule* (Hanson, 2007).

Taxanes are the best known and attract the attention of researchers due to their interesting biological activities. In 1999, More than 400 compounds of this class were already isolated from natural sources and new molecules continue to be taken into account today (Pinto *et al*., 2019). The best known taxane is taxol (**79)**, a compound which is very active against human cancers, isolated for the first time by Wani *et al*. (1971) from the Pacific yew tree called *Taxus brevifolia* (Taxaceae).

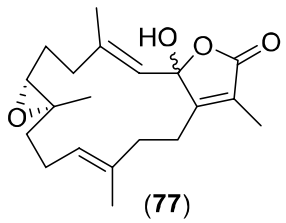

(**77**)

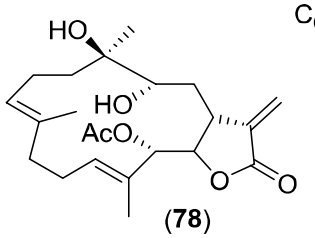

(**78**)

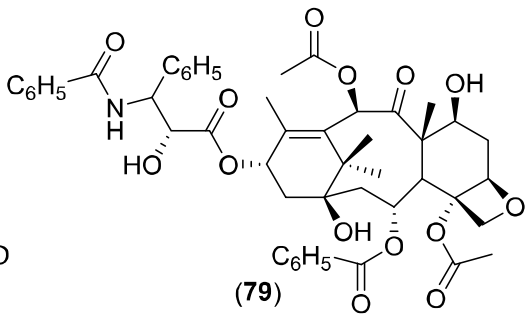

(**79**)

I.7.3.2.2. Bicyclic diterpenoids

This class contains two main structural types, namely the labdane type and the clerodane type.

- **The labdane series**

Conifers are the main source of labdane-type diterpenes. However, they are also found in botanical families such as Verbenaceae, Compositeae, Zingiberaceae, Caesalpiniaceae…etc

(Chingwaru et al., 2015). From the structural point of view, labdanes comprise in their structures a *trans*-decaline type nucleus substituted in position C-4 by a gem-dimethyl group and in positions 8 and 10 by an angular methyl as in compound **64**. The numbering used for their nomenclatures is that recommended by Rowe in 1992 (Rowe, 1992). On the *trans*-decaline nucleus is grafted in position C-9, a side chain with 6 carbon atoms corresponding to a methylpentane.

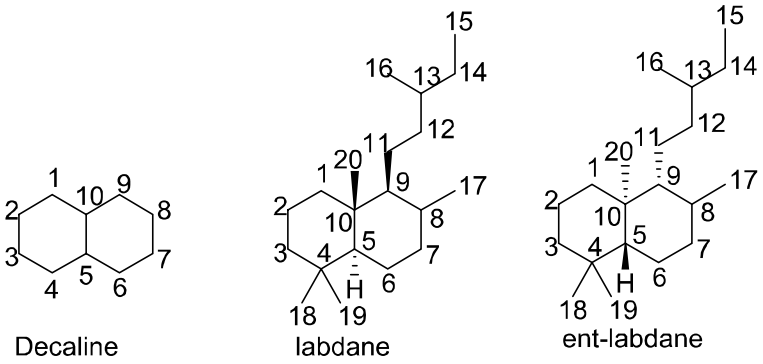

(**80**)

Very often, this *trans*-decaline nucleus may undergo structural modifications. The main ones concern the oxidation of one of the gem-dimethyl groups in position 4 to carboxylic acid or to alcohol **65** and the transformation of methyl in position 8 to exomethylene. The side chain can also undergo modifications, which can lead either to functionalization such as the oxidation of carbons C-16 and C-15 to carboxylic acid, to aldehyde (**82)** or to alcohol (**81)**, or to a cyclization leading to a furan nucleus (**84)** or to a lactone (**83)**.

Certain modifications can lead either to a loss of one or more carbon atoms, or to the rupture of a bond in the carbon skeleton of decalin thus leading, respectively to two other structural types of labdane namely the nor-labdanes (**85**) and the seco-labdane (**86**). Depending on the number of carbon atoms lost, we can have: nor-labdanes (one lost atom), bisnor-labdane (two atoms lost), trinor-labdanes (three atoms lost), tetranor-labdanes (four atoms lost) etc…

Sometimes, two molecules of labdane can combine to form a dimer. This is the case for ent-methylisoozate (**87**) isolated for the first time by Dirceu *et al*. (1999) of *Xylopia aromatica* (Annonaceae).

Table VII : Some structural types of labdanes

Structure and name	Source	Reference
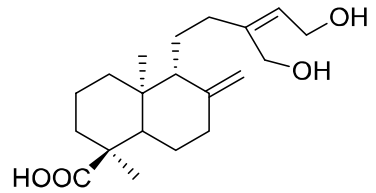 ent-15,16-dihydroxylabda- 8, 13-dien-18- oïc acid (**81**)	*Brickellia lemmonii* (Compositeae)	Hanson, 1998
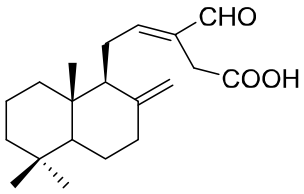 Zerumine A (**82**)	*Alpinia zerumbet* (Zingiberaceae)	Xu *et al*., 2006
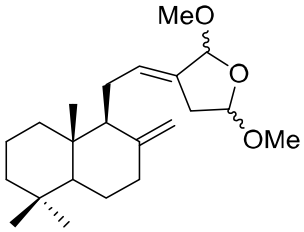 Aulacocarpine D (**83**)	*Aframomum aulacocarpos* (Zingiberaceae)	Sob *et al*., 2007
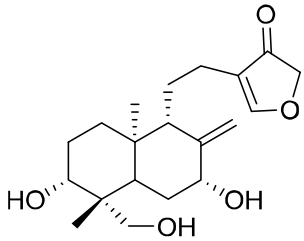 7(*R*)-hydroxy-14-deoxyandrographolide (**84**)	*Andrographis paniculata* (Acanthaceae)	Chen *et al*., 2008
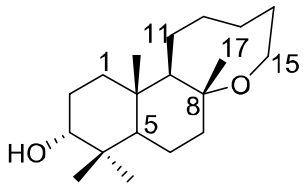 8α ,15-epoxy-16-norlabdane (**85**)	*Eragrostis viscosa* (Poaceae)	N'Soki *et al*., 2010
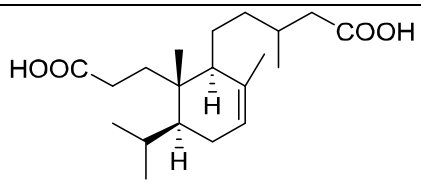 Cativin-7-en-3, 15-dioicacid-3-4-secolabdane (**86**)	*Brickellia veronicaefolia*	Wang *et al*., 2012

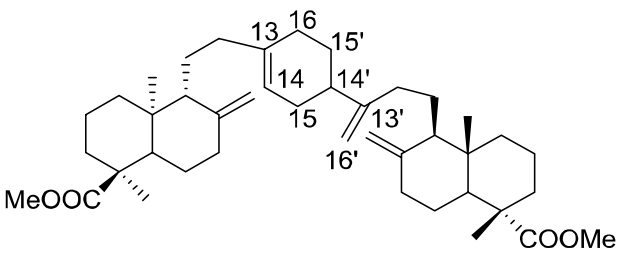 *ent*-methylisoozate (**87**)	*Xylopia aromatica* (Annonaceae)	Dirceu *et al*., 1999

- **The clerodane series**

They are abundant in the Asteraceae, Compositeae and Labiatae families (Hanson, 2004). Like the labdanes, the clerodanes are cyclic diterpenes enclosing in their structures the decaline type nucleus. However, the difference between these two types lies from the structural point of view, at the level of the position of the various methyl groups as well as the stereochemistry at the level of the junction of the decalin cycles. Indeed, while in the labdane type, gem-dimethyl occupies position C-4, and in position C-5 there is hydrogen, in clerodane type, position C-4 is only occupied by a single methyl, the second having migrated to position C-5. The presence of a hydrogen in position C-10 is also very regularly noted as well as the omnipresence of a methyl group at position C-9. In addition, while in labdanes the stereochemistry of the decalin junction is *trans*, in the clerodane type, it can be sometimes *cis* or *trans*. Some structural types of clerodanes are given in Table IV.

Table VIII : Some structural types of clerodanes

Structure and name	Source	Reference
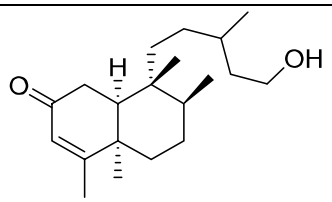 15-hydroxy-3-cleroden-2-one (**88**)	*Casearia sylvestris* (Flacourtiaceae)	Dos santos *et al*., 2007
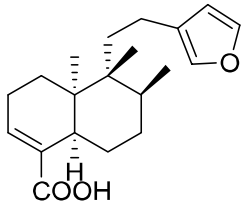 (-)-hardiwickiic acid (**89**)		

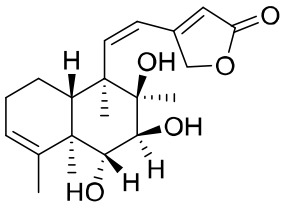 Barbatine C (**90**)	*Scutellaria barbata* (Labiatae)	Sheng-Jun *et al*., 2006

I.7.3.2.3. Labdane and clerodane type diterpenoids from *D. microcarpum*

Given their structural similarities (decalin), the isolated diterpenoids of *Detarium microcarpum* species belong to the labdane and clerodane type, with a side chain of varied structure. This is a methylpentane comprising a carboxylic function.

Table X : Some isolated diterpenoids of the *D. microcarpum*

Structures	Name	Sources	References
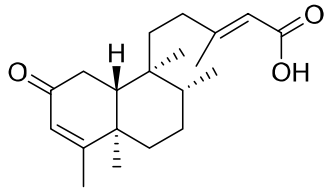	2-oxokolavenic acid or 2-oxo-3,13E-clerodiene-15-oïc acid (**33**)	Leave and Bark	Aquino *et al*., 1992
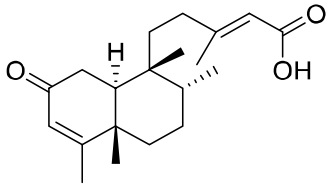	Cis-2-oxokolavenic acid (**34**)	Bark	Ikhiri et Llagouma.,1995
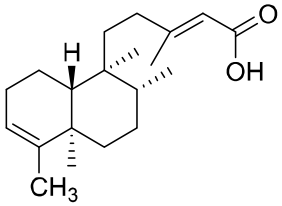	Kolavenic acid (**35**)	Leaves	Lajide *et al*., 1995
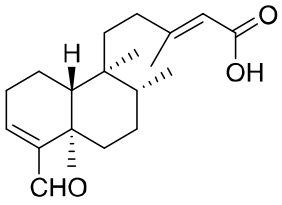	5-(5-formyl-1,2,3,4,4a,7,8,8a-octahydro-1,2,4a-trimethyle-1-naphtalenyle)-3-methyle-[1S-[1α(E),2β,4aβ,8aα]] Pent-2-enoïc acid (**36**)		
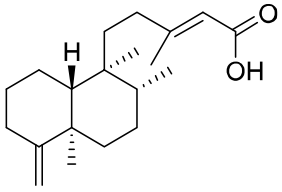	Ent-4(18)-13E-clerodien-15-oic acid (**37**)		

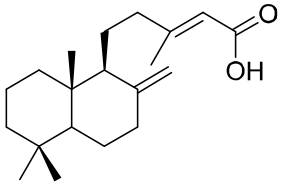	Copalic acid (**38**)	Bark	Ikhiri et Llagouma.,1995
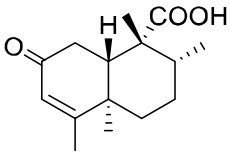	Naphtalene acetic-7-oxo-1,2,3,4,4a,7,8,8a-octahydro-1,2,4a,5-tetramethyl acid (**39**)	Bark	Aquino *et al*., 1992
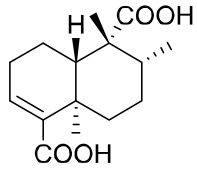	Naphtalene acetic-5-carboxyl-1,2,3,4,4a,7,8,8a-octahydro-1,2,4a-trimethyl acid (**40**)		

I.7.3.2.4. Tricyclic diterpenes

There are several types of tricyclic diterpenes including pimaranes, abietanes, cassanes, rosanes, vouacapanes, and podocarpanes, which are the most encountered (Pablo, 2007).

- The abietane type is found in most species of the genus *Salvia* (Lamiaceae) (Hanson, 2007). This is the case with danshexinkume (**91**) isolated from *Salvia miltiorrhisa* (Ikeshiro *et al*., 1991).

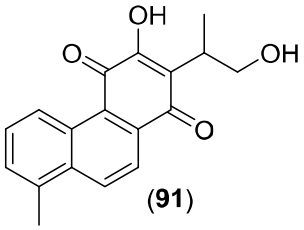

(**91**)

- The pimarane type like scopararane A (**92**), was isolated from *Eutypella scoparia* (Pongeharoen *et al*., 2006).

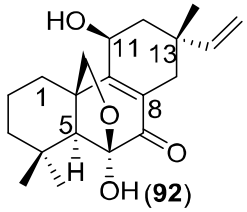

(**92**)

- The cassane-type is abundant in the genus *Ceasalpinia* (Hanson, 2006). This is the case for caesaldecane (**93**) isolated from Caesalpinia decapetala (Kiem *et al*., 2005).

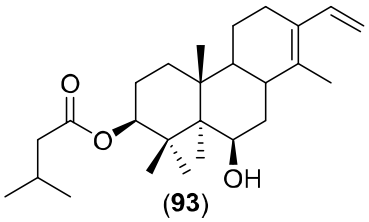

(**93**)

From a structural point of view, tricyclic diterpenes differ from bicyclic ones by the presence in their skeleton of a third cycle joined to that of decaline. This third cycle can be either with 6 carbons for pimaranes (**92**) and cassanes (**93**), or with 6 or 7 carbon atoms for abietanes (**91**). All have in position 13, a side chain with 2 carbon atoms for pimaranes and casanes, and with 3 carbon atoms for abietanes, corresponding to isopropyl. The side chain of abietanes can be cyclized to lead to the ring with 7 carbon atoms (**94**), while in pimaranes and cassanes, it can either form a double bond (92 and 93) or be cyclized in furan nucleus or in furanolactone (Casane) (**95**). It is also noted that cassanes and pimaranes have a methyl group in position 13, which is absent in abietanes, and another in position 10, which can be oxidized to alcohol or to carboxylic acid. Finally, it is note in these three types, the presence of a gem-dimethyl, which sometimes can be absent in abietanes.

Table IX : Some structural types of tricyclic diterpenes

Structure and name	Source	Reference
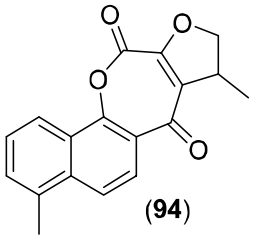 (**94**)	*S. miltiorrhiza*	Xu. *et al*., 2016
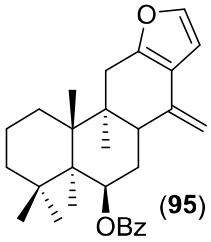 (**95**) Isovoucapenol A	*Ceasalpinia pulcherrina*	Ragasa *et al*., 2002

I.7.3.2.5. Tetracyclic diterpenoids

This class includes kauranes, beyranes, atiseranes, gibberelines, trachilobanes, aphidicolanes, stemodanes etc... (Hanson, 2007; Pablo, 2007). However, the structural types mainly encountered are:

- Kauranes of which the plants of the genus *Xylopia* (Annonaceae) constitute a main source, are also found in the Asteraceae, Compositeae and Rubiaceae (Takahashi *et al*., 2001; Hanson, 1998). An example is that of ent-kaur-16-en-19-oic acid (**96**), isolated from the seeds of *Xylopia sericea* (Takahashi *et al*., 2001).

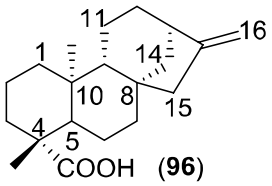

(**96**)

- The atiseranes are commonly found in plants of the genus *Stevia*, *Xylopia* or in certain cell cultures (Hanson, 1998). For example, kaurenoic acid methyl ester (**97**) and scopadulcic acid (**98**) were isolated, respectively from the seeds of *Xylopia sericea* and a tissue culture of *Scoparia dulcis* (Takahashi *et al*., 2001; Hayashi *et al*., 1996).

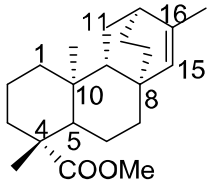

(**97**)

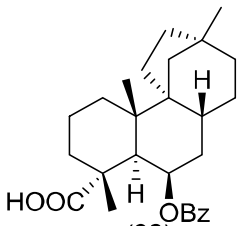

(**98**)

- Gibberellins are considered as hormones in plants. Many of them have been isolated from Leguminoseae. This is the case of 17-hydroxy-16,17-dihydrogibberellin A4 (**99**), isolated from a Leguminoseae called *Cytisus simensis* (Picciarelli *et al*., 1991).

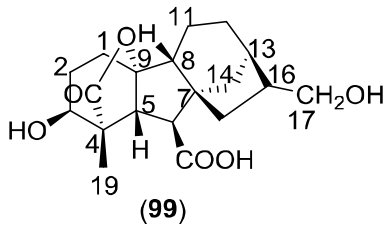

(**99**)

Atiseranes and kauranes from a structural point of view, have a decalin-type nucleus, which is not the case with gibberellins whose structure has a five-cycle interspersed between two six-cycle. The fourth cycle being pentatonic forms with the hexatonic cycle, a bicyclic bridged of the bicyclo [3.2.1] octane type for gibberellins and kauranes and bicyclo [2.2.2] for compound **97** or [3.2.1] **98**, and octanes for atiseranes. *Gem*-dimethyl in position 4 is omnipresent in atiseranes and kauranes, which is not the case for gibberellins from which one of the methyl groups has migrated in position C-6. In addition, kauranes and gibberellins have a methyl group at the C-16 position. These various methyl groups can undergo oxidation to carboxylic acid or to alcohol.

I.7.3.2.6. Diterpenes with various structures

One of the main sources of this class is marine organisms. The structural types encountered are briaranes, xerulans, xemicanes etc ... (Hanson, 2004). This is the case with briaexcavatolide (**100**), a briarane isolated from a coral called *Briareum excavatum* (Wu *et al*., 2003).

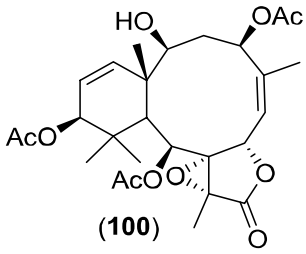

(**100**)

I.7.4. Method for determining the structure and stereochemistry of labdanes

I.7.4.1. Structure determination method

As with other families of organic compounds, the elucidation of compounds of labdane-type diterpenes is based on spectroscopic techniques such as IR, UV, one- and two-dimensional NMR, mass spectrometry (MS).

The vast majority of labdane type diterpenes are recognized by the presence on their ^{1}H NMR spectra of a set of three singlets integrating three protons each, with resonances in the range of δ_H 0.50 to 1.00 attributable to the three methyl groups occupying the positions C-4 and C-10 from the decalin nucleus. For the labdanes having an exocyclic double bond $\Delta^{8(17)}$, we observe two large singlets integrating for an olefinic proton each between δ_H 4.00 and 5.00. The presence of the exomethylene is confirmed on the ^{13}C NMR spectrum by two characteristic signals appearing at about δ_C 148.0 for C-8 carbon and 107.0 for C-17 carbon (Bastard *et al*., 1984).

On the IR spectrum, this methylene group is characterized by a set of valence vibration bands appearing around λ_{max} 3080, 1640 and 890 cm^{-1}. In the absence of other substituents on the decalin-type nucleus, there are signals on the ^{13}C NMR spectrum at about δ_C 42.0, 33.0 and 38.0 corresponding to the chemical shifts of carbons C-3, C-4 or C-18 and C-7 (Bastard *et al*., 1984).

The skeletons of the labdane type can be characterized from their EI mass spectrum which showed an intense signal at *m/z* 137, a variable value depending on the substituents carried by the nucleus of the decaline type (Hong-Xi *et al*., 1996). The formation of this ion fragment is rationalized as scheme 8.

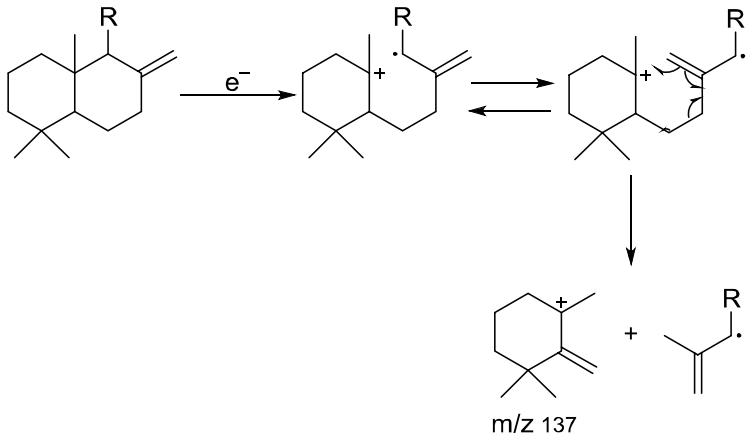

Scheme 7 : Characteristic fragmentation of skeletons of the labdane type

I.7.4.2. Method for determining stereochemistry

The main difference between "normal labdane" and "*ent*-labdane" comes from the stereochemistry at the level of carbons C-5, C-9 and C-10 as in compound **64**. In normal labdanes, the side chain in position C-9 and the methyl group fixed at C-10 have a *β*-stereochemistry and the hydrogen in C-5. In *ent*-labdanes, these orientations are reversed giving rise to an *α*-sterereochemistry. In practice, in order to distinguish between these two series, certain chiroptic methods are used. From the work of Hasegawa *et al*., (1985) and Waridel *et al*., (2004), it appears that the measurement of optical rotation is one of the methods used to establish the difference between normal and *ent*-labdanes, where the sign of the optical rotation is positive for normal labdanes and negative for *ent*-labdanes. However, the opposite is observed in structures whose side chain has, in addition to a furan nucleus, a carbonyl function in position C-12 (DellaGrecaa *et al*., 2001; 2000). For the skeletons containing an exomethylene in position 8 (**17**), the measurement of the circular dichroism spectrum (CD) makes it possible to observe a positive cotton effect for normal labdanes and negative for ent-labdanes (Zdero *et al*., 1991; Itokava *et al*., 1988; Morita *et al*., 1988).

I.7.5. Biological activities of labdane-type diterpenes

Although to our knowledge, there is no labdane to date with a recognized therapeutic effect, many compounds of this type, which are of synthetic origin or isolated from terrestrial plants and sailors have been reported to exhibit diverse pharmacological properties. Some of these pharmacological properties include antibacterial, antifungal, anti-inflammatory, cytotoxic and enzyme inhibitory activities.

I.7.5.1 Antibacterial activity

The ethanol extract of the bark of *D. microcarpum* has been reported to exhibit moderate antibacterial activity against *Pseudomonas aeruginosa*, *Klebsiella pneumoniae*, *Citrobacter freundii*, *Staphylococcus aureus* and *Listeria monocytogenes* (Abreu *et al*., 1998). Two labdane-type diterpenoid, (-) copalic acid or ent-8 acid (**38**), 13*E*-labdadien-15-oic isolated from the methanolic bark extract of *D. microcarpum* displayed a strong *in vitro* inhibition on some bacteria growth including *Bacillus subtilis*, *Staphylococcus aureus* and *S. epidermis* (Ikhiri and Ilagouma, 1995; Tincusi *et al*., 2002). Two other tetranorditerpenoids isolated from the chloroform extract of the bark of *D. microcarpum* including 1-naphthalene acetic-7-oxo-1,2,3,4,4a, 7,8,8a-octahydro-1,2,4a, 5-tetramethyl (**24**) and 1-naphthalene acetic-5-carboxy-1,2,3,4,4a, 7,8,8a-octahydro-1,2,4a-trimethyl (**25**) have been reported to inhibit the growth of *Candida albicans* and *Cryptococcus neoformans* (Aquino *et al*., 1992); (Hosoe *et al*., 1999).

Chinou *et al*., (1994), working on the leaves of *Cistus incanus* (Cistaceae) isolated several labdane-type diterpenoids among which, labdan-14-ene-8,13-diol (**101**); 5*R*, 8*R*, 9*R*, 10*R*-labdan-13*E*-8*a*-15-diol (**102**) and acetate of 5*R*, 8*R*, 9*R*, 10*R*-labdan-13*E*-en-8*a*-ol-15-yl (**103**). All these compounds exhibited an activity on Gram-positive (*S. aureu*s and *S. epidermis*) and Gram-negative bacteria (*K. pneumoniae, P. aeruginosae* and *E. coli*) on *Klebsiella pneumoniae, Staphylococcus aureus* and *Pseudomonas aeruginosae*.

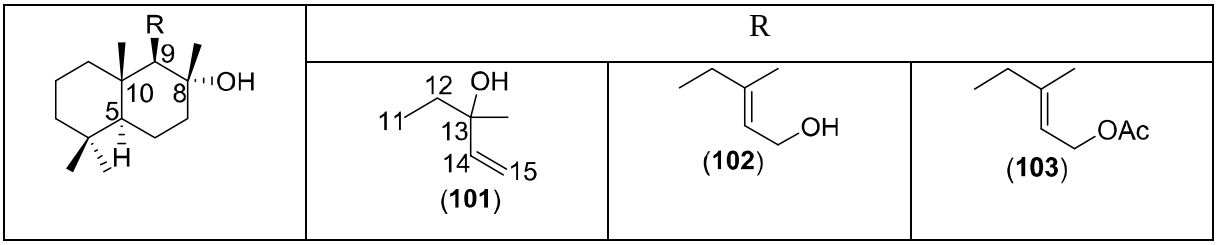

Gomojosides including gomojosides K104 and L105 isolated from *Viburnum suspensum* showed remarkable antibacterial activity against *Aeromonas salmonishida* at the concentration of 100 ppm (Iwagawa *et al*., 1993).

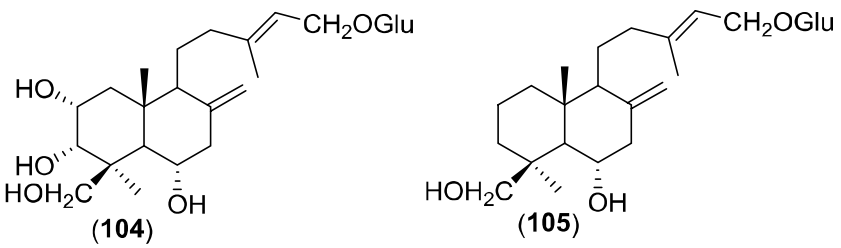

I.7.5.2. Antifungal activity

Aframodial or 8*β*,17-epoxy-12*E*-labdene-15,16-dial isolated from the seeds of *Aframomum danielli* (Zingiberaceae) displayed a wide spectrum of biological activities among which antifungal activity was the most important (Kimbu *et al*., 1979; Ayafor *et al*., 1994). Tested on the strains of *Candida albicans*, *Candida tropicalis* and *Candida utilis*, Aframodial (**106**) revealed a higher antifungal activity than that of amphotericin B (**107**) which is one of the reference antifungal molecules used in modern medicine to combat fungal infections, although its toxicity somehow limits its use (Ayafor *et al*., 1994). Four years later, Morita *et al*., (1998), studying the seeds of *Alpinia galanga* (Zingiberaceae), also isolated a large amount of aframodial (**106**), and this antifungal activity was confirmed.

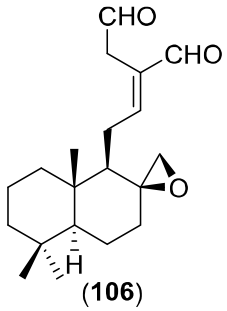

(**106**)

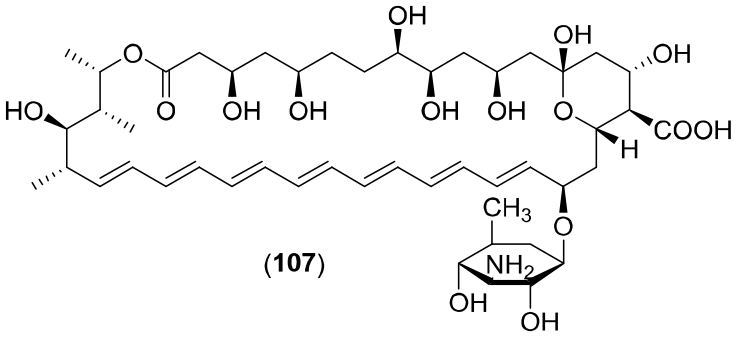

(**107**)

I.7.5.3. Anti-inflammatory activity

The leaves of *Cryptomeria japonica* (Taxodiaceae) are used in the traditional Japanese pharmacopoeia for the treatment of inflammation in the event of injuries, abscesses and eczema. The phytochemical and pharmacological study of these leaves allowed Shimizu *et al*., (1998) to show that this anti-inflammatory activity was due to a labdane, namely cis-communic acid (**107**). These authors thus reported for the first time, the anti-inflammatory activity of a labdane-type diterpene.

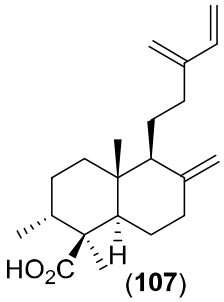

(**107**)

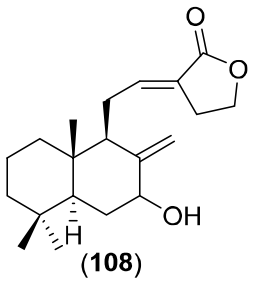

(**108**)

Hedychilactone A (**108**) isolated the same year from *Hedychium coronarium* (zingiberaceae) by Itokawa *et al*., (1998) also exhibited interesting anti-inflammatory properties.

I.7.5.4. Cytotoxic activity

Many labdane-type diterpenes have been tested for their cytotoxic properties:

aframodial (**106**) exhibited strong cytotoxic activity against leukemic cells (L1210) with an ED_{50} of 2.5 μg/mL (Ayafor *et al*., 1994).

Labda-8(17),12(*E*),14-triene-2α,18-diol (**109**), isolated from the ethanolic extract of *Orthosiphon labiatus* (Labiatae) has shown cytotoxic activity on the MCF-7 cancer cell line lung, with an IC_{50} of 82 μM (Ahmed *et al*., 2007).

Damrong *et al*., (2003), tested 12,17-dihydroxylabda-7,13(*E*)-diene (**110**) on five human cancer cell lines, namely BT474, CHAGO, HEP-G2, KATO3 and SW620, with concentrations inhibition (IC_{50}) respectively of 2.5 μg/mL; 6.1 μg/mL; 5.5 μg/mL; 0.6 μg/mL and 6.1 μg/mL. This compound exhibited a very interesting cytotoxic activity with respect to the KATO3 line (IC_{50} = 0.6 μg/mL), compared to doxorubicin 100 (IC_{50} = 1.7 μg/mL), an active ingredient belonging to the family of anthracyclines, used in medicine in cancer chemotherapy, taken here as a positive control.

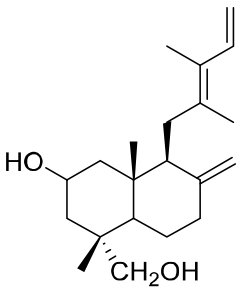

(**109**)

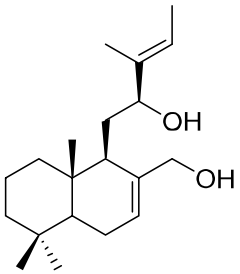

(**110**)

Working on the leaves of *Renealmia alpinia* (Zingiberceae) Bing-Nang *et al*., (1997), isolated and characterized several labdane-type diterpenes among which, 11, 15-hemiacetal-11-hydroxy-8(17),12(*E*)-labdadiene-15,16-dial (**106**). Tested on M109 cells from colon cancer, this compound exhibited interesting cytotoxic activity with an IC_{50} of 2.6 μg/mL.

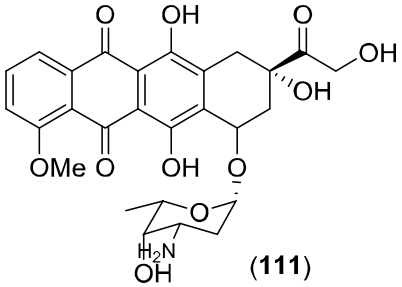

(**111**)

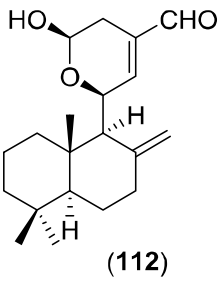

(**112**)

I.7.5.5. Enzyme-inhibiting activity

Roots of *Scoparia dulcis* (Scrophulariaceae), Kawasaki *et al*., (1987) isolated scoparic acid (**113**). This compound exhibited an inhibitory activity of bovine β-glucuronidase with an IC_{50} value of 6.8×10^{-5} μg/mL.

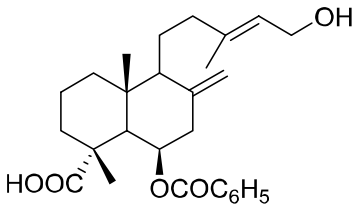

(**113**)

The inhibitory activities of various enzymes as well as the antiviral, anti-tuberculosis, antihypertensive, antiplasmodial, hepatoprotective, etc. properties of many labdane-type diterpenes of natural or synthetic origin have also been highlighted by many researchers (Chinou I., 2005; Hanson, 2007).

These various biological properties of labdane-type diterpenes, which appear moreover to be the predominant class of compound of the species *D. microcarpum*, come to rekindle our interest in the study of this species with a view to isolating other also interesting biomolecules.

CHAPTER II :
RESULTS AND DISCUSSION

II.1. EXTRACTION AND ISOLATION OF COMPOUNDS

The different parts of *Detarium Microcarpum* (Fruits, twigs, stem bark, leaves, root barks and root wood) were harvested in Gamba savanna (Mvina division, Adamaoua region of Cameroon) on March 2017. Air-dried powder of those different part of *D. microcarpum* were extracted by maceration at room temperature (about 25°C) firstly with methanol, on one hand, and with a mixture of ethanol-water (7:3) solvent system (3×10 L) on the other hand, for 48 h. After filtration, the resulting solutions were concentrated under reduced pressure to give crude extracts. The extraction results obtained are shown in the tables below.

Table XI : Methanol extraction results of the different parts of *D. microcarpum*

Organ	**Code**	**Powder mass (g)**	**Extract mass (g)**	**Extraction percentage** (%)
Fruits	DMF	545	340	62.38
Leaves	DML	400	116	29.00
Root barks	DMRb	752	320	42.55
Root wood	DMR	1900	600	31.57

Table XII : ethanol-water extraction results of the different parts of *D. microcarpum*

Serie	**Code**	**Organ**	**Powder mass (g)**	**Extract mass (g)**	**Extract dissolution solvent**	**Extraction percentage** (%)
A	DMA	Seeds	154	25	MeOH	16,23
B	DMB	Fruits	457	279	MeOH	61,05
C	DMC	Branches	185	96	MeOH	51,89
D	DMD	Young leaves	210	49	MeOH-H_2O	23,33
E	DME	Old leaves	501	73	MeOH-H_2O	14,57
F	DMF	Root barks	868	373	MeOH	42,97
G	DMG	Root wood	2400	832	MeOH	34,66

For the methanol extracts, only fruit extract was fractionated using successively *n*-hexane (*n*-hex), dichloromethane (CH_2Cl_2), ethyl acetate (EtOAc) and *n*-butanol (*n*-BuOH) through flash chromatography over silica gel (200 g), to yield five fractions as indicated in table 13 below.

Table XIII : Fractionation results of the methanol extract of fruits.

Organ	Solvent	Fraction code	Fraction mass (g)
Fruits	*n*-hex	DMf1	15
	CH_2Cl_2	DMf2	19
	EtOAc	DMf3	30
	n-Butanol	DMf4	57
	Water	DMf5	210

The *n*-butanol fraction **(DMf4)** (57 g), was subjected to CC over silica gel and eluted with a DCM/MeOH (1:0-0:1) to give **DMf41**, **DMf42** and **DMf43**, respectively. The dichloromethane Fraction **(DMf2)** (19 g), was subjected to CC over silica gel, eluted with a gradient of *n*-hexane/EtOAc and then EtOAc/MeOH to afford **DMf21**. The ethyl acetate fraction **(DMf3)** (30 g) followed the same separation method to yield **DMf31**, **DMf32** and **DMf33**, respectively.

The different ethanol-water extracts were firstly submitted to antisalmonella test and then fractionated using successively *n*-hexane (*n*-hex), dichloromethane (CH_2Cl_2), ethyl acetate (EtOAc), *n*-butanol (*n*-BuOH) and water through flash chromatography over silica gel, to yield five fractions for each part. Thus, after evaporation and lyophilization, 35 crude extracts were obtained. The results of the fractionation are recorded in table 14.

Table XIV : Fractionation results of the different organs of *D. microcarpum*

Organ	Solvant	Fraction code	Fraction mass (g)
Seeds	Hexane	DMA1	4
	CH_2Cl_2	DMA2	5
	AcOEt	DMA3	6
	Water	DMA4	9
Fruits	Hexane	DMB1	15
	CH_2Cl_2	DMB2	17
	AcOEt	DMB3	22
	n-Butanol	DMB4	27
	Water	DMB5	168
Branches	Hexane	DMC1	5
	CH_2Cl_2	DMC2	7
	AcOEt	DMC3	10
	n-Butanol	DMC4	14
	Water	DMC5	30
Young and Old leaves	Hexane	DMDE1	8
	CH_2Cl_2	DMDE2	11
	AcOEt	DMDE3	13
	n-Butanol	DMDE4	18
	Water	DMDE5	52
Root barks	Hexane	DMF1	7
	CH_2Cl_2	DMF2	9
	AcOEt	DMF3	10

	n-Butanol	DMF4	62
	Water	DMF5	275
Root wood	Hexane	DMG1	9
	CH_2Cl_2	DMG2	12
	AcOEt	DMG3	23
	n-Butanol	DMG4	135
	Water	DMG5	637

Fractions from roots wood, roots bark and fruits were subjected to successive column chromatography over silica gel. Twenty compounds were obtained from this study as illustrated in the schemes below (Scheme 8-11).

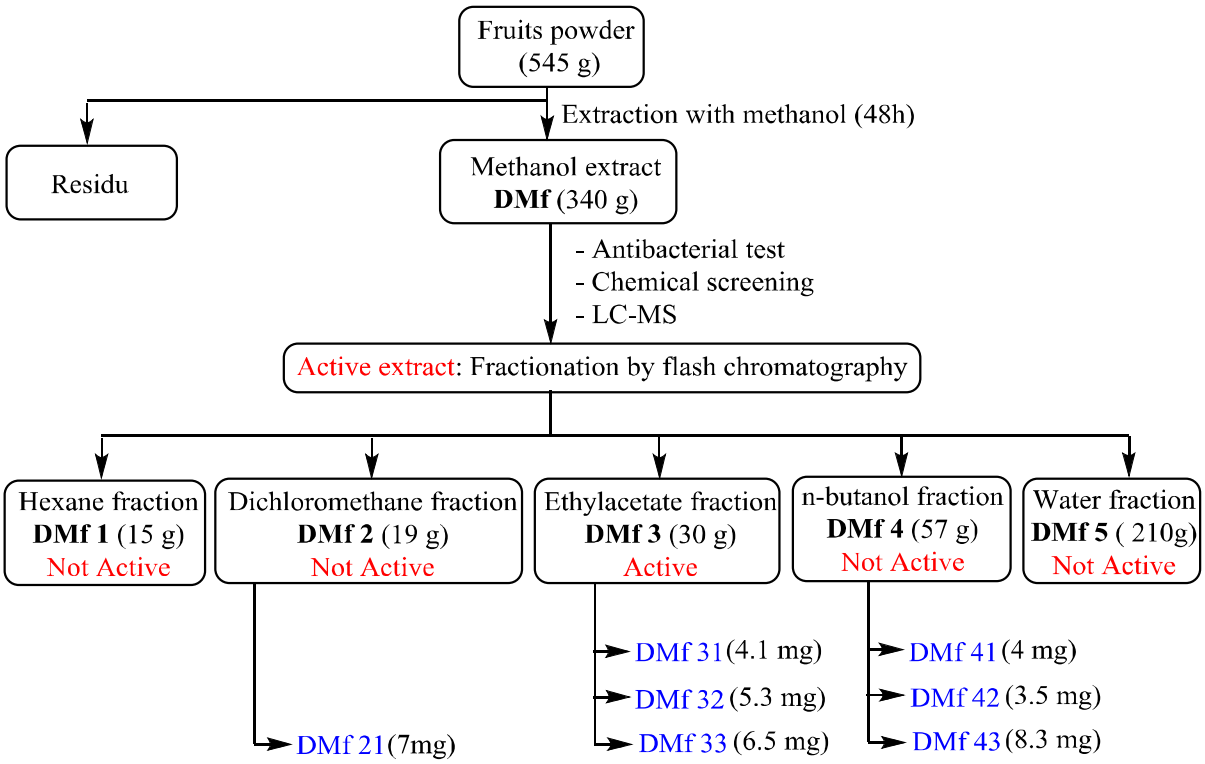

Scheme 8 : Extraction and isolation protocol of fruit methanolic extract of *D. microcarpum*

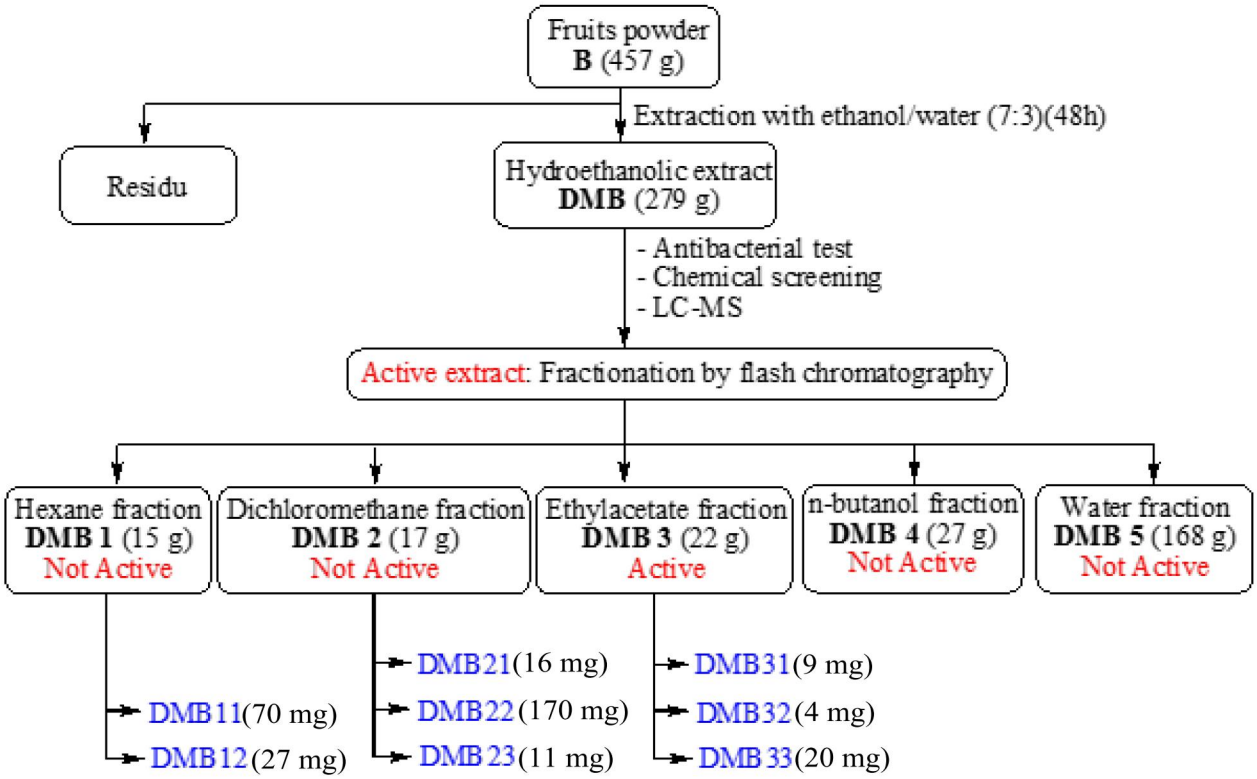

Scheme 9 : Hydro-ethanolic extraction and isolation pathway of compounds from fruits of *D. microcarpum*

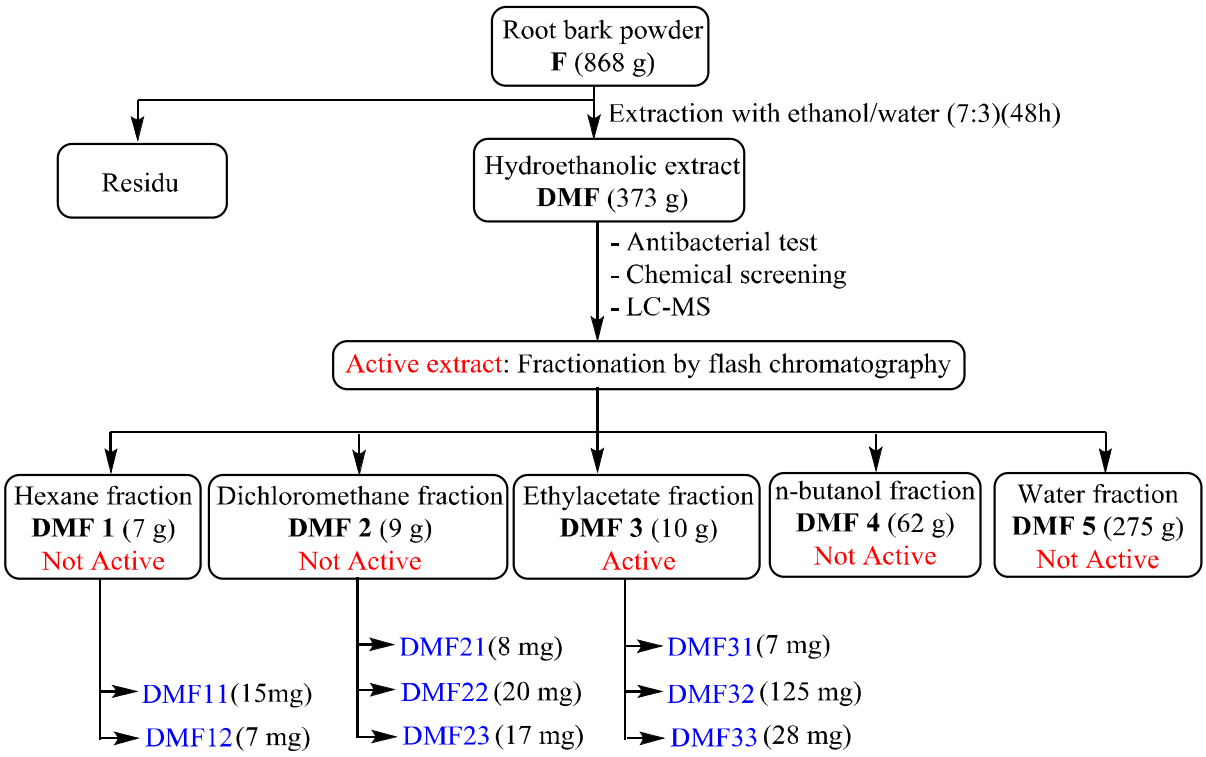

Scheme 10 : Extraction and isolation pathway of compounds from root bark of *D. microcarpum*

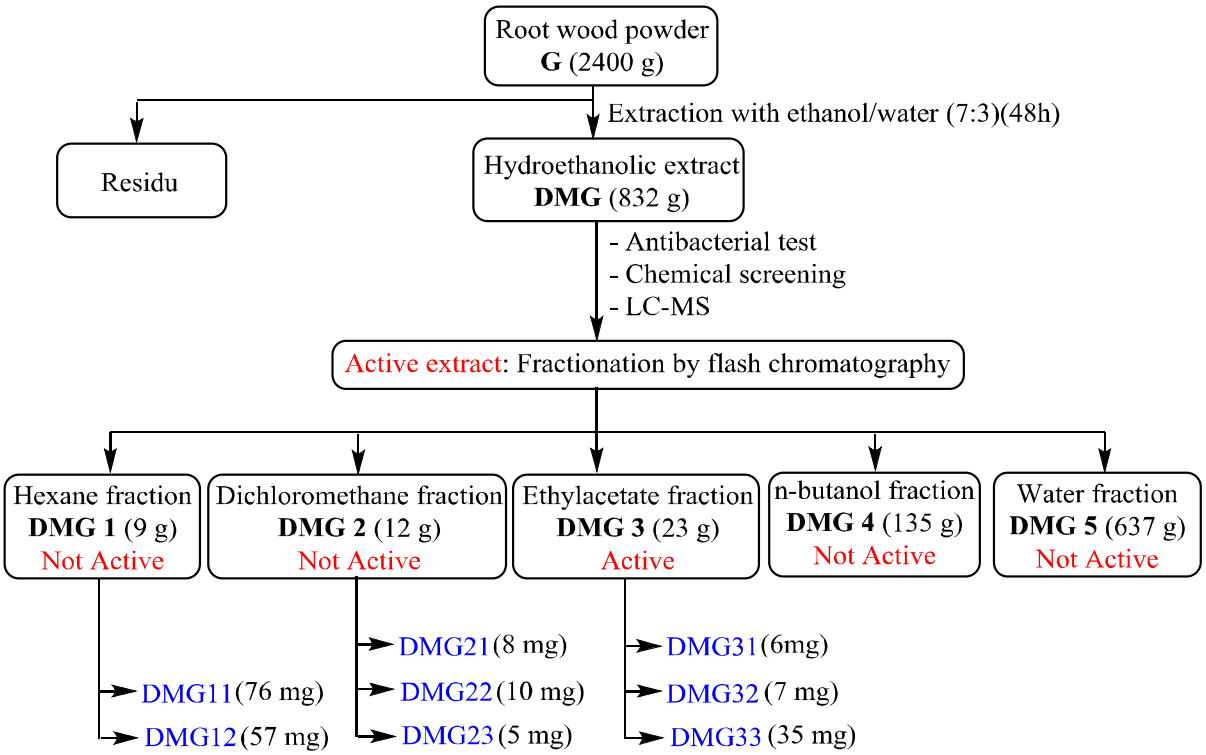

Scheme 11 : Extraction and isolation pathway of compounds from roots wood of *D. microcarpum*

Table XV : Informations on isolated compounds

Solvants	Compounds from fruits				Compounds from roots bark		Compounds from roots wood		Comments
	Methanol extract		Hydroethanolic extract		Hydroethanolic extract		Hydroethanolic extract		
Hex	Codes	Weight (mg)	Codes	Weight (mg)	Codes	Weight (mg)	Codes	Weight (mg)	/
	/	/	DMB11	70	DMF11	15	DMG11	76	DMB11 identical to DMG11
	/	/	DMB12	27	DMF12	7	DMG12	57	DMB12, DMB21 and DMG12 are identical
CH_2Cl_2	DMf21	7	DMB21	16	DMF21	8	DMG21	8	DMF11 identical to DMF21
	/	/	DMB22	170	DMF22	20	DMG22	10	DMB22 identical to DMG22
	/	/	DMB23	11	DMF23	17	DMG23	5	
AcOEt	DMf31	4.1 mg	DMB31	9	DMF31	7	DMG31	6	DMf21, DMF22 and DMF31 are identical

	DMf32	5.3 mg	DMB32	4	DMF32	125	DMG32	7	
	DMf33	6.5 mg	DMB33	20	DMF33	28	DMG33	35	
n-But	DMf41	4 mg	/	/	/	/	/	/	DMB32 and DMf41 are identical
	DMf42	3.5 mg	/	/	/	/	/	/	DMB33 and DMf42 are identical
	DMf43	8.3 mg							

II.2. CHARACTERIZATION OF COMPOUNDS ISOLATED FROM *D. MICROCARPUM* AND CHEMICAL TRANSFORMATIONS.

From what has been mentioned above, a total of eighteen (18) compounds were isolated from the different parts (fruits, roots wood and root bark) of *D. microcarpum* during our investigations. These compounds belong to six classes of secondary metabolites including:

- 01 Cyanogenic derivetive (**DMf43**)
- 01 Ceramide (**DMG31**)
- 03 Diterpenoids (**DMG23, DMB12, DMG22)**
- 05 Triterpenoids (**DMF23**, **DMF31**, **DMF32**, **DMf33** and **DMF41**)
- 05 Steroids (**DMF21, DMf42**, **DMG11, DMB31** and **DMG33**)
- 04 Phenolic compounds (**DMG21**, **DMf31**, **DMf32** and **DMf33**)

The structures of these compounds were elucidated by spectroscopic data analysis. To complete the structure determination of some isolated compounds, chemical transformations including methanolisis and the reduction, and X-rays analysis were carried out. In the following pages, the structural elucidation of all those different compounds will be described.

II.2.1. Characterization and identification of isolated compounds.

II.2.1.1. Cyanogenic derivative

II.2.1.1.1. Structure elucidation of compound DMf43 (Microcarposide)

Compound DMf43 was obtained as a white powder in EtOAc/MeOH (95:05) mixture. It reacts positively both with Molish's and the cyanogenic reagents, suggesting respectively the presence of a sugar and a cyanide moiety in its structure. The molecular formula, $C_{17}H_{29}NO_{10}$, implying 4 degrees of unsaturation, was deduced from its HR-ESI-TOF-MS (Figure 5), which showed in the positive mode, the protonated molecular ion peak $[M+H]^+$ at *m/z* 408.1865 (calcd for $C_{17}H_{30}NO_{10}^+$, 408.1864).

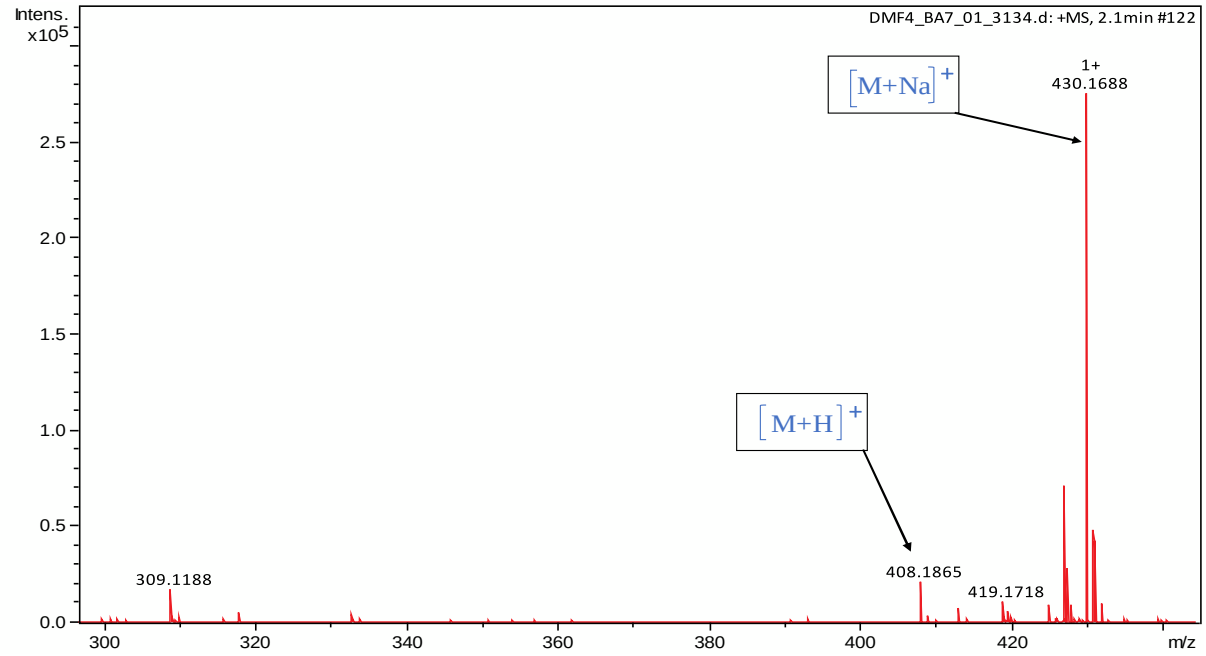

Figure 5 : HR-ESI-MS spectrum of DMf43

The IR spectrum of compound DMf43 (Figure 6) exhibited a vibration band at ῡ 2356 cm^{-1} characteristic of the stretching vibration of cyanide groups. This spectrum also displays characteristic vibration bands of hydroxyl groups and C_{sp3}–H of aliphatic carbons at ῡ 3363 cm^{-1} and ῡ 2920 cm^{-1}, respectively.

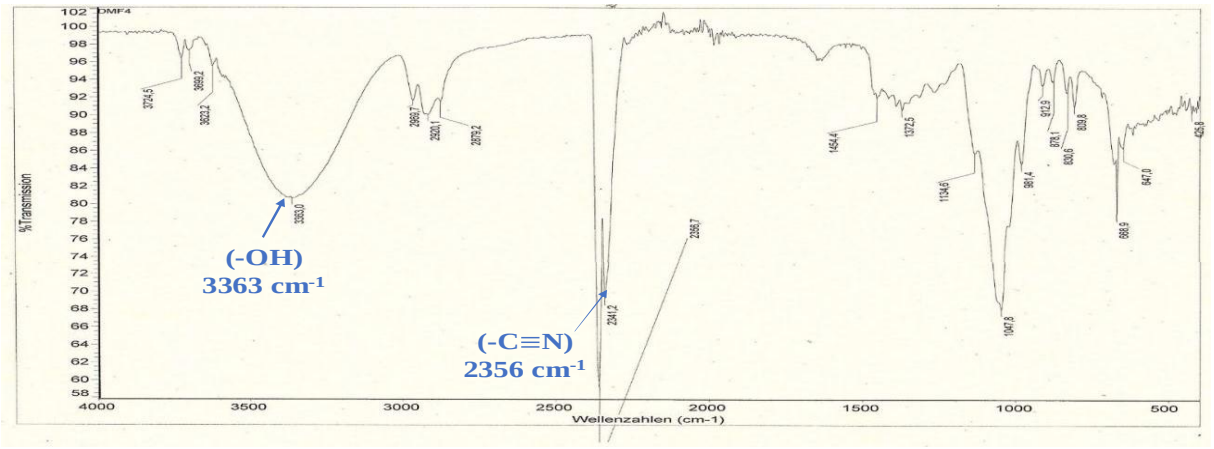

Figure 6 : IR spectrum of DMf43

The broad band proton decoupled ^{13}C NMR spectrum (Figure7, Table 17) shows seventeen signals corresponding to the seventeen carbon atoms contained in the molecular formula. These signals were sorted by DEPT coupled with HMQC (Figure 11) techniques into twelve sp^3 methines among which eleven oxymethines appearing at δ_C 101.9 (C-1′), 101.2 (C-1″), 76.9 (C-5′), 76.1 (C-3′), 73.4 (C-2′), 72.4 (C-4″), 71.9 (C-2), 68.8 (C-3″), 70.9 (C-2″), 70.4 (C-4′), 71.1 (C-5″) and one tertiary methine at δ_C 31.7 (C-3); one sp^3 oxymethylene at δ_C 67.0 (C-6′); three methyles at δ_C 18.4 (C-6″), 18.2 (C-4) and 17.6 (C-5) and a quaternary carbon signal at δ_C 118.1 (C-1) corresponding to carbon of cyanide group.

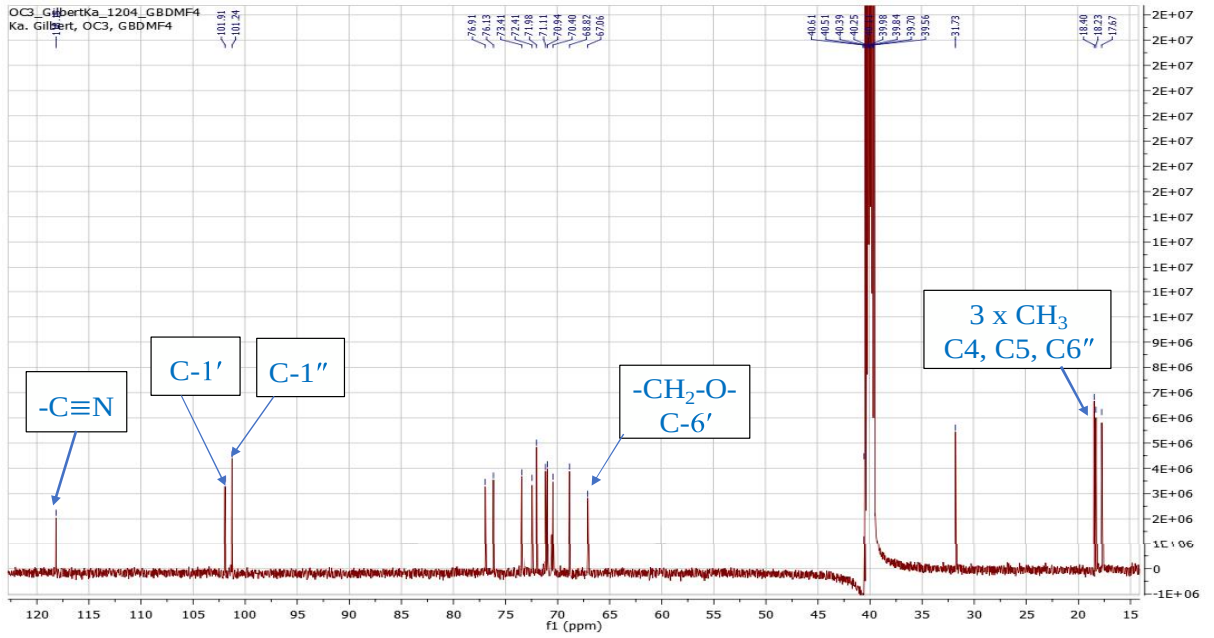

Figure 7 : ^{13}C NMR spectrum (125 MHz, DMSO) of DMf43

The combined analysis of the ^1H NMR (Figure 8; Table 17) and HMQC spectra of DMf43 showed a set of signals at δ_H 4.51 (1H, d, J=5.6 Hz, H-2)/ δ_C 71.9 (C-2), δ_H 2.06 (1H, m, H-3)/

δ_C 31.7 (C-3), δ_H 0.97 (3H, d, *J*=6.8 Hz, H-4)/ δ_C 18.2 (C-4) and δ_H 1.11 (3H, d, *J*=6.7 Hz, H-5)/ δ_C 17.6 (C-5) assignable to an isovaleronitrile aglycone type moiety (C_5H_9NO) (Nielsen et *al*., 2002). The ^{1}H NMR spectrum of DMf43 also exhibited two doublets of one proton each at δ_H 4.34 (1H, d, *J* = 7.8 Hz, H-1′) and δ_H 4.59 (1H, d, *J* = 5.8 Hz, H-1″) which correlated in the HMQC spectrum with the corresponding carbons C-1′ at δ_C 101.9 and C-1″ at δ_C 101.2, indicative of the presence of two sugar moieties. Were also observed in these spectra, two sets of signals. The first set constituted of hydroxy methine and methylene signals at δ_H/ δ_C 4.34 (1H, d, *J* = 7.8 Hz, H-1′)/ 101.9 (C-1′), 2.99 (1H, dd, *J* = 9.9, 6.5 Hz, H-2′)/ 73.4 (C-2′), 3.32 (1H, s, H-3′)/ 76.1 (C-3′), 3.05 (1H, dt, *J* = 8.9, 4.5 Hz, H-4′)/ 70.4 (C-4′), 3.18 (1H, dt, *J* = 12.6, 6.5 Hz, H-5′)/ 76.9 (C-5′), 3.81 (1H, dd, *J* = 11.9, 4.3 Hz, H-6a′)/ 67.0 (C-6′) and 3.46 (1H, dd, *J* = 11.9, 2.2 Hz, H-6b′)/ 67.0 (C-6′) were characteristic of an D-glucopyranosyl moiety (Yu SS *et al*., 1999), whereas the second ~~set~~, including signals at δ_H/ δ_C 4.59 (1H, d, *J* = 5.8 Hz, H-1″)/ 101.2 (C-1″), 3.63 (1H, d, *J* = 9.0, H-2″)/ 70.9 (C-2″), 3.43 (1H, d, *J* = 3.9, H-3″)/ 68.8 (C-3″), 3.20 (1H, d, *J* = 4.2, H-4″)/ 72.4 (C-4″), 3.42 (1H, d, *J* = 3.2, H-5″)/ 71.1 (C-5″) and 1.13 (3H, d, *J* = 6.2, H-6″)/ 18.4 (C-6″) were attributable to an L-rhamnopyranosyl moiety (Yu SS *et al*., 1999; Yu-jie *et al*., 2014). Complete assignment of the protons and carbons of the two sugar units was achieved by the analysis of the COSY, HMQC and HMBC spectra of this compound.

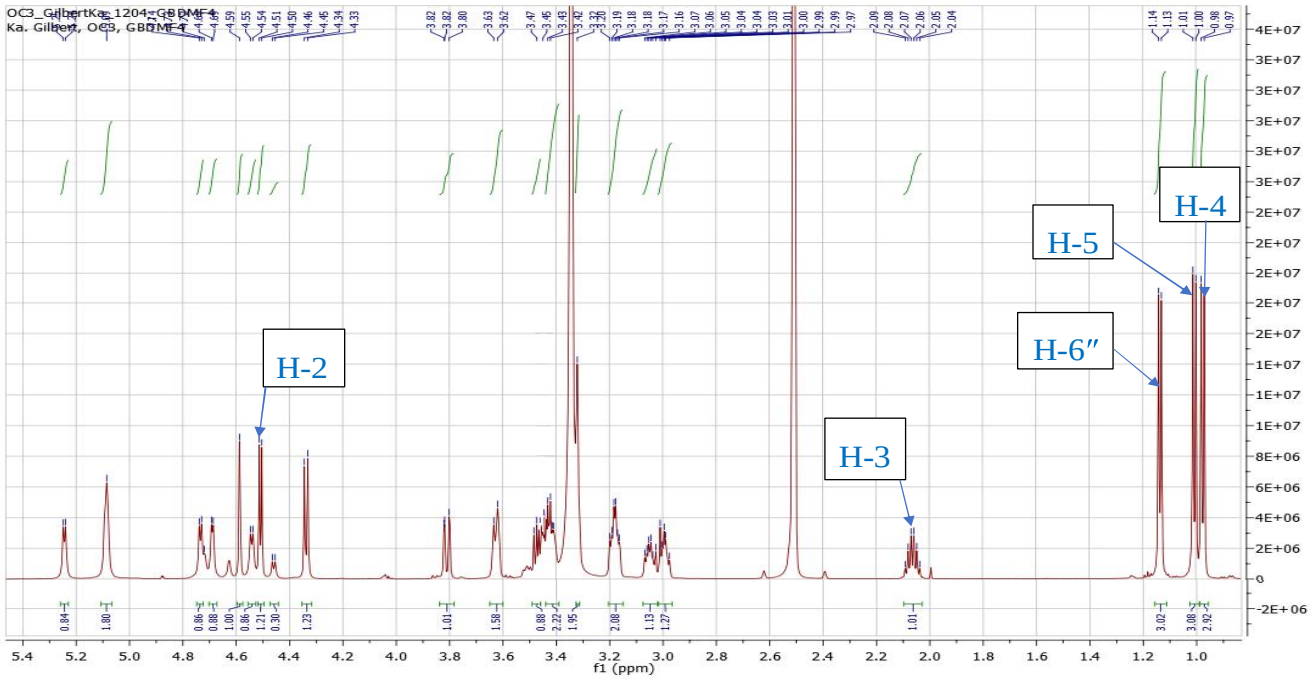

Figure 8 : ^{1}H NMR spectrum (500MHz, DMSO) of DMf43

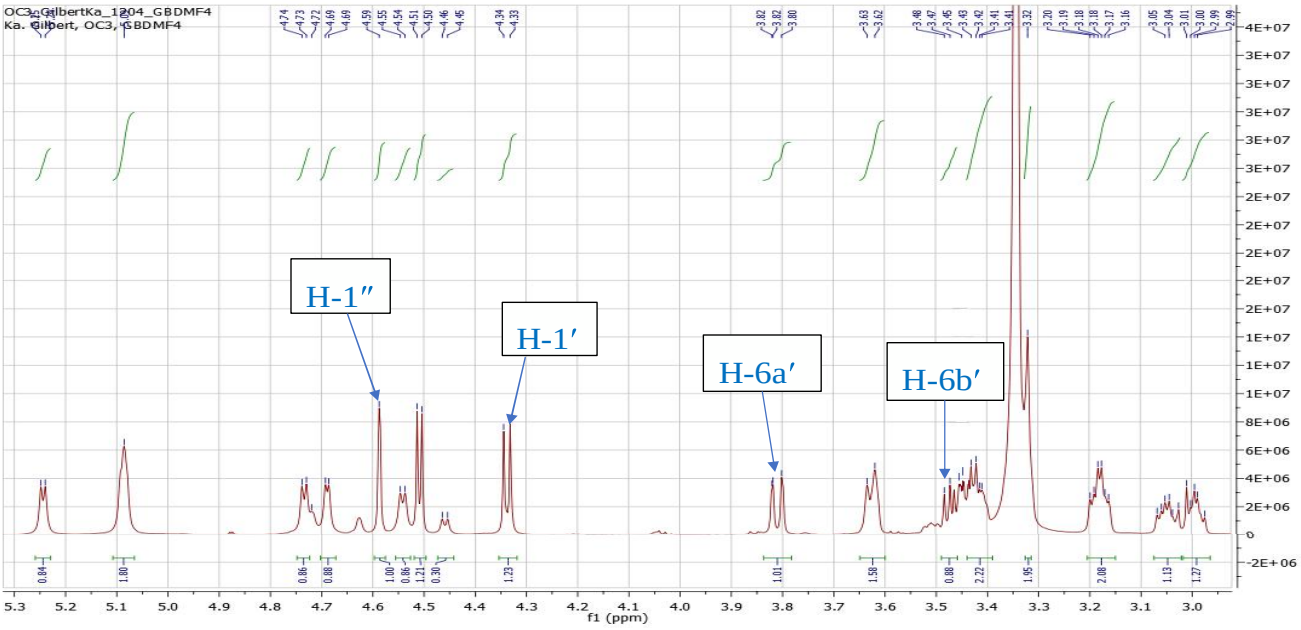

Figure 9 : Extended ^{1}H NMR spectrum (500MHz, DMSO) of DMf43

At this stage of our discussion, it remains to us to determine the linkage between the two sugar moieties and the aglycone unit.

The fragment ion observed at *m/z* 309 (M^+ - 99), in the HR-ESI-TOF-MS of DMf43, corresponding to the loss of the aglycone confirmed that the aglycone was linked to the sugar moieties through an oxygen atom (scheme 12).

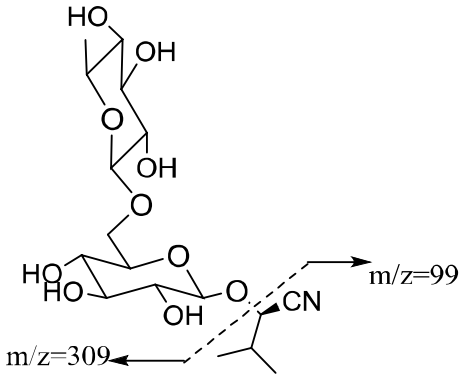

Scheme 12: Mass fragmentation pattern of DMf43

Furthermore, the HMBC (Figure 11) correlations observed between the anomeric proton H-1′ of the D-glucose unit at δ_H 4.34 (1H, d, J = 7.8 Hz) and carbon C-3′ (δ_C 76.1), C-5′ (δ_C 76.9) and C-2 (δ_C 71.9) of the aglycone, clearly confirmed its direct attachment to the aglycone. The HMBC correlations were used once again to establish the linkage between the two sugar units. Indeed, the HMBC cross signals observed on the one hand, between protons H-6′ of the D-glucose moiety at δ_H 3.81 (1H, dd, J = 11.9, 4.3 Hz, H-6a′) and 3.48 (1H, dd, J = 11.9, 2.2 Hz, H-6b′) and the anomeric carbon C-1″ of the L-rhamnose unit at δ_C 101.2, and on the other

hand between the anomeric proton H-1″ of the L-rhamnose unit at δ_H 4.49 (1H, d, *J*=5.8 Hz) and carbon C-6′ (δ_C 67.0) of the D-glucose unit allowed a C-1'-O-C-6' junction between the two sugar units.

The relative stereochemistry of the two anomeric protons was established as β from the ^3J coupling constant values of 5.0 Hz found both between H-1′and H-2′ ($^3J_{H1'-H2'}$=5.0 Hz), and between H-1″ and H-2″ ($^3J_{H1''-H2''}$=5.0 Hz (Yu-jie *et al*., 2014; Yu SS *et al*., 1999).

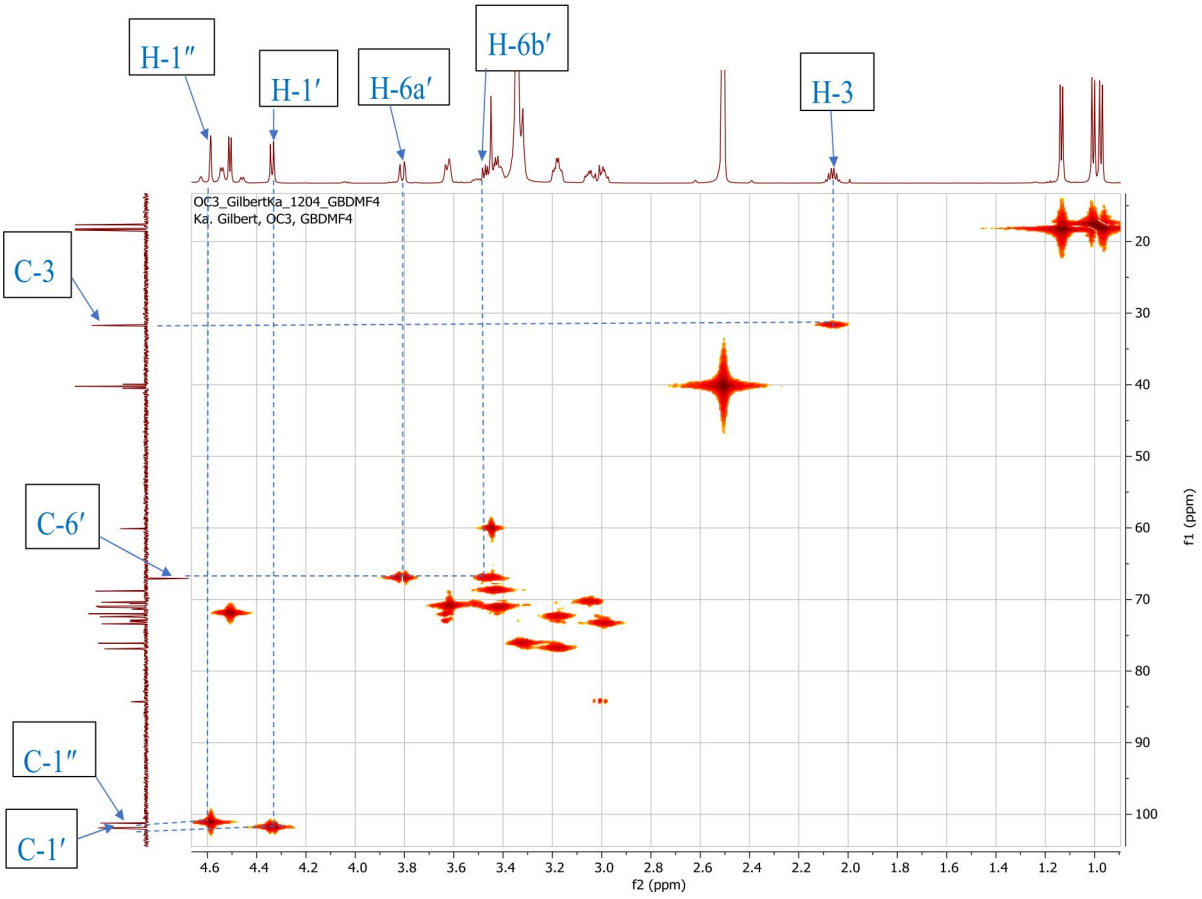

Figure 10 : HMQC spectrum of DMf43

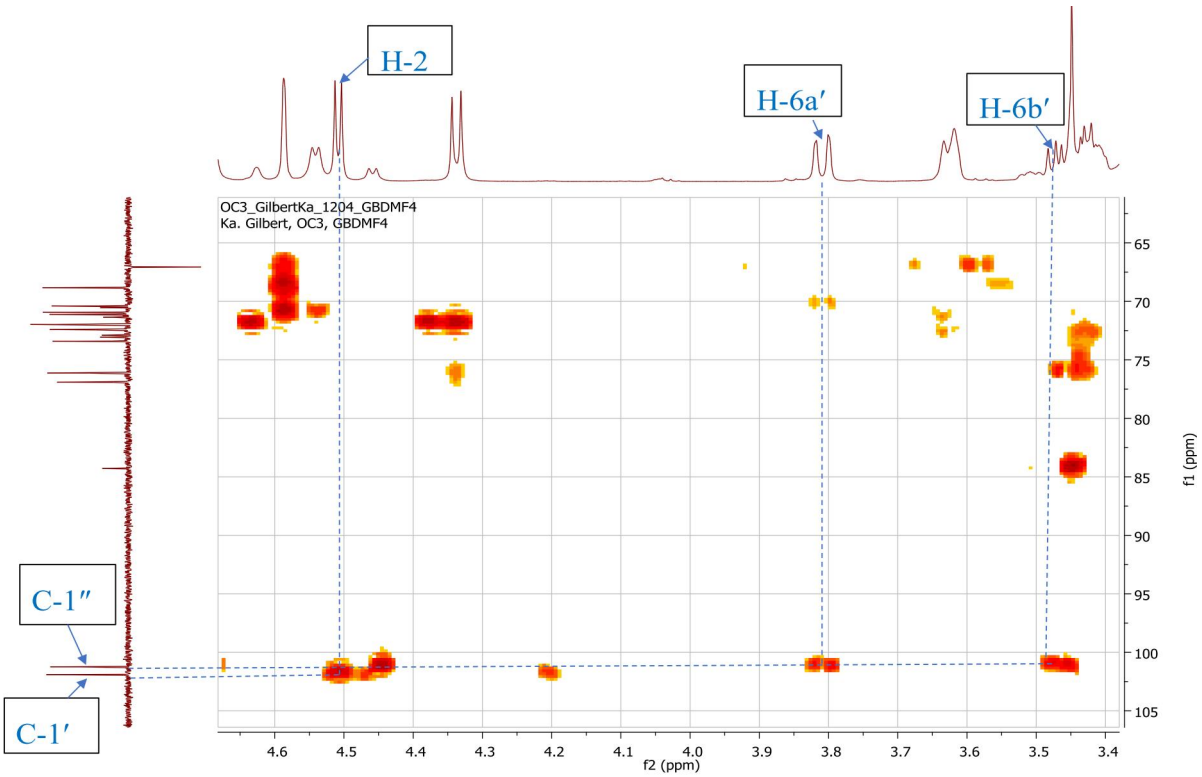

Figure 11 : HMBC spectrum of DMf43

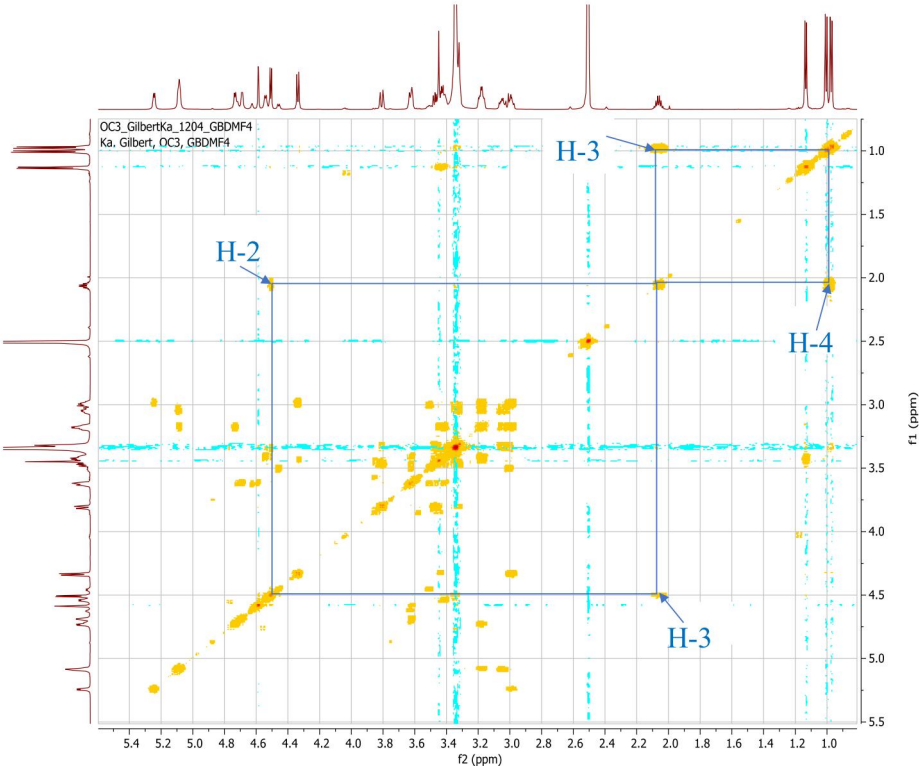

Figure 12 : COSY spectrum of DMf43

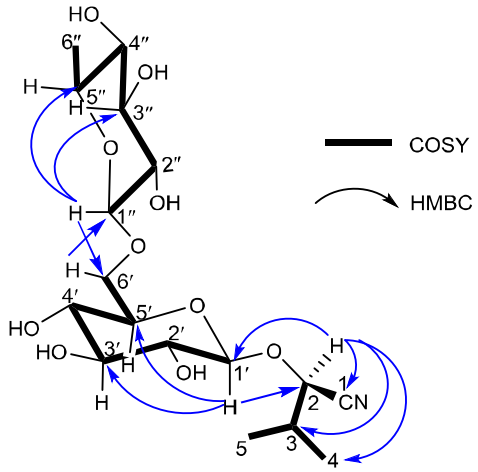

Scheme 12 : Some COSY and HMBC correlations of DMf43

The absolute configuration of the stereogenic center C-2 of the aglycone was established by comparing the chemical shifts and coupling constants of its proton with those of the two closely related epimers heterodendrin and epi-heterodendrin (**Figure S12**) (Lechtenberg et al., 1996). These two compounds are glucosides possessing in their structures the same aglycone part directly link to the same sugar unit as in DMf43.

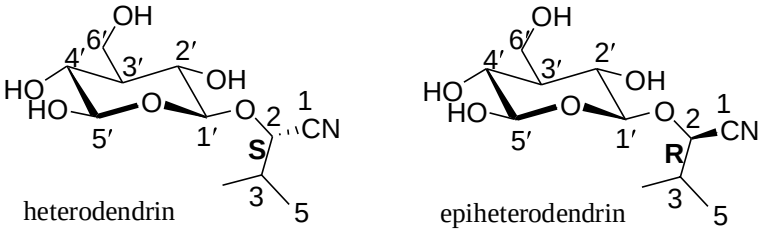

Figure 13 : Absolute configuration of Heterodendrin and Epiheterodendrin

The fact that the ^{1}H NMR data of our compound (Chemical shifts and coupling constant) (Table 15) showed very close similarities with those of epihetrodendrin allowed us to assign the «*R*» configuration to carbon C-2, as in epihetrodendrin epimer (Lankhorst *et al.*, 1995).

Table XVI : Some NMR data for Heterodendrin, Epiheterodendrin (Lankhorst et *al.*, 1995) and Compound DMf43

Position	(*S*)-heterodendrine		(*R*)-epiheterodendrine		Compound **1**	
	δ_H (600 MHz, DMSO-d6)	δc (150 MHz, DMSO-d6)	δ_H (600 MHz, DMSO-d6)	δc (150 MHz, DMSO-d6)	δ_H (500 MHz, DMSO-d6)	δc (125 MHz, DMSO-d6)
1	-	117.8	-	118.6	-	118.1
2	4.74 (*J* = 6.2 Hz)	70.7	4.55 (*J* = 5.4 Hz)	72.6	4.51 (*J* = 5.6 Hz)	71.9
1′	4.32 (*J* = 7.6 Hz)	100.9	4.29 (*J* = 7.7 Hz)	103.4	4.34 (*J* = 7.8Hz)	101.9

Thus, from the above data, compound DMf43, to which trivial name microcarposide was attributed, was assigned as (2*R*)-3-methyl-2-[*β*-L-rhamnopyranoside-1(1→6)-*β*-D-glucopyranosyl] butanenitrile or (2*R*)-2-[*β*-L-rhamnopyranoside-1(1→6)-*β*-D-glucopyranosyl] isovaleronitrile or 6′-*O*-rhamnosyl-(*R*)-epiheterodendrine.

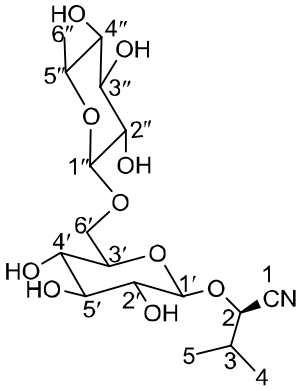

(114)

Table XVII : ^{1}H (500 MHz) and ^{13}C (125 MHz) NMR spectral data and HMBC correlations of DMf43 in DMSO.

Position	δ_H (nH, m, *J* in Hz)	δc (m)	HMBC
1	-	118.1 (s)	
2	4.51 (1H, d, 5.6)	71.9 (d)	$C_{1'}$, C_1, C_3, C_4
3	2.06 (1H, dq, 13.3, 6.7)	31.7 (d)	
4	0.97 (3H, d, 6.8)	18.2 (q)	
5	1.11 (3H, d, 6.7)	17.6 (q)	
1′	4.34 (1H, d, 7.8)	101.9 (d)	C_1
2′	3.63 (1H, d, 9.0)	70.9 (d)	
3′	3.48 (1H, d, 3.9)	68.8 (d)	$C_{1''}$
4′	3.20 (1H, d, 4.2)	72.4 (d)	
5′	3.43 (1H, d, 3.2)	71.1 (d)	
6a′	3.80 (1H, dd, 11.9, 4.3)	67.0 (t)	
6b′	3.82 (1H, dd, 11.9, 2.2)		
1″	4.59 (1H, s)	101.2 (d)	$C_{3'}$
2″	2.99 (1H, dd, 9.9, 6.5)	73.4 (d)	
3″	3.32 (1H, s)	76.1 (d)	
4″	3.05 (1H, dt, 8.9, 4.5)	70,4 (d)	
5″	3.18 (1H, dt, 12.6, 6.5)	76.9 (d)	

6″	1.13 (3H, d, 6.2)	18.4 (q)

II.2.1.2. Ceramide

II.2.1.2.1. Structure elucidation of DMG31 (Microcarpamide)

DMG31 was obtained as colorless crystals in *n*-Hex/EtOAc 9:1, , $[\alpha]_D^{20} + 9$ (*c* 0.17, CH_3OH-CH_2Cl_2), mp 133 °C. Its molecular formula, $C_{44}H_{89}NO_5$, containing one degree of unsaturation, was deduced from the analysis of NMR data and HRESIMS (Figure 14) which showed the pseudo-molecular ion peak $[M+H]^+$ at *m/z* 712.6819 (calcd 712.6819 for $C_{44}H_{90}NO_5^+$). The IR spectrum (Figure 15) exhibited vibration bands for hydroxyl groups at ῡ 3333-3208 cm^{-1} and for a secondary amide carbonyl group at ῡ 1633 and 1512 cm^{-1}.

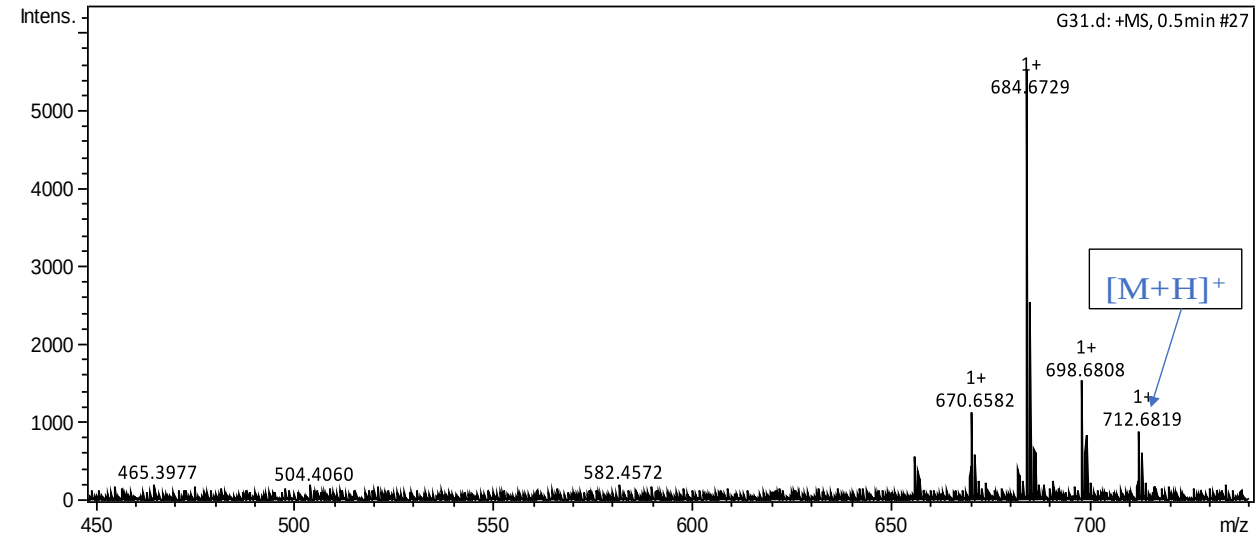

Figure 14 : HR-ESI-MS spectrum of DMG31

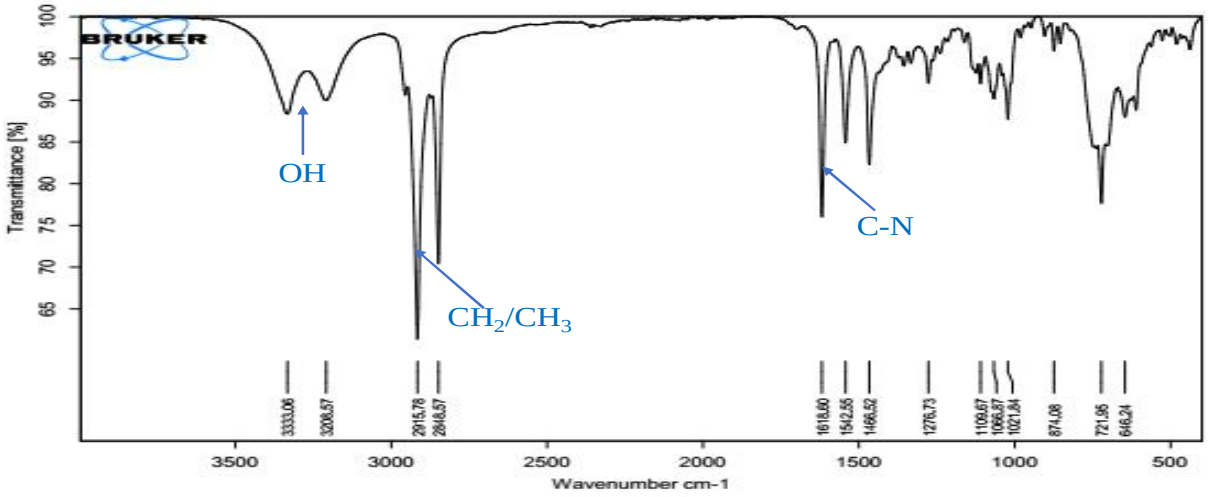

Figure 15 : IR spectrum of DMG31

The ^{1}H NMR spectrum (Figure 16; Table 19) of DMG31 revealed the presence of characteristic signals for a secondary *amide* proton at δ_H 8.73 (1H, d, J = 9 Hz) and a downfield H-2 azomethine proton of ceramide at δ_H 5.16 (1H, m, H-2) (Simo et *al*., 2008). This spectrum also displayed resonances for three oxymetine protons at δ_H 4.79 (1H, m; H-4), 4.37 (1H, m; H-3) and 4.30 (1H, t, J=6.5, H-2′), an oxygenated methylene at δ_H 4.50 (1 H, dd, J = 4.8, 10.8 Hz, H-1b) and 4.45 (1H, dd, J = 4.9, 10.8 Hz, H-1a), a very strong aliphatic methylene signal appearing as broad singlet at δ_H 1.25-1.38 and two terminal methyl groups at δ_H 0.86 (3H, d, J = 5.6 Hz, H-18′) and 0.84 (3H, d, J = 5.6 Hz, H-26) indicating of the ceramide nature of DMG31 (Bankeu et *al*. 2017, Garg et *al*., 1995).

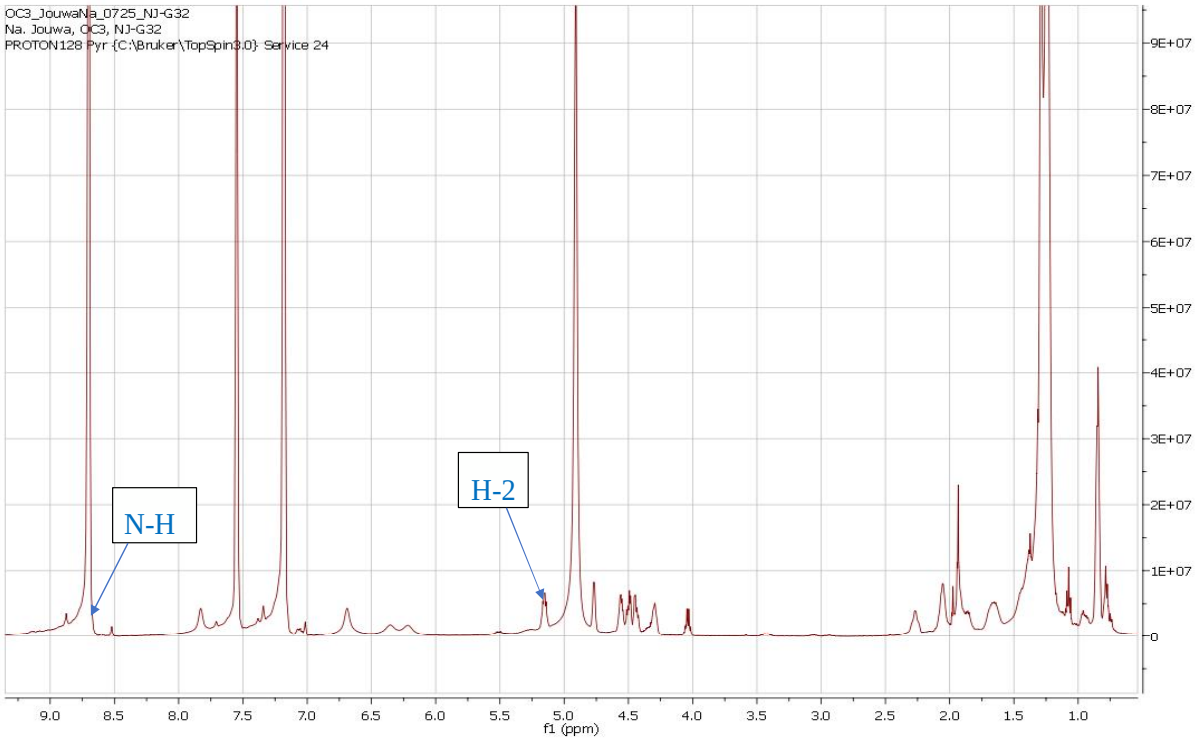

Figure 16 : ^{1}H NMR spectrum (500 MHz, C_5D_5N) of DMG31

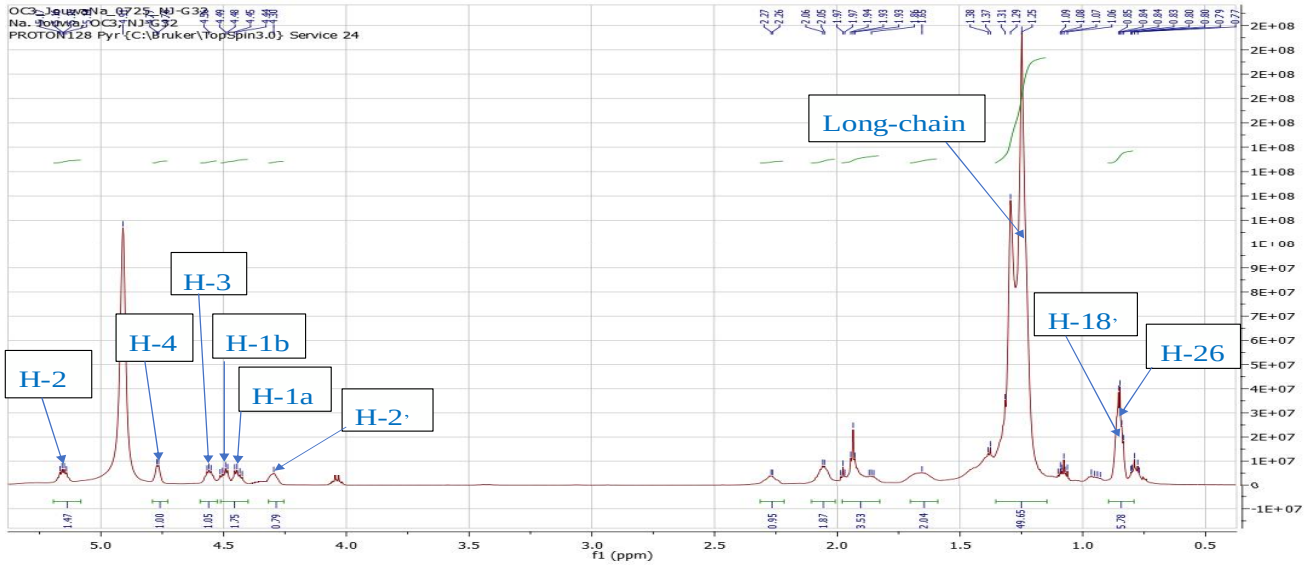

Figure 17 : Extended ^{1}H NMR spectrum (500 MHz, C5D5N) of DMG31

The broadband proton decoupled ^{13}C NMR spectrum of DMG31 (Figure 18; Table 19) analyzed with the aid of APT technic supported the above assumption, showing carbon resonances for an amide carbonyl at δ_C 173.6 (C-1′), an azomethine at δ_C 52.8 (C-2), an oxymethylene at δ_C 61.6 (C-1), three oxymethines at δ_C 76.4 (C-3), 73.4 (C-4) and 72.2 (C-2′), aliphatic methylenes at δ_C 22.0-34.0 and two methyl carbons appearing at δ_C 14.0 (C-26 and C-18') (Naheed *et al.*, 2007).

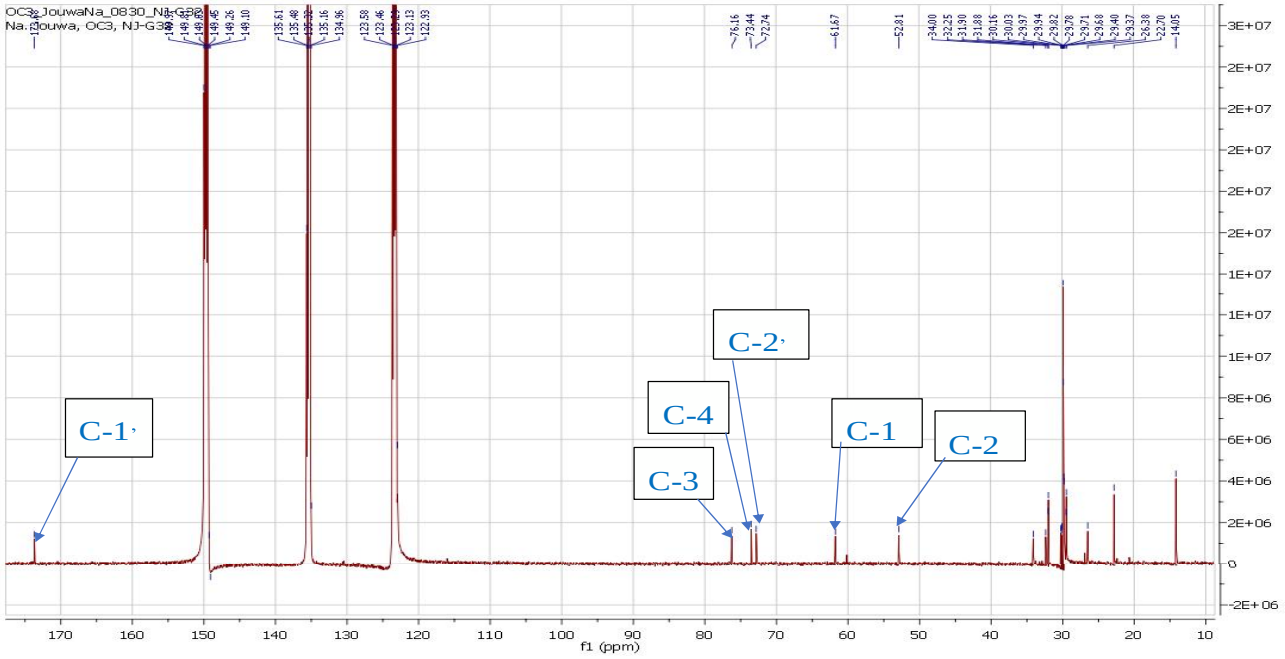

Figure 18 : ^{13}C NMR spectrum (125 MHz, C5D5N) of DMG31

Analysis of the ^{1}H-^{1}H COSY, HMQC and HMBC spectra (Figures 22, 25 and 26) led to the assignments of proton and carbon resonances. The COSY spectrum displayed correlations between the oxymethylene protons at δ_H 4.50 (1 H, dd, J = 4.8, 10.8 Hz, H-1b) and 4.45 (1H, dd, J = 4.9, 10.8 Hz, H-1a) and the azomethine at δ_H 5.16 (1H, m, H-2) which in turn correlated with the oxymethine proton at δ_H 4.37 (1H, m; H-3) and the amide proton at δ_H 8.73 (1H, d, J = 9 Hz, N-H). Were also observed, the presence of hydroxy methine protons H-3 (δ_H 4.37) and H-4 (δ_H 4.79), suggesting the presence of hydroxyl groups at C-1, C-3 and C-4, which was further confirmed by the HMBC spectrum where correlations between the oxymethylene protons H-1 (δ_H 4.45, H-1a and δ_H 4.50, H-1b) and the azomethine carbon C-2 (δ_C 52.8) were observed; in turn, carbon C-2 (δ_C 52.8) was observed by the amide proton N-H (δ_H 8.73) and by the oxymethine proton H-3 (δ_H 4.37). This spectrum exhibited also correlation between proton H-4 (δ_H 4.79) and carbon C-3 (δ_C 76.4). The location of a hydroxy group at C-2′ was supported by the coupling observed on the COSY spectrum between the oxymethine proton H-2′ (δ_H 4.30) and protons H-3′ [δ_H 1.94 (1H, t, 5.0) and 2.27 (1H, td, 11.8, 4.6)]. The HMBC spectrum also showed correlations between both the amide proton N-H (δ_H 8.73) and the oxymethine proton H-2′ (δ_H 4.30) with amide carbonyl carbon C-1′ at δ_C 173.6. These correlations also indicated the presence of a -NH-COCH(OH)CH_2- moiety in DMG31 which in turn confirmed the presence of sphingosine and fatty acid chains in this compound.

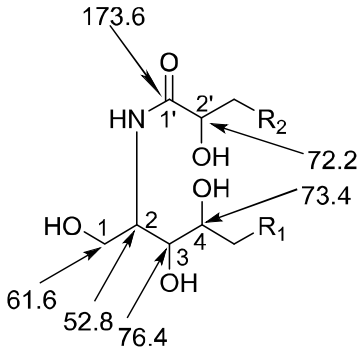

In order to determine the lengths of the sphingosine and fatty acid chains and the absolute configuration of DMG31, the acid methanolysis method of Graver and Sweeley was applied (Su et *al*., 2002).

When DMG31 was methanolysed, this reaction yield to fatty acid methyl ester (FAME) and to long-chain base (LCB) (Scheme 13).

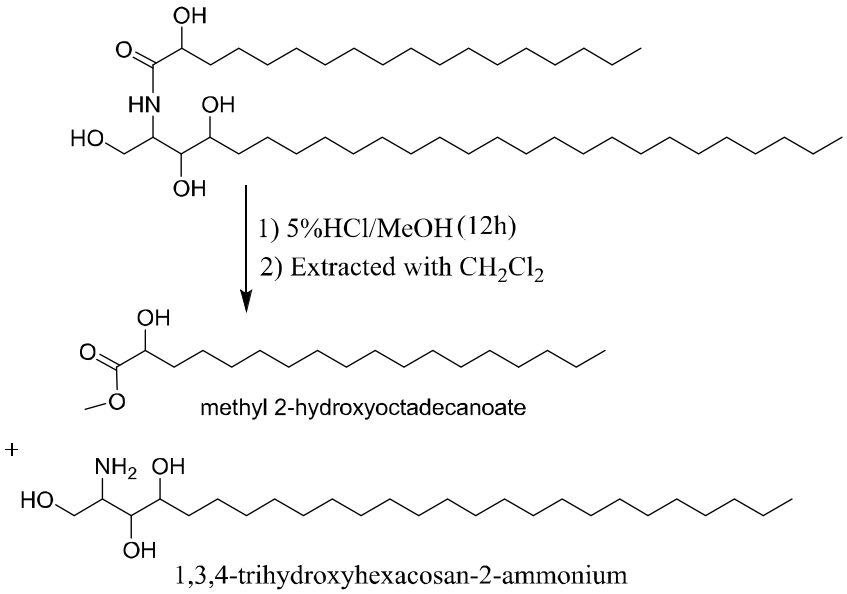

Scheme 13 : Methanolysis and organic extraction of DMG31

The LCB was found to be constituted of twenty-six carbon atoms from its HRESIMS (Figure 19) which exhibited the ion peak at m/z 430.6860 (calcd 712.6819 for $C_{44}H_{90}NO_5$) for $[HOCH_2CH(NH_3)(CHOH)_2(CH_2)_{21}CH_3]^+$ ($C_{26}H_{56}O_3N$) corresponding to 1,3,4-trihydroxyhexacosane-2-ammonium. On the basis of this evidence and in accordance with the molecular formula and NMR data of DMG31, the FAME was deduced as containing nineteen carbon atoms with carbonyl and hydroxyl groups, notably as methyl 2-hydroxyoctadecanoate.

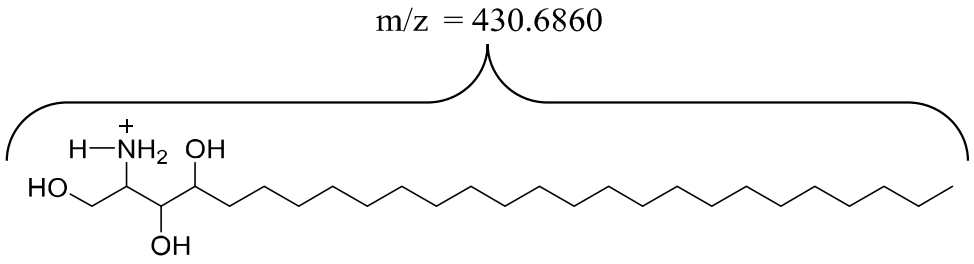

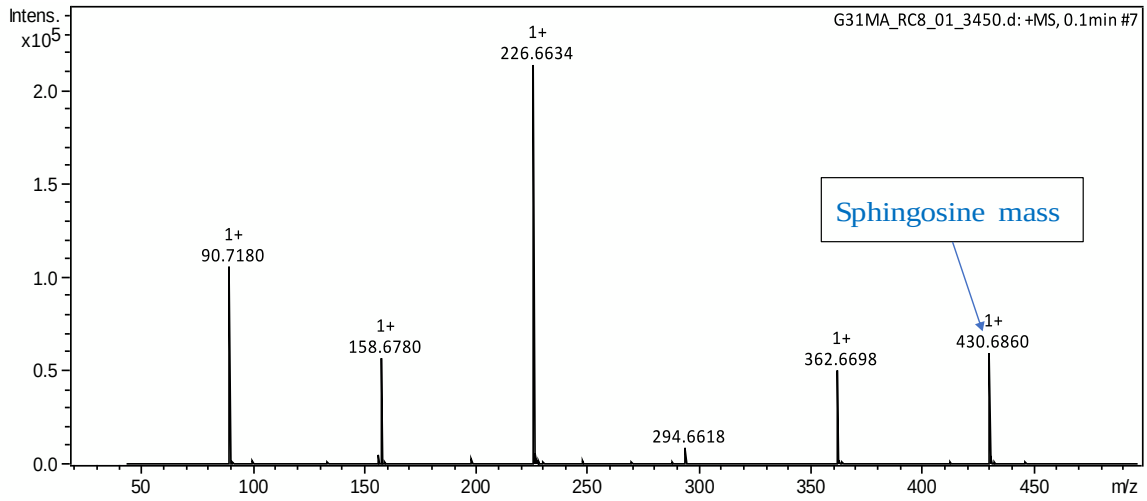

Figure 19 : HR-ESI-MS spectrum of organic phase

Thus, the structure of DMG31 was determined as *N*-(2′-hydroxyoctadecanoyl)-2-amino-hexacosane-1,3,4-triol.

This compound possesses four stereogenic carbons at C-2, C-3, C-4 and C-2′. The relative stereochemistry around these stereogenic centers, was established by comparison their ^{13}C NMR data, with those of a similar molecule in the literature. In particular, the ^{13}C NMR chemical shifts of C-2 (δ_C 52.8), C-3 (δ_C 76.4), C-4 (δ_C 73.4) and C-2′ (δ_C 72.2) in DMG31, were very close to those of a similar reported compound (2*S*, 2′*R*, 3*S*, 4*R*, 11*E*)-*N*-(2′-hydroxyhenicosanoyl)-2-aminononadec-11-ene-1,3,4-triol, which showed values of δ_C 53.0 (C-2) , 76.8 (C-3), 73.1 (C-4) and 72.5 (C-2') (**1a**) (Figure18) (Dos Santos *et al*., 2012). The fact that the optical rotation value ($[\alpha]_D^{20}$ = +10 (*c* = 0.2, CH_3OH)) of **1a**, was found to be close (in term of sign and value) with that of compound DMG31 ($[\alpha]^{20}_D$ = +9 (*c* = 0.17, CH_3OH-CH_2Cl_2)), suggested that in our compound, the stereochemistry around the stereo genic carbons C-2, C-3, C-4 and C-2' is the same (2*S*, 3*S*, 4R and 2′R respectively) as in compound **1a**. Hence, the structure of compound DMG31 was assigned as (2S, 2′R, 3S, 4R)-N-(2′-hydroxyoctadecanoyl)-2-amino-hexacosane-1,3,4-triol, trivially named microcarpamide.

Table XVIII: ^{13}C NMR spectral data (δ_C in ppm) of compound DMG31 and a natural ceramide (Dos Santos *et al*., 2012) 1a **in pyridin-d$_5$.**

Position	DMG31	1a
C-2	52.8	53.0
C-3	76.4	76.8
C-4	73.4	73.0
C-2′	72.2	72.5

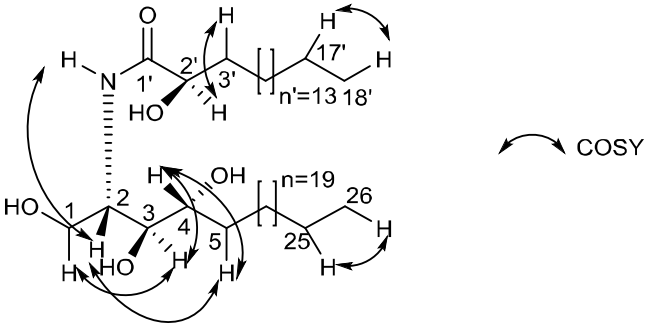

Scheme 14 : Important COSY connectivity in DMG31

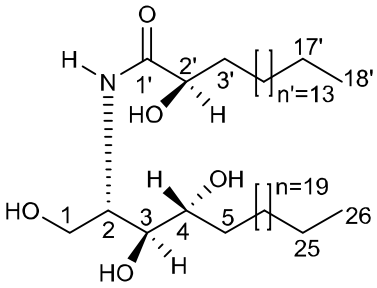

microcarpamide (115)

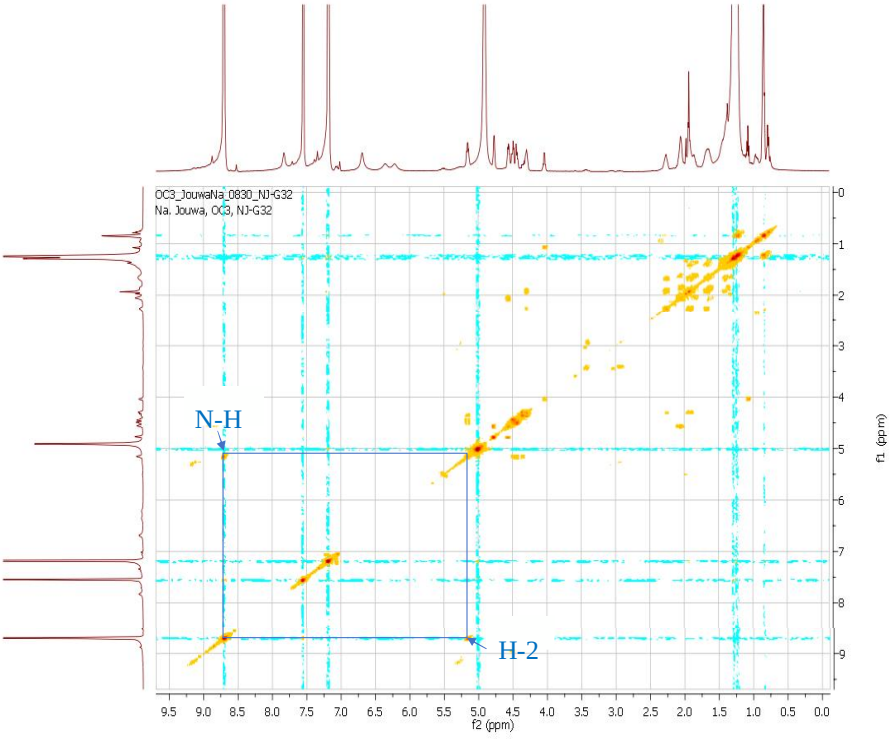

Figure 20 : COSY spectrum of DMG31

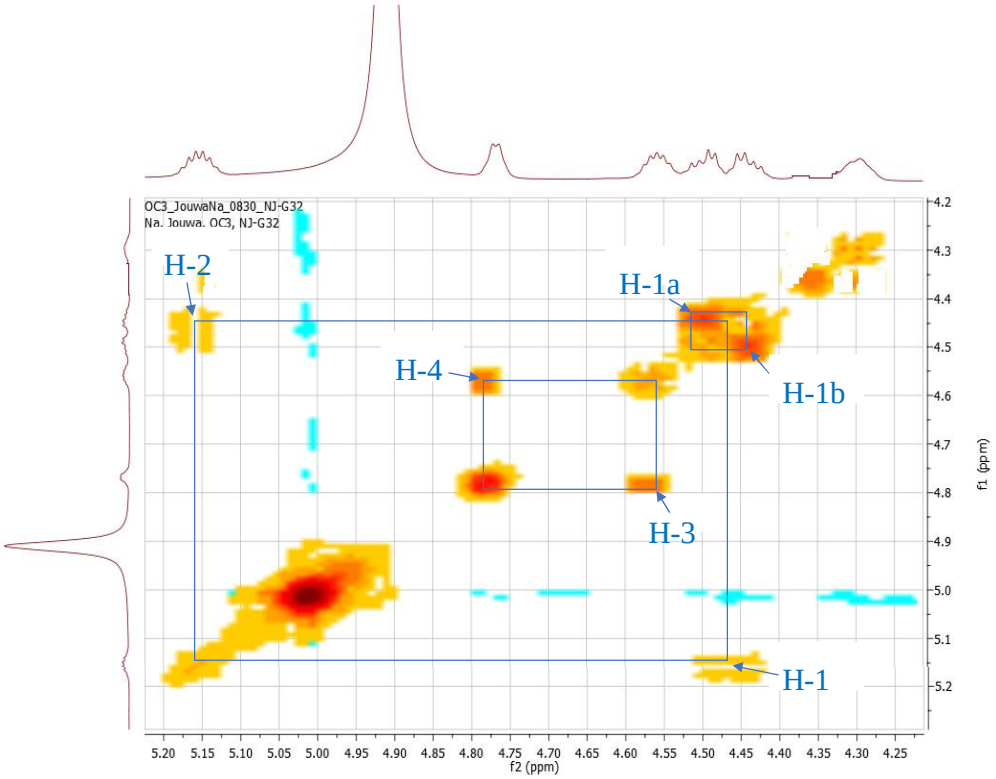

Figure 21 : Extended COSY spectrum of DMG31

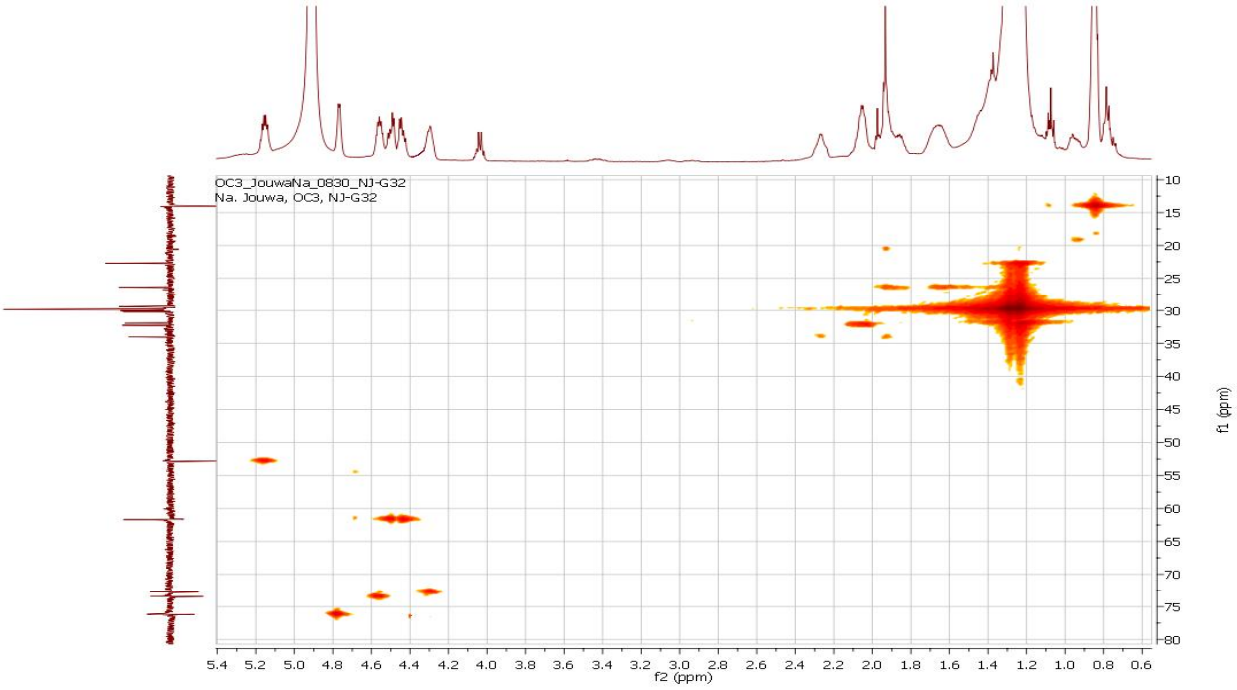

Figure 22 : HMQC spectrum of DMG31

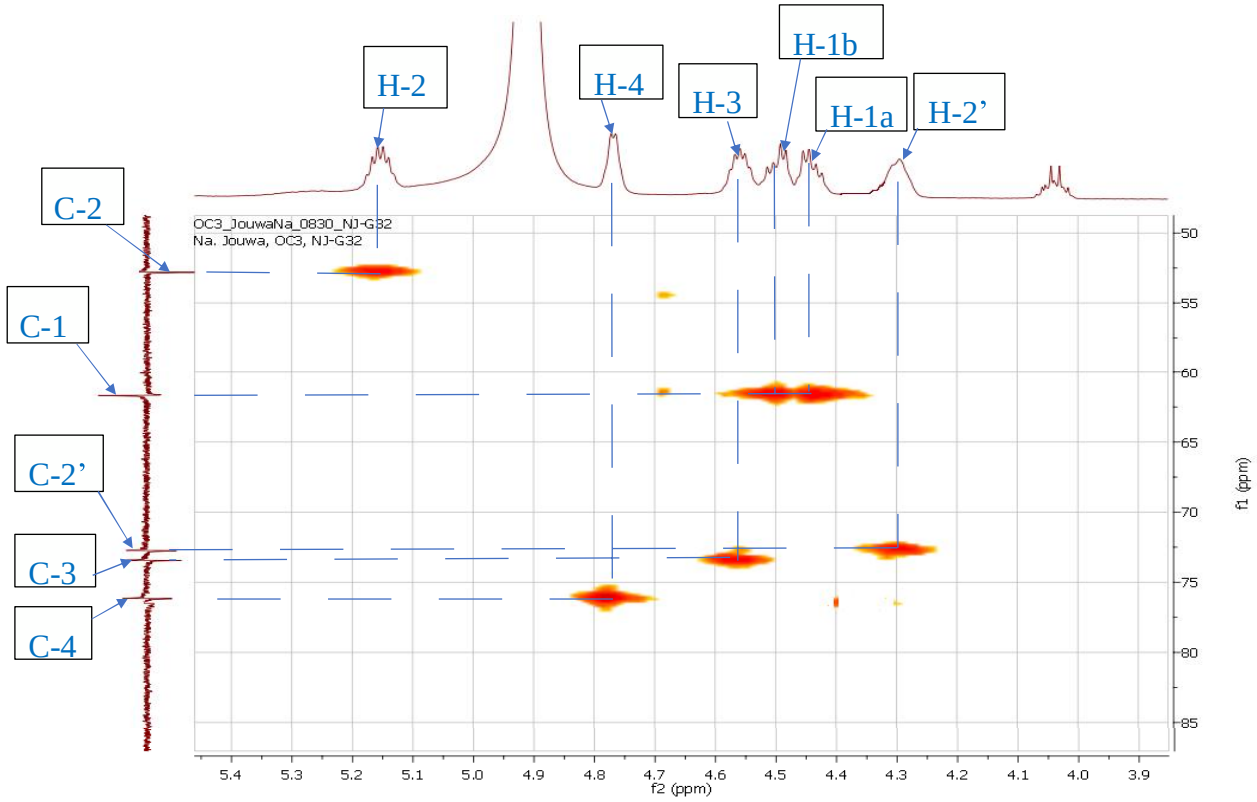

Figure 23 : Extended HMQC spectrum of DMG31

Table XIX : ^{1}H (500 MHz) and ^{13}C (125 MHz) NMR spectroscopic data of DMG31 in pyridin-d_5.

Position	δ_H ; m ; *J* in Hz	δ_C *(ppm)*
1a 1b	4.45 ; dd, *J*=10.8, 4.9 4.50 ; dd, *J*=10.8, 4.8	61.2
2	5.13-5.20 ; m	52.8
3	4.79 ; m	76.4
4	4.56 ; m	73.4
5a 5b	1.94 ; t, *J*= 5.0 2.27 ; td, *J*= 11.8, 4.6	34.0
6	1.82-1.89 ; m	26.4
7-24	1.18-1.27 ; m	26.3-34.0
25	1.36-1.42 ; m	22.7
26	0.84 ; t, *J*=5.6	14.0
1′	-	173.6
2′	4.30 ; d, 5.5,	72.2
3a′ 3b′	1.94 ; t, *J*= 5.0 2.27 ; td, J= 11.8, 4.6	34.0

4a′ 4b′	1.60-1.72 ; m 1.82-1.89 ; m	30.1
5′-16′	1.27-1.32	29.3-30.0
17′	1.43-1.48 ; m	22.7
18′	0.86 ; t, *J*=5.6	14.0
NH	8.73 ; d, *J*=8.8	-

II.2.1.3. Diterpenoids.

II.2.1.3.1. Structure elucidation of DMG23 (Microcarpin).

Compound DMG23 was obtained as a white powder from the mixture of *n*-Hex/EtOAc (15:7) with $[\alpha]_D^{20}$ = + 20.5 (*c* =1.00, $CHCl_3$/MeOH). Its molecular formula, $C_{16}H_{30}O_3$ implying two degrees of unsaturation was deduced from HRESIMS (Figure 24**)** which displays in negative mode, the chloride adduct ion peak $[M+Cl]^-$ at *m/z* 305.1901 (calcd for $C_{16}H_{30}O_3Cl^-$, 305.1889).

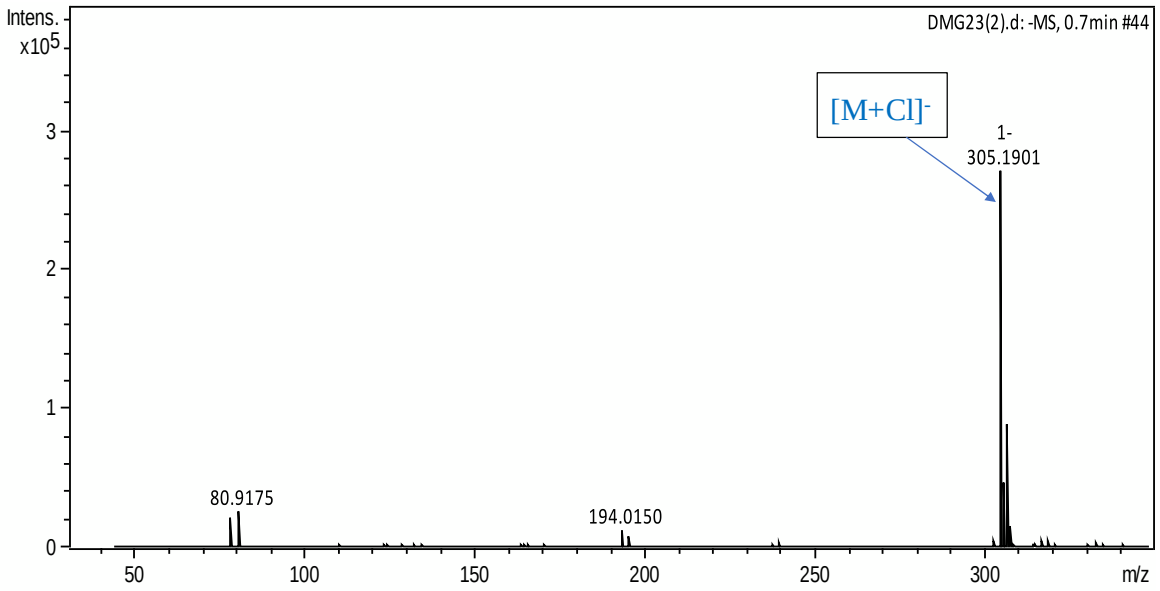

Figure 24 : HR-ESI-MS spectrum of DMG23

In accordance with this molecular formula, 16 carbon signals were observed in the ^{13}C broad band proton decoupled spectrum of this compound (Figures 25). These signals were sorted by DEPT 135 (Figures 26) and HMQC (Figures 27) techniques as four methyls at δ_C 16.4, 17.7, 18.4 and 21.8; six sp^3 methylenes of which one oxymethylene at δ_C 57.7, the five others appearing at δ_C 17.4, 27.1, 31.4, 32.9, 42.4; three sp^3 methines among with one oxymethine at δ_C 76.2, the two other being at δ_C 37.4 and 41.8. From the above information, it

was deduced that compound DMG23 possesses three quaternary sp^3 carbons, among which one oxygenated at δ_C 75.8 and the two remaining others at δ_C 38.8 and 42.0. Furthermore, the absence in the ^{13}C NMR data of unsaturated carbon led to the conclusion that the two degrees of unsaturation, calculated from the molecular formula are due to the presence in the structure of compound DMG23 of two rings. The bicyclic nature, in conjunction with the molecular formula $C_{16}H_{30}O_3$, suggested that compound DMG23 is a labdane type diterpene presumably a tetranorlabdane, possessing in its structure a decalin skeleton. (Hasnah et *al*., 1993 ; Arun et *al*., 1988)

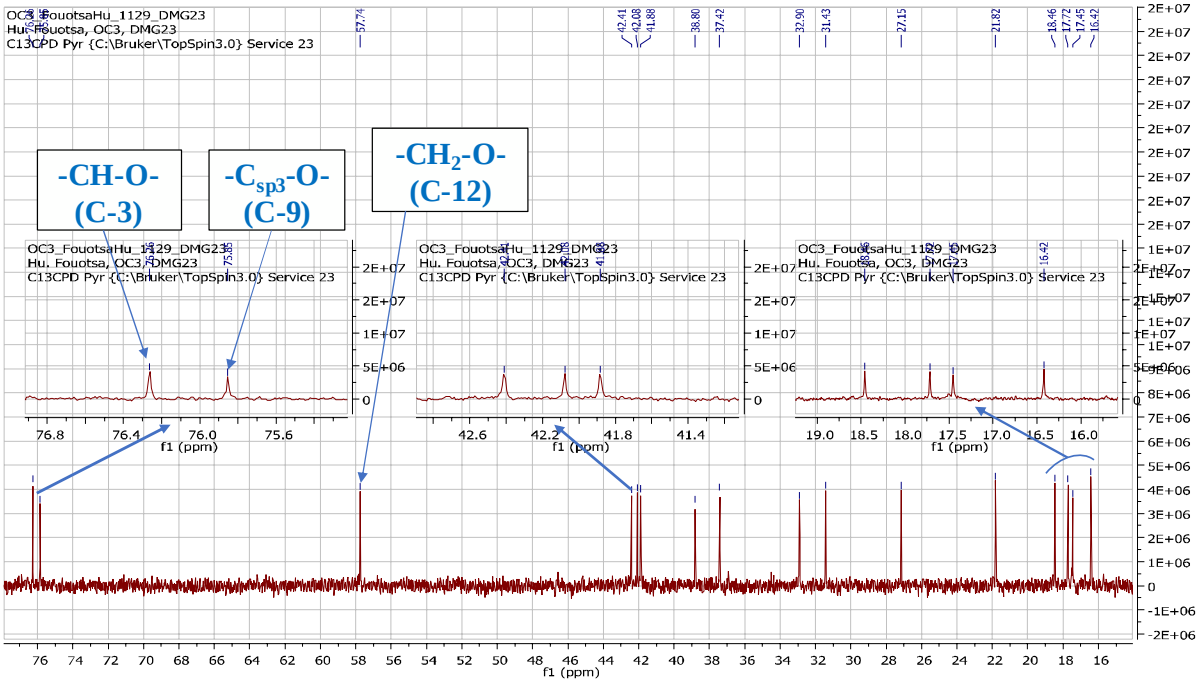

Figure 25 : ^{13}C NMR spectrum (125 MHz, C_5D_5N) of DMG23

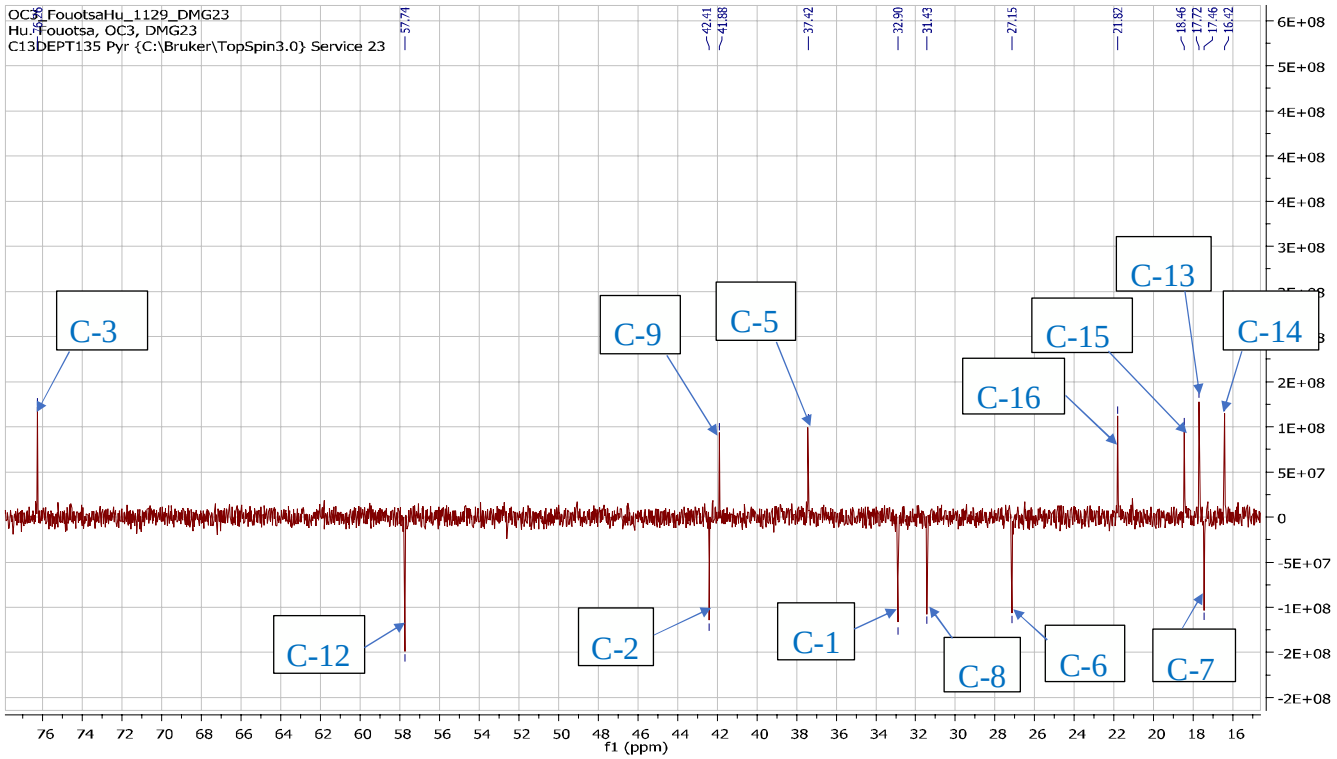

Figure 26 : DEPT 135 spectrum of DMG23

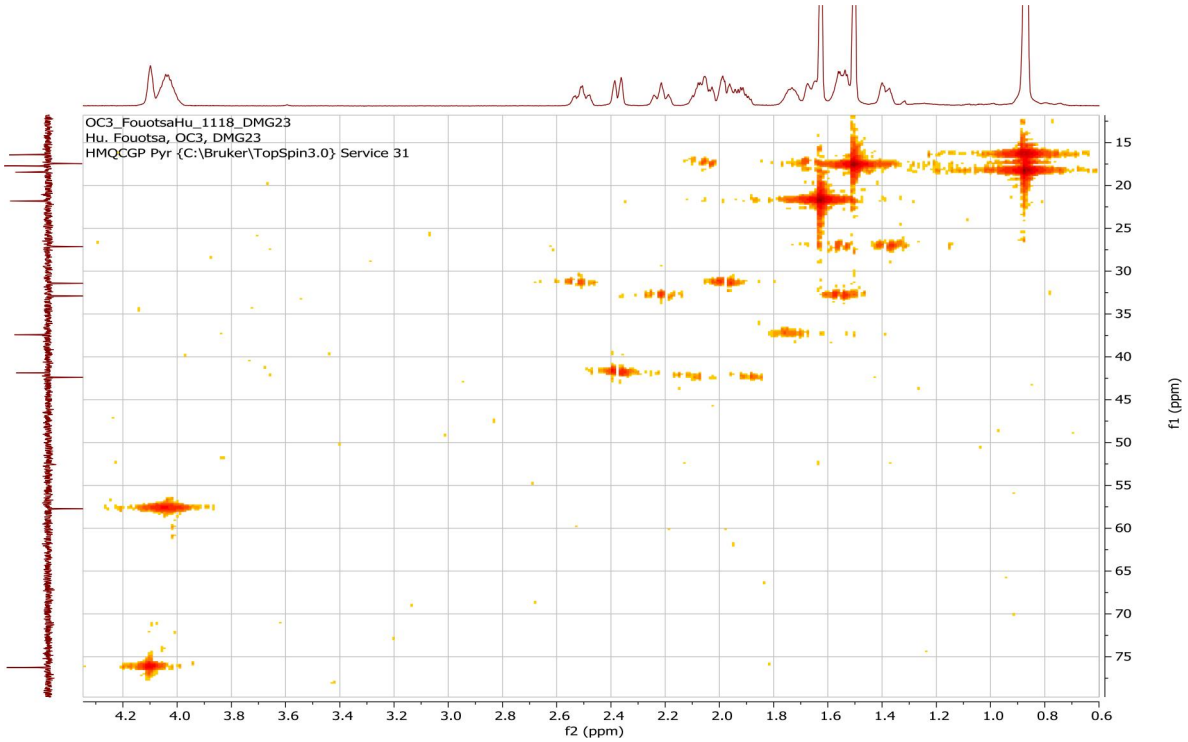

Figure 27 : HMQC spectrum of DMG23

Analysis of the ^{1}H-NMR spectrum (**Figure 31**) combined with the HMQC informations supported the presence of a labdane diterpene moiety in DMG23. Indeed, these NMR data

revealed the presence of three-proton singlets at δ_H/δ_C 0.88 (3H, s)/16.4; 0.87 (3H, s)/18.4 and 1.62 (3H, s)/21.8 attributable, respectively to two geminal methyl groups at position C-4 (δ_C 42.0) and a tertiary methyl group at position C-10 (δ_C 38.8) of a labdane-type skeleton. A subsequent methyl group appeared at δ_H/δ_C 1.50 (3H, d, 3.4)/17.7. Signals of two diastereotopic protons at δ_H/δ_C 2.07 (1H, dd, 1.5, 3.6)/31.4 and 1.92 (1H, dd, 1.5, 4.3)/31.4 exhibiting ^{1}H-^{1}H COSY (Figures 29) correlations with the oxymethylenic protons at δ_H/δ_C 4.04 (2H, t, 6.3)/57.7 were also observed, indicating the presence of a -CH_2-CH_2-O- spin system in DMG23.

The ^{1}H-NMR spectrum also displayed a set of three one proton broad singlets at δ_H/δ_C 5.25 (1H, s), 5.71 (1H, s) and 5.98 (1H, s) corresponding to three hydroxyl groups, confirming the presence in the structure of this compound of three oxygenated carbons as suggested by ^{13}C NMR and among which, one oxymethylene (δ_C 57.7), one oxymethine (δ_C 76.2) and one oxygenated quaternary carbon (δ_C 75.8) bearing a hydroxyl group. The oxymethine carbon was assigned to be at C-3 position of the labdane skeleton according to the correlation ^{1}H-^{1}H COSY (Figures 30) observed between H-3 (δ_H/δ_C 4.10 (1H, t, 8.5)/ 76.2) and Hb-2 (δ_H/δ_C 1.98 (1H, dd, 14.7, 10.4)/ 32.9). This was also confirmed by ^{1}H-^{13}C HMBC spectrum (Figures 31) which showed correlations between hydroxyl proton OH-3 at δ_H 5.98 (1H, s) and carbon C-3 (δ_C 76.2), on one hand, and between H-14 (δ_H/δ_C 0.87 (3H, s)/ 18.4) and carbon C-3 (δ_C 76.2) on the other hand. Among the four methyls observed in ^{1}H and ^{13}C NMR, three of them have already been located at position 4 and 10 of the labdane skeleton (Reddy, 2009). The remaining methyl group was positioned at C-8 from the COSY correlations observed between the H-13 (δ_H/δ_C 1.50 (3H, d, 3.4)/ 17.7) and H-8 (δ_H/δ_C 2.37 (1H, dd, 14.7, 12.1)/ 41.8) protons on the one hand, and from the HMBC correlation observed between the H-13 protons and the C-8 (δ_C 41.8) carbon on the other hand. The oxygenated quaternary carbon (δ_C 75.8) was found to be at C-9 due to the HMBC cross-peaks exhibited between both H-13 (δ_H/δ_C 2.37 (1H, d, 12.0)/ 41.8), H-16 (δ_H/δ_C 1.62 (3H, s)/ 21.8) and C-9 (δ_C 75.8). At this stage of the discussion, the only free position on the labdane skeleton was at C-9 on which the -CH_2-CH_2-O-H moiety was located. This was confirmed on the one hand, from biogenetic considerations (Reddy, 2009) and on the other hand, by the HMBC correlations observed between proton H-8 (δ_H/δ_C 2.37 (1H, dd, 14.7, 12.1)/41.8) and the methylenic carbon C-11(δ_C 31.4).

All these informations led us to proposed for this compound, the following partial structure (8-methyl-tetranorlabdane-3, 9, 12-triol) possessing five chiral centers around C-3, C-5, C-8, C-9 and C-10.

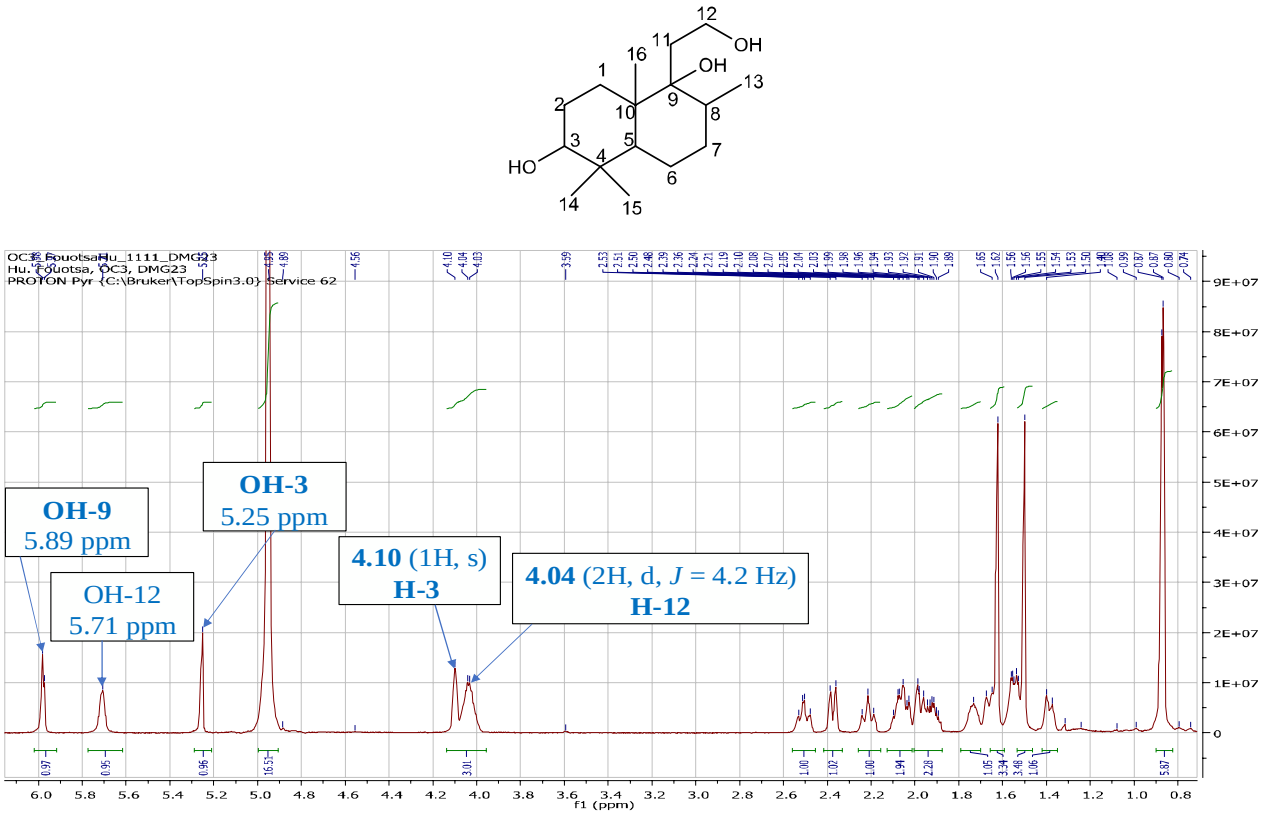

Figure 28 : ^{1}H NMR spectrum (500 MHz, C_5D_5N) of DMG23

The relative stereochemistry around those chiral centers (C-3, C-5, C-8, C-9 and C-10) was established from the comparison of this structure with a similar labdane diterpenoid, vitepyrroloid C described in the literature (Luo et al., 2017). The substituent patterns on stereogenic centers were identical in both structures except at position C-3 where vitepyrroloid C carried an acetyl group while in DMG23, it was a hydroxyl group. In addition, compound DMG23 exhibited positive optical rotation value $[\alpha]_D^{20} + 20.5$ similar to that of vitepyrroloid C $[\alpha]_D^{20} + 18$, assuming that DMG23 had the same stereochemistry like vitepyrroloid C. Thus, DMG23 was established to be (3S, 5S, 8R, 9R, 10S)-8-methyl-tetranorlabdane-3, 9, 12-triol, to which the trivial name Microcarpin was assigned.

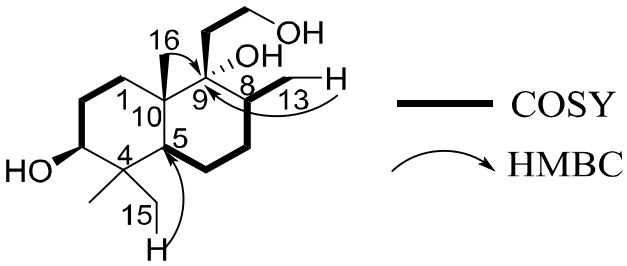

Scheme 15 : Some correlations COSY and HMBC of DMG23

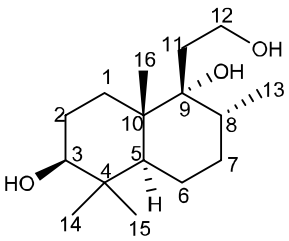

Microcarpin (116)

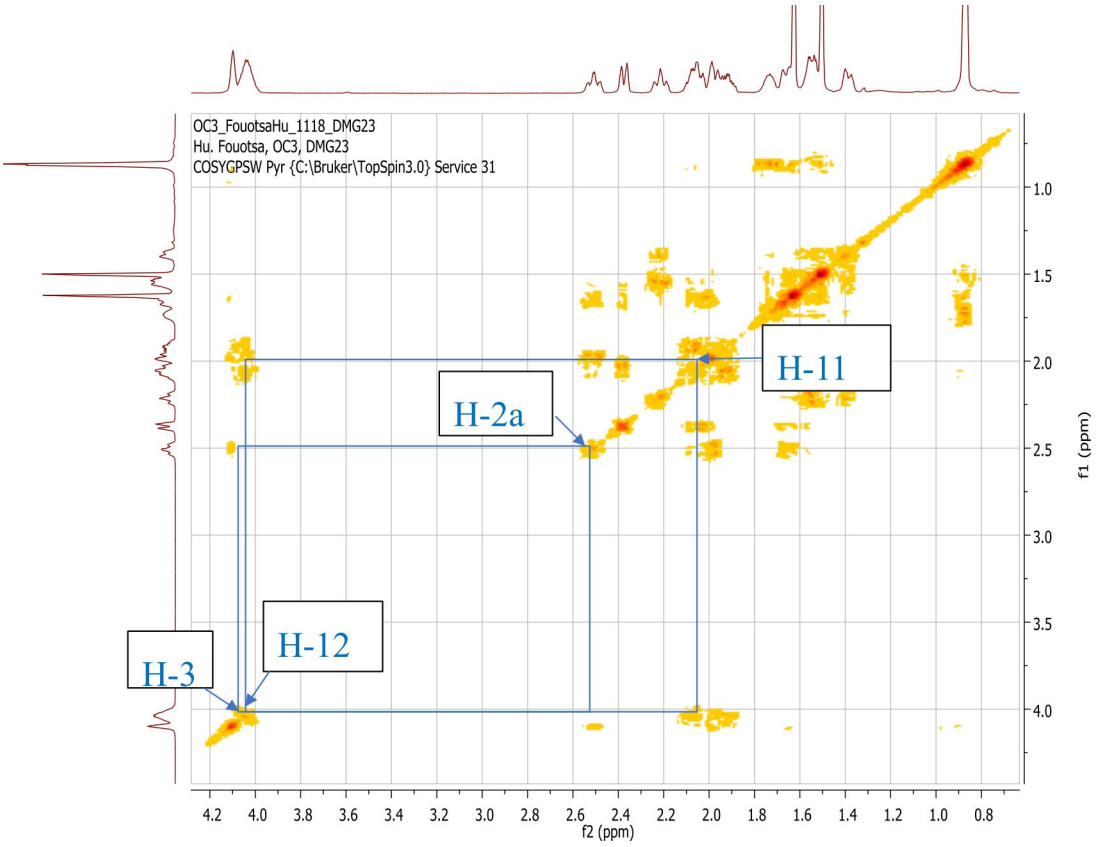

Figure 29 : COSY spectrum of DMG23

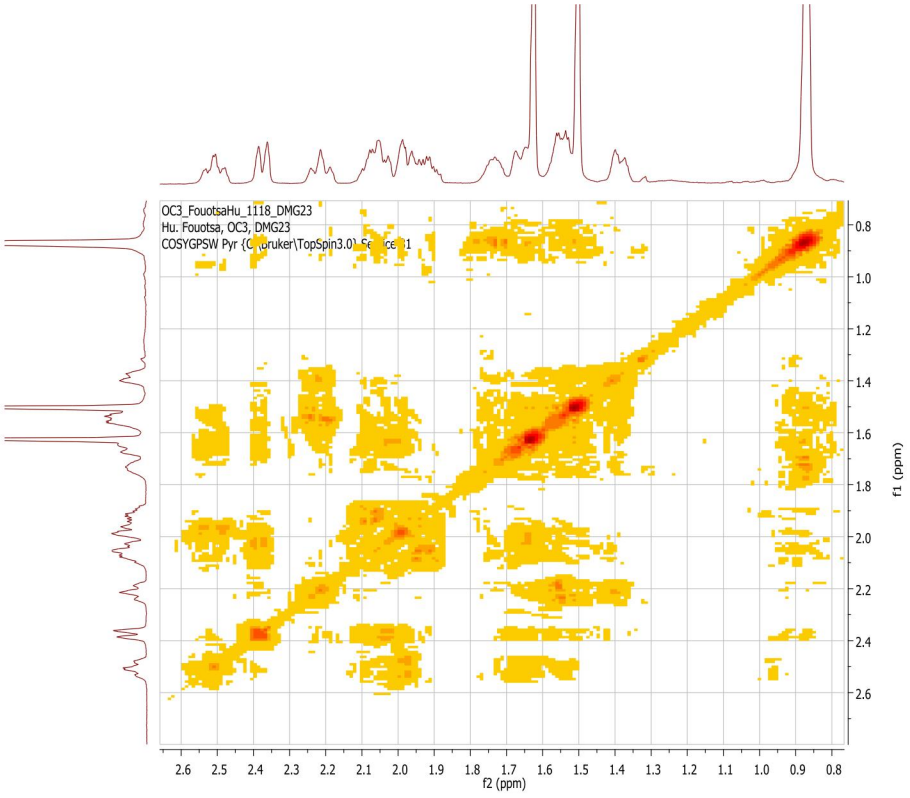

Figure 30: Extended COSY spectrum of DMG23

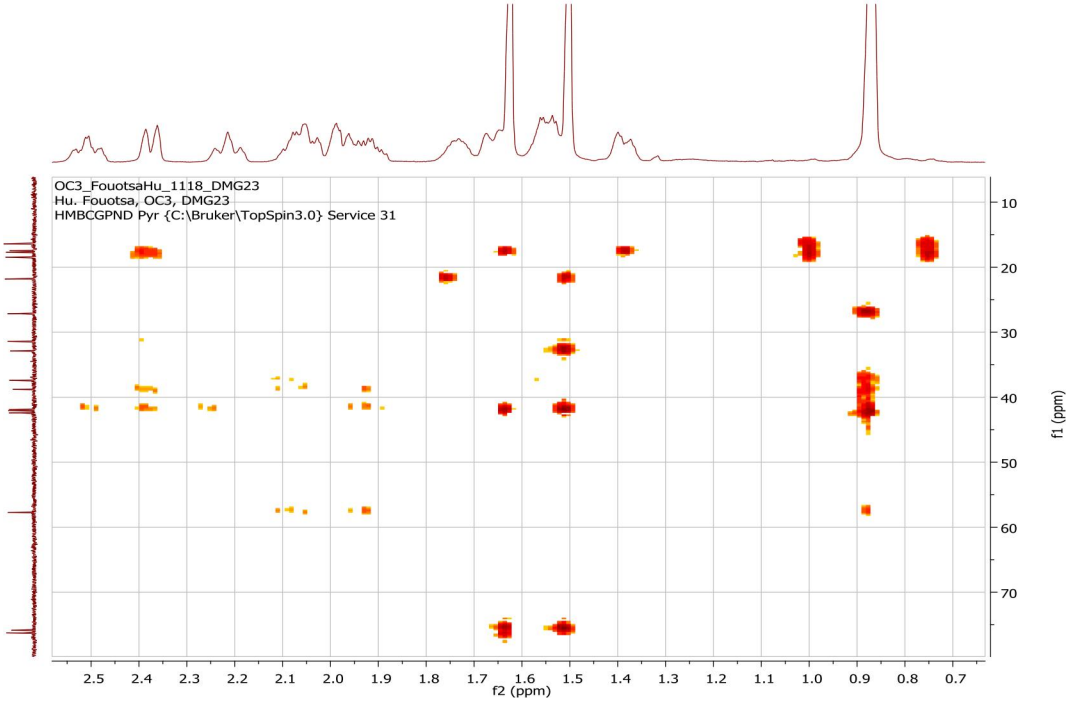

Figure 31 : HMBC spectrum of DMG23

Table XX : ^{1}H (500 MHz) and ^{13}C (125 MHz) NMR spectroscopic data of DMG23 in pyridin-d_5.

Position	δ_H ; m ; *J* in Hz	δ_C
1a	2.21 (1H, t, 13.2)	42.4
1b	1.56 (1H, d, 3.8)	
2a	2.51 (1H, dd, 14.7, 11.6)	32.9
2b	1.98 (1H, d, 3.7)	
3	4.10 (1H, s)	76.2
4	-	42.0
5	1.73 (1H, d, 12.1)	37.4
6a	2.05 (1H, s)	17.4
6b	1.67 (1H, dt, 4.6, 11.8)	
7a	1.54 (1H, d, 3.0)	27.1
7b	1.38 (1H, t, 12.1)	
8	2.37 (1H, d, 12.0)	41.8
9	-	75.8
10	-	38.8
11a	2.07 (1H, d, 3.6)	31.4
11b	1.92 (1H, d, 4.3)	
12	4.04 (2H, d, 4.2)	57.7
13	1.50 (3H, s)	17.7
14	0.87 (3H, d, 3.4)	18.4
15	0.88 (3H, d, 3.4)	16.4
16	1.62 (3H, s)	21.8
OH-3	5.98 (1H, s)	-
OH-9	5.25 (1H, s)	-
OH-12	5.71 (1H, s)	-

II.2.1.3.2. Identification of DMB12 (Rhinocerotinoic acid)

Compound DMB12 was obtained as a white crystal from the *n*-Hex/EtAcO (13: 7) mixture. The molecular formula $C_{20}H_{30}O_3$ was deduced from analysis of its HRESIMS (Figure 32) which showed in positive mode, the sodium adduct ion peak $[M+Na]^+$ at *m/z* 341.2108 (calcd 341.2098 for $C_{20}H_{30}O_3Na^+$), corresponding to six degrees of unsaturation. The twenty carbon atoms present in molecular formula argued in favor of diterpenoid type skeleton.

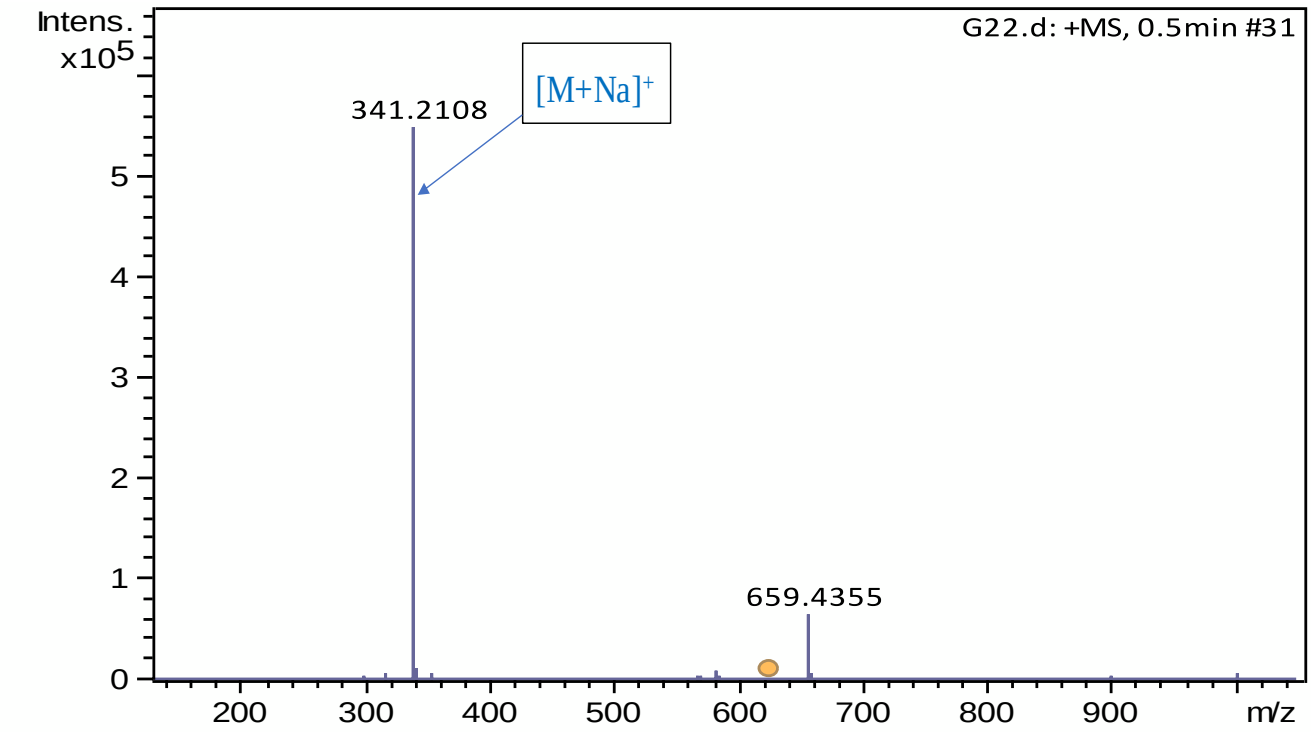

Figure 32 : HRESIMS spectrum of DMB12

The broadband proton decoupled ^{13}C NMR spectrum of DMB12 showed 20 carbon signals which were assigned with the aid of DEPT technique (Figure 36 and 37) as five methyl (δ_C 27.7, 21.5, 19.1, 18.6, 11.4), six methylenes (δ_C 39.1, 18.6, 41.2, 35.4, 32.7, 35.2) , two methines (δ_C 116.6, 50,2) and seven quaternary carbon (δ_C 33.2, 198.9, 129.7, 167.0, 41.0, 158.3, 167.8). The quaternary carbon signals at δ_C 198.9 (C-7) and 167.8 (C-15) suggested the presence of two carbonyl functions attributable to conjugated ketone and carboxylic acid respectively. The ^{13}C NMR spectrum of DMB12 also displayed resonances for four sp^2 carbons at δ_C 129.7 (C-8), 167.0(C-9), 158.3 (C-13) and 116.6 (C-14) corresponding to two conjugated double bonds of which one tetrasubstituted (C-8 and C-9) and one trisubstituted (C-13 and C-14).

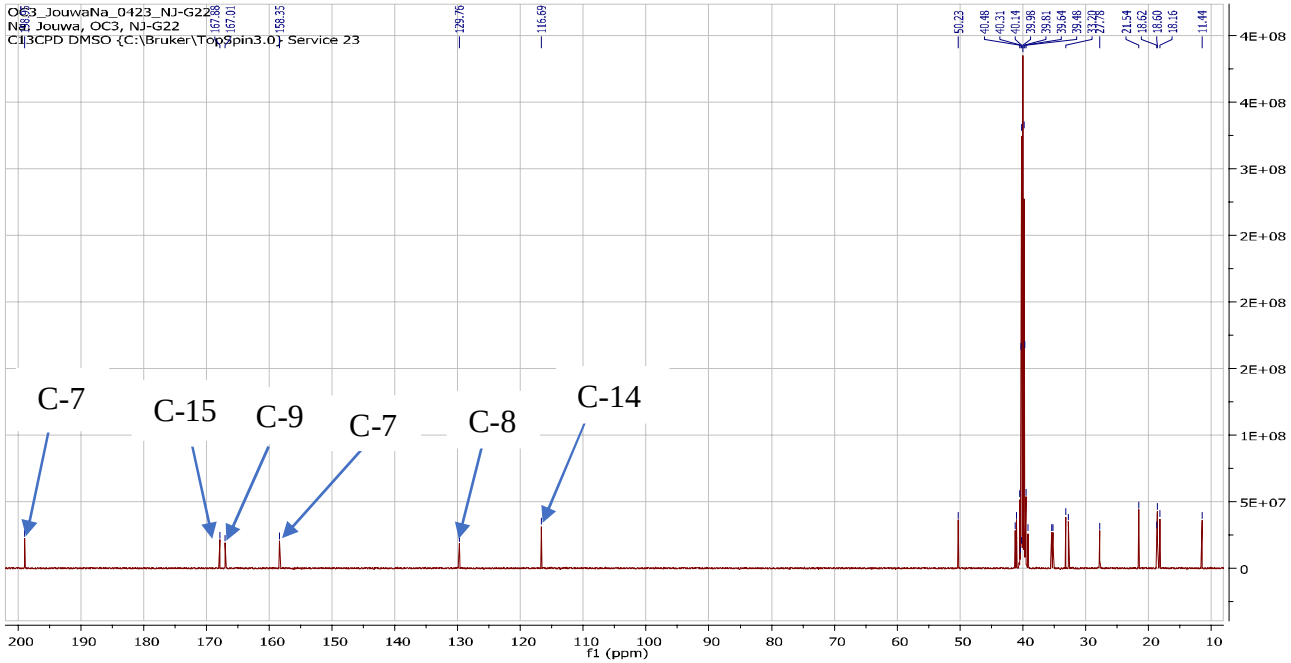

Figure 33: ^{13}C NMR spectrum (125MHz; DMSO) of DMB12

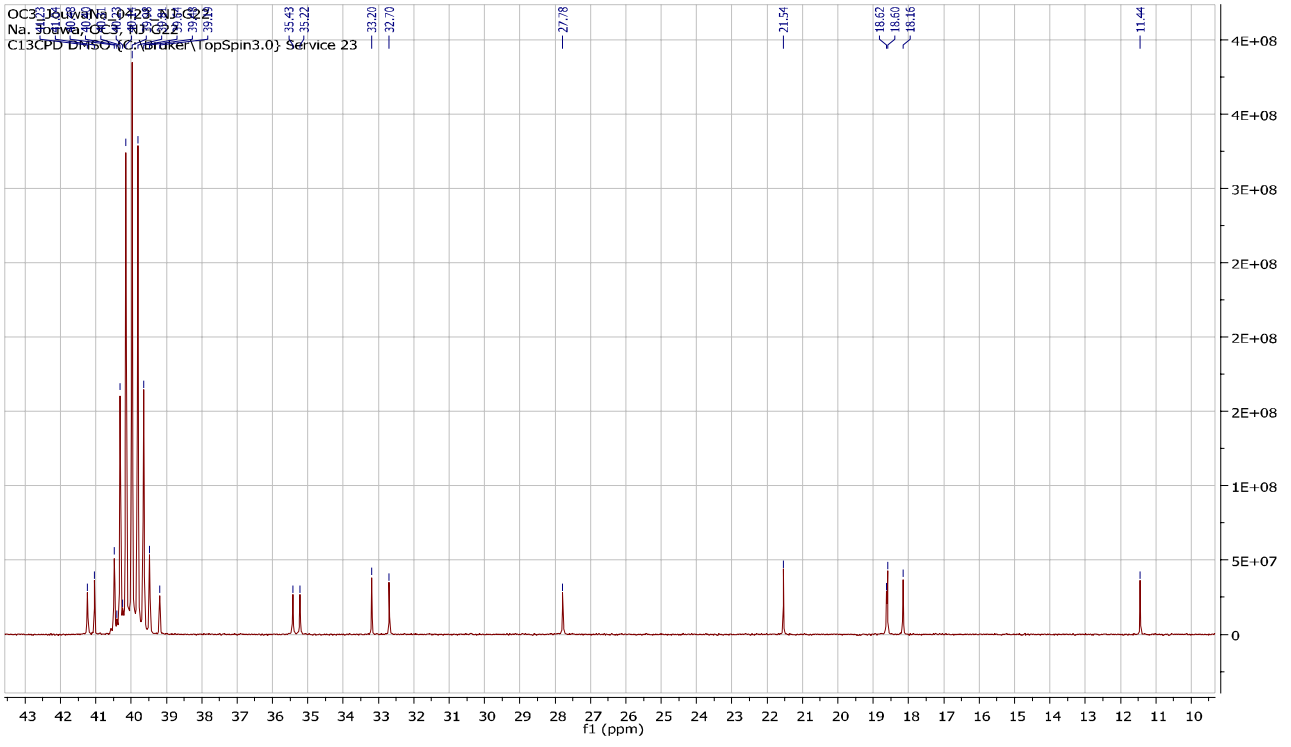

Figure 34 : expanded ^{13}C NMR spectrum (125MHz; DMSO) of DMB12

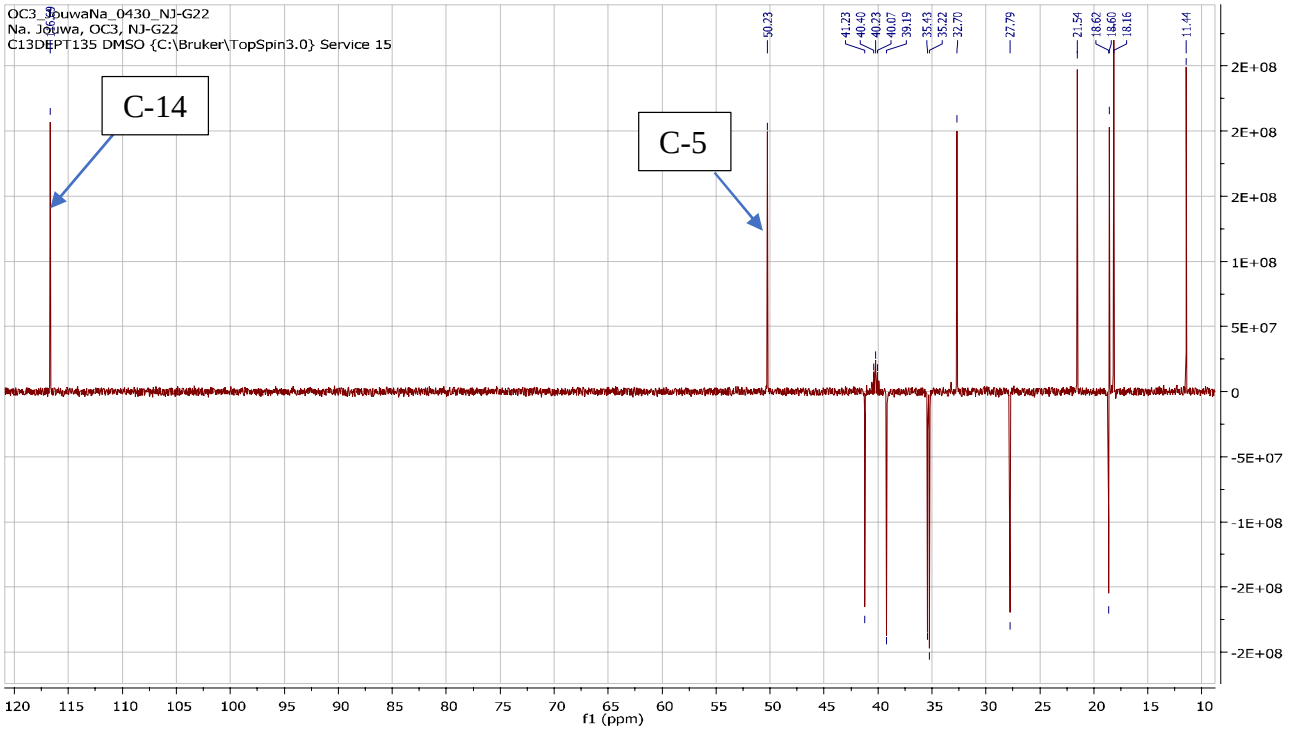

Figure 35 : DEPT 135 spectrum of DMB12

The ^{1}H NMR spectrum (Figure 33) of DMB12 showed four singlets of three protons at δ_H 1.68, 1.06, 0.89 and 0.85, characteristic of methyl groups located on the decaline moiety of a labdane-type skeleton. A signal of a vinylic proton was also observed at δ_H 5.68 (1H, d, J = 0.6 Hz, H-14) showing a HMBC correlation with the conjugated carboxylic acid carbonyl at δ_C 167.8 (C-15), which confirmed this latter to form with C-13 (δ_C 158.3) and C-14 (δ_C 116.6), a conjugate system. Further HMBC correlations were observed between the methyl protons H-17 (δ_H 1.68) and the conjugated ketone carbonyl at δ_C 198.9 (C-7) on the one hand, and between this methyl protons H-17 and both sp^2 carbons C-8 (δ_C 129.7) and C-9 (167.0) on the other hand, suggesting the methyl group and the conjugated double bond to be located on C-8 (δ_C 129.7).

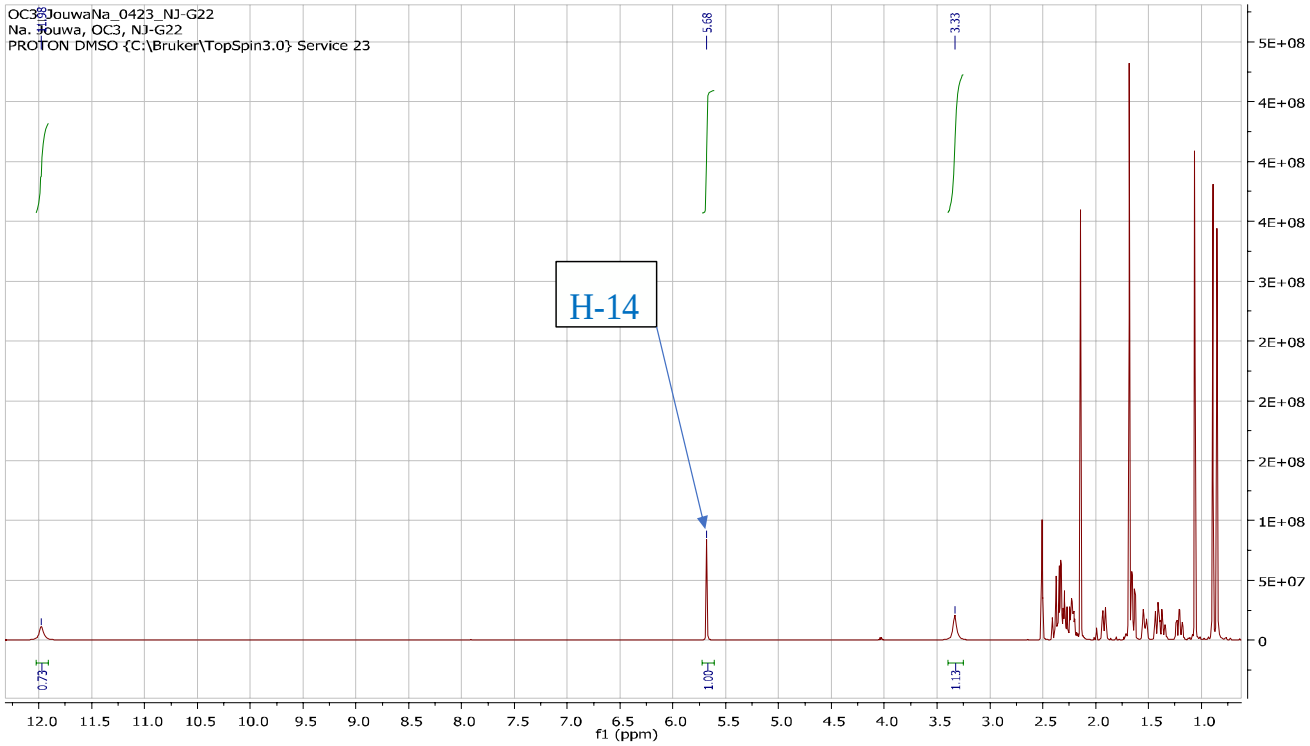

Figure 36 : ^{1}H NMR spectrum (500MHz; DMSO) of DMB12

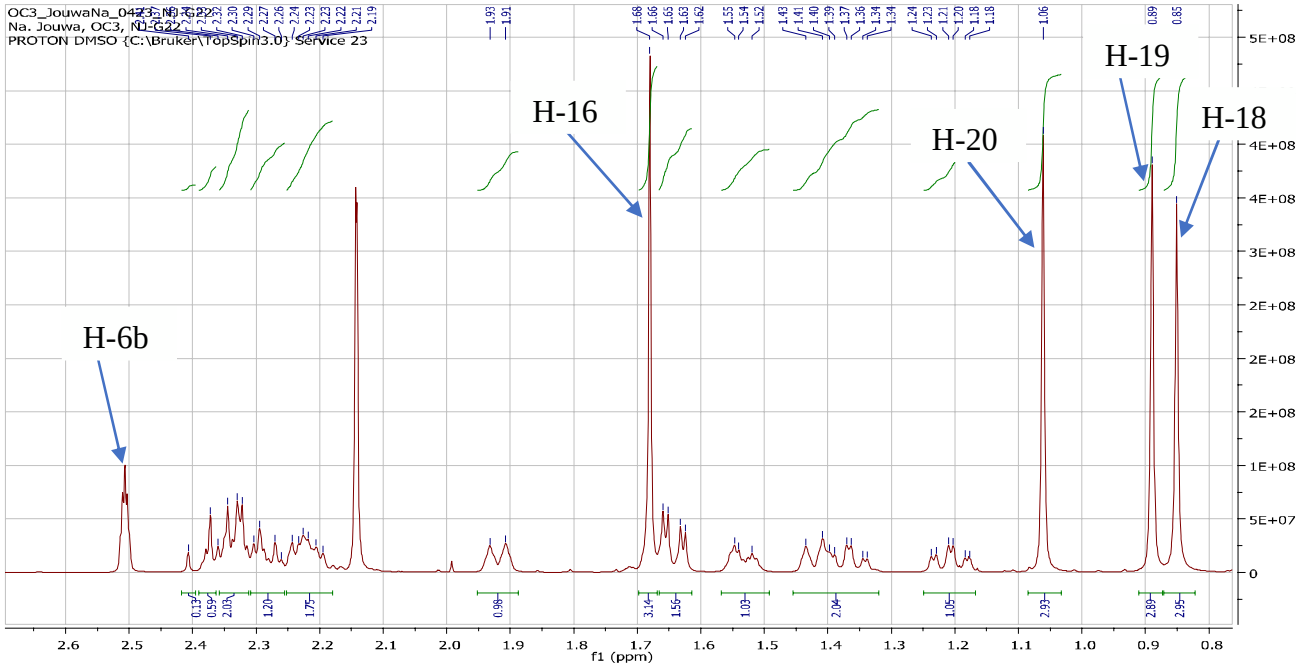

Figure 37 : Expanded part ^{1}H NMR spectrum (500MHz ; DMSO) of DMB12

By comparing these spectral data with those described in the literature, DMB12 was identified as rhinocerotinoic acid (**117**)**,** an anti-inflammatory labdane diterpene isolated for the first time from *Elytropappus rhinocerotis* (Asteraceae) (Dekker et *al.*, 1988). It is the first time that this compound is reported from the genus *Detarium*.

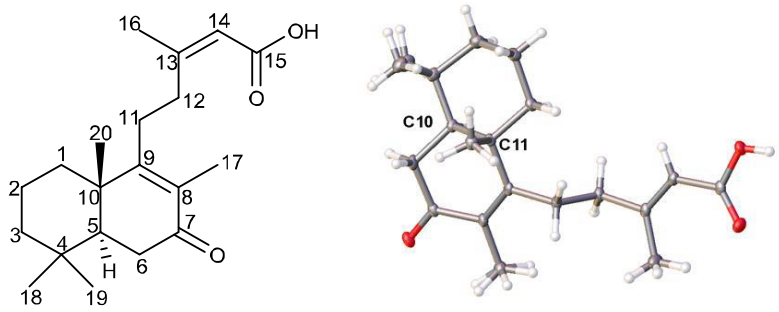

(117)

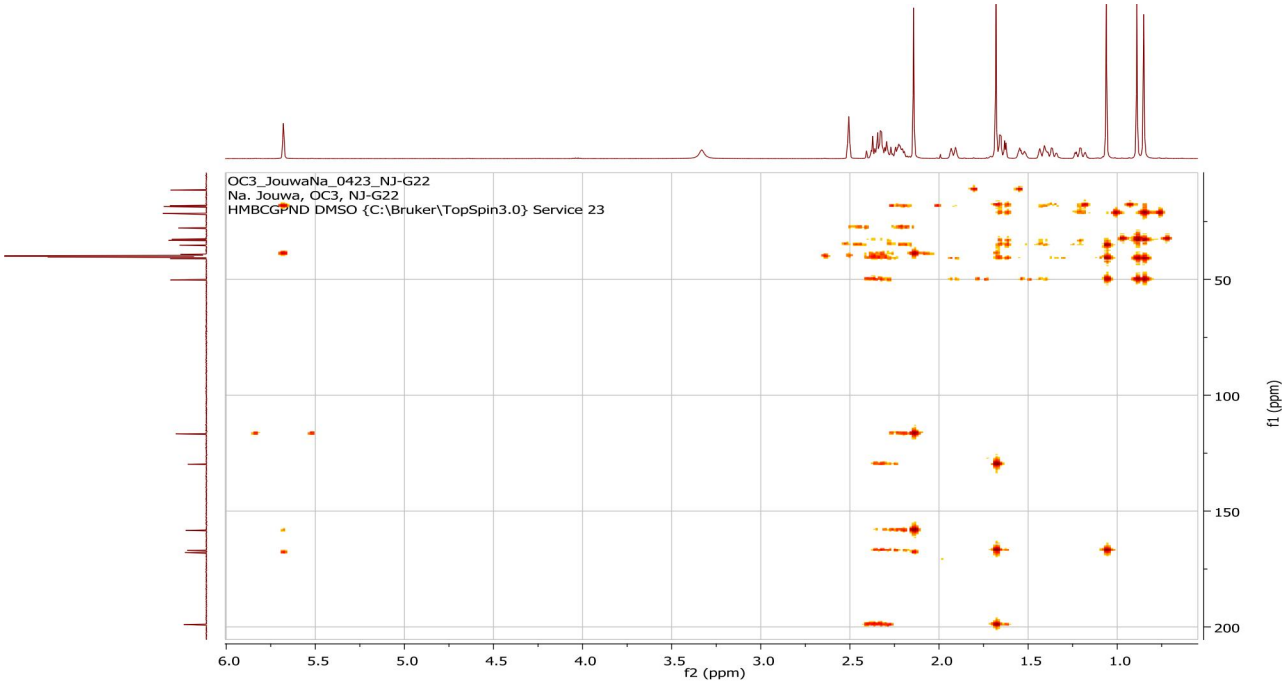

Figure 38 : HMBC spectrum of DMB12 (4) (125MHz; DMSO)

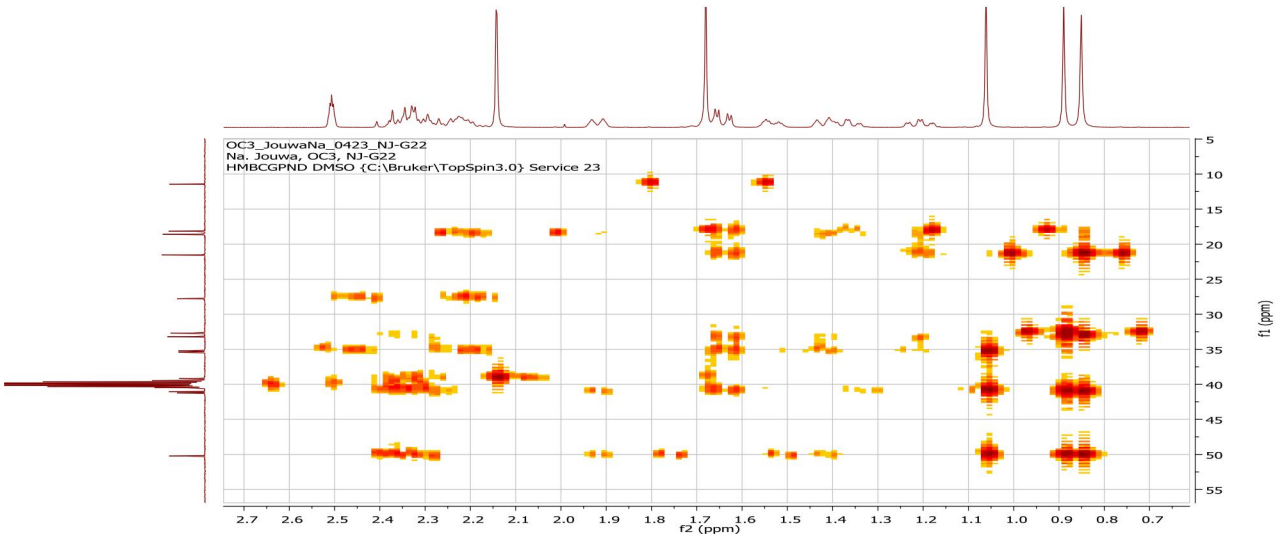

Figure 39 : Expanded part of HMBC spectrum of DMB12 (4) (125MHz; DMSO)

Table XXI : ^{1}H and ^{13}C NMR data (500 MHz and 125 MHz; *in pyridin*-d_5) of DMB12 with that reported by Rijo.

Position	δ_H (mH, m, J_{HH} in Hz)	δ_C	δ_C (Dekker et *al.*, 1988)
1a	1.92 (1H, d, 12.4)	39.1(t)	35.8
1b	1.35 (1H, dd, 12.9, 3.3)		
2	1.53 (1H, dd, 10.2, 6.9)	18.6(d)	18.5
3a	1.41 (1H, dd, 13.9, 8.6)	41.2(t)	41.2
3b	1.21 (1H, dd, 13.2, 3.7)		
4	-	33.2(s)	33.1
5	1.64 (1H, dd, 13.7, 4.1)	50.2(d)	50.2
6a	2.22 (1H, dd, 3.7, 17.5)	35.4(t)	35.1
6b	2.50 (1H, dd, 14.3, 17.5)		
7	-	198.9(s)	200.1
8	-	129.7(s)	130.5
9	-	167.0(s)	166.2
10	-	41.0(s)	41.0
11	2.37 (2H, t, 4.7)	32.7(t)	32.4
12	2.33 (2H dd, 7.5, 3.7)	35.2(t)	39.7
13	-	158.3(s)	161.7
14	5.68 (1H, d, 0.6)	116.6(d)	115.1
15	-	167.8(s)	171.1
16	2.14 (3H, d, 1.1)	18.6(q)	19.1
17	1.68 (3H, s)	11.4(q)	11.4
18	0.85 (3H, s)	27.7(q)	27.6
19	0.89 (3H, s)	21.5(q)	21.2
20	1.06 (3H, s)	18.1(q)	18.1

II.2.1.3.3. Identification of DMG22 (5-(carboxymethyl)-5,6,8a-trimethyl-3,4,4a,5,6,7,8,8a-octahydronaphthalene-1-carboxylic acid)

Compound DMG22 was obtained as a white crystal in the mixture of *n*-Hex/EtOAc (3 :1). Its HRESIMS (Figure 40**)** gave in positive mode, a pseudo molecular ion peak $[M+H]^+$ at *m/z* 281.1721 corresponding to the molecular formula $C_{16}H_{24}O_4$ with five degrees of unsaturation. The sixteen carbon atoms present in the molecular formula argued in favor of a tetranorditerpenoid type skeleton.

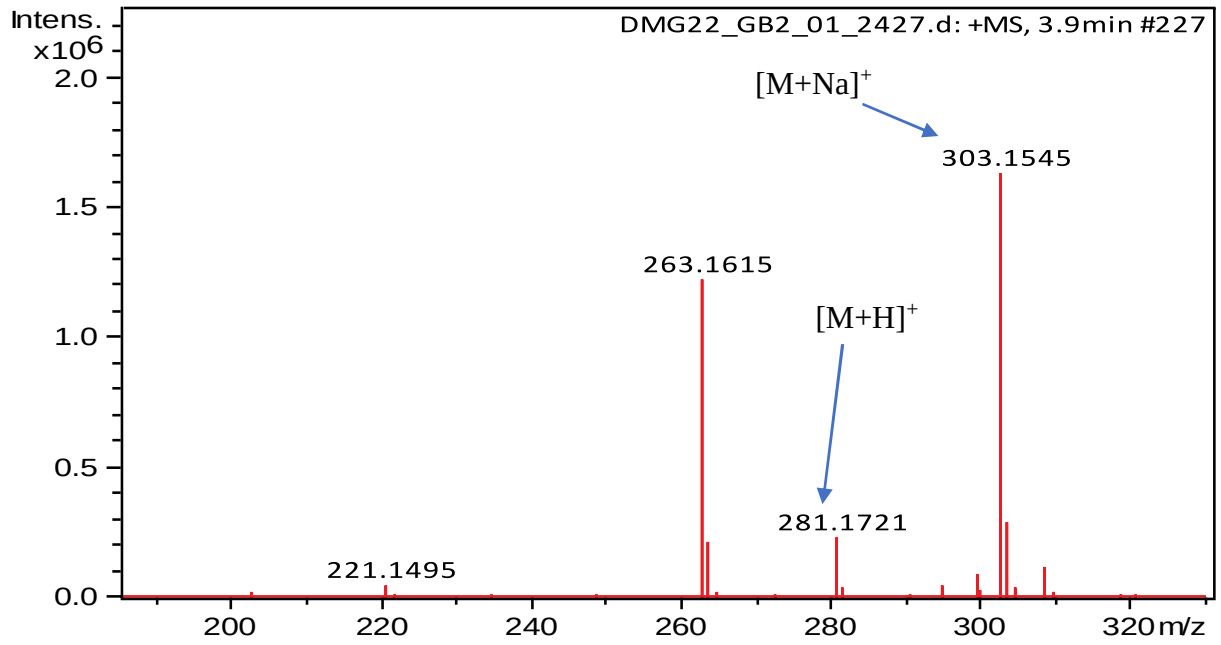

Figure 40 : HR-ESI-MS spectrum of DMG22

The ^{13}C NMR data coupled with DEPT technique (Figure 42 and 43) indicated the presence of sixteen carbons resonances including those of two carboxylic acid carbonyls at δ_C 175.2 and 170.5, two sp^2 carbons at δ_C 144.2 and 138.1, three methyls of which two tertiary methyls at δ_C 21.8 and 17.4, and one secondary methyl at δ_C 39.3.

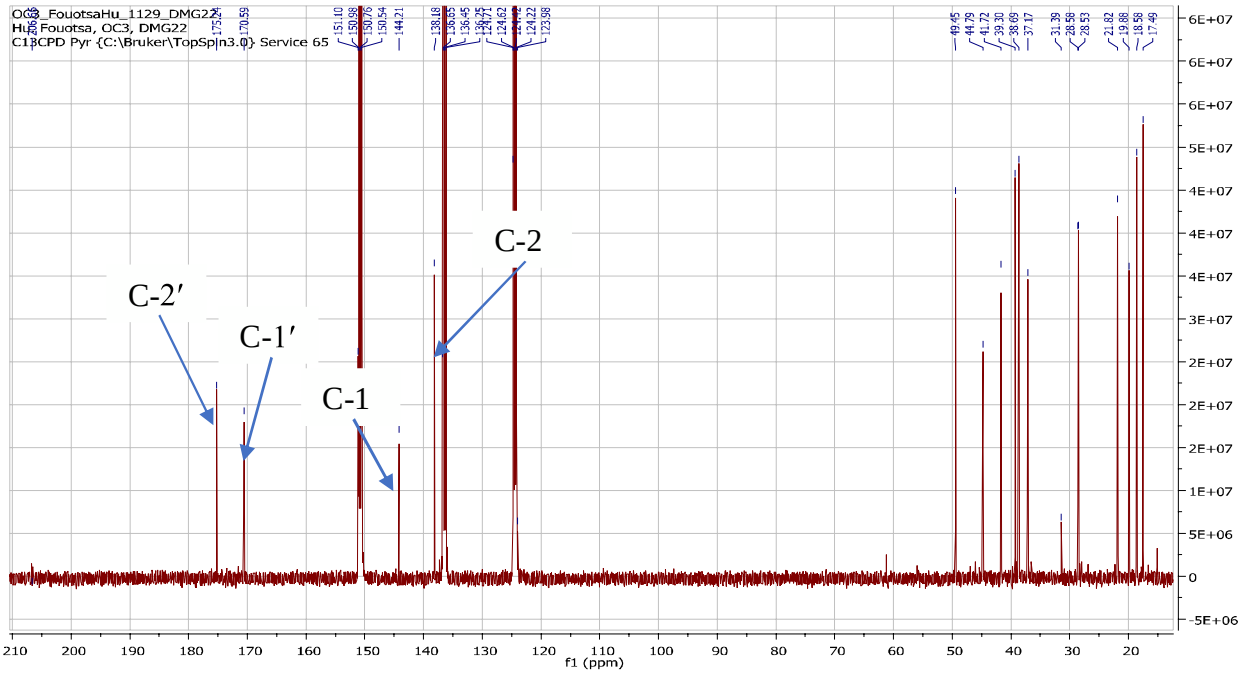

Figure 41 : ^{13}C NMR spectrum (125MHz; C_5D_5N) of DMB12

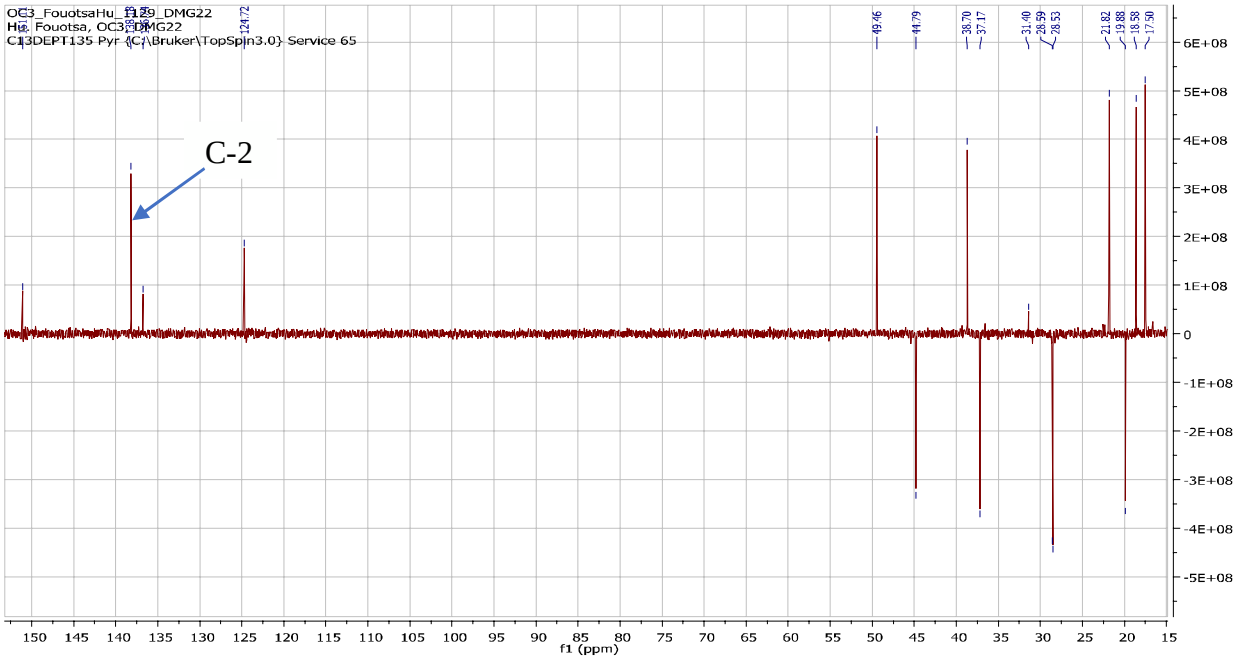

Figure 42 : DEPT 135 spectrum of DMB12

Analysis of the ^{1}H NMR spectrum of DMG22 revealed the presence of one olefinic methine proton resonance at δ_H 7.01 (1H, br s) and three methyl proton signals at δ_H 1.53 (3H, m), 0.98 (3H, d, 6.6), 0.80 (3H, d, 2.4). These ^{1}H and ^{13}C NMR spectroscopic data were consistent with a clerodane diterpenoid type skeleton containing two carboxylic acid functions. One of the carboxylic acid function were evidenced from the fragment ion peak observed on the HRESIMS at *m/z* 221.1495 $[M+H-60]^+$ due to the loss of a -CH_2CO_2H group.

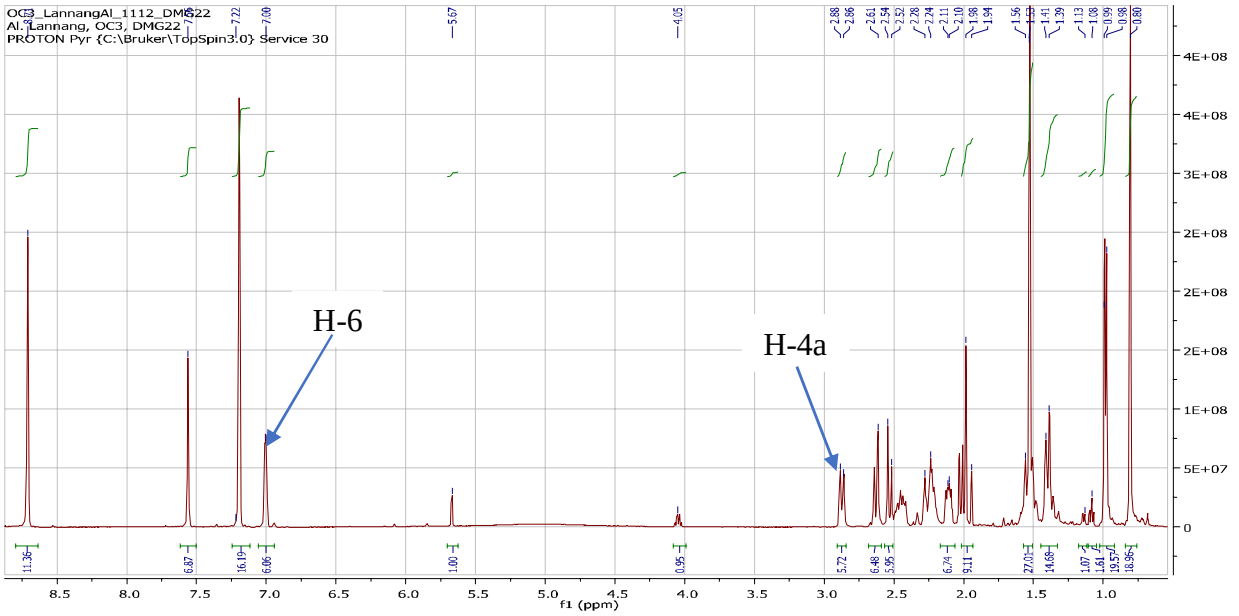

Figure 43 : ^{1}H NMR spectrum of (500MHz; C_5D_5N) of DMB12

The comparison of these NMR and MS data with those described in the literature allowed us to attribute to DMG22, the structure of 5-(carboxymethyl)-5,6,8a-trimethyl-3,4,4a,5,6,7,8,8a-octahydronaphthalene-1-carboxylic acid (**118).** It is a tetranorditerpenoid previously isolated from the bark of *Detarium microcarpum* harvested in Dakar, Senegal (Aquino *et al*., 1992).

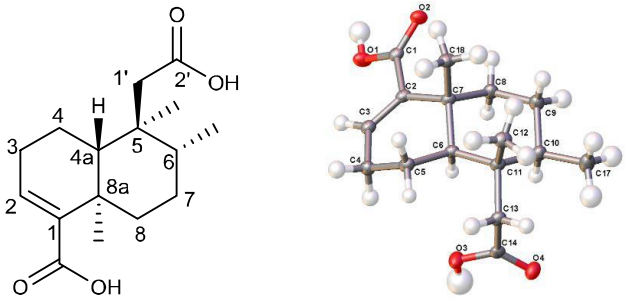

(118)

Table XXII: ^{1}H NMR (500 MHz, C_5D_5N), and ^{13}C NMR (125 MHz, C_5D_5N) spectral data of compound DMG22

Position	DMG22		Aquino et *al*., 1992 ($CHCl_3$)
	δ_H (m, J_{HH} in Hz)	δ_C	δ_C
1	-	144.2	140.6
2	7.01 (1H, t, 4.3)	138.1	141.4
3-a	2.22 (1H, m)	28.6	27.4
3-b	1.56 (1H, t, 7.5)		
4-a	2.11 (1H, dd, 12.5, 6.9)	19.8	18.4
4-b	0.80 (3H, m, 2.4)		
4a	1.99 (1H, dd, 3.1, 7.3)	49.4	47.8
5	-	41.7	41.1
6	2.20 (1H, m)	39.3	37.4
7-a	2.43 (1H, dd, 10.8, 6.6)	28.5	27.1
7-b	1.33 (1H, m)		
8-a	2.87 (1H, m)	37.1	35.3
8-b	1.40 (2H, d, 11.5)		
8a	-	38.6	37.8
1′a	2.63 (1H, d, 13.5)	44.7	43.0
1′b	2.53 (1H, d, 13.5)		
2′	-	175.2	177.8
5-CH_3	1.53 (3H, s)	17.4	16.2
6-CH_3	0.98 (3H, d, 6.6)	18.5	17.4
8a-CH_3	0.80 (3H, s)	21.8	20.5
1-COOH	-	170.5	172.2

II.2.1.4. Triterpenoids

II.2.1.4.1. Identification of DMB32 (lup-20(29)-en-28-oic acid)

Compound DMB32 was isolated as a white powder in the *n*-Hex/EtOAc mixture (3/1). Soluble in chloroform, it reacted positively to the Liebermann-Burchard test suggesting its triterpenoidic nature. Its HRESIMS showed the pseudo molecular ion peak $[M+H]^+$ at *m/z* 426.3045 compatible with the molecular formula $C_{30}H_{50}O$ implying 6 degrees of unsaturation.

The ^1H NMR spectrum (Figure 44) of DMB32 showed in the upfield region, seven tertiary methyl singlets between δ_H 0.68 and 1.67 among which six appeared to be linked to sp^3 carbons (δ_H 0.68-1.03) and one to a sp^2 carbon (δ_H 1.67) (Teixeira et al., 2017).

The ^1H and ^{13}C NMR (Figure 45) spectra also displayed two olefinic methylene proton singlets at δ_H 4.68/δ_C 109.3 and δ_H 4.56/δ_C 109.3 assignable to a terminal methylene group, one downfield allylic methine proton at δ_H 2.37/ δ_C 48.0, one oxymethine proton at δ_H 3.18/ δ_C 78.9 attributable to H-3 proton of triterpene and one olefinic tertiary carbon signal at δ_C 150.9 (Table 23) (Teixeira et al., 2017).

The comparison of these spectral data with those reported the literature allowed us to assign to compound DMB32 the structure **119** which is that of 3β,23-dihydroxylup-20(29)-en-28-oic acid (Lupeol) (**Teixeira et al., 2017)**.

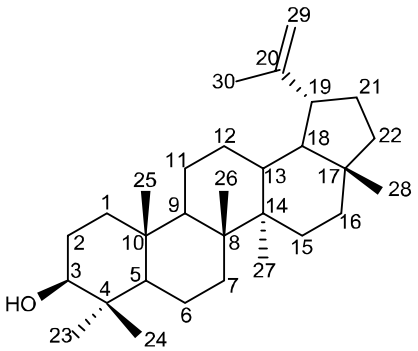

(119)

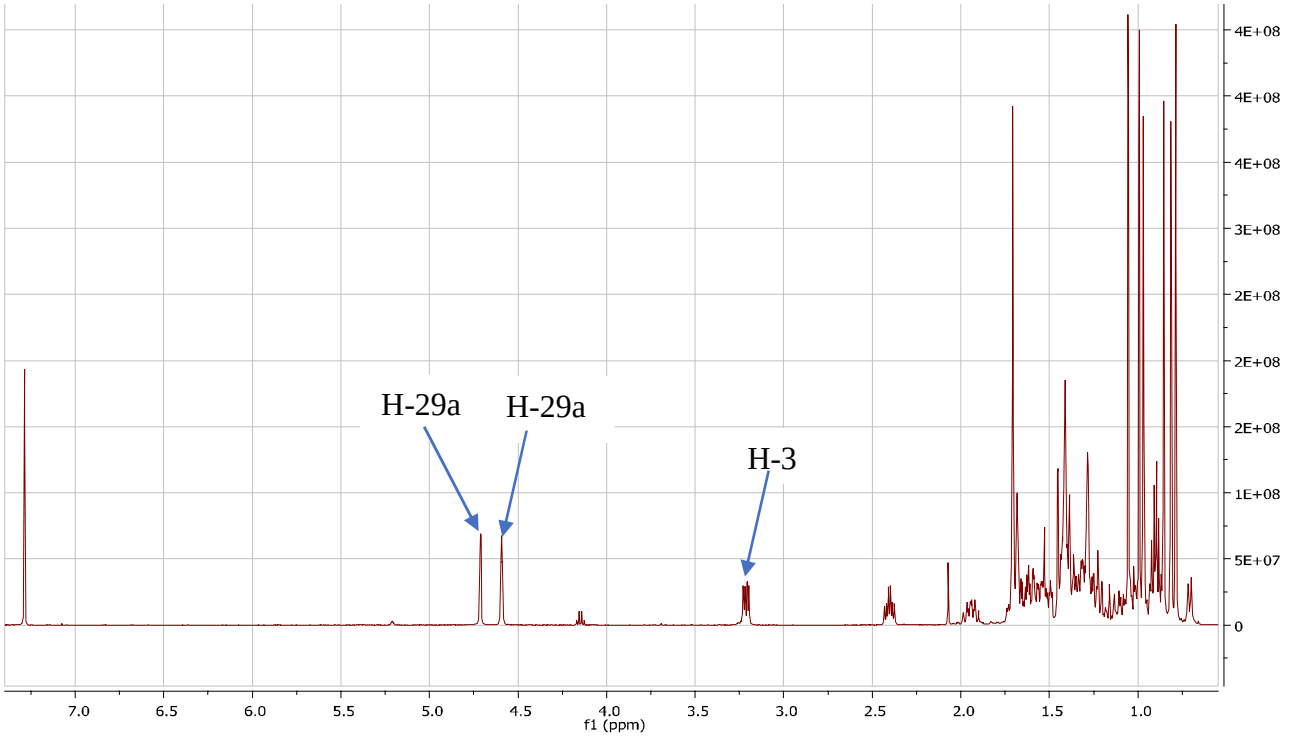

Figure 44 : ^{1}H RMN spectrum (500 MHz, $CDCl_3$) of compound DMB32

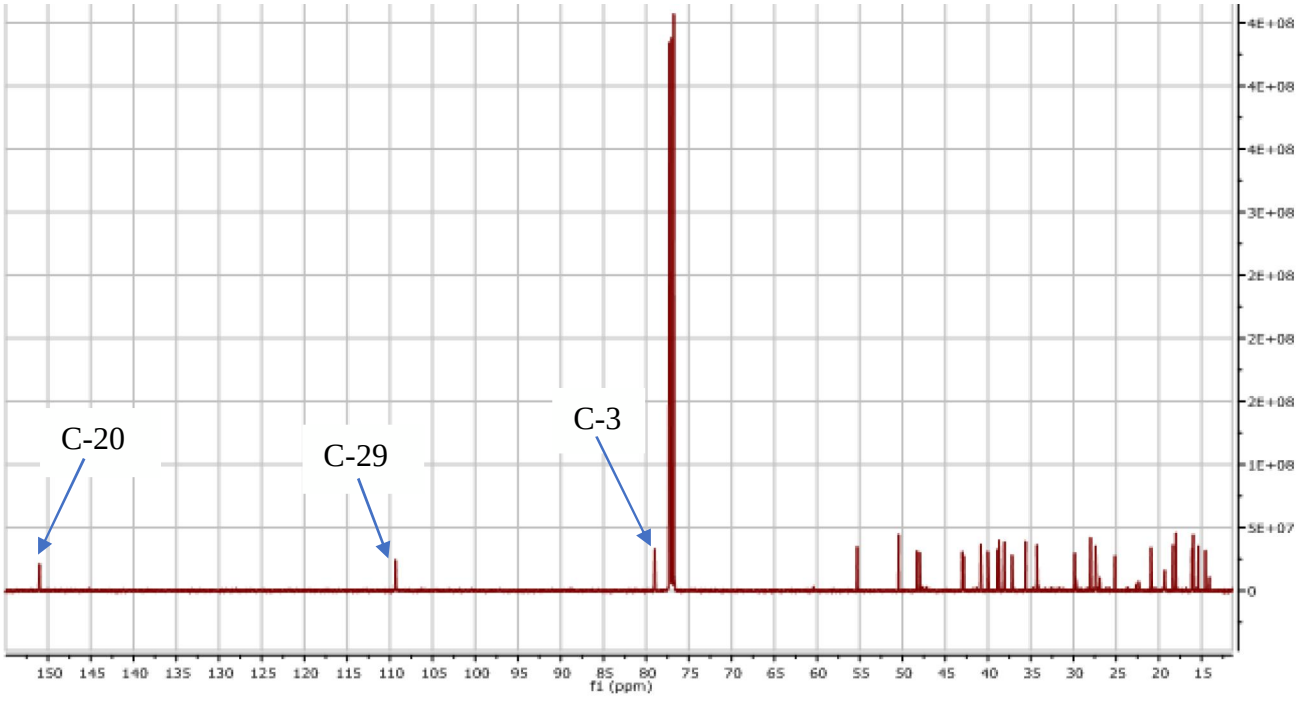

Figure 45 : ^{13}C NMR (125 MHz, $CDCl_3$) spectrum of DMB32

Table XXIII: ^{1}H NMR (500 MHz, $CDCl_3$), and ^{13}C NMR (125 MHz, $CDCl_3$) spectral data of compound DMB32

Position	δ_H in ppm (nH, m, *J* in Hz)	δ_C (m)	δc in ppm (Teixeira et al., 2017)
1	1.47 (1H, m); 1.37 (1H, m)	38.7(t)	38.1
2	2.20(1H, m); 2.14 (1H, m)	27.5(t)	24.4
3	3.18 (1H, dd, 11.6-5.2)	79.0(d)	79.1
4	-	38.8(s)	38.7
5	1.38 (1H, t, 9.1)	55.3(d)	55.3
6	1.41 (1H, d, 6.1) ; 1.36 (1H, d, 12.5)	18.3(t)	18.3
7	1.45 (1H, m) ; 1.33 (1H, m)	34.3(t)	34.3
8	-	40.8(s)	40.9
9	1.38 (1H, t, 9.3)	50.4(d)	50.5
10	-	37.1(s)	37.2
11	1.45 (1H, m) ; 1.23 (1H, m)	20.9(t)	20.9
12	1.52 (1H, m) ; 1.39 (1H, m)	25.1(t)	25.2
13	1.45 (1H, m)	38.1(d)	38.9
14	-	42.8(s)	42.9
15	1.45 (1H, m) ; 1.24 (1H, m)	27.4(t)	27.5
16	1.48 (1H, m) ; 1.32 (1H, m)	35.6(t)	35.6
17	-	43.0(s)	43.0
18	1.53 (1H, t, 10.1)	48.3(d)	48.3
19	1.19 (1H, m)	48.0(d)	48.0
20	-	151.0(s)	150.9
21	1.47 (1H, m) ; 1.28 (1H, m)	29.8(t)	29.9
22	1.49 (1H, m) ; 0.92 (1H, m)	40.0(d)	40.0
23	0.86 (3H, d, 6.2)	28.0(q)	28.0
24	0.74 (3H, s)	15.4(q)	15.4
25	0.80 (3H, s)	16.1(q)	16.1
26	0.95(3H, s)	15.9(q)	16.0
27	1.00 (3H, s)	14.5(q)	14.6
28	0.90 (3H, s)	18.0(s)	18.0
29	4.66 (1H, s); 4.55 (1H, s)	109.3(t)	109.3
30	1.66 (3H, s)	19.3(q)	19.3

II.2.1.4.1. Identification of DMF31 (Betulinic acid)

DMF31 was isolated as a white powder, in the *n*-Hex/EtOAc mixture (3/1). Soluble in chloroform, it gave positive reaction in Liebermann Burchard test characteristic of triterpenoids. Its HRESI mass spectrum (Figure 46) showed the pseudo molecular ion peak $[M+H]^+$ at *m/z* 457.3721 compatible with the molecular formula $C_{30}H_{48}O_3$ containing 7 degrees of unsaturation.

The comparison of the ^{1}H and ^{13}C NMR spectra of compound DMF31 (Fig 47 and 48, respectively) with those of compound DMB32 showed close similarities including the presence

of two olefinic protons at δ_H 4.93/δ_C 109.5 and δ_H 4.76/δ_C 109.5, a downed methyl group at δ_H 1.78/δ_C 19.5, a vinylic methine at δ_H 3.52/δ_C 49.7 and an oxymethine proton H-3 of triterpenoids at δ_H 3.44/δ_C 78.1, indicating that compound DMF31 as compound DMB32 was a pentacyclic triterpene of the lup-20(29)-ene series.

The only difference between the two compounds was the disappearance of signals corresponding to the C-28 quaternary methyl group in compound DMF31 NMR spectra, which was replaced by a carboxylic acid function resonating at δ_H 12.4/δc 177.2. All these ^{1}H- and ^{13}C- NMR data (Table 24) were in accordance with those described in the literature for betulinic acid **(120)** (Siddiqui *et al.*, 1988).

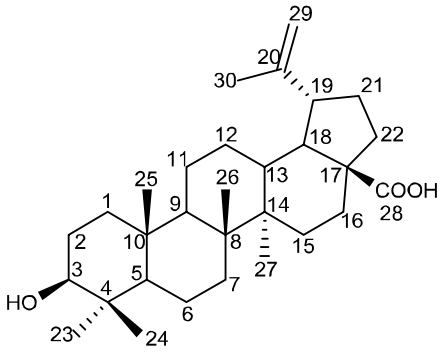

(120)

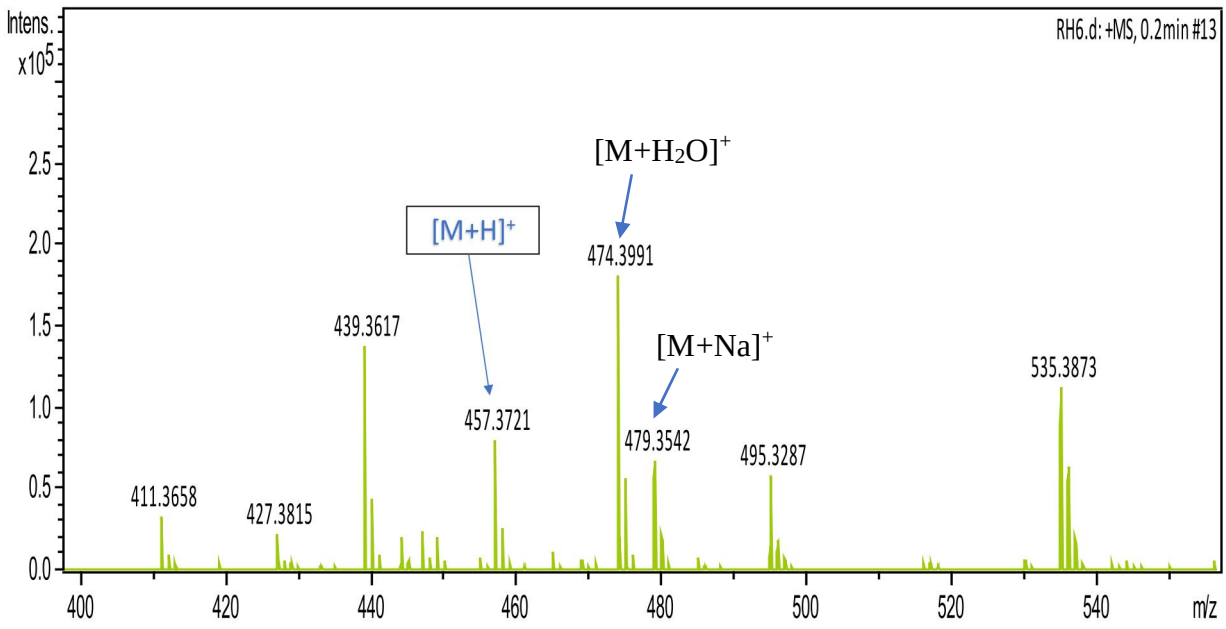

Figure 46 : HR-ESI-MS spectrum of DMF31

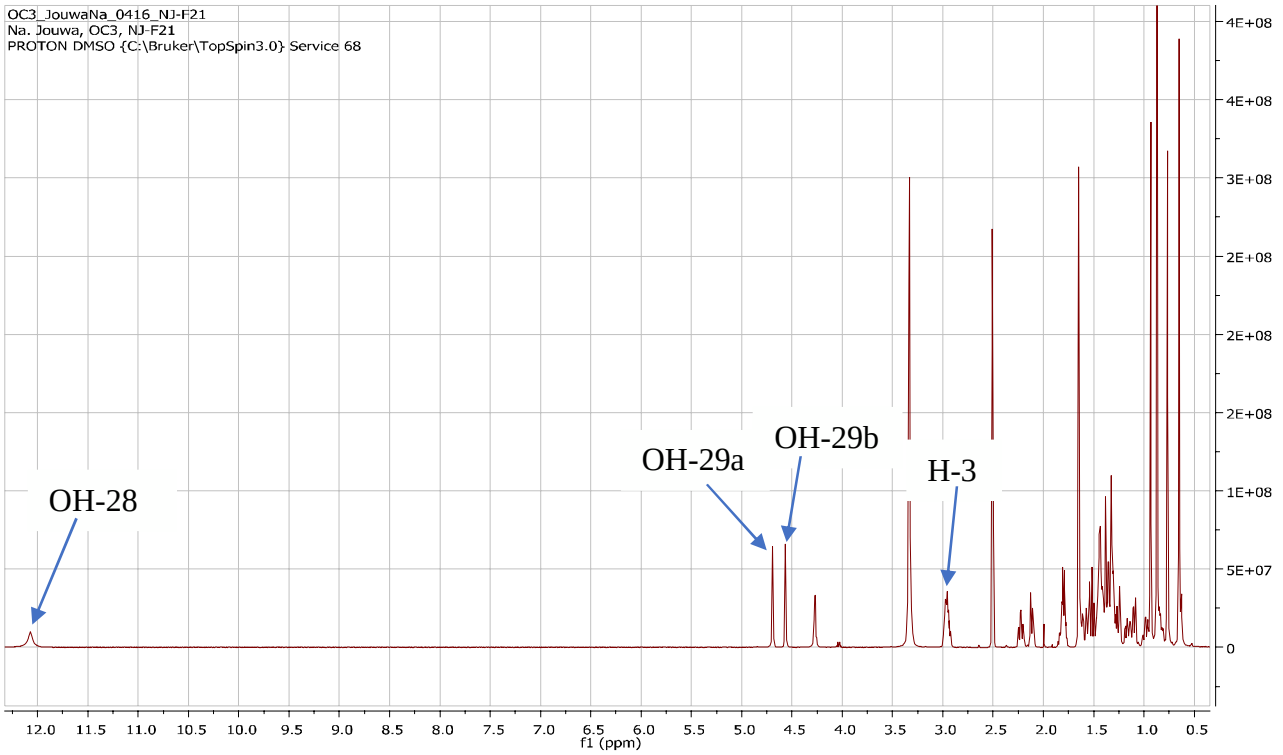

Figure 47 : ^{1}H-NMR spectrum (500 MHz, C_5D_5N) of DMF31

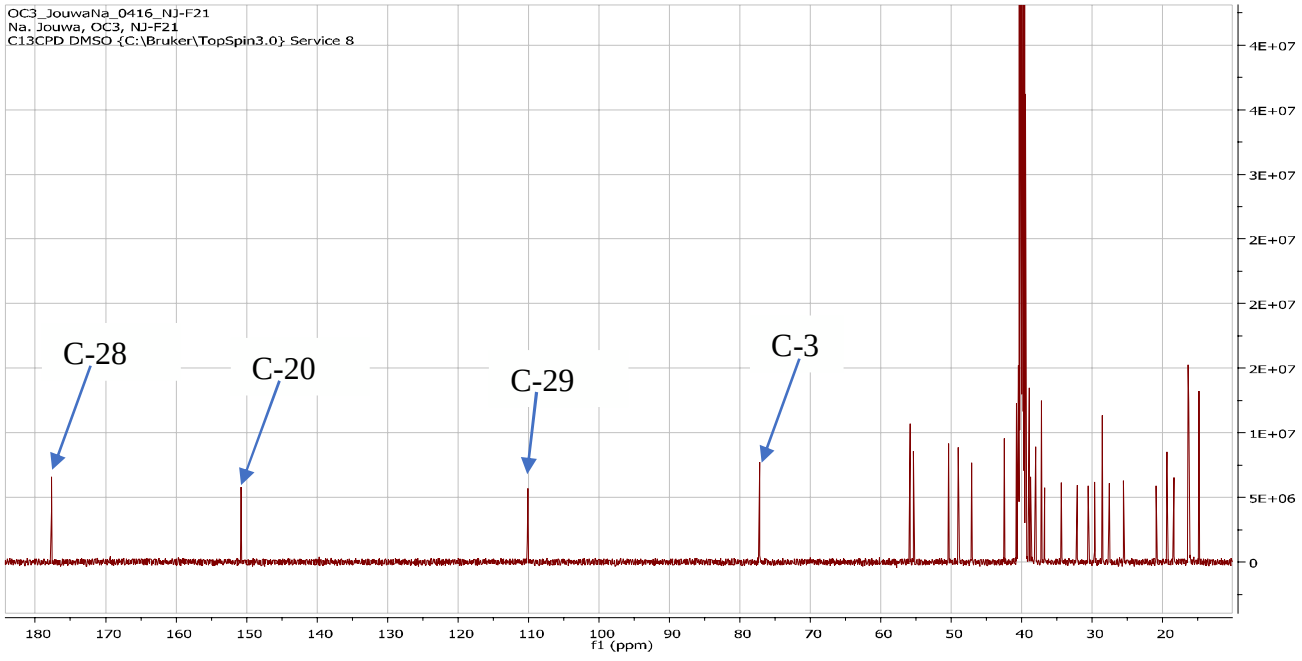

Figure 48 : ^{13}C-NMR spectrum (500 MHz, C_5D_5N) of DMF31

Table XXIV: ^{1}H NMR (400 MHz, $CDCl_3$), and ^{13}C NMR (125 MHz, $CDCl_3$) spectral data of DMF31

Position	δ_H in ppm (nH, m, *J* en Hz)	δc in ppm (m)	δc in ppm (Siddiqui *et al*., 1988)
1	1.47 (1H, m); 1.37 (1H, m)	38.5(t)	38.7
2	2.20 (1H, m); 2.14 (1H, m)	37.6(t)	37.4
3	3.37 (1H, t)	77.4(d)	78.9
4	-	35.6(s)	38.8
5	-	56.5(d)	55.3
6	1.41 (1H, d) ; 1.36 (1H, d)	32.3(t)	18.3
7	1.45 (1H, m) ; 1.33 (1H, m)	34.3(t)	34.3
8	-	41.0(s)	40.7
9	1.38 (1H, t)	50.4(d)	50.5
10	-	37.4(s)	37.2
11	1.45 (1H, m) ; 1.23 (1H, m)	20.8(t)	20.8
12	1.52 (1H, m) ; 1.39 (1H, m)	25.5(t)	25.5
13	1.45 (1H, m)	37.2(d)	38.4
14	-	42.6(s)	42.4
15	1.45 (1H, m) ; 1.24 (1H, m)	25.6(t)	30.5
16	1.48 (1H, m) ; 1.32 (1H, m)	29.7(t)	32.1
17	-	47.1(s)	56.3
18	1.53 (1H, t)	42.6(d)	46.8
19	1.19 (1H, m)	49.1(d)	49.2
20	-	150.6(s)	150.3
21	1.47 (1H, m) ; 1.28 (1H, m)	28.4(t)	29.7
22	1.49 (1H, m) ; 0.92 (1H, m)	33.3(t)	37.0
23	0.86 (3H, d)	22.2(q)	27.0
24	0.70 (3H, s)	18.3(q)	15.3
25	0.85 (3H, s)	16.0(q)	16.0
26	0.99(3H, s)	16.1(q)	16.1
27	1.03 (3H, s)	14.7(q)	14.7
28		177.2(s)	180.5
29	4.72 (1H, s); 4.59 (1H, s)	109.6(t)	109.6
30	1.67 (3H, s)	19.4(q)	19.4

II.2.1.4.3. Identification of DMF33 (Alphitolic acid)

Compound DMF33 was isolated as white powder, in the *n*-Hex/EtOAc mixture (1/1). It was soluble in chloroform and reacted positively to Liebermann-Burchard's test suggesting its triterpenoid nature. The molecular formula, $C_{30}H_{48}O_4$ with 07 degrees of unsaturation, was deduced from NMR data and its HR-EIMS (figure 49) which showed a molecular ion peak $[M]^+$ at *m/z* 472.3.

The ^{1}H and ^{13}C NMR data of DMF33 (figure 51) were very similar to those of DMF31, suggesting DMF33 to be also a pentacyclic triterpene close to betulinic acid. The only

difference observed between them was the absence of a methylene group at C-2 in DMF33, which was replaced by an oxymethine appearing at δ_H 3.41 (1H, ddd, 4.4, 9.3, 11.3, H-2)/δc 70

By comparing these ^{1}H and ^{13}C NMR data with those previously reported, compound DMF33 was identified as a pentacyclic triterpene **(121)** namely Alphitolic acid (Aguirre *et al.*, 2006).

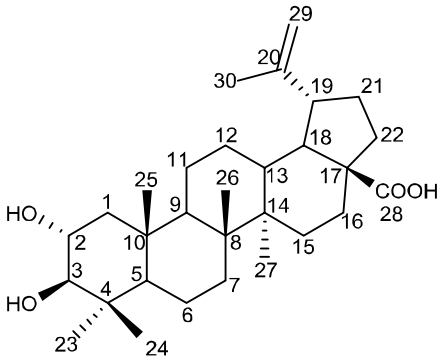

(121)

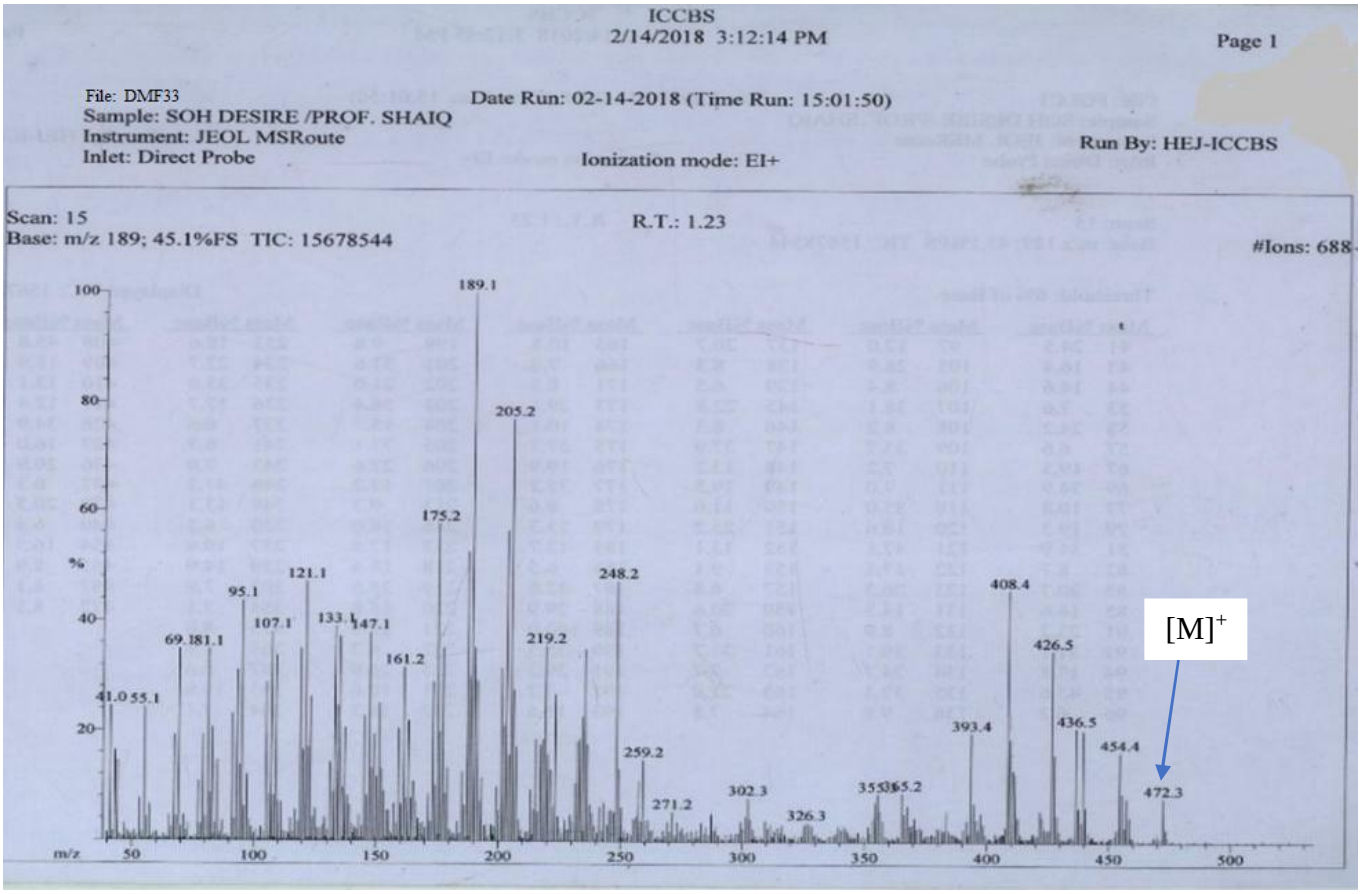

Figure 49 : Mass spectrum of DMF33

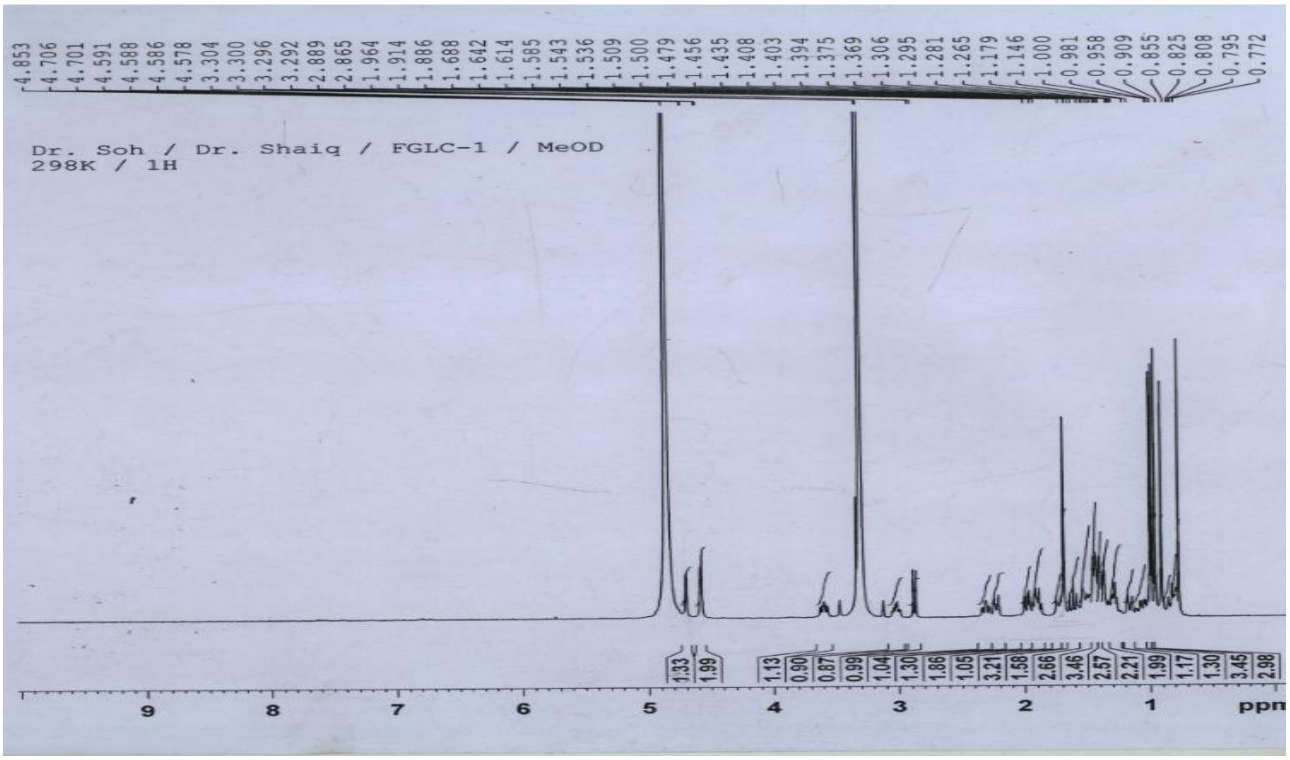

Figure 50 : ^{1}H NMR (400MHz, MeOD) spectrum of DMF33

Figure 51:

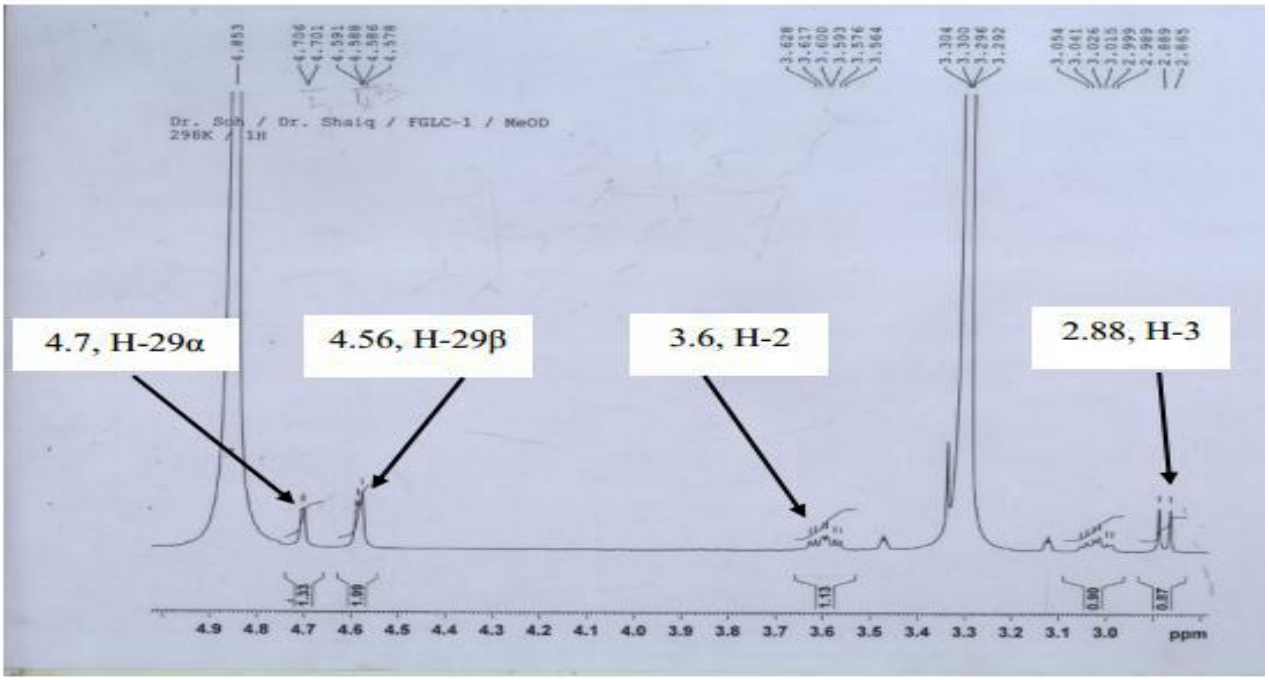

Figure 51 : Expended ^{1}H NMR spectrum (400MHz, MeOD) of DMF33

Table XXV: ^{1}H NMR (500 MHz, MeOD), and ^{13}C NMR (125 MHz, MeOD) spectral data of compound DMF33.

Position	DMF33		(Aguirre *et al* 2006) DMSO-d_6	
	δ_H (nH, m, *J* in Hz)	δ_C in ppm (m)	δ_H (nH, m, *J* in Hz)	δ_C (ppm)
1		48.1(t)		47.5
2	3.60 (1H, ddd, 4.4, 9.3, 11.3)	70.0(d)	3.51 (1H, ddd, 4.4, 9.3, 11.3)	67.8
3	2.81 (1H, d, 9.3)	84.1(d)	2.72 (1H, d, 9.3)	82.6
4		40.3(s)		39.4
5		56.5(d)		55.3
6		17.6(t)		18.4
7		38.1(t)		34.3
8		40.2(s)		40.7
9		49.8(d)		50.3
10		40.5(s)		38.3
11		20.9(t)		21.0
12		26.1(t)		25.4
13	2.26 (1H,ddd, 3.4, 12.7, 12.7)	40.2(d)	2.22 (1H,ddd, 3.4, 12.7, 12.7)	38.0
14		42.0(s)		42.5
15		31.4(t)		30.6
16		33.1(t)		32.1
17		53.9(s)		55.8
18	1.52 (1H, t, 11.3)	51.8(d)	1.52 (1H, t, 11.3)	49.0
19	2.93 (1H, m)	50.0(d)	2.96 (1H, m)	47.1
20		151.2(s)		150.7
21		31.5(t)		29.6
22		34.7(t)		36.7
23	0.90 (3H, s)	30.4(q)	0.90 (3H, s)	29.1
24	0.68 (3H, s)	18.1(q)	0.68 (3H, s)	17.3
25	0.82 (3H, s)	18.0(q)	0.82 (3H, s)	17.5
26	0.77 (3H, s)	17.2(q)	0.87 (3H, s)	16.2
27	0.95 (3H, s)	16.1(q)	0.94 (3H, s)	14.8
28		180.1(s)		177.6
29	4.70(1H, d, 1.8, H-29α) 4.56 (1H, d, 1.8, H-29β)	110.0(t)	4.70 (1H, d, 1.8, H-29α) 4.57 (1H, d, 1.8, H-29β)	110.0
30	1.68 (3H, s)	19.7(q)	1.66 (3H, s)	19.4

II.2.1.4.4. Identification of DMF23 (3β,23β-dihydroxylup-20(29)-en-28-oic acid)

DMF23 was isolated as a white powder in a mixture of *n*-Hex/EtOAc (1/1). It was soluble in pyridine and gave positive reaction to the Liebermann Burchard's test characteristic of triterpenoids. The analysis of its HR-ESI-MS showed the pseudo-molecular ion peak $[M+H]^+$ at *m/z* 472.3545 from which the molecular formula $C_{30}H_{48}O_4$ was deduced, containing seven degrees of unsaturation.

These molecular formula and degrees of unsaturation were identical to those of compound DMF33 described above, indicating that compounds DMF23 and DMF33 had the same skeleton. Comparison of their ^{1}H and ^{13}C NMR data (Figure 53 and 54) revealed very close similarity. The main difference observed between the two compounds was the presence of five methyl group signals in DMF23 instead of six presented by NMR data of DMF33.The remaining methyl group were replaced by an oxymethylene appearing at δ_H/ δ_C 3.89 (d, 11.4)/ 71.9; 3.70 (d, 11.4)/ 71.9. By comparing these data with those previously reported in the literature, compound DMF23 was identified as 3*β*,23*β*-dihydroxylup-20(29)-en-28-oic acid (Valencia-Chan et *al*., 2017).

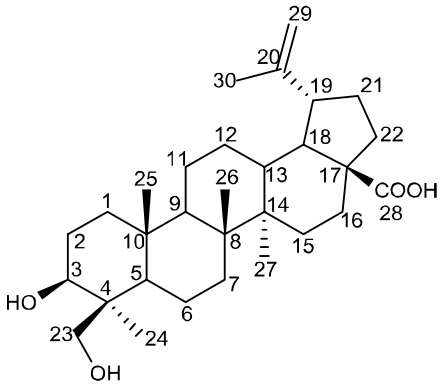

(122)

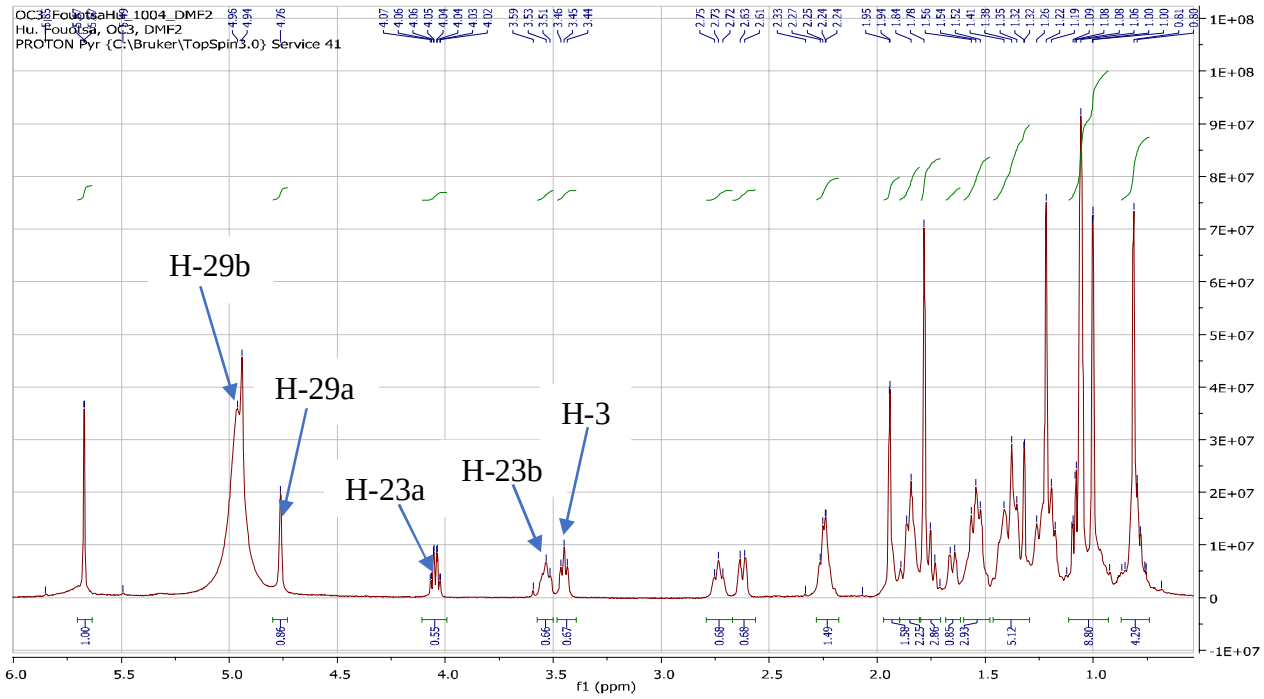

Figure 52 : ^{1}H NMR spectrum (500 MHz, C_5D_5N) of DMF23

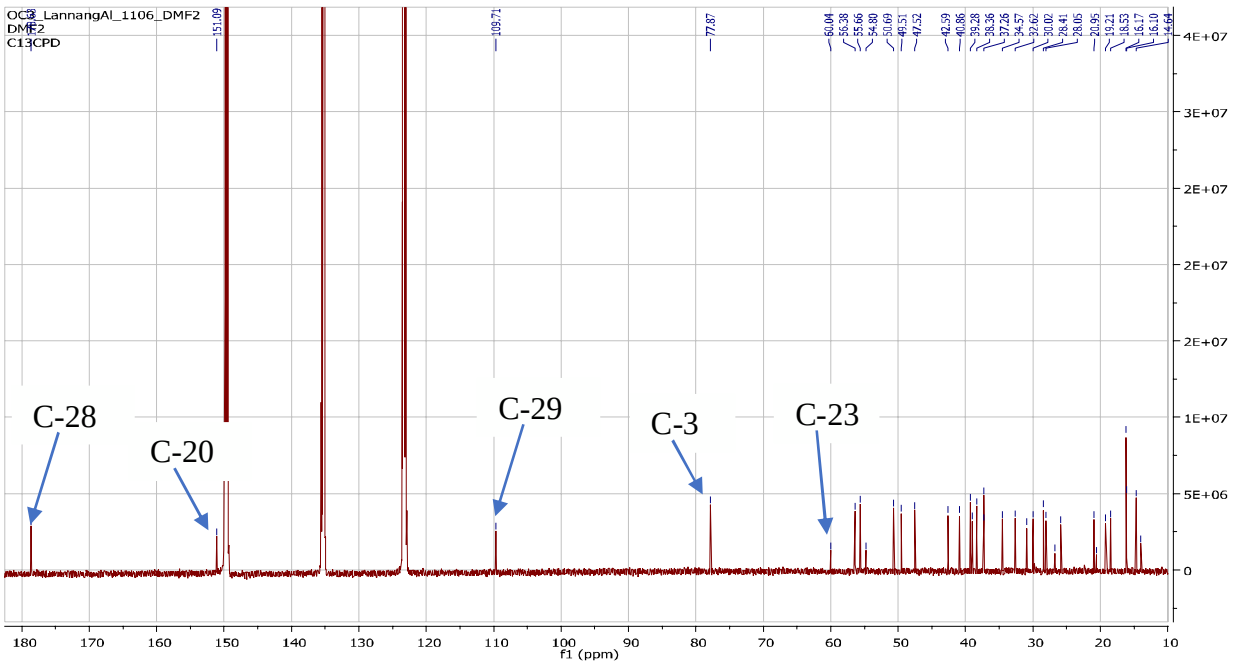

Figure 53 : ^{13}C NMR spectrum (125 MHz, C_5D_5N) of DMF23

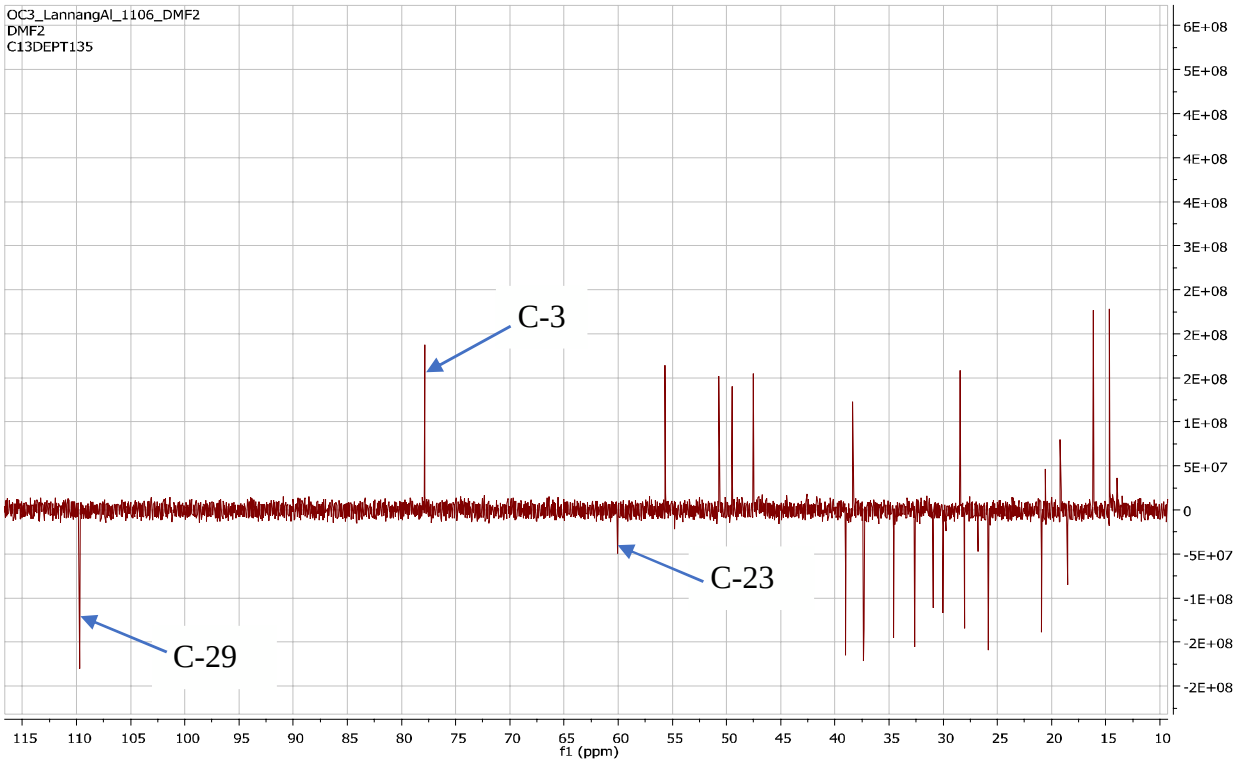

Figure 54 : DEPT 135 spectrum of DMF23

Table XXVI : ^{1}H NMR (500 MHz, C_5D_5N), and ^{13}C NMR (125 MHz, C_5D_5N) spectral data of compound DMF23

Position	DMF23		(Valencia-Chan et *al*., 2017) C_5D_5N 125 MHz
N°	δ_H (mult., *J* in Hz)	δ_C (m)	δ_C
1a 1b	1.79, m 1.37, m	34.2(t)	34.2
2a 2b	1.97, m 1.76, m	27.2(t)	27.6
3	3.95, br	76.3(d)	75.8
4	-	41.3(s)	41.8
5	2.12, d, 12	44.2(d)	44.4
6a 6b	1.59, m 1.39, m	18.9(t)	19.0
7a 7b	1.63, m 1.35, m	35.0(t)	35.4
8	-	41.8(s)	41.2
9	1.65, t, 11.4	51.4(d)	52.1
10	-	38.1(s)	38.2
11a 11b	1.51, m 1.22, m	21.7(t)	21.7
12a 12b	1.95, m 1.19; m	33.3(t)	33.5
13	2.74, t, 12	39.1(d)	38.9
14	-	43.4(s)	43.7
15a 15b	1.86, t, 13.2 1.21, d, 13.2	30.7(t)	30.7
16a 16b	2.61, d, 12.6 1.48, m	33.7(t)	34.0
17	-	57.1(s)	57.6
18	1.70	50.2(d)	50.3
19	3.55, m	48.3(d)	48.5
20	-	151.8(s)	149.9
21a 21b	2.25, m 1.51, m	31.7(t)	32.7
22a 22b	2.25, m 1.59, m	38.0(t)	36.8
23a 23b	4.04, d, 11.4 3.59, d, 11.4	71.9(t)	72.0
24	0.78, s	18.5(q)	18.7
25	0.89, s	17.0(q)	17.3
26	0.99, s	15.4(q)	14.8
27	1.22, s	17.1(q)	17.5
28	-	179.4(s)	178.8
29a 29b	4.76, br s 4.94, br s	110.4(t)	109.9
30	1.79, s	19.9(q)	19.5

II.2.1.4.5. Identification of DMF32 (ursolic acid)

Compound DMF32 was isolated as a white powder in a mixture of *n*-Hex/EtOAc (13/7). It is soluble in pyridine and responds positively to the Liebermann Burchard's test characteristic of triterpenoids. The analysis of its HRESIMS (Figure 55) showed the pseudo-molecular ion peak $[M+H]^+$ at *m/z* 457.3731 from which the molecular formula $C_{30}H_{48}O_3$ was deduced, containing seven degrees of unsaturation.

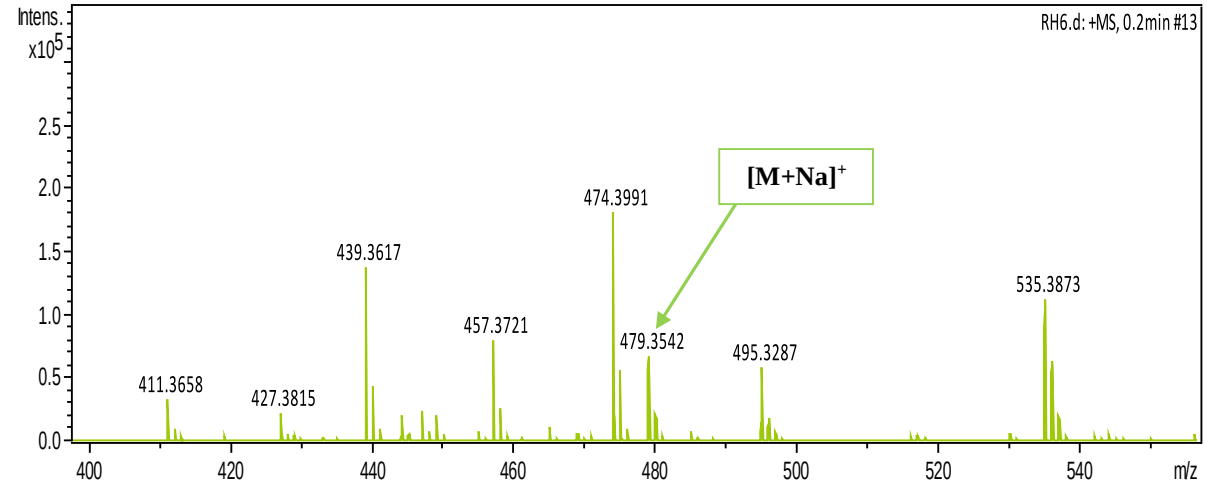

Figure 55 : HR-ESI-MS spectrum of DMF32

The ^1H and ^{13}C NMR spectral data of this compound (Figure 56 and 57, respectively) displayed signals for seven methyl groups in the region δ_H 0.88 - 1.24 among which five angular methyls and two secondary one at δ_H 0.95 (3H, *d*, *J*= 6.2 Hz) / δ_C 21.2 and δ_H 1.00 (3H, *d*, *J* = 6.4 Hz) / δ_C 16.4.

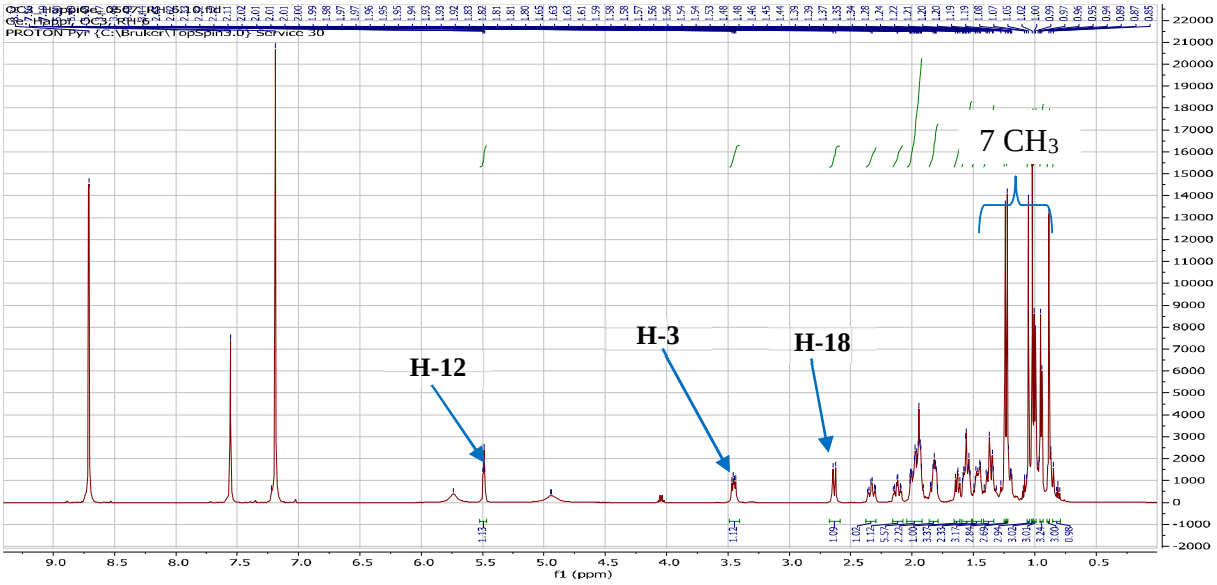

Figure 56 : ^1H NMR spectrum (500 MHz, C_5D_5N) of DMF32

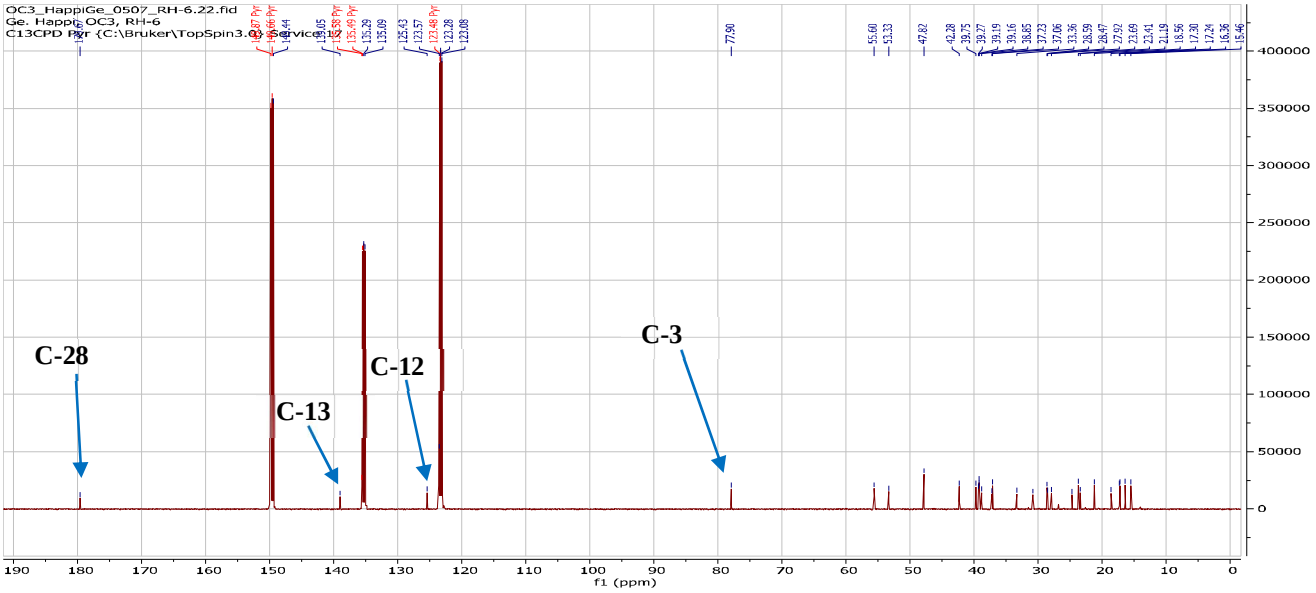

Figure 57 : ^{13}C NMR spectrum (125 MHz, C_5D_5N) of DMF32

These NMR spectra also showed the presence of one olefinic proton at δ_H 5.49 (dd, J = 10.4, 5.6 Hz) / δ_C 125.4, one allylic proton at δ_H 2.63 (d, J = 11.1 Hz) / δ_C 53.3, and signals for two olefinic sp^2 carbons at δ_C 125.4 and δ_C 139.1 characteristic of a pentacyclic triterpene belonging to the urs-12-ene series (Table 26). In addition to the urs-12-ene skeleton signals, an hydroxymethine at δ_H 3.45 (dd, J = 10.1, 5.8 Hz) / δ_C 77.9 and a carboxylic group at δ_C 179.7 were also observed.

From the above spectroscopic data, compound DMF32 was identified as ursolic acid **(122)**, a known compound previously isolated from *Arctostaphylos uva-ursi* **(Mahato and Kundu, 1994)**.

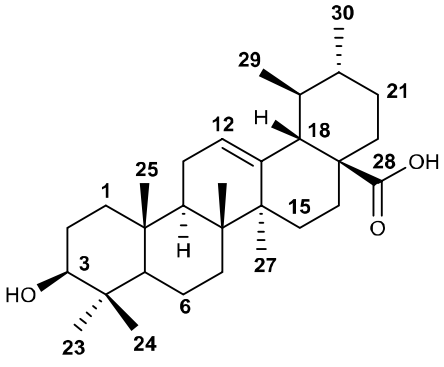

(123)

Table XXVII : ^{1}H NMR (500 MHz, C_5D_5N) and ^{13}C NMR (125 MHz, C_5D_5N) spectral data of DMF32

Position	DMF32		(Mahato and Kundu, 1994) CD_3OD 125 MHz
	δ_H (nH, m, *J* in Hz)	δ_C (m)	δ_C
1	1.55 (2H, dd, 14.0 and 6.5)	38.9(t)	39.8
2		27.9(t)	27.9
3	3.45 (1H, dd, 10.1 and 5.8)	77.9(d)	79.7
4		39.2(s)	40.0
5	0.86 (1H, *d*, 11.9)	55.6(d)	56.8
6		18.6(t)	19.5
7		33.4(t)	34.4
8		39.7(s)	40.8
9	1.62 (1H, dd, 17.9 and 10.0)	47.8(d)	47.9
10		37.1(s)	38.1
11		23.4(t)	24.4
12	5.49 (1H, dd, 10.4 and 5.6)	125.4(d)	128.9
13		139.1(s)	139.7
14		42.3(s)	43.3
15	2.33 (2H, td, 13.4 and 4.6)	28.5(t)	29.2
16	2.12 (2H, td, 13.3 and 4.2)	24.7(t)	25.3
17		47.8(s)	47.9
18	2.63 (1H, d, 11.3)	53.3(d)	54.4
19		39.3(d)	40.5
20		39.2(d)	40.4
21		30.9(t)	31.8
22		37.2(t)	38.1
23	1.24 (3H, s)	28.6(q)	28.8
24		17.3(q)	16.4
25		15.5(q)	16.0
26		17.2(q)	17.7
27	1.22 (3H, s)	23.7(q)	24.1
28		179.7(s)	181.8
29	1.00 (3H, d, 6.4)	16.4(q)	17.8
30	0.95 (3H, d, 6.2)	21.2(q)	21.6

II.2.1.5. Steroïdes

II.2.1.5.1. Identification of DMF21 (mixture of *β*-sitosterol and stigmasterol)

Compound DMF21 was isolated in the form of white needles in the hexane-ethyl acetate mixture (9: 1). Soluble in chloroform, it melts between 123 and 124 °C and responds positively to the Liebermann Burchard test by giving a blue coloration which quickly turns dark green, characteristic of sterols.

This compound was identified to be a mixture of stigmasterol and *β*-sitosterol 124 using its NMR data and mass spectrum. Indeed, on its ^{1}H NMR spectrum (Figure 58), we

observed on the one hand, the signals of H-6 and H-3 protons of these phytosterols at δ_H 5.30 and 3.52 respectively, and on the other hand, the signals of H-22 and H-23 protons of the stigmasterol at δ_H 5.10 and 5.14 respectively. This was corroborated by ^{13}C NMR spectrum which exhibited olefinic carbon signals at δ_C 140.7 and 121.7 (C-5 and C-6 respectively), and the signals at δ_C 138, 3 and 129.3 for the stigmasterol corresponding to carbons C-22 and C-23 respectively. We also observed the signal of oxymethyne carbons at δ_C 71.8 attributable to carbon C-3 (Pateh et al., 2009). The other signal values compared to those found in the literature led to the structures below which are those of stigmasterol and *β*-sitosterol (124).

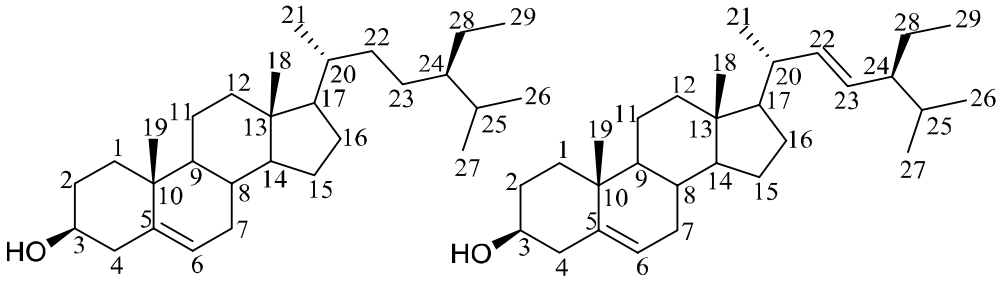

(124)

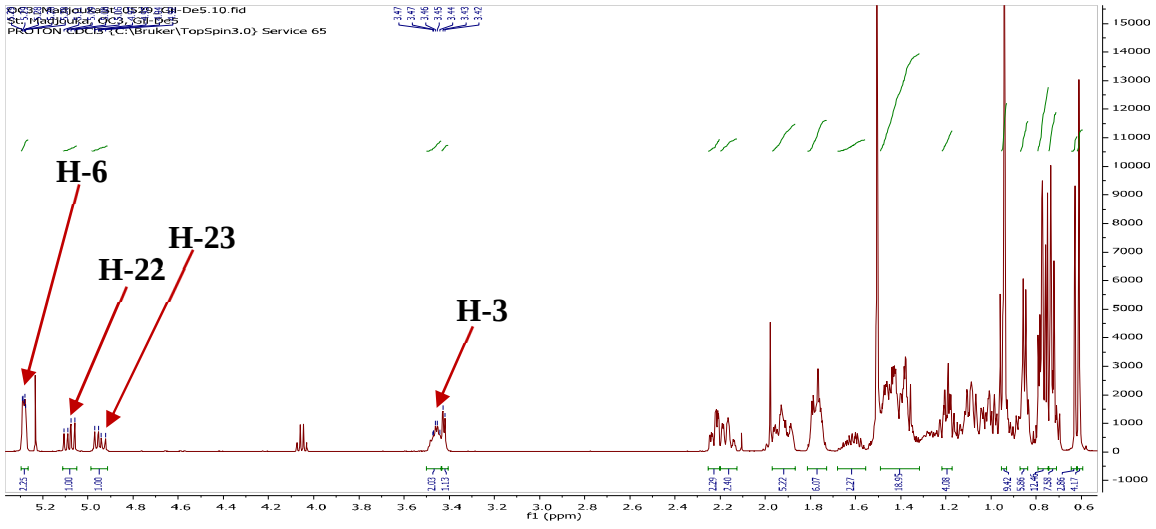

Figure 58 : ^{1}H NMR spectrum (500 MHz; CDCl3) of DMF21

II.2.1.5.2. Identification of DMf42 (*β*-sitosterol glucoside)

DMf42 was obtained as colorless crystals in the Hex/EtAcO mixture (25:75). Soluble in pyridine, it melts between 260-261 °C and responds positively to the Molish and Liebermann Burchard tests. This result suggests that the compound DMf42 is a glycosylated compound. The molecular formula, $C_{35}H_{60}O_6$, implying six degrees of unsaturation was determined on the

basis of NMR spectra data and the HRESI mass spectrum, which showed a pseudo molecular ion peak $[M+Na]^+$ at *m/z* 599.4279.

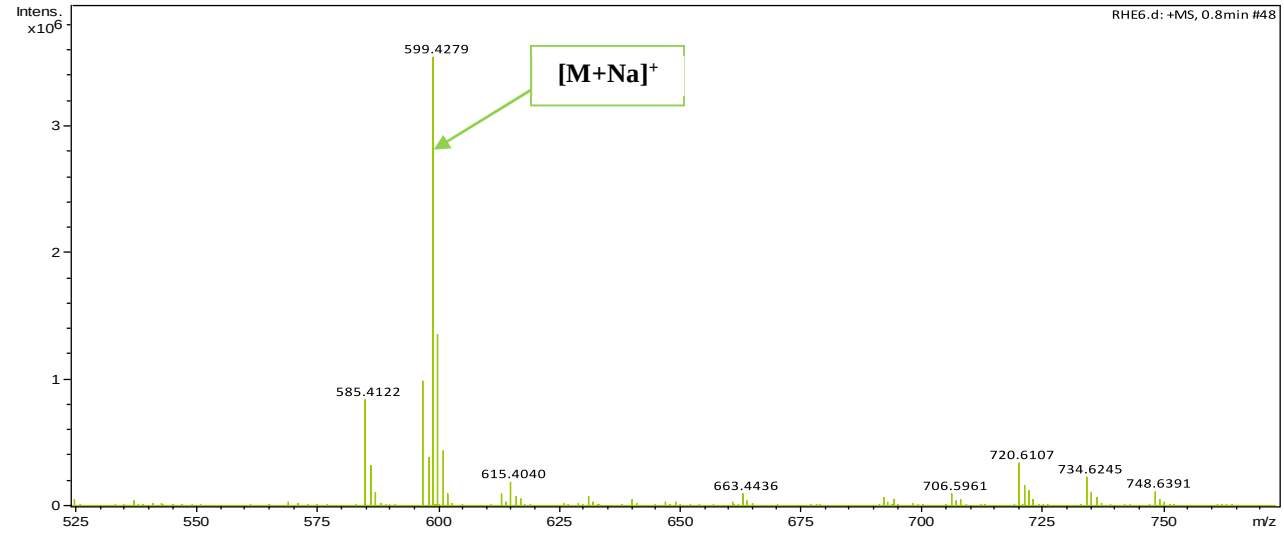

Figure 58 : HR-ESI-MS spectrum of DMf42

The broadband proton decoupled ^{13}C NMR spectrum recorded in the pyridine-d_5 (Figure 59) of this compound, presents two (02) categories of signals:

The first category, consisting of twenty-nine (29) resonant carbon signals between δ_C 12.4 and 141.7 including two (02) sp^2 hybridized carbon signals at δ_C 123.3 and 141.7 and one carbon signal oxygenated hybridized sp^3 at δ_C 80.3, the rest of the signals appearing between δ_C 12.9 and 58.2 are attributable to the signals of the carbons of a β-sitosterol type aglycone.

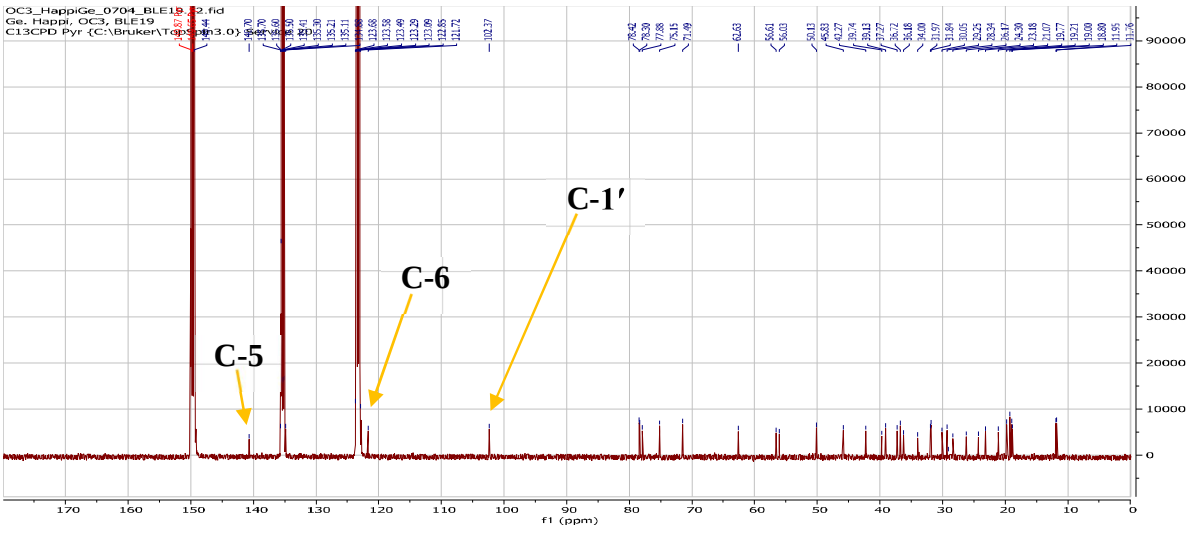

Figure 59 : ^{13}C RMN spectrum (125 MHz, C_5D_5N) of DMf42

This was confirmed by its ^1H NMR spectrum (Figure 60) on which we observed, among other things, a signal from an ethylenic proton at δ_H 5.37 characteristic of the H-6 proton and an oxymethine signal. at δ_H 3.59 characteristic of the H-3 proton.

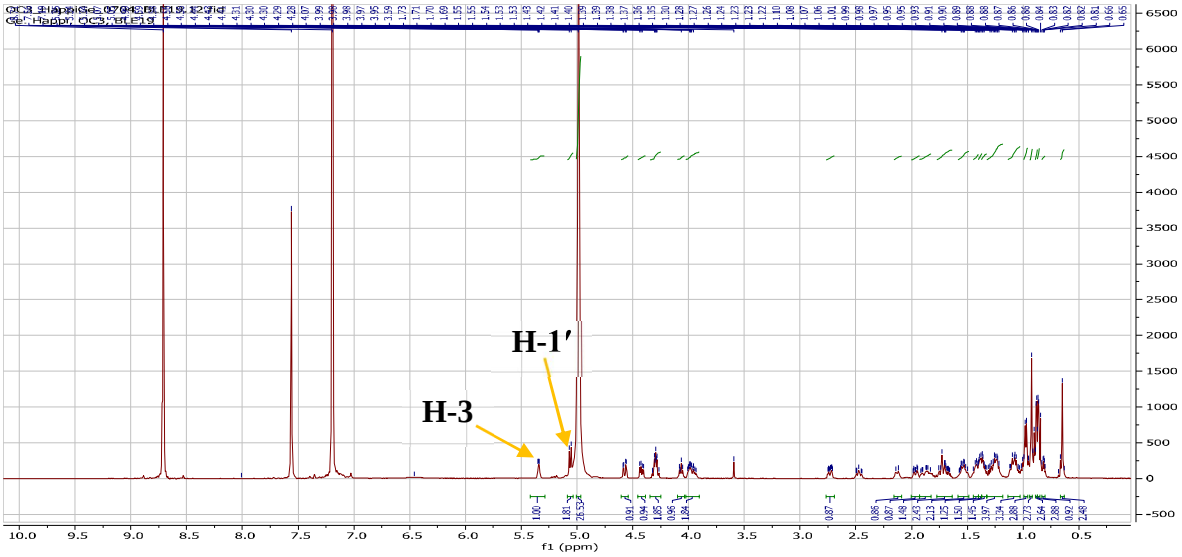

Figure 60 : ^{1}H NMR spectrum (500 MHz, C5D5N) of compound DMf42

The second category of carbon signals consists of six (06) peaks whose chemical shifts vary from δ_C 63.0 to 102.5 corresponding to an osidic unit of the hexose type. Comparison of these chemical shifts with those in the literature (Viswanah *et al*., 2006) indicates that it is glucose. This was also confirmed by its 1H NMR spectrum on which we observed the protons of oxymethines and methylenes resonating between δ_H 2.28 and 4.44.

All these data, compared to those reported in the literature (Viswanagh *et al*., 2006), allowed the identification of the compound DMf42 as being the 3-*O*-*β*-*D*-glucopyranoside of *β*-sitosterol (125).

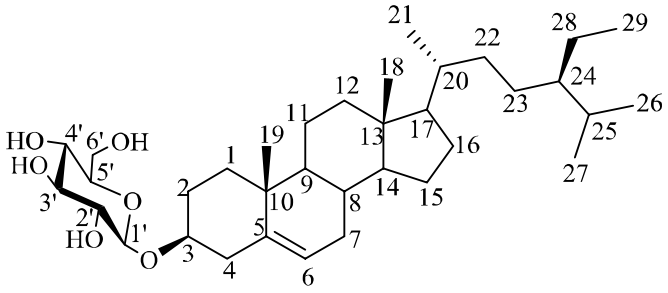

(125)

II.2.1.5.3. Identification of DMG33 (stigmasterol glucoside)

Compound DMG33 was isolated in the form of a white powder in the Hex / AcOEt mixture (40: 60). Soluble in pyridine, it melts between 274-276 °C and responds positively to the tests of Molish and Liebermann Burchar. Its ^{1}H and ^{13}C NMR spectra (Figure 61 and 62) shows the characteristic peaks of a sterol glucoside. Its broadband proton decoupled ^{13}C NMR spectrum is almost superimposable to that of DMf42. Similarities are observed in the following characteristic signals: the $\Delta^{5,6}$ double bond at δ_C 141.7 and 123.3, the C-3 oxymethine at δ_C 80.3, as well as the signals at δ_C 51.6; 58.1 and 57.4 corresponding to carbon C-9, C-14 and C-17 respectively. The only difference is observed in the presence of signals attributable to the $\Delta^{22,23}$ bond at δ_C 138.7 and 130.6. All of these data compared to those found in the literature confirm the structure below which is that of stigmasterol glucoside (**126**).

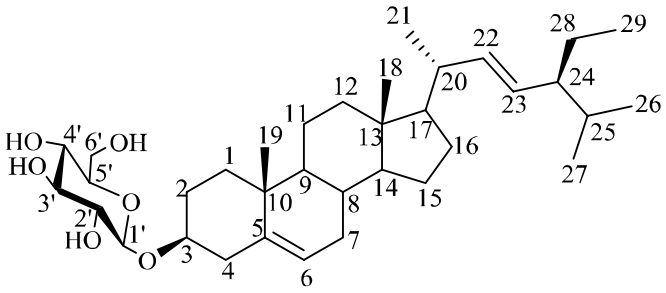

(126)

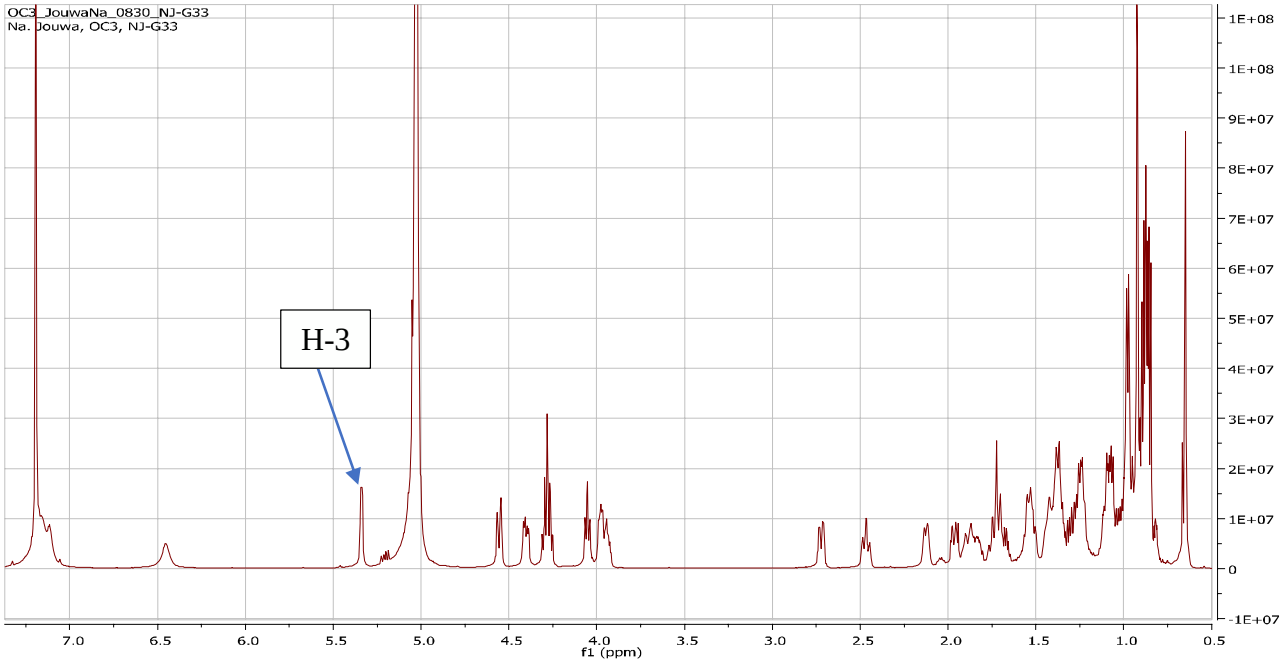

Figure 61 : ^{1}H RMN spectrum (500 MHz, C_5D_5N) of compound DMG33

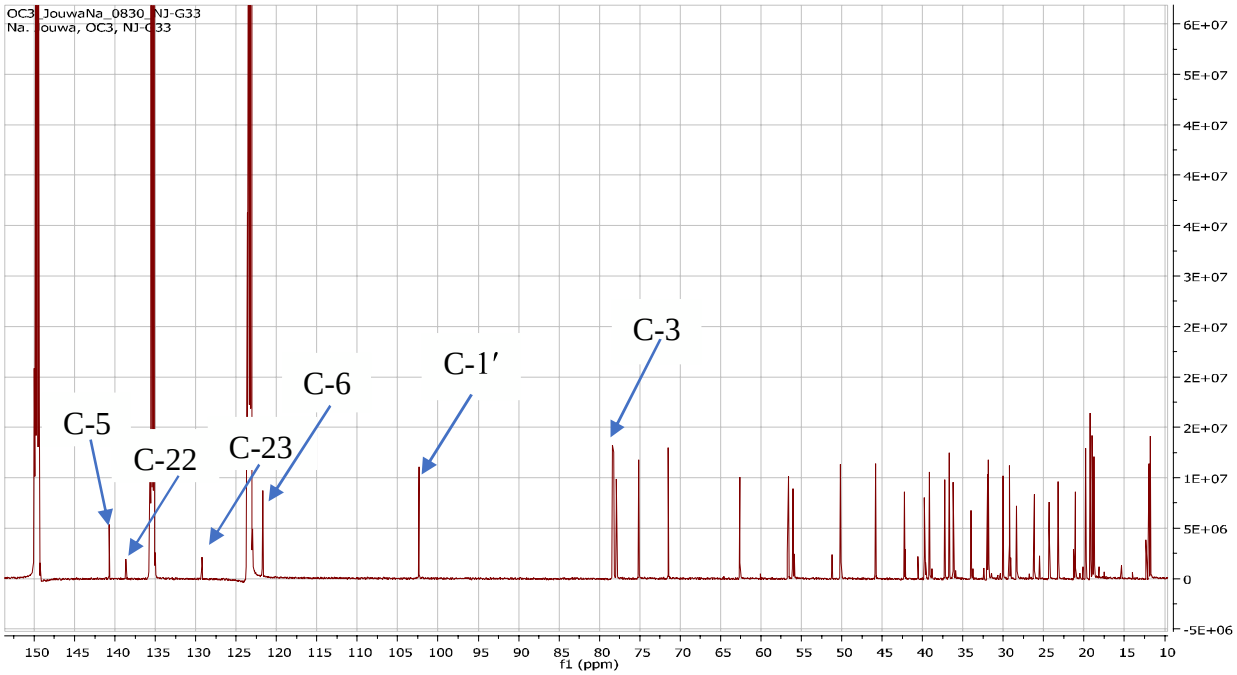

Figure 62 : ^{13}C RMN spectrum (125 MHz, C_5D_5N) of compound DMG33

Table XXVIII : ^{1}H NMR (500MHz, C_5D_5N) and ^{13}C NMR (125MHz, C_5D_5N) Spectral data of compounds DMf42 and DMG33.

Position	DMG33 **(stigmasterol glucoside)**		DMf42 **(*β*-sitosterol glucoside)**	
	^{1}H (ppm) (mult., *J* en Hz)	**^{13}C (ppm)**	**^{1}H (ppm) (mult., *J* en Hz)**	**^{13}C (ppm)**
1		38.6		38.0
2		35.2		30.9
3	3.59 (1H, m)	80.3	3.80 (1H, m)	80.3
4		43.6		43.5
5		141.7		141.7
6	5.37 (t, 6.1)	123.3	5.38 (t, 6.4)	123.3
7		30.4		30.3
8		30.4		30.3
9		51.6		51.6
10		35.2		35.0
11		22.3		22.3
12		39.9		39.9
13		43.6		43.5
14		58.2		58.1
15		26.7		25.6
16		30.2		29.5
17		57.4		57.3
18	0.72 (s)	12.9	0.70 (s)	12.9
19	1.03 (s)	20.0	0.93 (s)	20.5
20		41.9		37.4
21	0.86 (d)	22.4	084 (d, 6.3)	22.3

22	5.14 (dd, 12.0, 8.0)	139.7	4.51 (m)	33.2
23	5.03 (dd, 12.0, 8.0)	129.6	5.14 (m)	25.6
24		52.7		47.2
25		33.2		30.4
26	0.82 (d, 6.6)	22.3	0.83 (d, 6.4)	22.3
27	0.80 (d, 6.6)	20.8	0.81 (d, 6.4)	20.4
28		24.3		22.4
29		13.3		13.2
1'	4.44 (d, 7.8)	102.5	4.40 (d, 7.8)	102.5
2'	3.31 (m)	77.9	3.29 (m)	74.9
3'	3.62 (m)	77.9	3.58 (m)	77.4
4'	3.31 (m)	71.6	3.30 (m)	71.6
5'	3.39 (m)	80.3	3.35 (m)	77.4
6'	2.28 (m)	63.0	2.39 (m)	63.0

II.2.1.5.4. Identification of DMB31 (stigmasterol)

Compound DMB31 was obtained as colorless needles (85:15 *n*-Hexane/EtOAc), mp 137─138 °C. It reacted positively to the Liebermann-Burchard test for steroids (blue -violet colour). The molecular formula, $C_{29}H_{48}O$, implying five degrees of unsaturation was determined on the basis of NMR spectra data and the HRESI-MS, which showed a molecular ion peak $[M+H]^+$ at *m/z* 412.3452 with further fragment peaks which are characteristically attributed to stigmasterol. Its ^{13}C NMR spectrum shows signals attributable to the $\Delta^{22,23}$ bond at δ_C 138.4 and 129.4. Its ^1H NMR spectrum (Figure 63), we observe the presence of the signal of the proton H-3 at δ_H 3.51 in the form of a multiplet and that of the olefinic proton H-6 appearing at δ_H 5.35 also in the form of a triplet. The presence of the signals of six methyls were observed respectively at δ_H 1.03; 0.92; 0.83; 0.82; 0.80 and 0.71. All of these data compared to those found in the literature confirm the structure below which is that of stigmasterol (**127**).

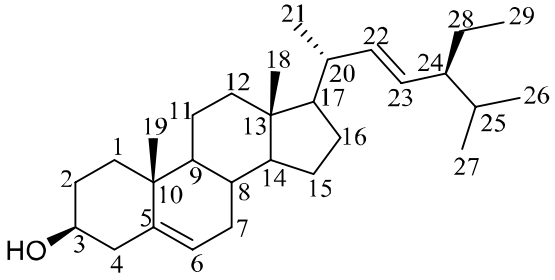

(127)

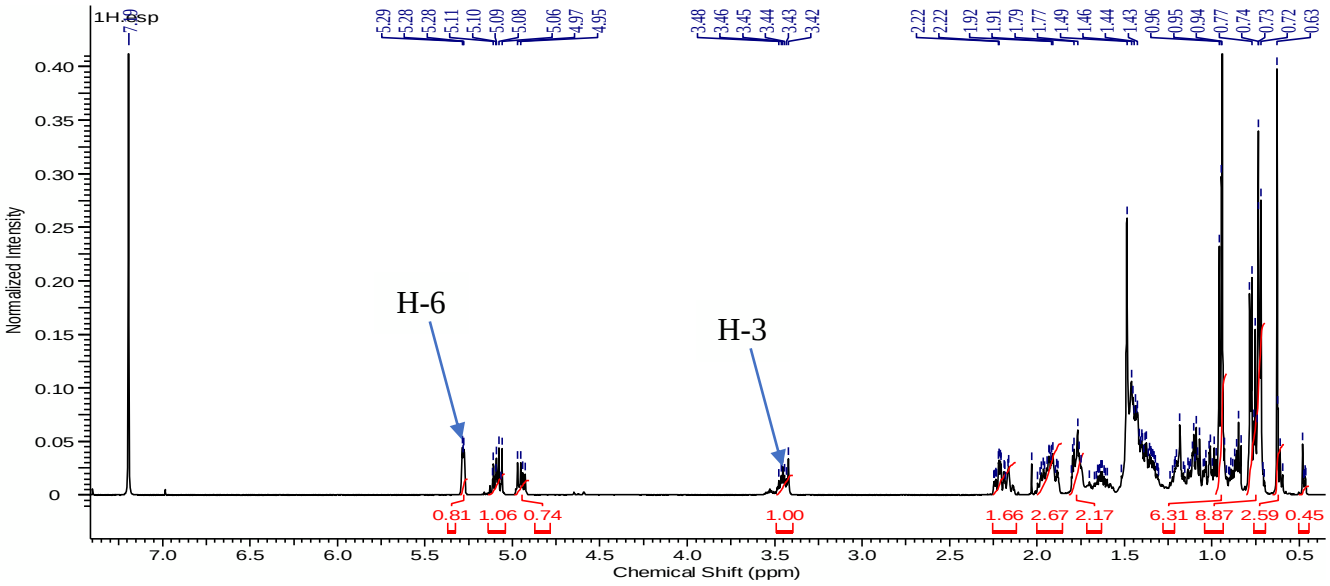

Figure 63 : ^{1}H NMR spectrum (500 MHz, $CDCl_3$) of DMB31

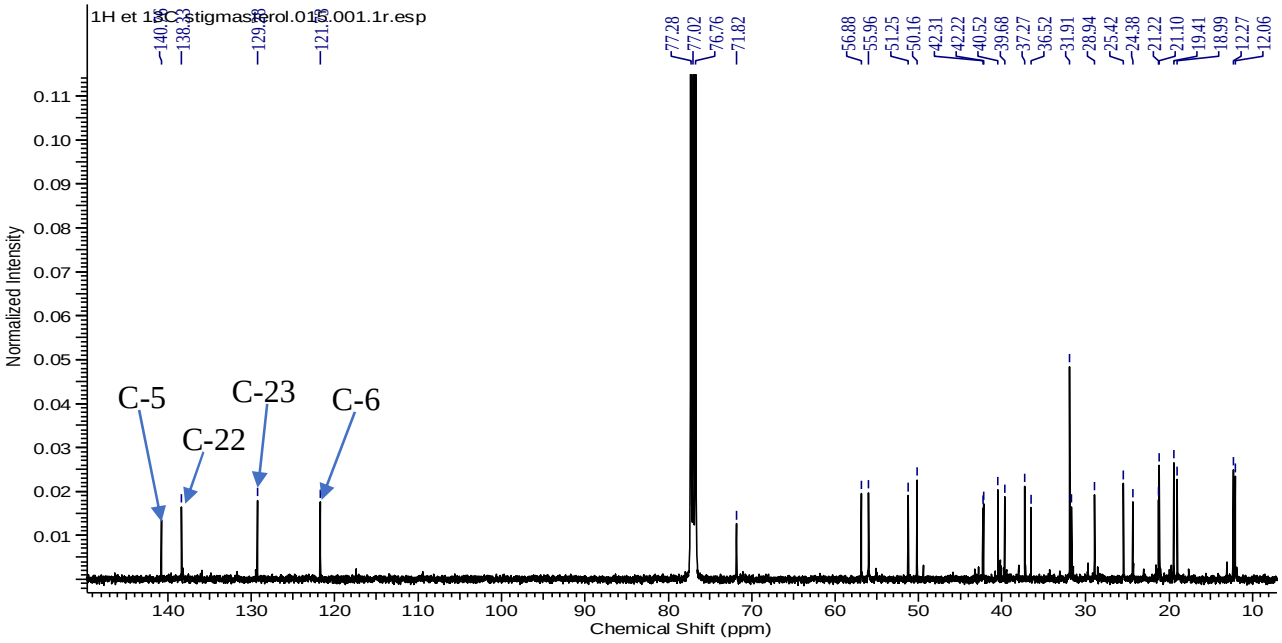

Figure 64 : ^{13}C NMR spectrum (125 MHz, $CDCl_3$) of DMB31

II.2.1.5.5. Identification of DMG11 (*β*-sitosterol)

Compound DMG11 was isolated in the form of a white powder from the Hex/EtOAc solvent system (19: 1). It gives a blue-green coloration to the Liebermann-Burchard test characteristic of steroids. Its broadband proton decoupled ^{13}C NMR spectrum is almost superimposable to that of DMB31. Similarities are observed in the following characteristic

signals: the $\Delta^{5,6}$ double bond at δ_C 140.8 and 121.8, the C-3 oxymethine at δ_C 71.8, as well as the signals at δ_C 50.1; 56.7 and 56.0 corresponding to carbon C-9, C-14 and C-17 respectively. The only difference lies in the absence of signals attributable to the $\Delta^{22,23}$ bond generally between δ_C 138 and 128. Moreover, on its ^{1}H NMR spectrum (Figure 65), we observe the presence of the proton signal. H-3 at δ_H 3.51 as a multiplet and that of the olefinic proton H-6 appearing at δ_H 5.33 also as a multiplet. But also, the presence of the signals of six methyls respectively at δ_H 1.00; 0.91; 0.84; 0.81; 0.80 and 0.66. All of these data compared to those found in the literature confirm the structure below which is that of *β*-sitosterol (**128**) (Nyigo et *al.*, 2016).

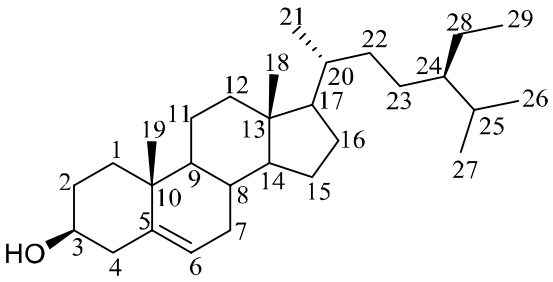

(128)

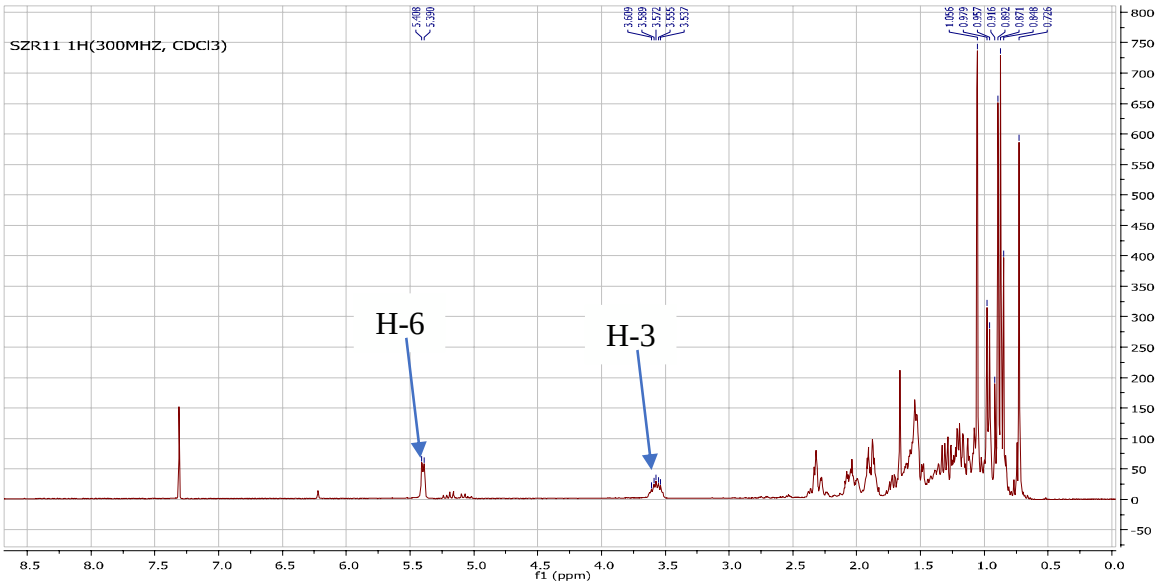

Figure 65 : ^{1}H NMR (500 MHz, $CDCl_3$) spectrum of DMG11

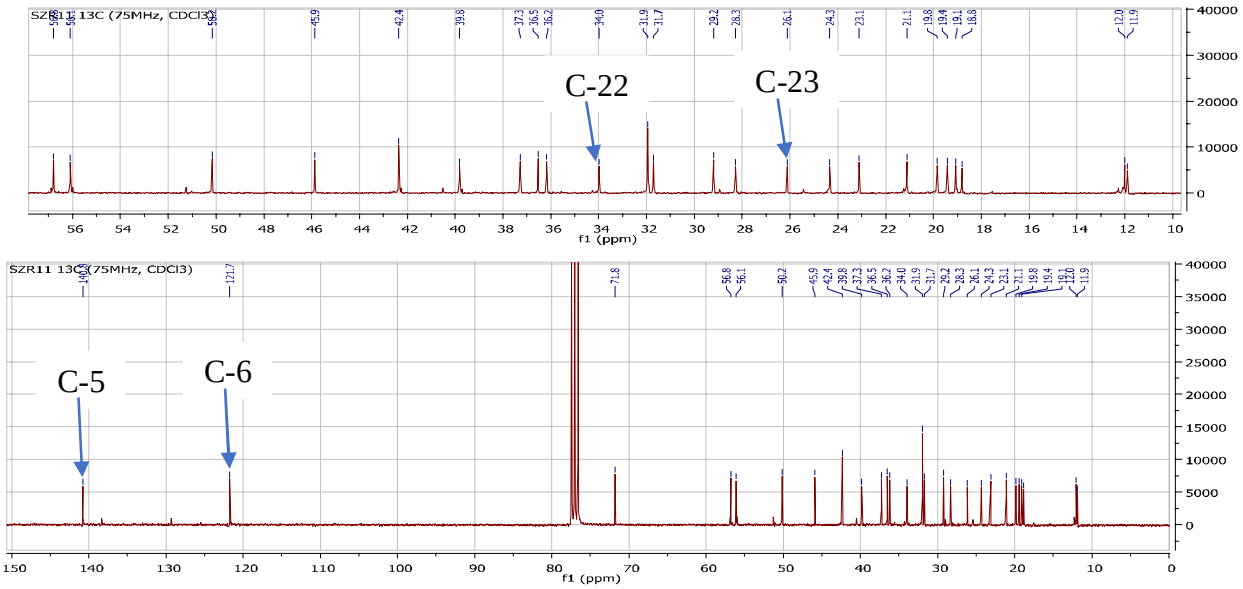

Figure 66 : ^{13}C NMR (125 MHz, $CDCl_3$) spectrum of DMG11

Table XXIX : ^{1}H NMR (500MHz, $CDCl_3$) and ^{13}C NMR (125MHz, $CDCl_3$) Spectral data of compounds DMB31 and DMG11

Position	DMB31 (stigmasterol)		DMG11 (*β*-sitosterol)	
	δ ^{13}C	δ ^{1}H (mult., *J* en Hz)	δ ^{13}C	δ ^{1}H (mult., *J* en Hz)
1	37.1		37.3	
2	31.7		31.7	
3	71.8	3.51 (1H, m)	71.8	3,53 (1H, m)
4	42.3		42.3	
5	140.8		140.8	
6	121.8	5.29 (t ; 6,1)	121.8	5,39 (t ; 6.4)
7	31.9		31.9	
8	31.9		31.9	
9	50.2		50.2	
10	36.5		36.5	
11	21.1		21.1	
12	39.7		39.7	
13	42.3		42.3	
14	56.8		56.9	
15	24.4		26.0	
16	29.0		28.3	
17	56.0		56.1	
18	12.3	1.03 (s)	12.1	1.01 (s)
19	18.8	0.71 (s)	19.0	0.68 (s)
20	40.5		36.2	
21	21.2	0.92 (d ; 6.2)	19.4	0.93 (d; 6.5)
22	138.4		34.0	4,99 (m)
23	129.3		26.0	5.14 (m)
24	45.8		45.8	

25	29.1		29.1	
26	21.1	0.82 (d; 6.6)	21.1	0.83 (d; 6.4)
27	19.8	0.80 (d; 6.6)	19.4	0.81 (d; 6.4)
28	25.4		23.1	
29	12.1	0.83 (t; 7.1)	12.3	0.84 (t; 7.2 Hz)

II.2.1.6. Phenolic compounds

II.2.1.6.1. Identification of DMG21 (1,7-dihydroxy-6-methylxanthone)

Compound DMG21 was isolated as a yellow crystal in the mixture of *n*-Hex/EtOAc (9:1). A positive test with ferric chloride revealed its phenolic nature. The analysis of its HRESIMS (Figure 68) showed in negative mode, the pseudo-molecular ion peak $[M-H]^-$ at *m/z* 241.0517 (calcd 241.0601, for $C_{14}H_{10}O_4$) from which the molecular formula $C_{14}H_{10}O_4$ was deduced, containing ten degrees of unsaturation.

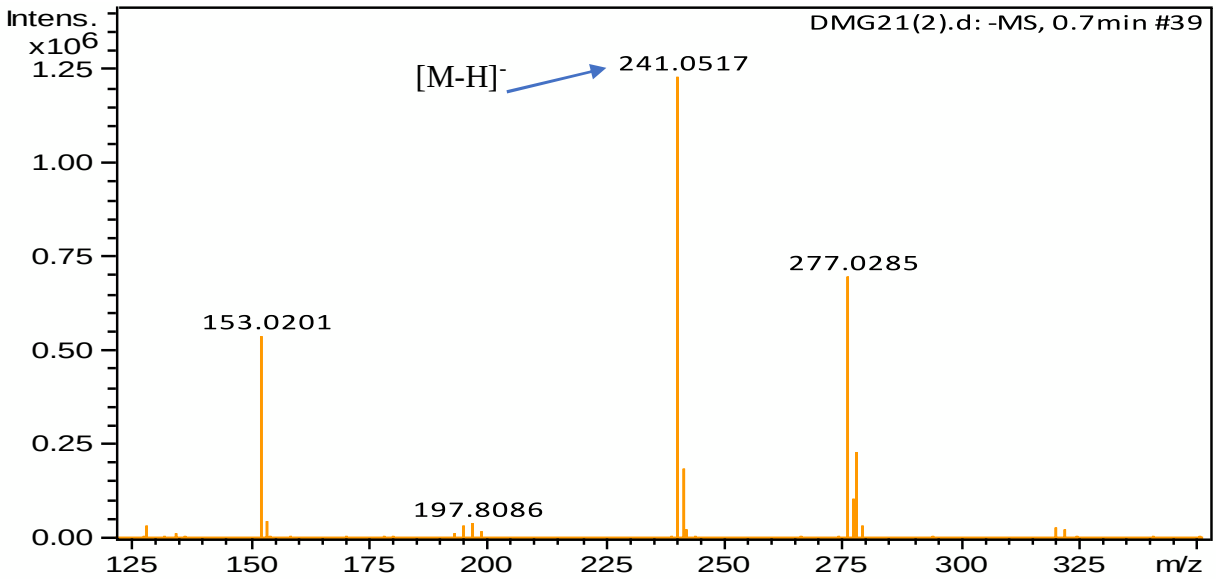

Figure 67 : HR-ESI-MS of compound DMG21

Its broadband decoupled ^{13}C NMR spectrum (Figure 70), displayed fourteen signals attributable to the fourteen carbon atoms as shown in its molecular formula. Among these signals, we note the presence of a signal at δ_C 182.0, corresponding to the conjugated carbonyl of ketone and another at δ_C 17.2, attributable to a non-oxygenated sp^3 carbon. Most data were similar to those of 1,7-dihydroxyxanthone (Yang et al. 2001). The only difference was that of H-6 where in the latter, was replaced by a methyl group in compound DMG21, which changed the chemical shift of C-6 from δ_C 125.5 to δ_C 137.4. In addition, the ^1H NMR data of DMG21

recorded in pyridine-d_5 were generally in agreement with those of the synthesised 1,7-dihydroxy-6-methylxanthone in $CDCl_3$ (Pockrandt et al. 2012). Hence, the structure of DMG21 was elucidated as 1,7-dihydroxy- 6-methylxanthone (**129**) (Yang et al. 2001). This compound is isolated for the first time from *D. microcarpum*.

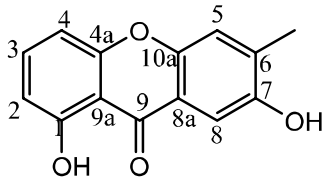

(129)

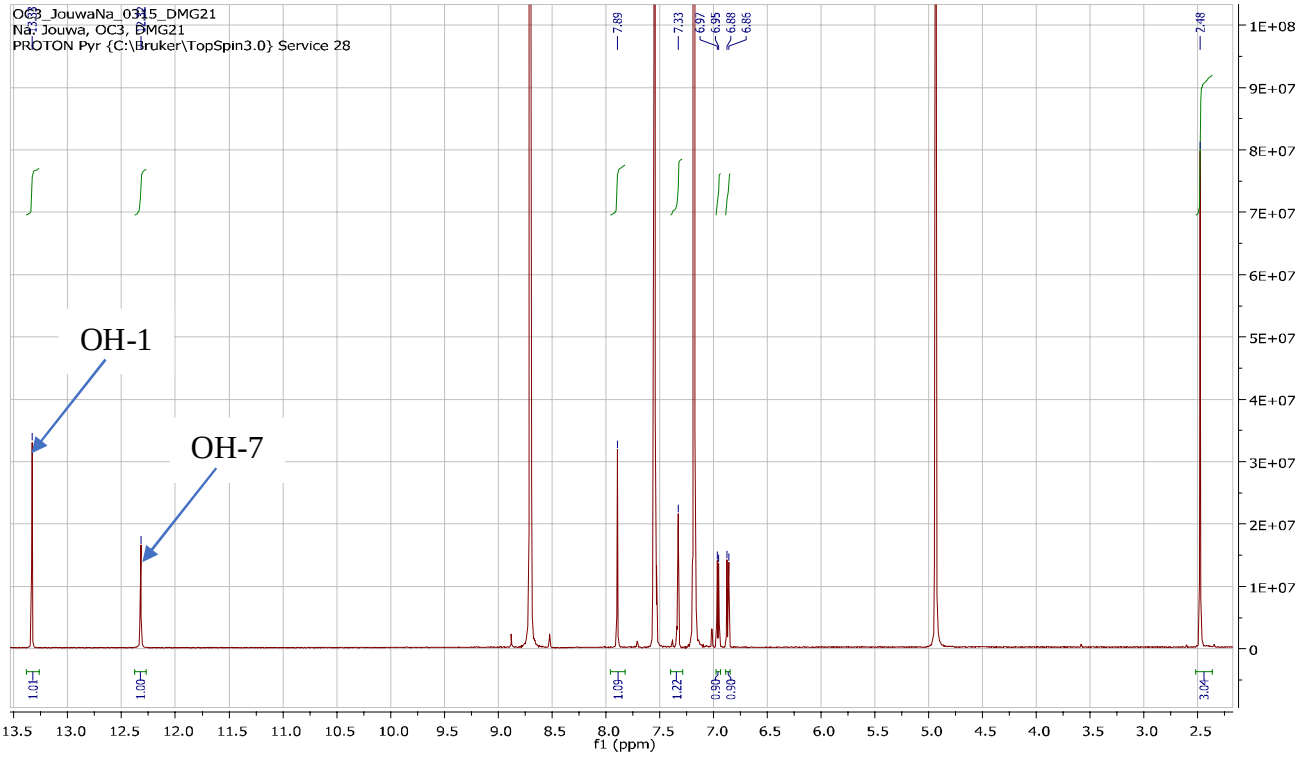

Figure 68 : ^{1}H NMR spectrum (500 MHz, C5D5N) of DMG21

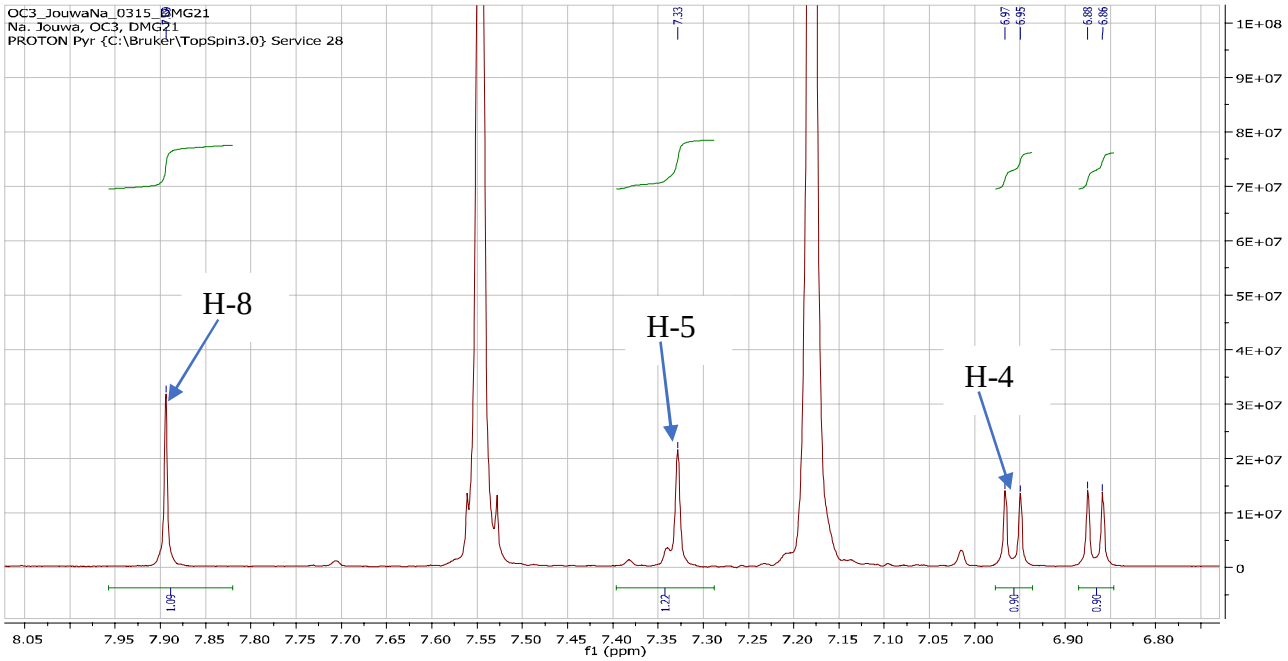

Figure 69 : Expended ^{1}H NMR spectrum (500 MHz, C_5D_5N) of DMG21

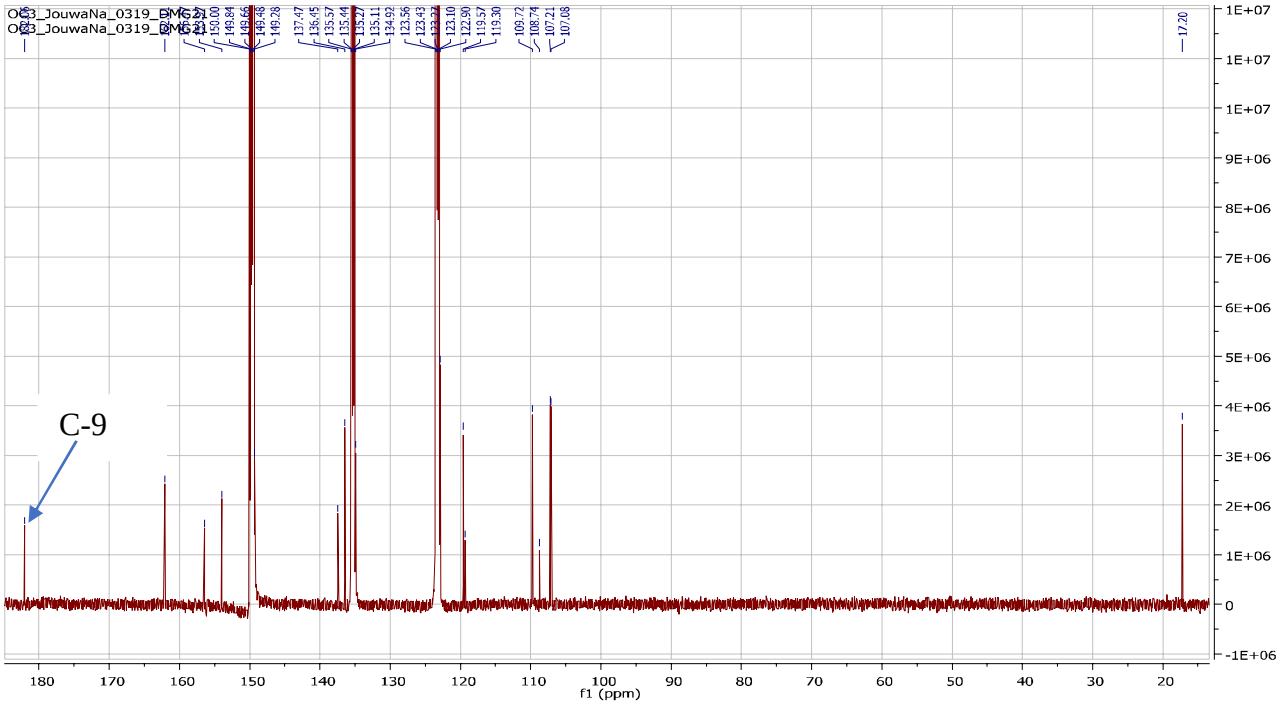

Figure 70 : ^{13}C NMR spectrum (125 MHz, C_5D_5N) of DMG21

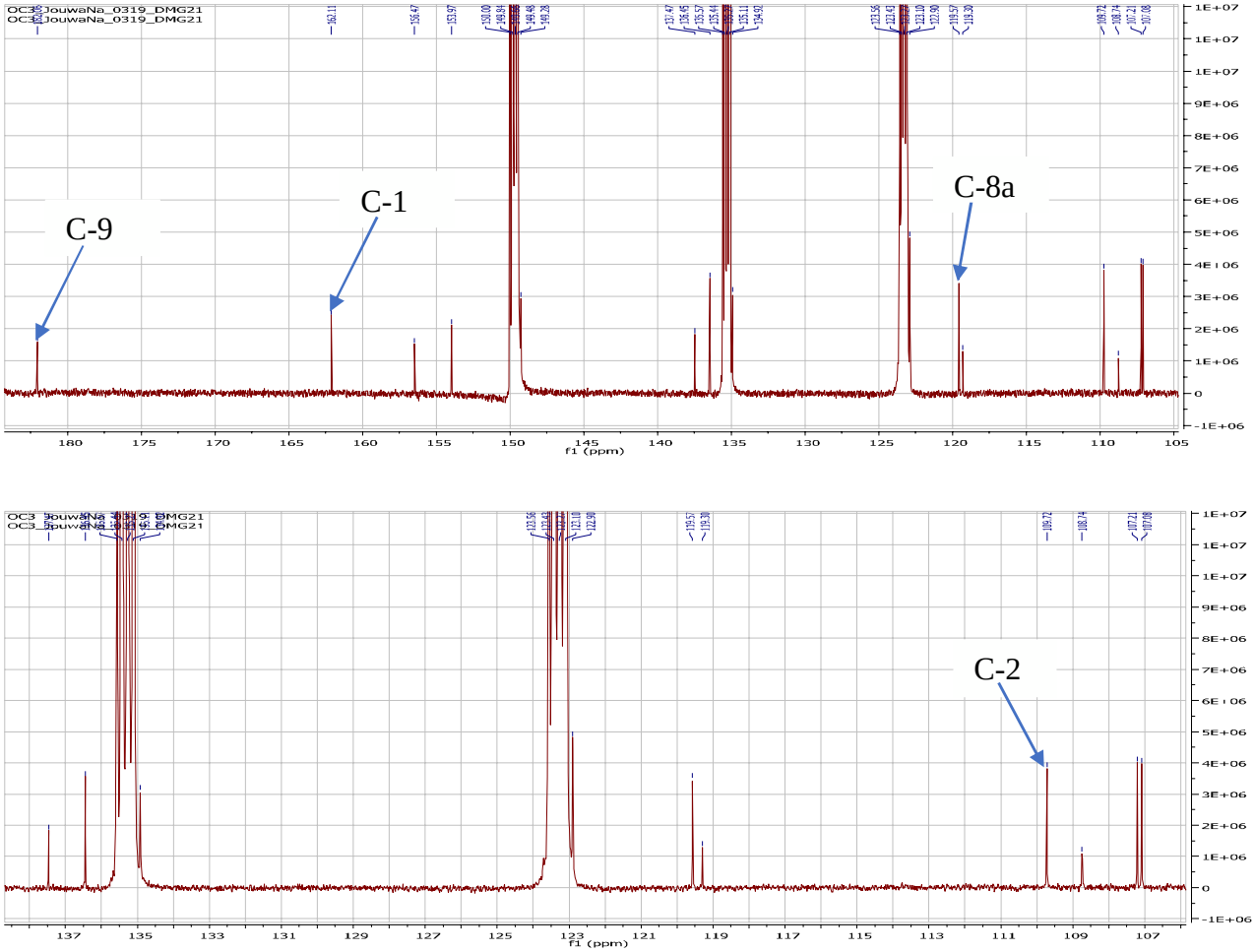

Figure 71 : Expended ^{13}C NMR (125 MHz, C5D5N) spectrum of DMG21

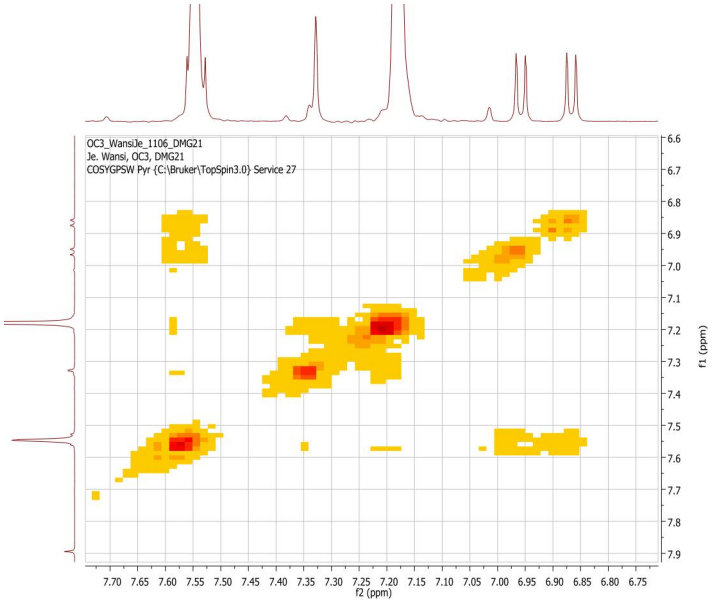

Figure 72 : Expended COSY spectrum of DMG21

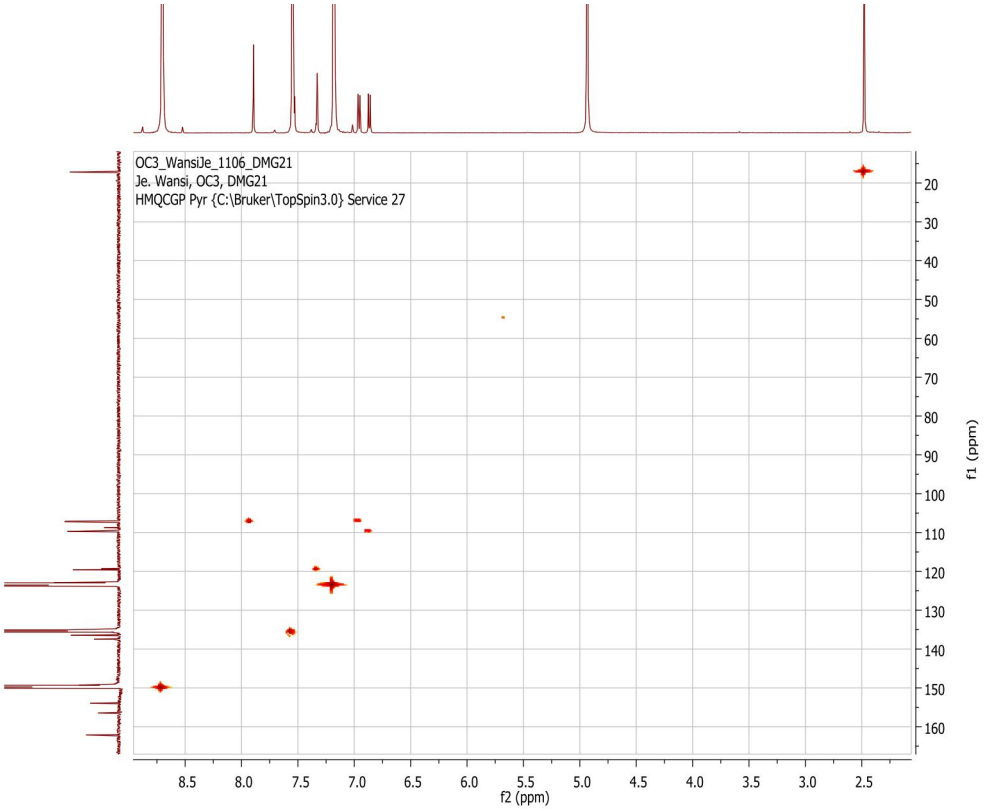

Figure 73 : HMQC spectrum of DMG21

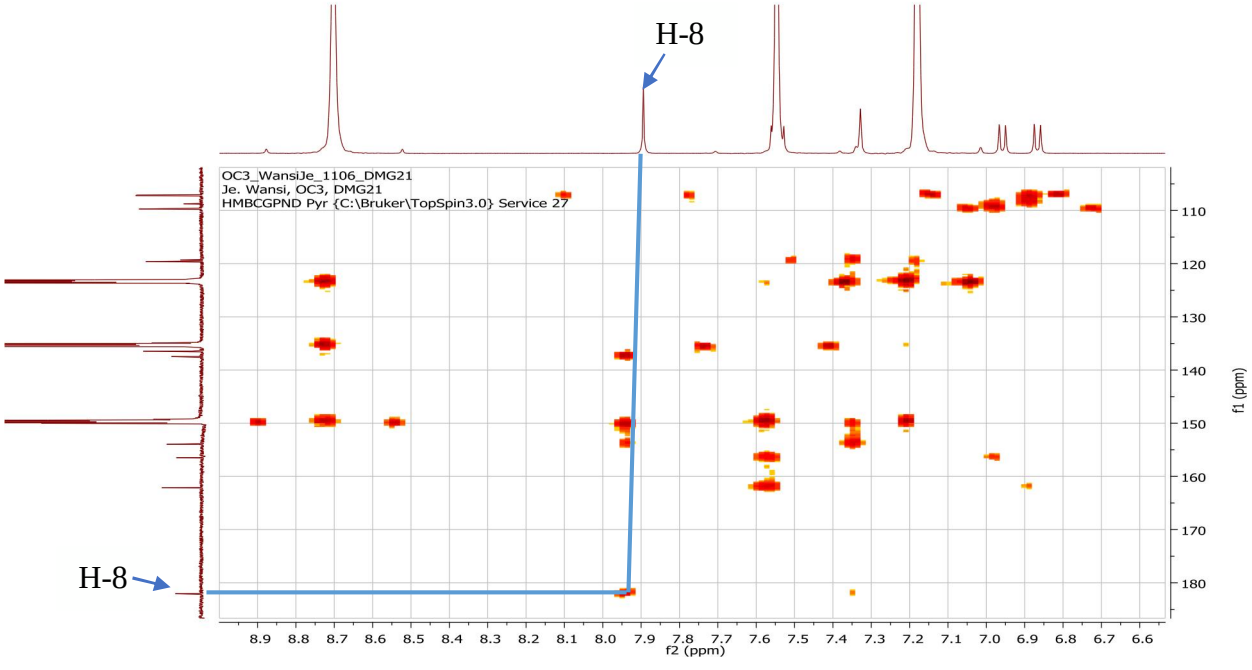

Figure 74 : HMBC spectrum of DMG21

Table XXX : Comparative ^{1}H NMR (500 MHz, C_5D_5N) and ^{13}C NMR (125 MHz, C_5D_5N) data of DMG21 with those of the literature.

Position	DMG21		Pockrandt et al. 2012	
	δ_C (m)	δ_H (ppm) (mult., *J* en Hz)	δ_C (m)	δ_H (ppm) (mult., *J* en Hz)
1	162.1(s)	-	160.9(s)	
2	109.7(d)	6.87 (1H, d, 7.3)	109.5(d)	7.70 (1H, d, 8.0)
3	136.4(d)	7.56 (1H, dd, 8.2, 7.3)	136.8(d)	6.79 (1H, dd, 8.0, 7.4)
4	107.0(d)	6.96 (1H, d, 8.2)	106.6(d)	7.05 (1H, d, 7.4)
4a	156.4(s)	-	155.8(s)	
5	119.5(d)	7.33 (1H, d, 0.9)	119.3(d)	7.48 (1H, d ; 0.8)
6	137.4(s)	-	136.9(s)	
7	153.9(s)	-	152.7(s)	
8	107.2(d)	7.89 (1H, d ; 0.9)	107.1(d)	8.05 (1H, d ; 0.8)
8a	119.3(s)	-	118.3(s)	
9	182.0(s)	-	181.3(s)	
9a	108.7(s)	-	107.8(s)	
10a	149.8(s)	-	149.4(s)	
6-Me	17.2(q)	2.48 (3H, s)	16.8(q)	2.42 (3H, s)
7-OH	-	12.32 (1H, s)	-	10.18 (1H, s)
1-OH	-	13.33 (1H, s)	-	12.75 (1H, brs)

II.2.1.6.2. Identification of DMf31 (methyl gallate)

Compound DMf31 was obtained as a white powder in the mixture of *n*-Hex/EtOAc (3:1). Soluble in DMSO, it melts between 240 and 242 °C and responds positively to the ferric chloride test by giving a violet coloration characteristic of phenolic hydroxyls. Its mass spectrum in EI (Figure 75) showed the peak of the molecular ion [M^+] at *m/z* 184, whose high-resolution analysis ([M^+] at *m/z* 184.0371) allowed it to be assigned the molecular formula $C_8H_8O_5$ containing 5 degrees of unsaturation. This high degree of unsaturation was in favor of an aromatic structure. Its broad band decoupled ^{13}C NMR spectrum (Figure 77; Table 31) exhibited six carbon signals instead of eight as it appeared in the molecular formula, suggesting the presence of two isochrones carbons within this molecule. These signals were assigned to a carbonyl ester at δ_C 166.3; two oxygenated sp^2 carbons at δ_C.145.6 and 138.4, two non-oxygenated sp^2 carbon at δ_C 119.3 and 108.5 and a carbomethoxyl at δ_C 51.6.

The ^{1}H NMR spectrum (Figure 76; Table 31), showed:

- a three protons broad singlet at δ_H 9.14 corresponding to hydroxyl protons,
- a signal of two isochronous aromatic protons at δ_H 6.92 corresponding to protons H-2 and H-6 of a 1, 3, 4, 5 tetrasubstituted aromatic nucleus,
- a three protons singlet at δ_H 3.92 confirming the presence of a carbomethoxyl group.

These data were compared to those described in the literature and allowed us to attribute to compound DMf31 the structure (**130**) which is that of methyl gallate (Ma *et al*., 2005). This compound has already been isolated from several plants.

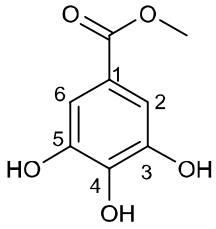

(130)

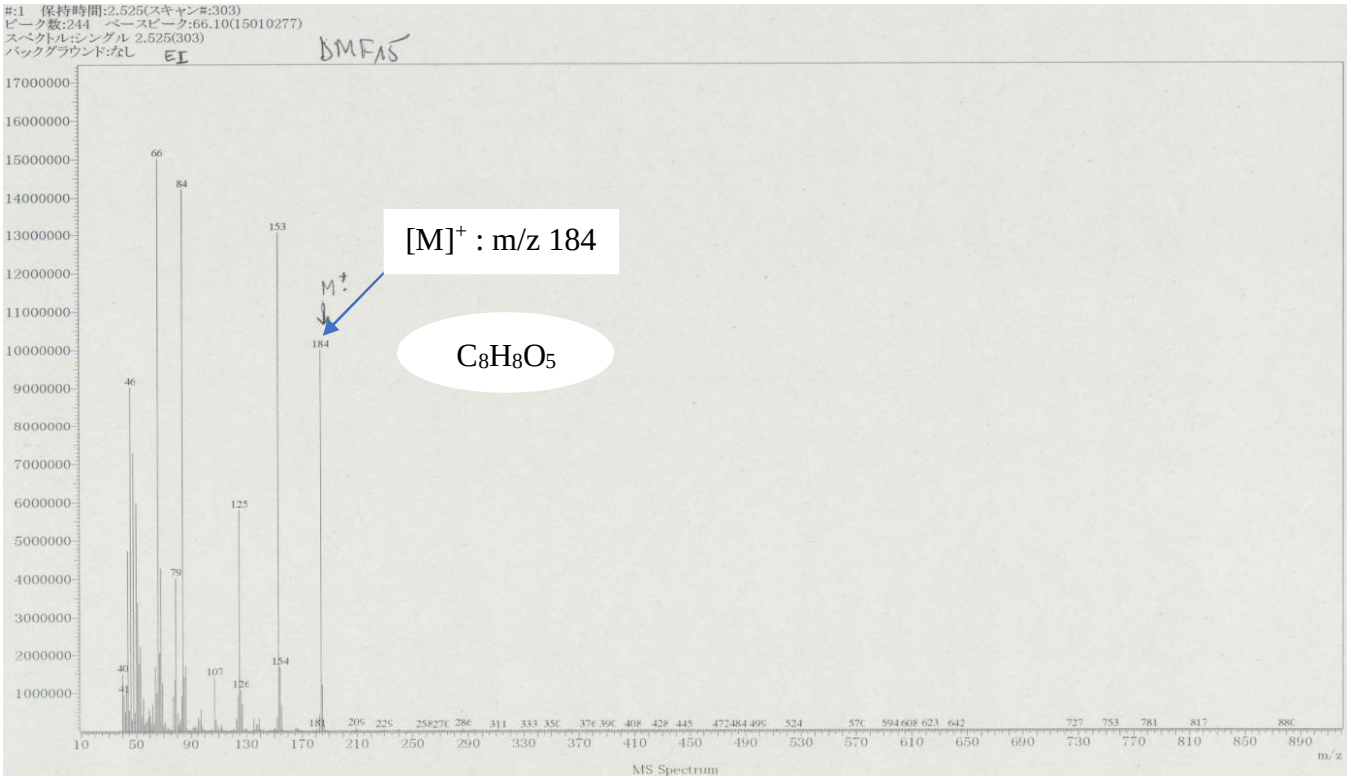

Figure 75 : Mass spectrum of DMf31

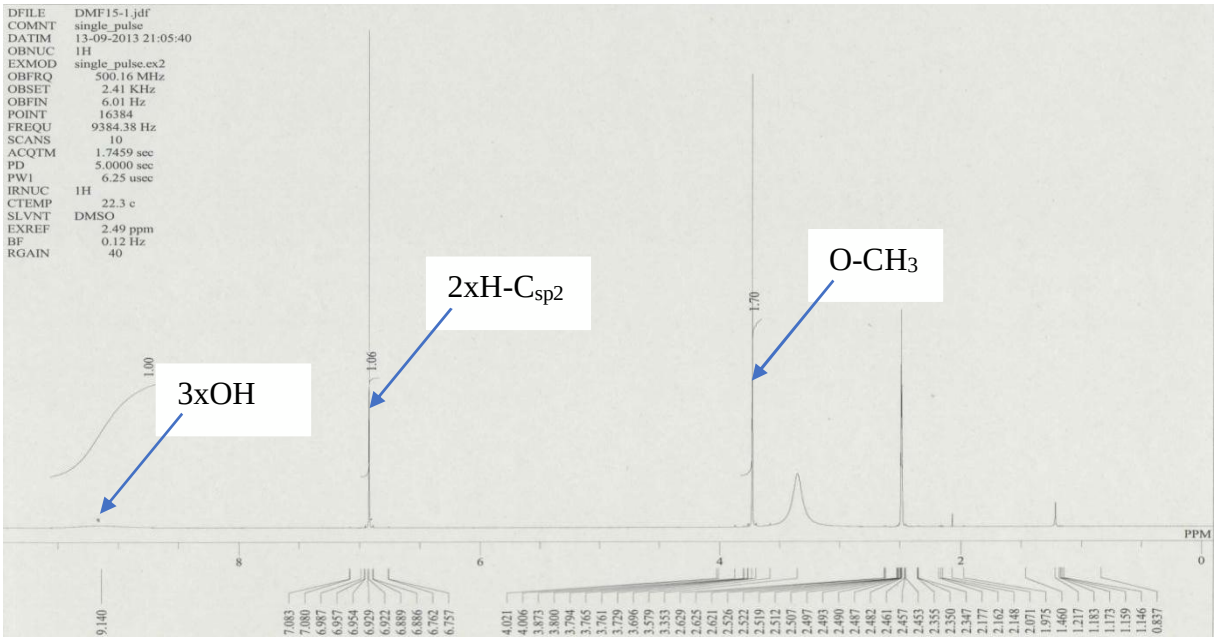

Figure 76 : ^{1}H NMR spectrum (500 MHz, DMSO) of DMf31

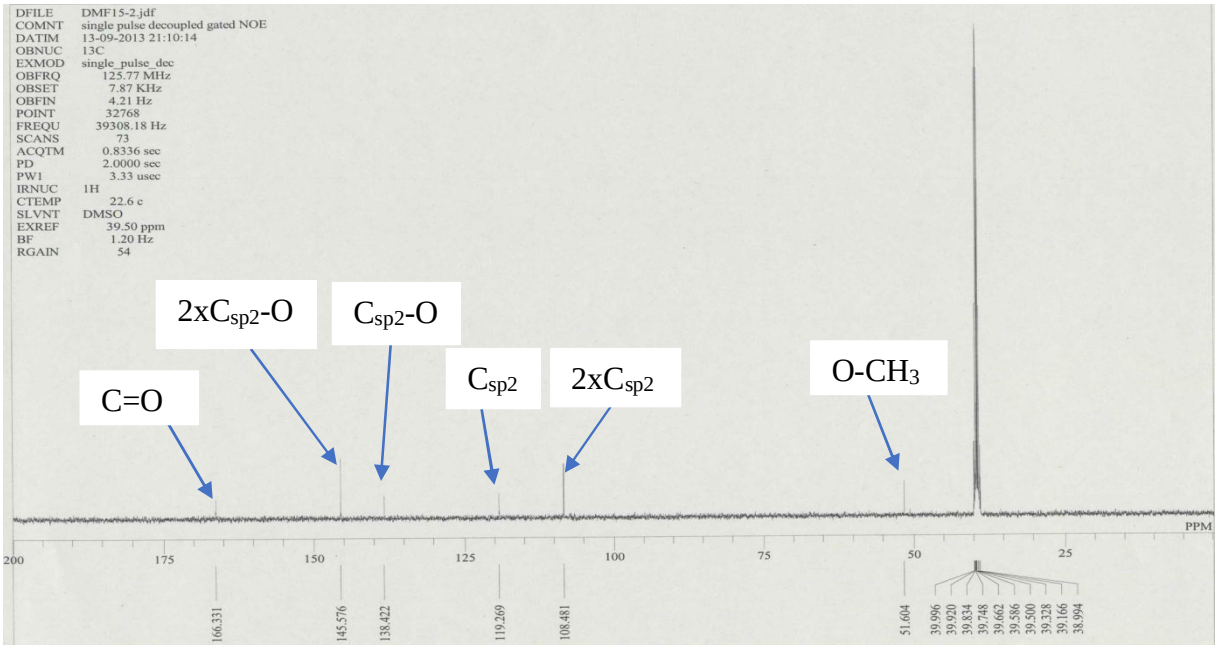

Figure 77 : ^{13}C NMR spectrum (125 MHz, DMSO) of DMf31

Table XXXI : ^{1}H NMR (DMSO; 500 MHz) and ^{13}C NMR (DMSO; 125 MHz) spectral data of DMf31.

Position	δ_H in ppm (nH, m, *J* in Hz)	δc in ppm (m)
1	/	119.2 (s)
2	6.92 (1H, s)	108.4 (d)
6	6.92 (1H, s)	108.4 (d)
7	/	116.3 (s)
7-OMe	3.92 (3H, s)	51.6 (q)
3-OH	9.14 (1H, s) large	145.5 (s)
4-OH	9.14 (1H, s) large	138.4 (s)
5-OH	9.14 (1H, s) large	145.5 (s)

II.2.1.6.3. Identification of DMf32 (luteolin)

Compound DMf32 was isolated as a white powder in the mixture of *n*-Hex/EtAcO (7:3) and melts between 278 and 280 °C. Soluble in DMSO it gave a violet coloration with ferric chloride characteristic of phenols. It reacted positively to the Shinoda test, characteristic of flavonoids. The EI mass spectrum of DMf32 indicated the molecular ion peak [M^+] at *m/z* 286. The high-resolution analysis of this molecular ion peak ([M^+] at *m/z* 286.0476 was in accordance with the molecular formula $C_{15}H_{10}O_6$ containing 11 degrees of unsaturation. This high degree of unsaturation was in favor of a strongly aromatic structure. Its ^{13}C NMR spectrum (Figure 80; Table 32) revealed fifteen carbon signals, corresponding to the fifteen carbon atoms appearing in the molecular formula. These signals included that of a carbonyl group at δ_C 181.7, the rest being signals of sp2 carbons including several oxygenated carbons.

Its ^{1}H NMR spectrum displayed:

- a one proton singlet at δ_H 6.66 characteristic of the H-3 proton of the C ring of a flavone type skeleton (Agrawal, 1989).

- An ABX system of three aromatic protons consisting of a doublet of doublet at δ_H 7.41 (1H, dd, 8.0, 2.9Hz) with ortho and meta coupling, a doublet at δ_H 7.37 (1H, d, 2.9 Hz) with a meta coupling and a further doublet at δ_H 6.87 (1H, d, 8 Hz) with otho coupling, characteristic of a 1, 3, 4 trisubstituted B aromatic nucleus of a flavone type skeleton (Agrawal, 1989).

- A pair of one proton doublets at δ_H 6.43 (1H, d, 2 Hz) and 6.17 (1H, d, 2 Hz) with ortho coupling corresponding to protons H-6 and H-8 of the A ring of a flavone type skeleton.

At this stage of the discussion; it remained to locate the four hydroxyl groups on the flavone skeleton. Three of them were located at position C-5 and C-7 of ring A and C-4’ of ring B based on biogenetic considerations, while the last one was located at C-3' on ring B, due to

the chemical shifts values of C-3' (δ_C 149.9) and C-4 '(δ_C 145.7), characteristic of those of two aromatic carbons carrying hydroxyl groups in the ortho position (Agrawal, 1989). These data were compared to those described in the literature and allowed us to assign to compound DMf32 the structure of luteolin (**131**). This compound has already been isolated from *Dendranthema morifolium* (Lin et *al*., 2015).

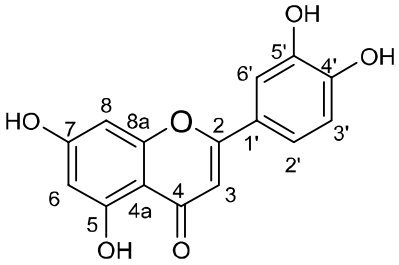

(131)

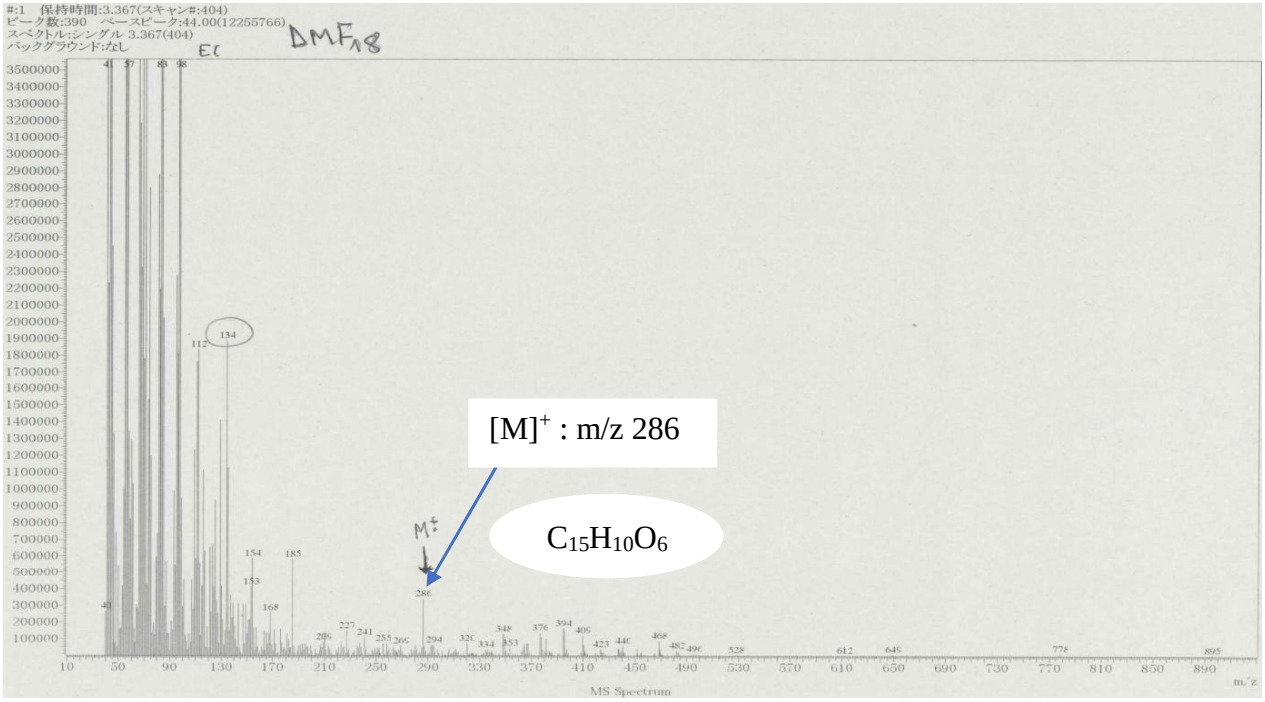

Figure 78 : Mass spectrum of DMf32

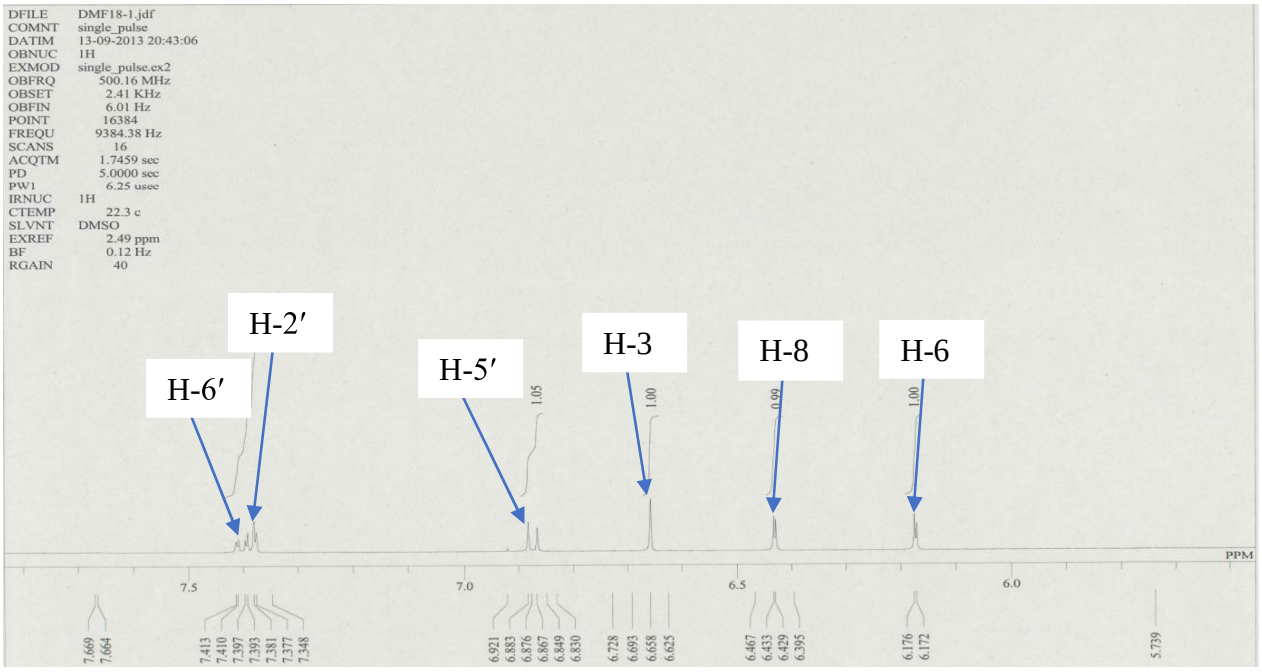

Figure 79 : ^{1}H NMR spectrum (500 MHz, DMSO) of DMf31

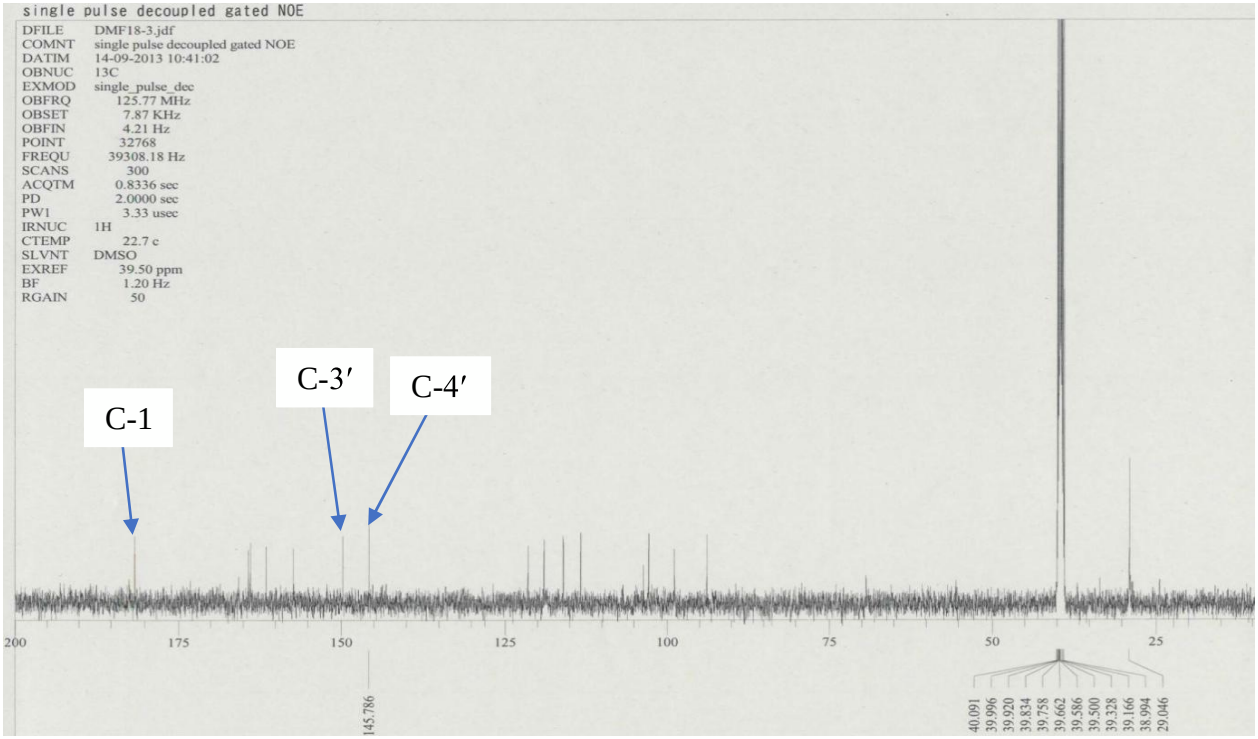

Figure 80 : ^{13}C NMR spectrum (125 MHz, DMSO) of DMf31

Table XXXII : ^{1}H NMR (DMSO; 500 MHz) and ^{13}C NMR (DMSO; 125 MHz) data of DMf32

positions	δ_H in ppm (nH, m, *J* in Hz)	δc in ppm (m)
1	-	-
2	-	164.2(s)
3	6.66(1H, s)	102.8(d)
4	-	181.7(s)
4a	-	103.6(s)
6	6.17 (1H, d, 2 Hz)	98.8(d)
8	6.43 (1H, d, 2 Hz)	93.6(d)
8a	/	157.2(s)
1’	/	121.8(s)
2’	7.37 (1H, d, 2.9 Hz)	113.5(d)
5’	6.87 (1H, d, 8 Hz)	115.9(d)
6’	7.41 (1H, dd, 2.9, 8 Hz)	118.1(d)
5-OH	8.71 (1H, s)	161.5(s)
7-OH	8.71 (1H, s)	163.6(s)
3’-OH	8.90 (1H, s)	149.9(s)
4’-OH	9.10 (1H, s)	145.7(s)

II.2.1.6.4. Identification of DMf33 ((-)-epicatechin)

Compound DMf33 was obtained as a brown solid in the mixture of *n*-Hex/EtOAc (13:5) and melts between 241-242 °C. It reacted positively both with ferric chloride (blue colour), indicating its phenolic and flavonoid nature. Its molecular formula was determined as $C_{15}H_{14}O_6$ on the basis of NMR data and EI-MS which showed a molecular ion peak $[M]^+$ at m/z 290, implying nine degrees of unsaturation. The UV spectrum of DMf33 showed an absorption band at λ_{max} 281 nm, suggesting a flavan skeleton (Agrawal, 1989). The broad band decoupled ^{13}C NMR spectrum of compound DMf33 (Figure 83; Table 33) displayed fifteen carbon signals, which were sorted by DEPT and HSQC spectra into seven quaternary carbon atoms, seven methines and one methylene group at δ_C 28.5.

The ^{1}H NMR spectrum exhibited two meta-coupled aromatic protons at δ_H 5.93 (1H, d, *J* = 2.0 Hz, H-6) and, at δ_H 5.90 (1H, d, *J* = 2.0 Hz, H-8) which were diagnostic for a C-5 and C-7 oxygenated ring A of flavan-3-ol (Jang et al., 2009). This spectrum also exhibited signals for an ABX spin system of aromatic protons at δ_H 6.76 (1H, d, *J* = 8.0 Hz), 6.79 (1H, dd, *J* = 2.0, 8.0 Hz), and 6.96 (1H, d, *J* = 2.0 Hz) assigned to trisubstituted B-ring. In addition to those aromatics protons, the ^{1}H NMR spectrum exhibited four aliphatic protons at δ_H 4.55 (1H, d, *J* = 6.5 Hz, H-2), 3.96 (1H, m, H-3), 2.79 (1H, dd, *J* = 16.0, 5.5 Hz, H-4), and 2.84 (1H, dd, *J* = 16.0, 8.0 Hz, H-4). The fact that H-2 appeared as a broad doublet indicated that this unit had

the 2,3 cis configurations (Ganapaty et *al*., 2008). Some significant HMBC correlations were observed between H-6 (δ_H 5.91) and C-8 (δ_C 95.4), C-10 (δ_C 100.9), C-5 (δ_C 157.9) and C-7 (δ_C 157.0), H-5′ (δ_H 6.83) and C-6′ (δ_C 120.1), C-1′ (δ_C 132.3), C-3′ (δ_C 146.2) and C-4′ (δ_C 146.3), and H-2 (δ_H 4.55) and C-4 (δ_C 28.6), C-3 (δ_C 68.9), C-2′ (δ_C 116.1), C-1′ (δ_C 132.3), C-6′ (δ_C 120.1), and C-9 (δ_C 157.6). The comparison of this data with those published (Jang et al., 2009) led to the identification of DMf33 as (-)-epicatechin (**132**) isolated for the first time from *Rubus parvifolius* (Do et *al*., 1988).

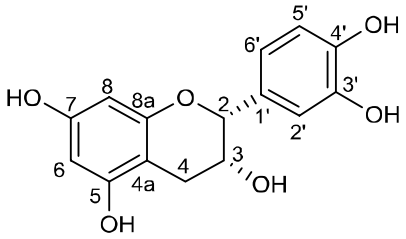

(132)

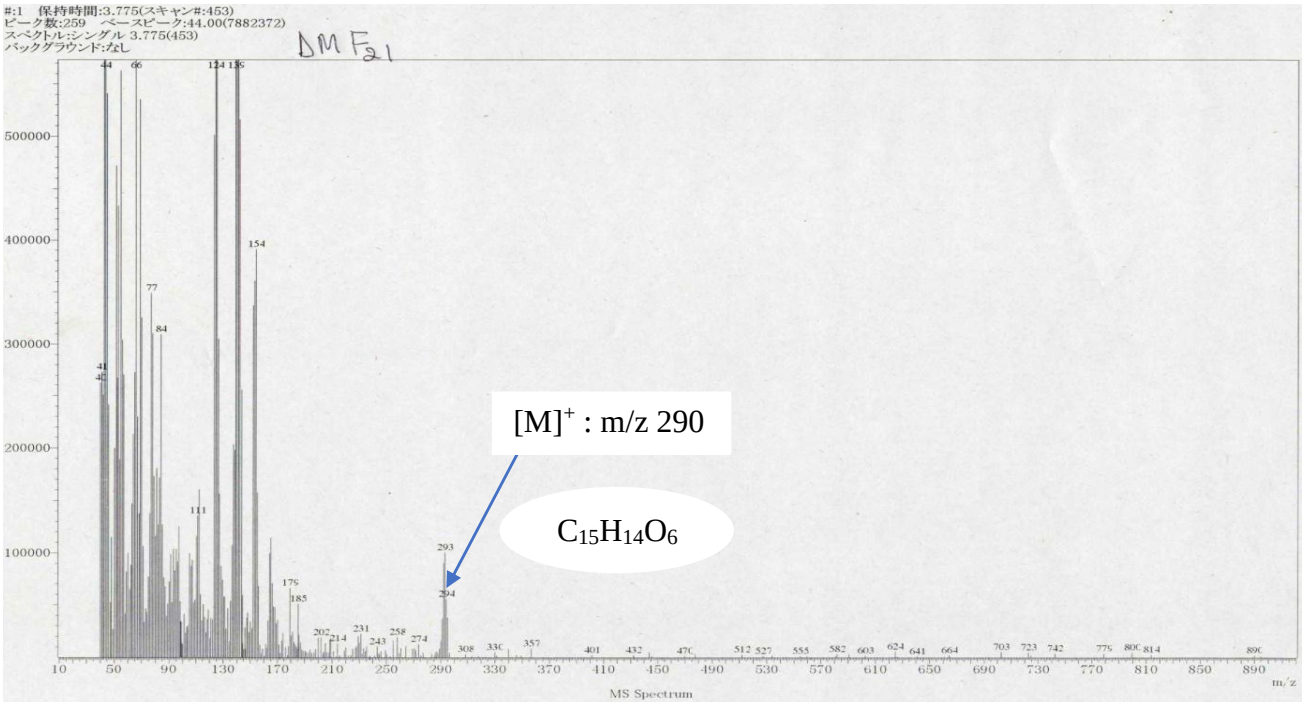

Figure 81 : Mass spectrum of DMf33

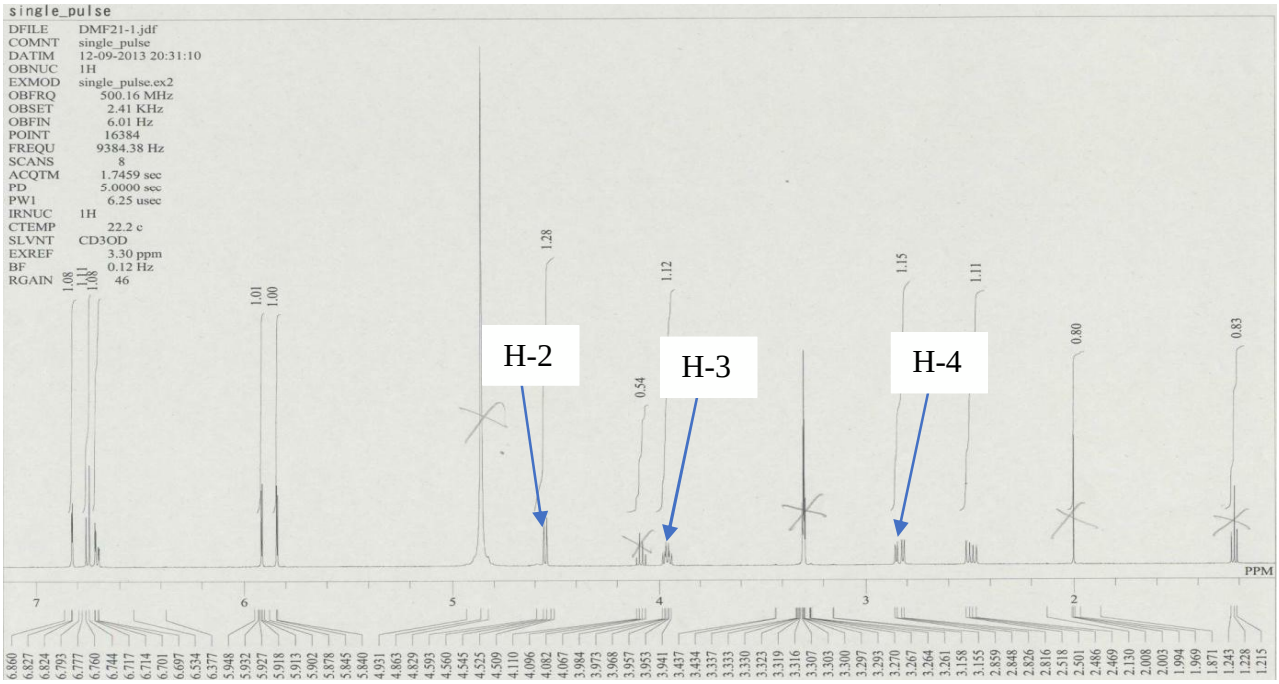

Figure 82 : ^{1}H NMR spectrum (500 MHz, DMSO) of DMf33

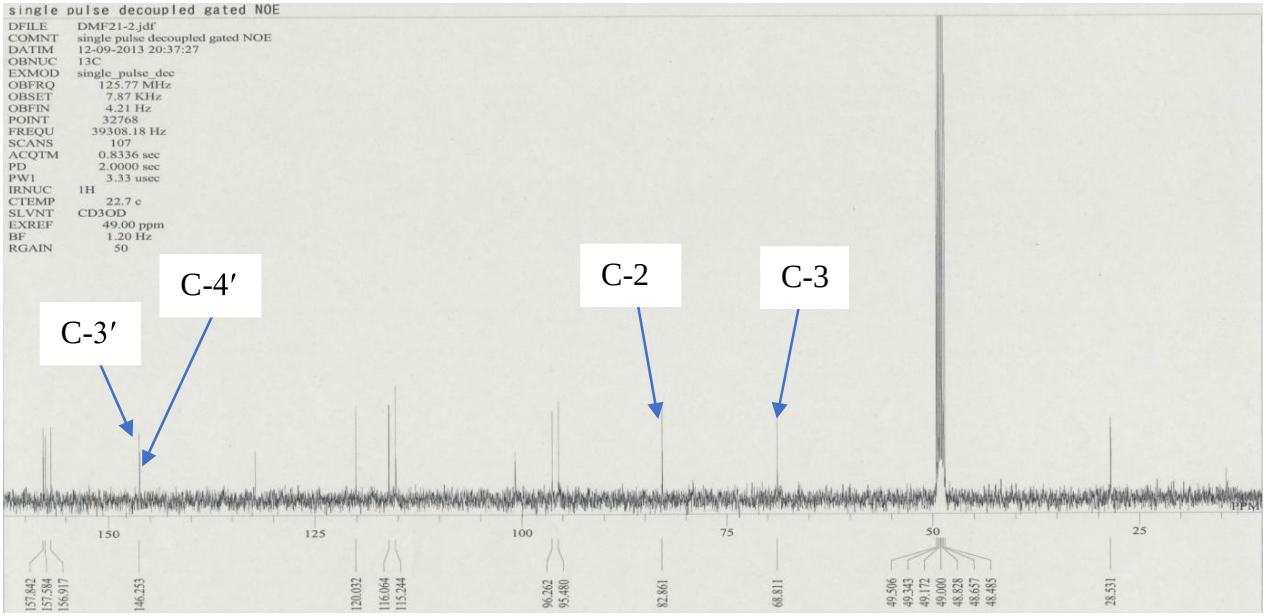

Figure 83 : ^{13}C NMR spectrum (125 MHz, DMSO) of DMf33

Table XXXIII : ^{1}H NMR (DMSO; 500 MHz) and ^{13}C NMR (DMSO; 125 MHz) data of DMf33

positions	δ_H in ppm (nH, m, *J* in Hz)	δc in ppm (m)
1	-	-
2	4.55 (1H, d, 6.5 Hz)	82.8 (d)
3	3.96 (1H, q, 5,4; 6.5 et 12 Hz)	68.8 (d)
4	2.79 (1H, d, 5.4 Hz)	28.5 (t)
	2.84 (1H, dd, 5.4et 12 Hz)	
4a	-	100.7 (s)
6	5.91 (1H, d, 2.5 Hz)	96.2 (d)
8	5.84 (1H, d, 2.5 Hz)	95.4 (d)
8a	-	156.9 (s)
1’	-	132.5 (s)
2’	6.83 (1H, d, 1.5 Hz)	115.2 (d)
5’	6.76 (1H, d, 8.5 Hz)	116.0 (d)
6’	6.70 (1H, dd, 1.5 et 8.5 Hz)	120.0 (d)
3-OH	4.45 (1H, s)	68.8 (d)
5-OH	8.70 (1H, s)	157.5 (s)
7-OH	8.73 (1H, s)	157.8 (s)
3’-OH	8.90 (1H, s)	146.2 (s)
4’-OH	9.10 (1H, s)	146.2 (s)

II.2.2. Chemical transformation

In the second aspect of our work, we undertook some chemical transformation to initiate a structure-activity relationship study of compound DMG12.

This compound (Rhinocerotinoic acid) was not only isolated in appreciable amounts, but it also exhibited antisalmonella activity. This reaction aimed to identify which of the carboxylic acid (C-15) and ketone (C-7) functions was responsible of the antisalmonella activity. Thus, the ketone function was reduced into alcohol using sodium borohydride NaBH4.

The chemical equation associated to this transformation is as follow:

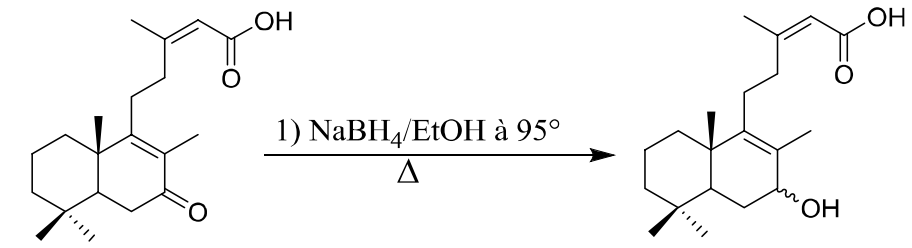

Rhinocerotinoic acid **46%**

The formation of the alcoholic derivative was confirmed by the disappearance of the carbonyl signal at δ_C 198.9 (C-7) on the ^{13}C NMR spectrum of the obtained compound and the

appearance of an oxymethyne at δ_C 71.9 (Figure 90). Were also observed an additional oxymethyne proton signal at δ_H 3.68 (1H, t) on the 1H NMR spectrum (Figure 91).

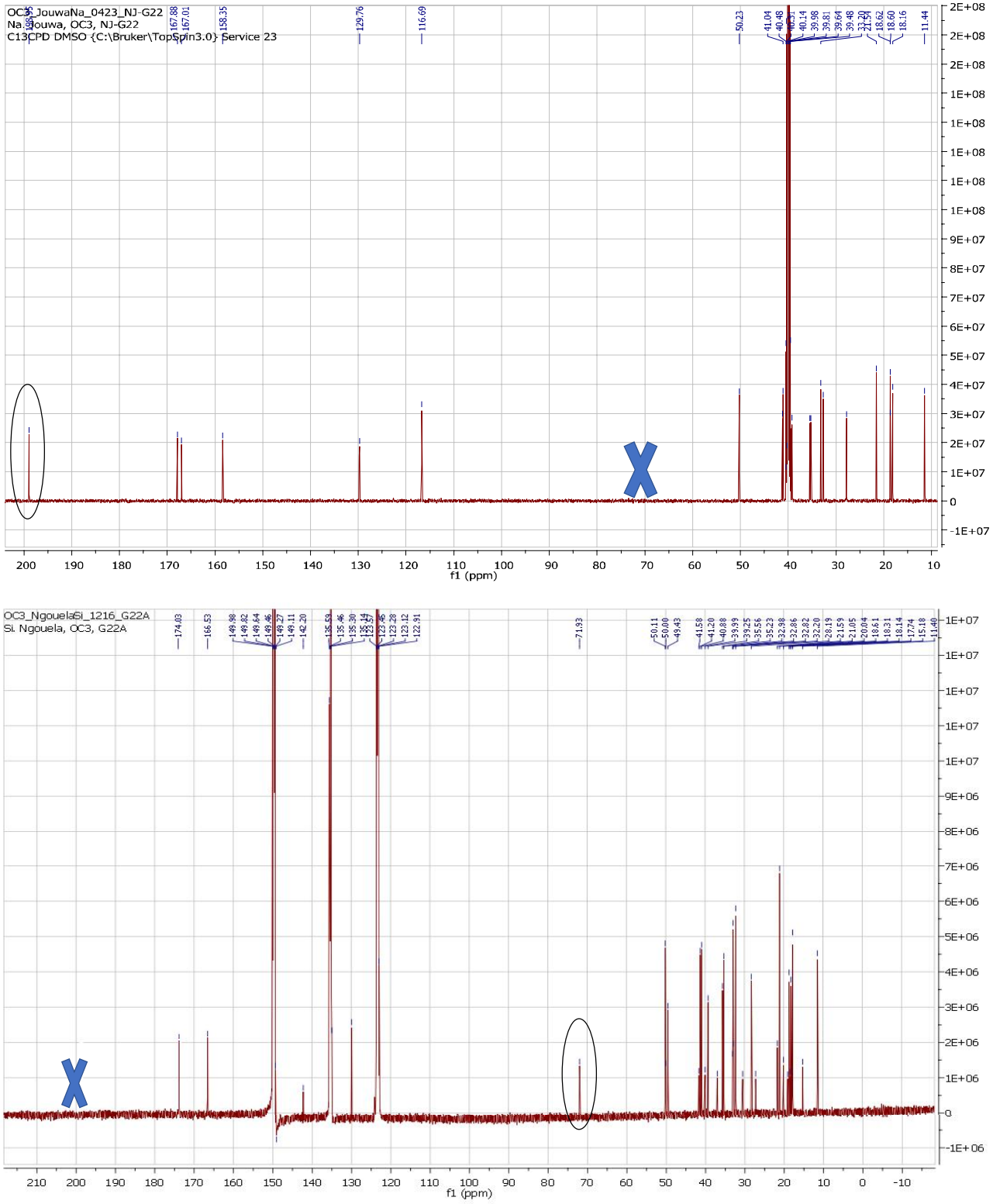

Figure 84 : Comparative ^{13}C NMR spectrum (125 MHz, $CDCl_3$) of DMG12 and of DMG12a

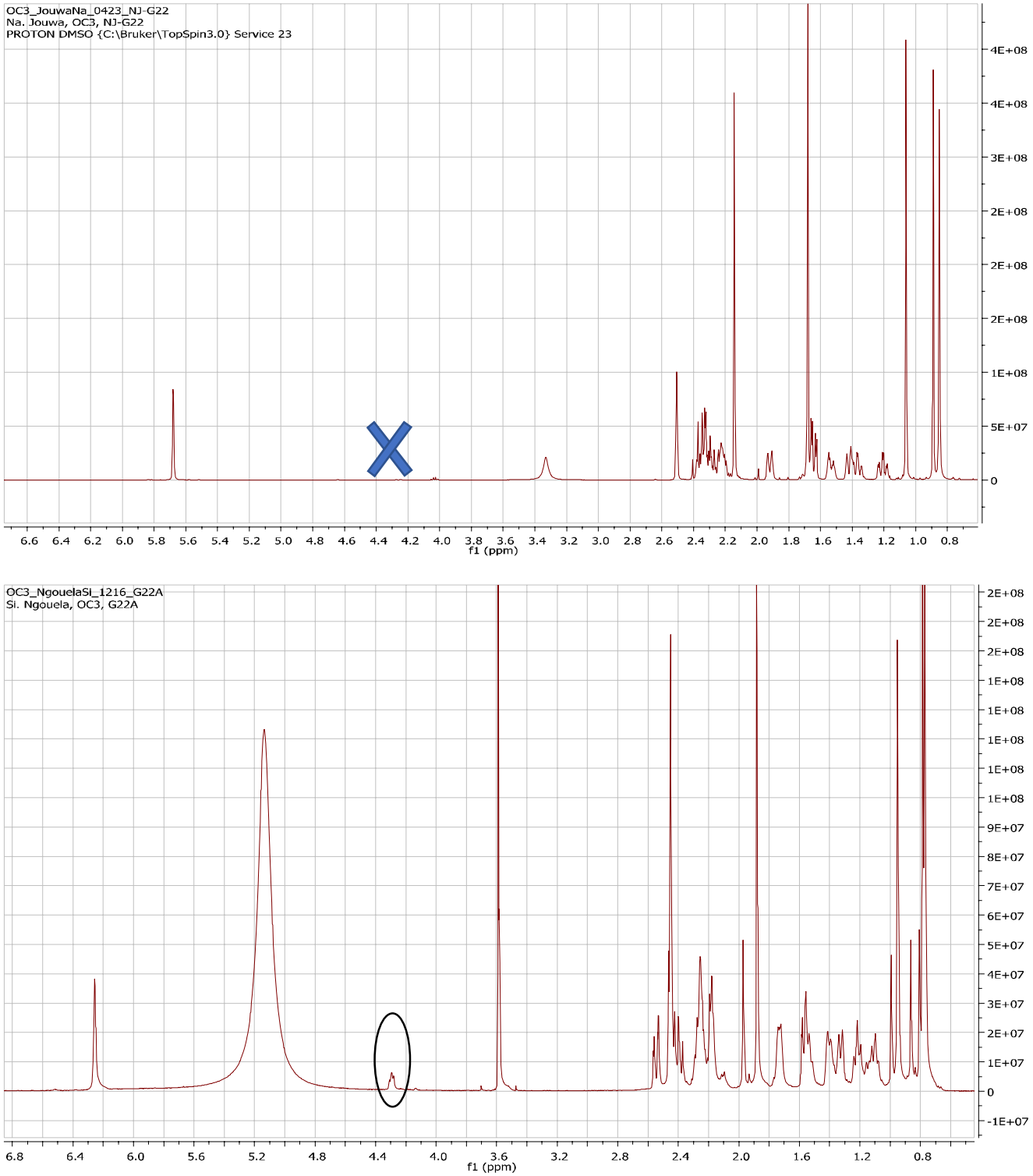

Figure 85 : Comparative ^{1}H NMR spectrum (125 MHz, $CDCl_3$) of DMG12 and of DMG12a

II.3. EVALUATION OF ANTISAMONELLA ACTIVITIES OF *D. MICROCARPUM*

Following the bio guided process, extracts, fractions and some isolated compounds were assayed *in vitro* and *in vivo* for their antisalmonella activity against three salmonella strains namely, *S. enteritidis* (SE), *S. typhi* (ST) and *S. tiphymurium* (STm). The minimal inhibition concentration (MIC) method was used.

II.3.1. *In vitro* antibacterial assays of crude extracts

Different extracts obtained were assayed for their antisalmonella activities against three salmonella strains namely, *Salmonella enteritidis* (SE), *Salmonella typhi* (ST) and *Salmonella typhimurium* (STm). The results obtained showed that each crude extract exhibited an activity on at least one salmonella strain with a MIC at 1.95 µg/mL for root-bark and root-wood, and at 250 µg/mL for leaves, branches, fruits and seeds. The results obtained are shown in the table below.

Table XXXIV : Antisalmonella activitiy of different extracts of *D. microcarpum* (MIC µg/mL)

Series	Codes	Plant organs	*Salmonella* strains		
			SE	ST	STm
A	DMA	Seeds	>500	250	>500
B	DMB	Fruits	>500	250	>500
C	DMC	Branches	250	>500	31.25
D and E	DMD	Leaves	NA	NA	250
F	DMF	Root-bark	250	3.90	1.95
G	DMG	Root-wood	NA	7.81	1.95

NA: Not Active

II.3.2. Antibacterial assays of fractions

The different fractions were also tested for their antimicrobial activities. Only the ethyl acetate fractions of the root-bark and root-wood showed activity on the three *Salmonella* strains with a MIC at 250 µg/mL. The obtained results are presented in the table below.

Table XXXV : Antisalmonella tests of the different fractions of *D. microcarpum* (MIC µg/mL)

ORGANS	Solvents	Fractions codes	*Salmonella* strains		
			SE	ST	STm
Seeds	*n*-hexane	DMA1	>500	>500	>500
	CH_2Cl_2	DMA2	>500	>500	>500
	EtOAc	DMA3	>500	>500	>500
	n-Butanol	DMA4	>500	>500	>500
	Water	DMA5	NT	NT	NT
Fruits	*n*-hexane	DMB1	>500	>500	>500
	CH_2Cl_2	DMB2	>500	>500	>500
	EtOAc	DMB3	>500	>500	>500
	n-Butanol	DMB4	NT	NT	NT
	Water	DMB5	NT	NT	NT
Branches	*n*-hexane	DMC1	>500	>500	>500
	CH_2Cl_2	DMC2	>500	>500	>500
	EtOAc	DMC3	>500	>500	>500
	n-Butanol	DMC4	NT	NT	NT
	Water	DMC5	NT	NT	NT
Leaves	*n*-hexane	DMDE1	>500	>500	>500
	CH_2Cl_2	DMDE2	>500	>500	>500
	EtOAc	DMDE3	>500	>500	>500
	n-Butanol	DMDE4	NT	NT	NT
	Water	DMDE5	NT	NT	NT
Root bark	*n*-hexane	DMF1	>500	>500	>500
	CH_2Cl_2	DMF2	>500	>500	>500
	EtOAc	DMF3	250	250	250
	n-Butanol	DMF4	NT	NT	NT
	Water	DMF5	NT	NT	NT
Root wood	*n*-hexane	DMG1	>500	>500	>500
	CH_2Cl_2	DMG2	>500	>500	>500
	EtOAc	DMG3	250	250	250
	n-Butanol	DMG4	NT	NT	NT
	Water	DMG5	NT	NT	NT

NT=Not Tested

II.3.3. Antibacterial assays of Compounds

Some of these compounds were tested for antimicrobial activities. Only three compounds namely microcarposide, microcarpamide and rhinocerotinoic acid, showed activity on the three *Salmonella* strains, with a MIC values of 62.50 and 31.25 μg/mL. The results are presented in the table below.

Table XXXVI : antibacterial tests of compounds (MIC µg/mL)

Compounds	Parameters	*Salmonella* strains		
		ST	STM	SE
Microcarposide (114)	**MIC (µg/mL)**	**62.5**	**31.25**	**31.25**
	MBC (µg/mL)	125	62.5	62.5
	MBC/MIC	2	2	2
Microcarpamide (115)	**MIC (µg/mL)**	62.5	62.5	62.5
	MBC (µg/mL)	125	125	125
	MBC/MIC	2	2	2
Rhinocerotinioc acid (117)	**MIC (µg/mL)**	62.5	62.5	62.5
	MBC (µg/mL)	125	125	125
	MBC/MIC	2	2	2
Ciprofloxacine (7)	**MIC (µg/mL)**	**0.5**	**0.5**	**1**
	MBC (µg/mL)	2	2	4
	MBC/MIC	4	4	4

II.3.4. Subacute toxicity test of root-bark extract

At the end of the *in vitro* tests, our extract showed good activity on three salmonella strains namely *S. typhi*, *S. enteritidis* and *S. typhimurium* whose values of the minimum inhibitory concentrations (MIC) were respectively at 250, 3.90 and 1.95 µg/mL.

In view of these interesting results, we first carried out the subacute toxicity test of our extract. It appears that no dose has shown signs of toxicity. The results are shown in the table below.

Table XXXVII : results of subacute toxicity

	Test groups				Satellite groups	
Parameters	Control	Dm 150 mg/kg	Dm 300 mg/kg	Dm 600 mg/kg	Control	Dm 600 mg/kg
Males						
ALT (I U /L)	38.55±6.975	51.02±12.81	40.71±3.066	59.51±9.532	72.55±21.16	54.48±17.39
AST (I U /L)	101.7±10.94	98.21±5.44	113.5±6.86	126.6±15.73	150.9±20.52	109.8±7.28
ALP (I U /L)	327±40.59	315.6±44.11	273.7±27.56	358.3±14.5	403.7±21.39	250.3±14.45
Albumin	541.12±16.99	608.99±4.11	582.26±5.45	586.52±6.10	584.79±12.36	552.44±11.78
Bilirubin	12.4±3.63	14.33±2.59	14.00±2.56	13.6±3.07	14.86±2.73	16.1±2.01
Creatinine (µmol/L)	1243±89.58	896.1±138	840.8±150.1	1062±47.8	1077±31.56	1106±34.28
Uric acid (µmol/L)	92.62±6.61	101.99±8.90	106.30±3.59	82.55±22.80	103.01±12.74	107.25±10.73
Females						
ALT (I U /L)	41.99±9.81	46.21±3.50	52.47±1.05	39.58±2.52	37.92±5.26	42.72±5.25
AST (I U /L)	101.7±10.94	107.8±4.61	114.1±4.98	109±7.47	94.77±14.99	108±7.07
ALP (I U /L)	291±25.95	252.5±41.56	257.2±31.74	254.3±54.68	246.1±40.17	197.3±27.81
Albumin	583.19±11.71	582.79±25.61	610.35±17.15	557.76±40.25	613.42±21.99	565.08±24.85
Bilirubin	10.77±0.45	12.62±0.80	11.89±0.58	10.68±1.63	13.58±0.89	11.56±0.80
Creatinine (µmol/L)	1207±56.24	964.7±134.51	1097±16.56	1115±16.56	1089±72.76	1089±22.56
Uric acid (µmol/L)	79.94±5.09	77.985±10.96	109.76±7.94	101.48±5.40	107.06±9.60	82.576±12.70

II.3.5. *In vivo* test of hydroethanolic root-bark extract

The histological analysis of liver, of salmonella-infected animals, treated with the *D. microcarpum* hydro-alcoholic root bark extract at the doses 75, 150 and 300 mg/kg.bw, is illustrated in (Figure 86). The liver section of normal control revealed normal parenchyma in which centrilobular vein, hepatocytes and sinusoids are well identified (Figure 86A) while some sinusoids clarification was observed in the immunosuppressed control (Figure 86B). It appears that typhoid fever provokes in liver section of salmonella control, some damages including inflammation with leukocyte infiltration, hepatocyte cytolysis (Figure 86C) which disappeared

in treated groups (Figures 86D, 86E, 86F and 86G). It emerges from this *in vivo* test that, all the doses have shown a curative effect both the dose 75, 150 and 300 mg/kg.bw. However, we note a correction of alterations (inflammation) caused by infection in the liver as shown the in the figure 86E, 86F and 86G of diagram below. Which is close to the values of normal and immunocompromised control.

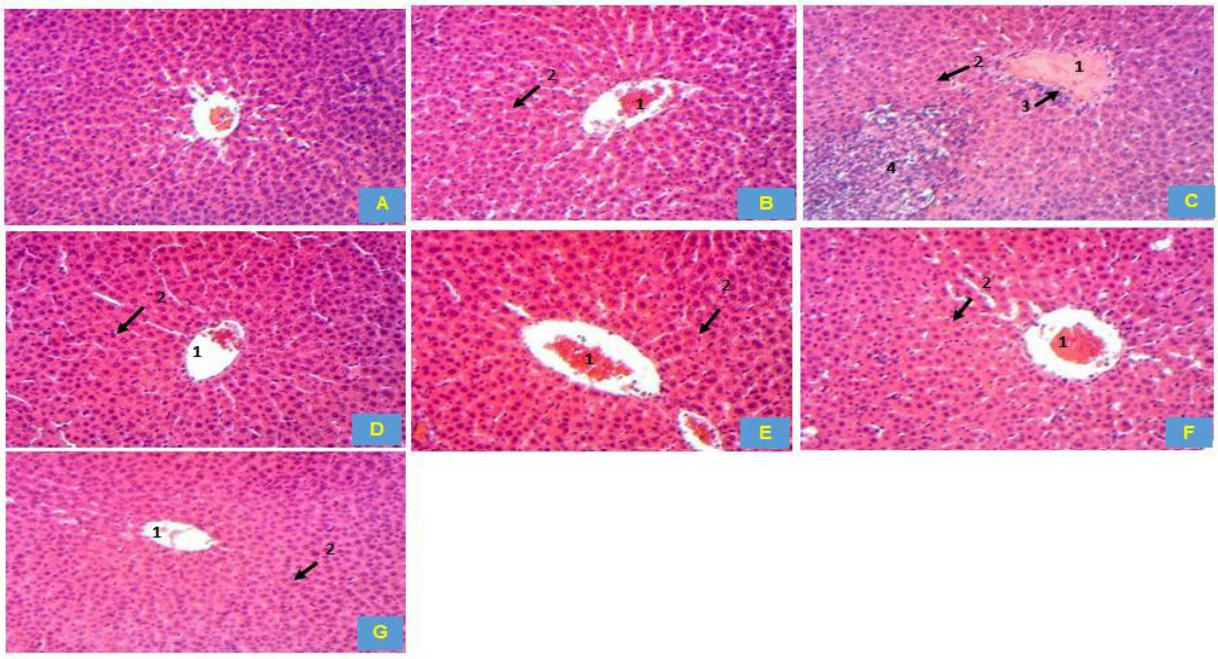

Figure 86 : 1-central lobular vein, 2-hepatocytes, 3-leukocyte inflammation, 4-hepatocytes cytolysis.

A-G: **A**: normal control, **B**: immunosuppressed control, **C**: *Salmonella* control, **D**: ciprofloxacin control, **E**: rats treated with 75 mg / kg of extract, **F**: rats treated with 150 mg/kg of extract, **G**: rats treated with 300 mg/kg of extract.

II.4.PRE-FORMULATION ASSAY

The objective of this work was, among other things, to develop a phytomedicine. The evaluation of the activities of the extracts (evaluation of the antibacterial activities and of the acute and subacute toxicity) having led to interesting results, it seemed judicious to us to attempt a pre-formulation.

After carrying out the in vitro tests on the *Salmonella* strains, the results obtained showed that the root bark of *D. microcarpum* was good candidates for the pre-formulation of a phytomedicine. Thus, the acute and subacute toxicity tests was first performed as well as the in

vivo tests. At the end of these tests, the extract showed no sign of toxicity, whereas the three doses of extract used to treat the rats infected with salmonella showed good activity. To optimize the use of our plant material, we have formulated our phytomedicine using the smallest curative dose (75 mg/mL). The protocol used is that of Reagan-Show and collaborators, set up in 2007, entitled "Dose translation from animal to human studies revisited". The following formula was used:

Formula for Dose Translation Based on BSA
$\text{HED (mg/ kg)} = \text{Animal dose (mg/kg)} \times \frac{Animal\ Km}{Human\ Km}$

In the present case, animal dose is 75 mg/ mL. From the above formula, the Km factor are constant and known. The animal Km vary from one animal to another according to the species (Km of rat is 6 while the human Km is 37 for adult and 25 for child). Our phytodrug has been pre-formulated as a syrup (Reagan-Shaw S et al., 2007), with the consumable doses evaluated as follows. This operation has several steps :

1er step : Human effective dose calculation

$$HED = 75 \times 6/\ 35 = 12.857\ mg/\ kg.$$

2nd step : Calculation of the daily dose for an adult

$$D = HED \times 60 = 12.857 \times 60 = 771.428\ mg/\ day$$

3th step : Preparation of simple syrup

The standard formula for a syrup saturated 6.7g of sugar for 3.3g of water. A total of 10g of simple syrup. It is advisable to use demineralized or deionized water.

4th step : Determination of quantity of each ingredient

- **Extract (active ingredient)**

The daily dose is 771,428 mg for an adult. The normal concentration of the active ingredient is 1.3mg/ mL. One teaspoon is 15mL; i.e. a concentration of 19.5 g/15 mL. For our extract, we will have 771.428/3 = 257.1426;

(257.1426/ 19500) x 100 = 1.3179% = 1.3% of active ingredient per spoon.

- **Conservator or stabilizer (Sodium benzoate)**

It is advisable to vary the percentage of stabilizers in order to determine which stabilizes the product over a long period. This percentage varies between 0.05 and 0.5%.

- **For orange essence:** The percentage is standard for essences and is 0.5%.
- **for Aroma:** The percentage is also standard for aromas and is 0.1%.
- **Simple syrup:**

Its percentage is deducted from the percentages of the other ingredients:

% syrup = 100% - (% extract +% stabilizer +% orange essence +% flavor)

= 100% - (1.3179% + 0.3% + 0.5% + 0.1%)

= 97.8

So, in 100 mg of phytomedicine, we will have 97.8 mg of saturated simple syrup (excipient), 1.3179 mg of crude extract (active principle), 0.3 mg of sodium benzoate (preservative), 0.5 mg of orange oil (ingredient) and 0.1 mg of flavor (ingredient).

GENERAL CONCLUSION AND PROSPECTS

General conclusion

The aim of this work was to assess the antisalmonellosis activity involved in typhoid fever of the hydro-ethanolic extracts and fractions of *D. microcarpum* and to chemically investigate the active fractions. This plant was chosen because of its uses in traditional medicine and on the basis of chemo-taxonomic data.

Bio-guided fractionation of the methanolic and the hydroethanolic extracts as well as the purification of fractions of the different parts of this plant, using liquid chromatography technics, led to the isolation of twenty-nine compounds of which nineteen have been fully characterized. They belong to six classes of natural substances and were classified as follows:

- Three diterpenoids: one of the clerodane type known as (4a*R*,5*S*,6*R*,8a*R*)-5-(carboxymethyl)-5,6,8a-trimethyl-3,4,4a,5,6,7,8,8a-octahydronaphthalene-1-carboxylic acid **118** and two of the labdane type, including a new one to which the trivial name microcarpin **116** was assigned and another known as rhinocerotinoic acid **117**,
- One new cyanogenic derivative to which we assigned the name Microcarposide **114**,
- One new ceramide to which the trivial name microcarpamide **115** has been assigned,
- One xanthone : 1,7-dihydroxy-6-methylxanthone **129**,
- Two flavonoids: luteolin **131** and epicatechin **132,**
- Five pentacyclic triterpenes: ursolic acid **123**, alphitolic acid **121**, betulinic acid **120**, 3*β*,23*β*-dihydroxylup-20(29)-en-28-oic acid **122** and lupeol **119** all known,
- Five phytosterols: *β*-sitosterol **128** and its 3-*O*-*β*-*D*-glucopyranoside derivative **125**, stigmasterol **127** and its 3-*O*-*β*-*D*-glucopyranoside derivative **126** and the mixture of *β*-sitosterol and stigmasterol **124**,
- One phenolic compound: methyl gallate **130**.

The determination of the structures of all these compounds was made possible by an analysis of their spectral data in particular, the ^{1}H and ^{13}C NMR one-and two-dimensional in conjunction with mass spectrometry, appealing not only to the electronic impact but also to soft ionization methods such as electrospray.

In the second part of this work, some of the structures such as, microcarposide, microcarpine and (4a*R*,5*S*,6*R*,8a*R*)-5-(carboxymethyl)-5,6,8a-trimethyl-3,4,4a,5,6,7,8,8a-octahydronaphthalene-1-carboxylic acid were recrystallized to record their crystallographic data, in order to determine their absolute stereochemistry and to confirm their structures. In addition, the ketone function in rhinocerotonoic acid was reduced by hemisynthesis and led to the formation of a novel hydroxylated derivative of hemisynthesis. This reduction was

performed in order to identify the chemical function responsible for antimicrobial activity within the molecule.

Extracts, fractions and some isolated compounds were evaluated for their antimicrobial activities on three salmonella strains, namely, *S. typhi*, *S. enteritidis* and *S. typhimurium*. The results obtained showed that :

- The hydroethanolic extracts of the different parts of our plant exert an activity on at least one strain of salmonella. The best activity was that of the root-bark and root-wood exerted on *S. typhimurium* with a MIC value of 1.95 μg/mL. Extracts from the root bark were also evaluated *in vivo* in infected rats with *S. enteritidis*. At the end of this curative test, we obtained good results from the interpretation of histological sections of the different organs of the rats used. Acute and subacute toxicity tests were also carried out and no toxicity signs or death were recorded when the plant extract was administered. This is an indication that the oral lethal dose-50 (LD_{50}) of the hydroethanolic root-bark extract of *D. microcarpum* was greater than 5000 mg/kg and is non-toxic at very low doses.
- Following the bio-guided process, the fractions that were obtained from the active extracts were evaluated for their antisamonella activities. Only the ethyl acetate fractions showed an activity, with a MIC value of 250 μg/mL. This value indicates that we lost the activity of our starting extracts during fractionation, an activity which could be due to the synergy of the compounds contained in the crude extract.
- Among the compounds isolated, some were tested for their antisalmonella activity. At the end of this test, three compounds: microcarposide, rhinocerotinoic acid and microcarpamide exhibited moderate antisalmonella activity *in vitro* against three strains namely *S. typhi*, *S. enteritidis* and *S. typhimurium* with minimum inhibition concentration values (MIC) of 153.4, 76.7, and 76.7 μM, respectively.

The third part of our work concerned the pre-formulation of a phyto-drug. The results of the *in vitro* and *in vivo* test on the same salmonella strains obtained, allowed us to perform a pre-formulation in the form of a syrup, to be used for the treatment of typhoid.

In view of all these results, we could conclude that the many uses of *D. microcarpum* in traditional medicine, would be due to the presence of terpenoids, in particular diterpenoids, a class of secondary metabolites endowed with interesting antimicrobial activities.

Perspective of our work, we plan to:

- Explain the mechanisms of action of *D. microcarpum*'s diterpenes in relation to their antimicrobial activities,

- Conduct a study of the stability, pharmacokinetics and dynamics of our preformulated phyto-drug,
- Standardize and perform clinical trials in order to formulate a phyto-drug,
- Submit all other isolated compounds to biological activity tests,
- Continue the structural elucidation of the five remaining compounds,
- Continue structural modifications on microcarpine and (4aR, 5S, 6R, 8aR)-5-(carboxymethyl)-5,6,8a-trimethyl-3,4,4a,5,6,7,8,8a-octahydronaphthalene-1-carboxylic acidin order to initiate the study of the structure activity relationship,
- Extend our investigations on other species of the genus *Detarium* such as *D. macrocarpum, D. senegalensis* ...

CHAPTER III:
EXPERIMENTAL PART

III.1. INSTRUMENTS AND GENERAL METHODS

Melting points were measured on a Buchii melting point apparatus. Optical rotations were recorded on a Perkin-Elmer-241 MC Polarimeter. IR spectra were recorded on a Bruker Fourier transform/infrared (ATR) spectrophotometer. Mass spectra (ESI–MS) were obtained with a Thermo-Finnigan LCQ DECA mass spectrometer and HRESIMS spectra were measured with a FTHRMS-Orbitrap (Thermo-Finnigan) mass spectrometer.

1D- and 2D- NMR spectra were recorded in deuterated solvents on either Bruker ARX 500 or AVANCE DMX 600 NMR spectrometers (proton at 500 MHz and carbon ^{13}C at 125 MHz). All chemical shifts (δ) were measured in parts per million (ppm) using a residual solvent signal as secondary reference relatively to tetramethyl silane (TMS) as internal standard, while coupling constants (*J*) are given in *Hz*. Solvents were distilled prior to their use. Analytical grade solvents were used for LCMS.

Column chromatography (CC) was performed using Merck MN silica gel 60 M (0.04–0.063 nm) and thin layer chromatography (TLC) was performed on aluminum silica gel 60 F_{254} (Merck) precoated plates (0.2 mm layer thickness). Spots were visualized on TLC either by UV lamp (254 and 366 nm) or by heating after spraying with 20% H_2SO_4 (v/v) solution. Diff erent mixtures of *n*-hexane, EtOAc, CH_2Cl_2 and MeOH were used as eluting solvents.

The antibacterial activity of compounds **1**-**5** was evaluated using the microdilution method (Newton et *al*., 2002). The determination of minimal inhibitory concentrations (MICs) and minimal bactericidal concentrations (MBCs) of these compounds were done using *Salmonella* strains: *S. typhi* (ST), *S. typhimirium* (STM) and *S. enteritidis* (SE).

The minimum inhibitory concentration (MIC) of compounds **1**-**5** were determined through the broth microdilution method in 96-well micro-titre plates. The 96-well plates were prepared by dispensing into each well 50 μL of Mueller Hinton broth. The test substances were initially prepared in DMSO in broth medium at 25mg/mL. A volume of 100 μL of each test sample was added into the first wells of the micro-titre plate. Serial two-fold dilutions of these test samples were made and 50 μL of inoculum standardized at 10^6 CFU/ml. The last wells (N°12) served as sterility controls (contained broth only) or negative control (broth plus inoculum). This gave final concentration ranges of 306.80-0.29 μM (for compound) and 386.30-0.37 μM (for reference drug: Ciprofloxacin), respectively. The plates were incubated at 37°C for 24 h. The MICs of the test compounds was detected following addition of 20 μL of rezasurin (a lamar blue TM Cell Viability Reagent) solution. Viable bacteria reduced the yellow due to a pink color. The MIC corresponded to the lowest well concentration where no color change was observed, indicating no growth of microorganism. The MBC was determined by adding 50 μL

aliquots of the clear wells to 100 μL of freshly prepared both medium and incubating at 37°C for 24h. The MBC was regarded as the lowest concentration of test sample which did not produce a color change as above. All tests were performed in triplicates at two different occasions.

III.2. EXPERIMENTAL

III.2.1. *In vitro* antisalmonella assays

The antibacterial activity of extracts, fractions and compounds was evaluated using the microdilution method (Newton et *al*., 2002). The determination of minimal inhibitory concentrations (MICs) and minimal bactericidal concentrations (MBCs) of these compounds was done using Salmonella strains: *S. typhi* (ST), *S. typhi mirium* (STM) and *S. enteritidis* (SE) (Supplemental material Table S3).

The minimum inhibitory concentration (MIC) of extracts, fractions and compounds were determined through the broth microdilution method in 96-well micro-titre plates. The 96-well plates were prepared by dispensing into each well 50 μL of Mueller Hinton broth. The test substances were initially prepared in DMSO in broth medium at 25mg/mL. A volume of 100 μL of each test sample was added into the first wells of the micro-titre plate. Serial two-fold dilutions of these test samples were made and 50 μL of inoculum standardized at 10^6 CFU/ml. The last wells (N°12) served as sterility controls (contained broth only) or negative control (broth plus inoculum). This gave final concentration ranges of 306.80-0.29 μM (for compound) and 386.30-0.37 µM (for reference drug: Ciprofloxacin), respectively. The plates were incubated at 37°C for 24 h. The MICs of the test compounds was detected following addition of 20 μL of resazurin (a Lamar blue TM Cell Viability Reagent) solution. Viable bacteria reduced the yellow due to a pink color. The MIC corresponded to the lowest well concentration where no color change was observed, indicating no growth of microorganism. The MBC was determined by adding 50 μL aliquots of the clear wells to 100 μL of freshly prepared both medium and incubating at 37°C for 24h. The MBC was regarded as the lowest concentration of test sample which did not produce a color change as above. All tests were performed in triplicates at two different occasions.

III.2.2 *In vivo* antisalmonella assay

III.2.2.1 Animals and ethics

The animals used in this study comprised of Wistar albino rats (7-8 weeks and 150-170 g) for antityphoid activity of the root back's extract of *D. microcarpum*. These animals

were bred in metabolic cage. They were housed in metabolic cage, fed with composed food (Appendix 4) and provided with tap water for drinking ad libitum. A quantity of composed feed (1 kg) was mixed with 500 ml of tap water. Small quantities of this mixture were rounded (ball-shaped) and given undried to the animals.

This test was carried out using a Salmonella typhimurium-induced typhoid model in rat. Only the hydroethanolic crude extract of the root barks was used in the treatment of infected animals. Prior to the test, animals were housed under the test conditions for a period of one week. The study was conducted with the approval of the Cameroon National Ethical Committee (Ref n°. FW-IRB00001954).

III.2.2.2 Immunosuppression of animals

Animals were immunosuppressed two days before infection by the oral administration of 30 mg/kg. of cyclophosphamide as previously described (Abhishek et *al*., 2008) with slight modifications. Immunosuppression prevents the rapid intervention of the immune system in the eradication of the disease condition.

III.2.2.3 Typhoid induction

A *Salmonella typhimurium* suspension was prepared at 0.5 Mc Farland turbidity scale as above. One millilitre (1 ml) of this solution containing about 10^8 CFU was orally administered to each animal (Havelaar et *al*., 2001). Only infected animals were selected on the basis of their faecal colony counts and used.

III.2.2.4 Experimental animal groups

Animals were arranged into fourteen groups of three animals. Groups M_0, M_1, M_2, M_3, M_4, M_5, and M_6 were males while groups F_0, F_1, F_2, F_3, F_4, F_5 and F_6 were females. The animals were treated as follows:

- Groups M_0 and F_0 (which were neither infected nor treated, and used as neutral control; they received distilled water).
- Groups M_1 and F_1 (which were neither infected nor treated, and used as immunosuppressed neutral control; they received also distilled water).
- Groups M_2 and F_2 (which were infected, but not treated) received distilled water during the treatment period, hence were used as negative control groups;
- Groups M_3 and F_3 received ciprofloxacin, and thus were used as positive control groups.
- Graded doses (75, 150, and 300 mg/kg) of the hydro-alcoholic extract root bark of *D. microcarpum* were administered to rats in groups M_4 and F_4, M_5 and F_5, M_6 and F_6,

respectively, by gastric intubation for ten consecutive days for the suppressive test and fourteen consecutive days for the curative test.

Food and water were given to the animals before and during the treatment ad libitum. Treatment was done by administering the extracts orally, every morning. After one day, the faecal matter was collected during the administration process. The collection of faecal matter was possible as the animals were a bit stressed up by the administration of the test substance, passing out the faeces spontaneous.

III.2.2.5 Assessment of stool bacterial density

The extent to which the animals complied with treatment was studied by counting the number of bacterial colonies in the faecal samples using the following protocol.

- 0.10 g of faecal matter was completely dissolved in 5 ml of autoclaved distilled water.
- 100 µl of the resulting solution was spread on the surface of solidified 0.9% saline SS agar in 90 mm type Petri dishes.
- After incubation for 18 hrs at 37 °C, the number of colonies following growth of Salmonella typhimurium in each Petri dish was counted and recorded.
- The results were converted into the number of colonies per gram of faecal matter per animal.

The time course for the bacteria treatment was assessed from the number of colonies obtained for each animal with time and this gave us an idea on how the animals were complying with treatment using the extract and thus the duration of treatment using the optimum dose regimen

Each time a group was completely healed (faecal bacterial charge comparable to that of the uninfected group M_2 and F_2), the animals were sacrificed and blood and organs were collected for haematological, biochemical and histological analyses.

III.2.3. Toxicity profile

The animals used in this investigation were male and female Wistar Albino rats provided by the animal house of the Faculty of Science of the University of Yaoundé I where they were housed under standard conditions with 12 hours photoperiod and had free access to water and food. The rats were 6-8 weeks old.

III.2.3.1 Sub-acute oral toxicity

The oral sub-acute toxicity of crude extract (Hydroethanolic root bark extract of *D. Microcarpum*) was evaluated in Wistar Albino rats according to the procedure outlined by the Organization for Economic Co-operation and Development (OECD) 425 protocol with some

modifications. A total of sixty rats were divided into six groups, each containing five males and five females. The test drug was administered at doses 150, 300 and 600 mg/kg to the test groups once daily for a period of 28 days, whereas the control group received distilled water. Satellite groups contained 10 males and 10 females and were administered the highest dose (600 mg/kg) and control for 28 days and then observed for the next 2 weeks (14 days). The animals were observed for mortality and signs of toxicity for a period of 28 days and 42 days. Individual body weights of rats were taken initially and at every two days intervals till day 28 and 42. Diethyl ether was used to anaesthetize the animals before blood samples were collected in EDTA tubes and dry tubes from all the animals through decapitation on 29th and 43th day.

III.2.4. Plant material

The fruits of *D. microcarpum* were harvested in Gamba savanna (Mvina division, Adamaoua region of Cameroon) on March 2017. Identification was done by M. NGANSOP Eric, a Botanist of the Cameroon National Herbarium, Yaoundé, where a voucher specimen has been deposited under the registration number HNC/57227.

III.2.4.1. Extraction, fractionation and isolation

III.2.4.1.1. Extraction

Air-dried powder of fruit, leaves, root-bark and bark of *D. microcarpum* were extracted 3 times (3 × 10 L) by maceration at room temperature (about 25°C) with methanol and also with the mixture of ethanol and water (7:3) for 48 h. After filtration, the resulting solutions were concentrated under reduced pressure. The extraction results obtained are shown in the tables below.

Table XI (cf. chap II): Methanol extraction results of the different parts of *D. microcarpum*

Organes	**Codes**	**Powder Mass (g)**	**Mass Extract (g)**	**Extraction percentage** (%)
Fruits	DMF	545	340	62.38
Leaves	DML	400	116	29.00
Roots barks	DMRb	752	320	42.55
Roots	DMR	1900	600	31.57

Table XII(cf. chap II): ethanol water extraction results of the different parts of *D. microcarpum*

Serie	Code	Organs	Powder Mass (g)	Mass Extracts (g)	Extract dissolution solvent	Extraction percentage (%)
A	DMA	Seeds	154	25	MeOH	16,23
B	DMB	Fruits	457	279	MeOH	61,05
C	DMC	Branches	185	96	MeOH	51,89
D	DMD	Young leaves	210	49	MeOH et H_2O	23,33
E	DME	Old leaves	501	73	MeOH et H_2O	14,57
F	DMF	Bark	868	373	MeOH	42,97
G	DMG	Root	2400	832	MeOH	34,66

III.2.4.1.2. Fractionation

In parallel with the evaluation of the biological activities, we proceeded with the bio-guided fractionation of these various extracts. The fractionation was carried out using different solvents ranging from the least polar (hexane), to the more polar (water) via intermediate-polar solvents (methylene chloride, ethyl acetate and n-butanol). Thus, after evaporation and lyophilization, several crude extracts were obtained. The results of the fractionation obtained are recorded in the table below.

For the methanol extracts only fruits extract was fractionated using successively *n*-hexane (hex), dichloromethane (DCM), ethyl acetate (EA) and *n*-butanol (*n*-BuOH) through flash chromatography over silica gel, to yield five fractions.

Table XIII (cf. chap II): Fractionation results of the methanol extract of fruits.

Organs	Solvants	Fraction codes	Masses extracts (g)
Fruits	n-Hexane	DMf1	15
	CH_2Cl_2	DMf2	19
	AcOEt	DMf3	30
	n-Butanol	DMf4	57

The different ethanol-water extracts were first submitted to antisalmonella test and then fractionated using successively *n*-hexane (hex), dichloromethane (DCM), ethyl acetate (EA), *n*-butanol (*n*-BuOH) and water through flash chromatography over silica gel, to yield five fractions for each part. Thus, after evaporation and lyophilization, 35 crude extracts were obtained. The results of the fractionation obtained are recorded in the table below.

Table 14: Fractionation results of the ethanol-water extract of different organs of *D. microcarpum*

Organs	Solvants	Fraction codes	Masses extracts (g)
Fruits	n-Hexane	DMB1	15
	CH_2Cl_2	DMB2	17
	EtOAc	DMB3	22
	n-Butanol	DMB4	27
	Water	DMB5	168
bark	n-Hexane	DMF1	7
	CH_2Cl_2	DMF2	9
	EtOAc	DMF3	10
	n-Butanol	DMF4	62
	Water	DMF5	97
Root	Hexane	DMG1	9
	CH_2Cl_2	DMG2	12
	EtOAc	DMG3	23
	n-Butanol	DMG4	135
	Water	DMG5	709

III.2.4.1.3. Isolation

a. Purification of fractions from methanol extract of fruit of *D. microcarpum*

a.1. Column chromatography of dichloromethane fraction (DMf2)

The dichloromethane fraction was subjected to CC over silica gel (0.04-0.063 nm) using n-hexane with a gradient of EtOAc. One hundred fractions of 100 mL each were collected and combined according to their TLC profiles on pre-coated silica gel 60 F_{254} plates developed with *n*-hexane/EtOAc mixture. The study of these subfractions led to the isolation of **betulinic acid** (160 mg).

Table XXXVIII : Chromatogram of fraction DMf2 from MeOH extract of fruit of *D. microcarpum*

Eluent	Fractions N°	Observations	Compounds
100 % *n*-hexane	1-20	Mixture of oily compounds and a white one	-
Hex- EtOAc (95 :05)	21-30	Oily complex mixture	-
Hex- EtOAc (85 :15)	31-40	Mixture of about four compounds	-
Hex- EtOAc (75 :25)	41-50	Mixture of about 3 compounds	DMf21 (160 mg)
Hex- EtOAc (65 :35)	51-60	Mixture of about 3 compounds	-
Hex- EtOAc (50 :50)	61-70	Complex mixture of about 3 compounds	-
Hex- EtOAc (40 :60)	71-80	Mixture of about 5 compounds	-
Hex- EtOAc (25 :75)	81-95	Mixture of about 3 compounds	-
100 % EtOAc	96-100	Complex mixture	-

a.2. Column chromatography of ethyl acetate fraction (DMf3)

The ethyl acetate fraction was subjected to CC using the same silica (0.04-0.063 nm) and eluted with *n*-hexane/EtOAc gradient of increasing polarity. One hundred and ten fractions of 100 mL each were collected and combined according to their TLC profiles on pre-coated silica gel 60 F_{254} plates developed with *n*-hexane/EtOAc. The study of these subfractions led to the isolation of **methyl gallate** (9 mg), **luteoline** (7 mg) and **epicatechin** (12 mg).

Table XXXIX : Chromatogram of fraction DMf3 from MeOH extract of fruit of *D. microcarpum*

Eluent	Fractions N°	Observations	Compounds
Hex- EtOAc (95 :05)	1-15	Mixture of about 4 compounds	-
Hex- EtOAc (90 :10)	16-30	Mixture of about 3 compounds	-
Hex- EtOAc (80 :20)	31-40	Mixture of about 5 compounds	-
Hex- EtOAc (75 :25)	41-50	Mixture of about 4 compounds	DMf31 (9 mg)
Hex- EtOAc (70 :30)	51-60	Mixture of about 3 compounds	DMf 32 (7 mg)
Hex- EtOAc (65 :35)	61-70	Mixture of about 6 compounds	DMf 33 (12 mg)
Hex- EtOAc (50 :50)	71-80	Mixture of about 7 compounds	-
Hex- EtOAc (25 :75)	81-95	Mixture of about 4 compounds	-
100 % EtOAc	96-110	Complex mixture	-

a.3. Column chromatography of *n*-butanol fraction (DMf4)

The *n*-butanol fraction was also subjected to successive CC over silica gel (0.04–0.063 nm) eluting successively with *n*-hexane/EtOAc, and EtOAc/MeOH gradients. One hundred and thirty fractions, each containing 100 mL, were collected and combined according to their TLC profiles on pre-coated silica gel 60 F_{254} plates developed with *n*-hexane/EtOAc. The study of this subfraction led to the isolation of **lupeol** (14 mg), **β-sitosterol glucoside** (10 mg) and **microcarposide** (15 mg).

Table XL : Chromatogram of fraction DMf4 from MeOH extract of fruit of *D. microcarpum*

Eluent	Fractions N°	Observations	Compounds
100 % *n*-hexane	1-20	Mixture of oily compounds and a white one	-
Hex- EtOAc (95 :05)	21-30	Oily complex mixture	-
Hex- EtOAc (85 :15)	31-40	Mixture of about 3 compounds	-
Hex- EtOAc (75 :25)	41-50	Mixture of about 4 compounds	DMf41 (14 mg)
Hex- EtOAc (65 :35)	51-60	Mixture of about 4 compounds	-
Hex- EtOAc (50 :50)	61-70	Complex mixture of about 5 compounds	-
Hex- EtOAc (40 :60)	71-80	Mixture of about 6 compounds	-
Hex- EtOAc (25 :75)	81-90	Mixture of about 4 compounds	DMf 42 (10 mg)
100 % EtOAc	91-100	Complex mixture of about 5 compounds	-
EtOAc-MeOH (95 :05)	101-115	Complex mixture of about 5 compounds	DMf 43 (15 mg)
EtOAc-MeOH (95 :05)	116-130	Complex mixture	-

b. Purification of fractions from hydroethanolic extract of fruit of *D. microcarpum*

b.1. Column chromatography of hexane fraction (DMB1)

The n-hexane fraction was subjected to CC over silica gel (0.04-0.063 nm) eluting with a *n*-hexane/AcOEt mixture of increasing polarity. A total of one hundred and five fractions of 100 mL each were collected and combined according to their TLC profiles on pre-coated silica gel 60 F_{254} plates developed with *n*-hexane/EtOAc systems to afford nine main subfractions. The study of these fractions led to the isolation of ***β*-sitosterol** (70 mg) and the **rhinocerotonoic acid** (27 mg).

Table XLI : Chromatogram of fraction DMB1 from hydroethanolic extract of fruit of *D. microcarpum*

Eluent	Fractions N°	Observations	Compounds
100 % *n*-hexane	1-20	Mixture of oily compounds and a white one	-
Hex- EtOAc (95 :05)	21-30	Oily complex mixture	DMB11 (70 mg)
Hex- EtOAc (85 :15)	31-40	Mixture of about four compounds	-
Hex- EtOAc (75 :25)	41-50	Mixture of about 3 compounds	-
Hex- EtOAc (65 :35)	51-60	Mixture of about 3 compounds	DMB12 (27 mg)
Hex- EtOAc (50 :50)	61-70	Complex mixture of about 3 compounds	-
Hex- EtOAc (40 :60)	71-80	Mixture of about 5 compounds	-
Hex- EtOAc (25 :75)	81-95	Mixture of about 3 compounds	-
100 % EtOAc	96-105	Complex mixture	-

b.2. Column chromatography of dichloromethane fraction (DMB2)

The dichloromethane fraction was also subjected to successive CC using silica gel (0.04-0.063 nm) and eluted with a mixture of *n*-hexane and EtOAc (1:9-100% EtOAc) to afford **rhinocerotonoic acid** (16 mg), **5-(carboxymethyl)-5,6,8a-trimethyl-3,4,4a,5,6,7,8,8a-octahydronaphtalene-1-carboxylic acid** (170 mg) and **DMB23** (11 mg).

Table XLII : Chromatogram of fraction DMB2 from MeOH extract of fruit of *D. microcarpum*

Eluent	Fractions N°	Observations	Compounds
Hex- EtOAc (95 :05)	1-15	Mixture of about 4 compounds	-
Hex- EtOAc (90 :10)	16-30	Mixture of about 3 compounds	-
Hex- EtOAc (80 :20)	31-40	Mixture of about 5 compounds	-
Hex- EtOAc (75 :25)	41-50	Mixture of about 4 compounds	-
Hex- EtOAc (70 :30)	51-60	Mixture of about 3 compounds	DMB21 (16 mg)
Hex- EtOAc (65 :35)	61-70	Mixture of about 6 compounds	-
Hex- EtOAc (50 :50)	71-80	Mixture of about 7 compounds	DMB22 (170 mg)
Hex- EtOAc (25 :75)	81-95	Mixture of about 4 compounds	-
100 % EtOAc	96-114	Complex mixture	DMB23 (11 mg)

b.3. Column chromatography of ethylacetate fraction (DMB3)

The ethylacetate fraction was also chromatographed over silica gel (0.04-0.063 nm) and eluted with *n*-hexane/EtOAc (3:7 to 100%) to give **stigmasterol** (9 mg), **lupeol** (4 mg), and **β-sitosterol glucoside** (20 mg).

Table XLIII : Chromatogram of fraction DMB3 from MeOH extract of fruit of *D. microcarpum*

Eluent	Fractions N°	Observations	Compounds
100 % *n*-hexane	1-17	Mixture of oily compounds and a white one	-
Hex- EtOAc (95 :05)	18-30	Oily complex mixture	-
Hex- EtOAc (85 :15)	31-40	Mixture of about 3 compounds	DMB31 (9 mg)
Hex- EtOAc (75 :25)	41-50	Mixture of about 4 compounds	DMB32 (4 mg)
Hex- EtOAc (65 :35)	51-60	Mixture of about 4 compounds	-
Hex- EtOAc (50 :50)	61-70	Complex mixture of about 5 compounds	-
Hex- EtOAc (40 :60)	71-80	Mixture of about 6 compounds	DMB33 (20 mg)
Hex- EtOAc (25 :75)	81-90	Mixture of about 4 compounds	-
100 % EtOAc	91-100	Complex mixture of about 5 compounds	-

c. Purification of fractions from hydroethanolic extract of root-bark of *D. microcarpum*

c.1. Column chromatography of hexane fraction (DMF1)

The *n*-hexane fraction was subjected to successive CC over silica gel (0.04–0.063 nm) eluting with a mixture of *n*-hexane and AcOEt of increasing polarity to yield ***β*-sitosterol and stigmasterol** mixture (15 mg) and **DMF12** (7 mg).

Table XLIV : Chromatogram of fraction DMF1 from hydroethanolic extract of fruit of *D. microcarpum*

Eluent	Fractions N°	Observations	Compounds
100 % *n*-hexane	1-15	Mixture of oily compounds and a white one	-
Hex- EtOAc (95 :05)	16-30	Oily complex mixture	DMF11 (15 mg)
Hex- EtOAc (85 :15)	31-40	Mixture of about four compounds	-
Hex- EtOAc (75 :25)	41-50	Mixture of about 3 compounds	-
Hex- EtOAc (65 :35)	51-60	Mixture of about 3 compounds	-
Hex- EtOAc (50 :50)	61-70	Complex mixture of about 3 compounds	DMF12 (7 mg)
Hex- EtOAc (40 :60)	71-80	Mixture of about 5 compounds	-

Hex- EtOAc (25 :75)	81-93	Mixture of about 3 compounds	-
100 % EtOAc	94-115	Complex mixture	-

c.2. Column chromatography of dichloromethane fraction (DMF2)

The dichloromethane fraction was subjected to successive CC using silica gel (0.04–0.063 nm) and eluting with a mixture of *n*-hexane and EtOAc (1:9-100%) to give ***β*-sitosterol and stigmasterol** mixture (8 mg), **betulinic acid** (20 mg) and **Lup-20(29)-en-28-oic acid, 3,23-dohydroxy-, (3α, 24α)**.

Table XLV : Chromatogram of fraction DMF2 from MeOH extract of fruit of *D. microcarpum*

Eluent	Fractions N°	Observations	Compounds
Hex- EtOAc (95 :05)	1-10	Mixture of about 4 compounds	-
Hex- EtOAc (90 :10)	11-25	Mixture of about 3 compounds	DMF21 (8 mg)
Hex- EtOAc (80 :20)	26-40	Mixture of about 5 compounds	-
Hex- EtOAc (75 :25)	41-50	Mixture of about 4 compounds	-
Hex- EtOAc (70 :30)	51-60	Mixture of about 3 compounds	DMF22 (20 mg)
Hex- EtOAc (65 :35)	61-70	Mixture of about 6 compounds	-
Hex- EtOAc (50 :50)	71-80	Mixture of about 7 compounds	DMF23 (17 mg)
Hex- EtOAc (25 :75)	80-98	Mixture of about 4 compounds	-
100 % EtOAc	99-107	Complex mixture	

c.3. Column chromatography of ethyl acetate fraction (DMF3)

The ethyl acetate fraction was also chromatographed and eluted with a mixture of *n*-hexane and EtOAc of increasing polarity (3:7-100%) to yield **betulinic acid** (7 mg), **ursolic acid** (125 mg), and **alphitolic acid** (28 mg).

Table XLVI : Chromatogram of fraction DMF3 from MeOH extract of fruit of *D. microcarpum*

Eluent	Fractions N°	Observations	Compounds
100 % *n*-hexane	1-20	Mixture of oily compounds and a white one	-
Hex- EtOAc (95 :05)	21-30	Oily complex mixture	-
Hex- EtOAc (85 :15)	31-40	Mixture of about 3 compounds	-
Hex- EtOAc (75 :25)	41-50	Mixture of about 4 compounds	DMF31 (7 mg)

Hex- EtOAc (65 :35)	51-60	Mixture of about 4 compounds	DMF32 (125 mg)
Hex- EtOAc (50 :50)	61-70	Complex mixture of about 5 compounds	DMF33 (28 mg)
Hex- EtOAc (40 :60)	71-80	Mixture of about 6 compounds	-
Hex- EtOAc (25 :75)	81-90	Mixture of about 4 compounds	-
100 % EtOAc	91-100	Complex mixture of about 5 compounds	-

d. Purification of fractions from hydroethanolic extract of root of *D. microcarpum*

d.1. Column chromatography of hexane fraction (DMG1)

The *n*-hexane fraction was subjected to CC over silica gel (0.04-0.063 nm) eluting with *n*-hexane, *n*-hexane/ EtOAc and EtOAc. One hundred fractions of 100 mL each were collected and combined on the basis of their TLC profiles to afford nine subfractions. The study of these subfractions led to the isolation of **β-sitosterol** (6 mg) and the **rhinocerotonoic acid** (14 mg).

Table XLVII : Chromatogram of fraction DMG1 from hydroethanolic extract of fruit of *D. microcarpum*

Eluent	Fractions N°	Observations	Compounds
100 % *n*-hexane	1-14	Mixture of oily compounds and a white one	-
Hex- EtOAc (95 :05)	15-30	Oily complex mixture	DMG11 (6 mg)
Hex- EtOAc (85 :15)	31-40	Mixture of about four compounds	-
Hex- EtOAc (75 :25)	41-50	Mixture of about 3 compounds	-
Hex- EtOAc (65 :35)	51-60	Mixture of about 3 compounds	DMG12 (14 mg)
Hex- EtOAc (50 :50)	61-70	Complex mixture of about 3 compounds	-
Hex- EtOAc (40 :60)	71-80	Mixture of about 5 compounds	-
Hex- EtOAc (25 :75)	81-95	Mixture of about 3 compounds	-
100 % EtOAc	96-100	Complex mixture	-

d.2. Column chromatography of dichloromethane fraction (DMG2)

The dichloromethane fraction followed similar separation and purification methods to provide **1,7-dihydroxy-6-methylxanthone** (8mg), **5-(carboxymethyl)-5,6,8a-trimethyl-3,4,4a,5,6,7,8,8a-octahydronaphtalene-1-carboxylic acid** (10 mg) and **detarine** (5 mg).

Table XLVIII : Chromatogram of fraction DMG2 from MeOH extract of fruit of *D. microcarpum*

Eluent	Fractions N°	Observations	Compounds
Hex- EtOAc (95 :05)	1-15	Mixture of about 4 compounds	-
Hex- EtOAc (90 :10)	16-30	Mixture of about 3 compounds	DMG21 (8 mg)
Hex- EtOAc (80 :20)	31-40	Mixture of about 5 compounds	-
Hex- EtOAc (75 :25)	41-50	Mixture of about 4 compounds	DMG22 (10 mg)
Hex- EtOAc (70 :30)	51-60	Mixture of about 3 compounds	DMG23 (5 mg)
Hex- EtOAc (65 :35)	61-70	Mixture of about 6 compounds	-
Hex- EtOAc (50 :50)	71-80	Mixture of about 7 compounds	-
Hex- EtOAc (25 :75)	81-95	Mixture of about 4 compounds	-
100 % EtOAc	96-110	Complex mixture	-

d.3. Column chromatography of ethyl acetate fraction (DMG3)

The ethyl acetate fraction was also chromatographed and eluted with the *n*-hexane and ethyl acetate mixture to give **microcarpamide** (13 mg) and **stigmasterol glucoside** (35 mg).

Table XLIX : Chromatogram of fraction DMG3 from MeOH extract of fruit of *D. microcarpum*

Eluent	Fractions N°	Observations	Compounds
100 % *n*-hexane	1-20	Mixture of oily compounds and a white one	-
Hex- EtOAc (90 :10)	21-30	Oily complex mixture	DMG31 (6 mg)
Hex- EtOAc (85 :15)	31-40	Mixture of about 3 compounds	DMG32 (7 mg)
Hex- EtOAc (75 :25)	41-50	Mixture of about 4 compounds	-
Hex- EtOAc (65 :35)	51-60	Mixture of about 4 compounds	-
Hex- EtOAc (50 :50)	61-70	Complex mixture of about 5 compounds	-
Hex- EtOAc (40 :60)	71-80	Mixture of about 6 compounds	DMG33 (35 mg)
Hex- EtOAc (25 :75)	81-90	Mixture of about 4 compounds	-
100 % EtOAc	91-100	Complex mixture of about 5 compounds	-

III.3 PHYSICO-CHEMICAL CHARACTERISTICS OF COMPOUNDS

III.3.1 Physico-chemical characteristics of compounds isolated from fruits

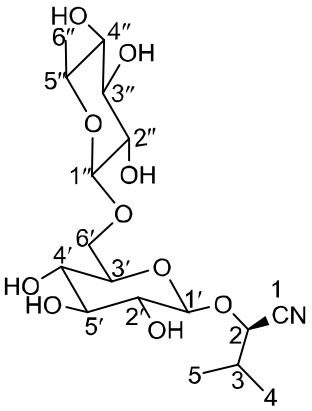

Compound DMf43: **Microcarposide, 3-methyl-2-[*β*-L-rhamnopyranoside-1(1→6)-*β*-D-glucopyranosyl] butanenitrile (114):** white crystals; $[\alpha]_{589}^{20} = -99$ (*c* =0.5, DMSO); IR (KBr) ν_{max} cm^{-1} : 3200-3500(OH), 1618(NH-C=O), *m/z* 408.1865 (calcd 408.1864 for $C_{17}H_{30}NO_{10}^{+}$ $[M+H]^{+}$), ^{1}H NMR (500 MHz, DMSO): and ^{13}C NMR (125 MHz, DMSO) NMR data see Table 17.

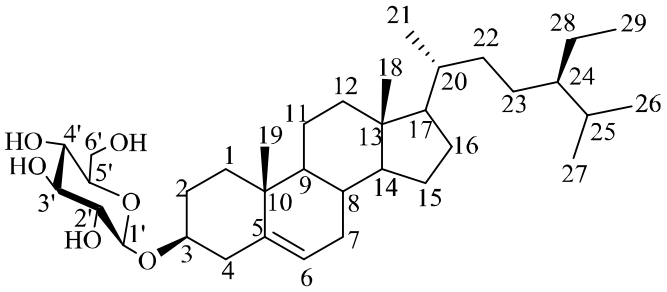

Compound DMf42=DMB33: ***β*-sitosterol-3-O-β-D-glucopyranoside (125)**: Colourless crystals; m. p. 260-261 °C; HRESI-MS m/z int (%) 414 (5), 396 (63), 381 (24), 255 (77), 159 (39), 81 (99), 55 (100), ^{1}H NMR (500 MHz, Pyridine-d_5) and ^{13}C (125 MHz, Pyridine-d_5) NMR data: see Table 28.

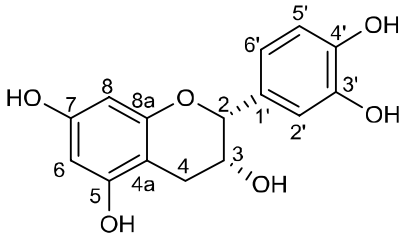

Compound DMf33: **(-)-Epicatechin (132)**: Brown solid; m. p. 241-242 °C; $[\alpha]^{30}_{D}$ -68.01 (c 0.24, MeOH); IR ν_{max} 3407, 1627, 1532, 1470, 1290, 1244, 1183, 1148, 1079, 1031, 819 cm-1

; UV (MeOH) λ_{max} 281; EI-MS m/z (rel. int.: %) 290 $[M]^+$ (29), 272 (40), 255 (9), 163 (18), 154 (60), 139 (100), 137 (70), 123 (63) and 110 (60). ^{1}H NMR (DMSO, 500 MHz) and ^{13}C NMR (DMSO, 125 MHz): see table 32.

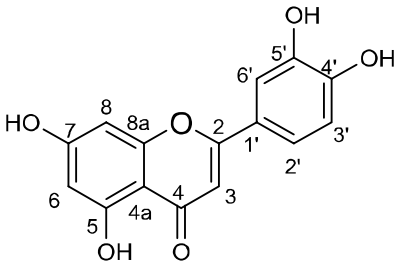

Compound DMf32: **Luteolin (131):** white powder; EI, $[M^+]$ at m/z 286.0476 (calcd 286.0477) for $C_{15}H_{10}O_6$; ^{1}H NMR (DMSO, 500 MHz) and ^{13}C NMR (DMSO, 125 MHz): see table 32.

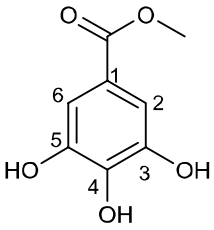

Compound DMf31: **Methyl gallate (130):** white powder; m. p. 240-242 ºC; EI, $[M^+]$ at m/z 184.0371 for $C_8H_8O_5$, ^{1}H NMR (DMSO, 500 MHz) and ^{13}C NMR (DMSO, 125 MHz): see table 31.

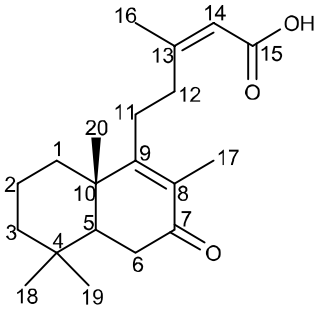

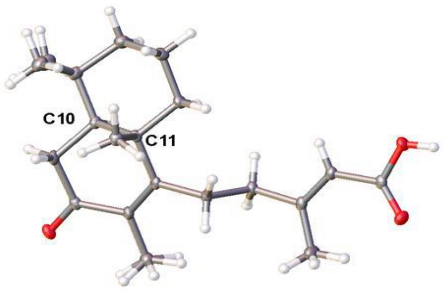

Compound DMB12=DMB21=DMG12: **Rhinocerotinoic acid (7-oxo-labda-8-13E-dien-15-oic acid) (118)**: white crystal, mp. 187–189 °C, $[\alpha]_D^{18}$ +38.9° (c 0.236, CHCl3). (+) HRESI-MS $[M+Na]^+$ at m/z 341.2108. ^{1}H NMR (DMSO, 500 MHz) and ^{13}C NMR (DMSO, 125 MHz) see table 21 (Rijo, 2011).

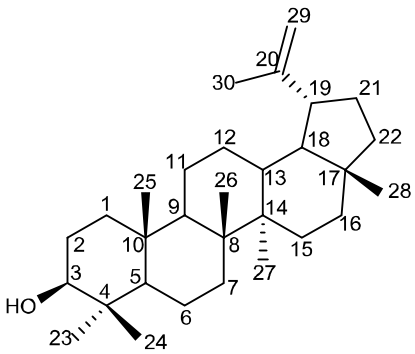

Compound DMB32=DMf41: **Lupeol (119):** white powder; HRESIMS, m/z 426.3045 for $C_{30}H_{50}O$; ^{1}H NMR ($CDCl_3$, 500 MHz) and ^{13}C NMR ($CDCl_3$, 125 MHz): see table 23 (Teixeira et al., 2017).

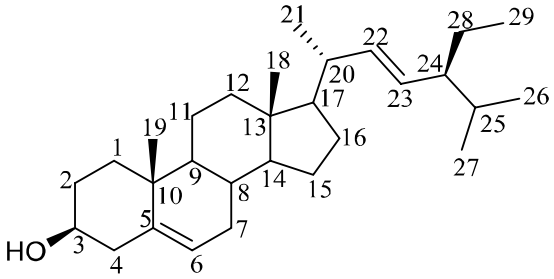

Compound DMB31: **Stigmasterol (127)**: Colorless needles; m. p. 137-138 °C; HRESI-MS $[M+H]^+$ m/z 412.3452 for $C_{29}H_{48}O$; ^{1}H NMR ($CDCl_3$, 500 MHz) and ^{13}C ($CDCl_3$, 125 MHz) NMR data: see Table 29.

III.3.2 Physico-chemical characteristics of compounds isolated from root bark.

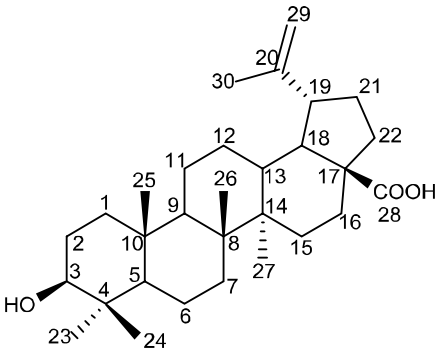

Compound DMF31=DMf21=DMF22: **Betulinic acid (120):** white powder; m.p 297 °C; HRESIMS: m/z 457.3721 for $C_{30}H_{48}O_3$; UV: 206 nm; IR (KBr): 3473, 3063, 2953, 2887, 2712, 1682, 1643, 1457, 1375, 1221, 1194, 1106, 1035, 980, 876, 871, 789 cm^{-1}; ^{1}H NMR ($CDCl_3$, 500 MHz) and ^{13}C NMR ($CDCl_3$, 125 MHz): see table 24 (Siddiqui *et al.*, 1988).

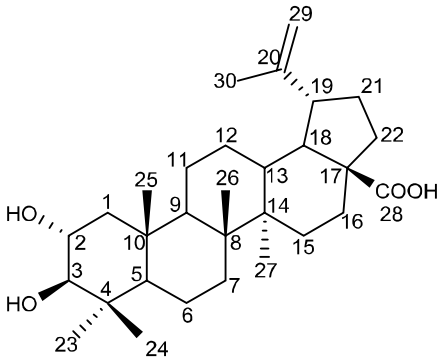

Compound DMF33: **Alphitolic acid (121)**: white powder; HR-EIMS: $[M]^+$ at m/z: 472.3; ^1H NMR ($CDCl_3$, 500 MHz) and ^{13}C NMR ($CDCl_3$, 125 MHz): see table 25

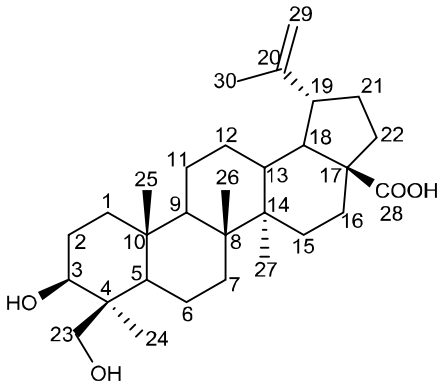

Compound DMF23: **3α,23α-Dihydroxylup-20(29)-en-28-oic acid (123):** white, amorphous powder; m. p. 199−200 °C; $[\alpha]^{26}_D$ −35.0 (c 0.2, CHCl3); IR (KBr) ν_{max} 3500, 3070, 2942, 1699, 1635 cm^{-1} ; HRESIMS m/z 472.3545 (calcd for $C_{30}H_{48}O_4$, 472.3552); ^1H (C_5H_5N, 500 MHz) and ^{13}C (C_5H_5N, 125 MHz) NMR data, see Table 27.

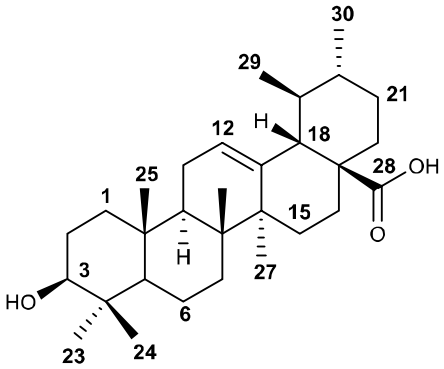

Compound DMF32: **Ursolic acid (122):** white powder; m. p. 197 °C; HRESI-MS $[M+H]^+$ at m/z 457.3731 for $C_{30}H_{48}O_3$; UV: 210 nm; IR (KBr): ν_{max} 3435, 3243, 3019, 2827, 2679, 2542,

1643, 1621, 1600, 1528, 1380, 1347, 1304, 1293, 1216, 963, 898, 843 cm^{-1}; ^{1}H NMR ($CDCl_3$, 500 MHz) and ^{13}C NMR ($CDCl_3$, 125 MHz) : see table 26 (Galgon et al., 1999).

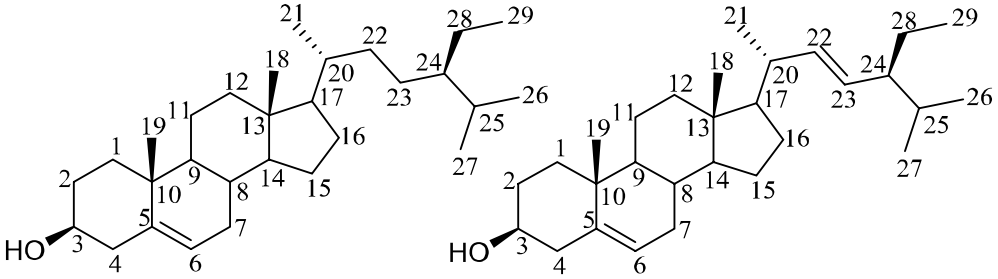

Compound DMF21: **Mixture of stigmasterol and β-sitosterol (124):** white needles, m. p. 123-124 °C

III.3.3 Physico-chemical characteristics of compounds isolated from root wood.

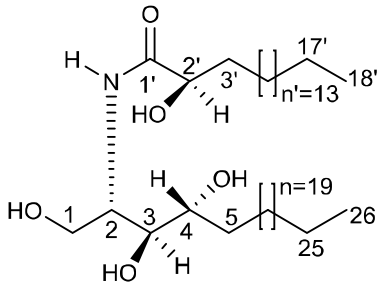

Compound DMG31=DMG32: **Microcarpamide, (2*S***, 2′*R***, 3*S***, 4*R***)-*N*-[2′-hydroxyhexadecanoyl]-2-amino-hexacosane-1,3,4-triol (115):** white crystals, mp 133 °C; $[\alpha]_D^{30}$ +27 (*c* =0.11, pyridine); IR (KBr) ν_{max} cm^{-1} : 3419(-OH), 2934(-C_{sp3}-H), 2201(-C≡N), 1422-812(-C_{sp3}-O), 665-417(-C_{sp3}-H); m/z 712.6819 (calcd 712.6814 for $C_{44}H_{90}NO_5^+$ $[M+H]^+$), ^{1}H NMR (500 MHz, pyridine-d_5): and ^{13}C NMR (125 MHz, pyridine-d_5) NMR data see Table 19.

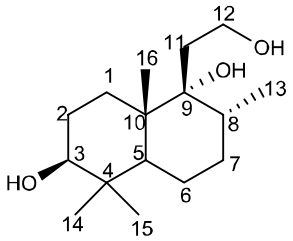

Compound DMG23: **Microcarpin, (3S, 5S, 8R, 9R, 10S)-8-methyl-tetranorlabdane-3, 9, 12-triol (116):** white crystals; $[\alpha]_D^{20}$ = + 20.5 (*c* =1.00, MeOH-$CHCl_3$); *m/z* 305.1901 (calcd

305.1889 for $C_{16}H_{30}O_3Cl^-$ [M+Cl]$^-$), ^{1}H NMR (500 MHz, pyridine-d_5) and ^{13}C NMR (125 MHz, pyridine-d_5) NMR data see Table 20.

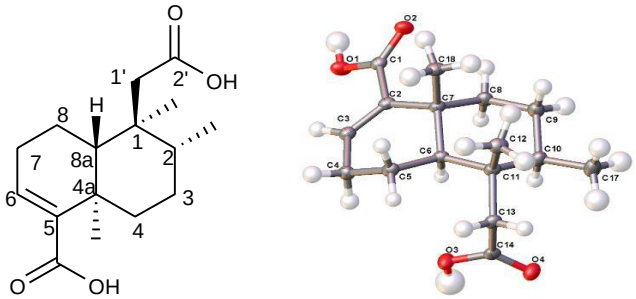

Compound DMG22=DMB22: **1-naphtbalene acetic-5-carboxy-1,2,3,4,4a, 7,8,8a-octahydro-1,2,4a-trimethyl acid (118)**: white crystals; m/z 279.1010, ^{1}H NMR (500 MHz, pyridine-d_5) and ^{13}C NMR (125 MHz, pyridine-d_5) NMR data see Table 22.

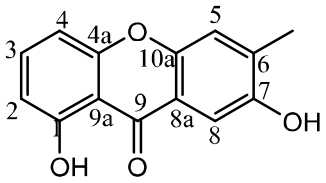

Compound DMG21: **1,7-dihydroxy-6-methylxanthone (129):** Yellowish cluster crystal; uV (MeOH) λ_{max} nm: 256.9, 288.9, 383.1; HRESIMS: m/z 241.0517, [M−H]$^-$ (Calcd 241.0506 for $C_{14}H_9O_4$,). ^{1}H (500 MHz, C_5D_5N) and ^{13}C (125 MHz, C_5D_5N) NMR data: see table 30.

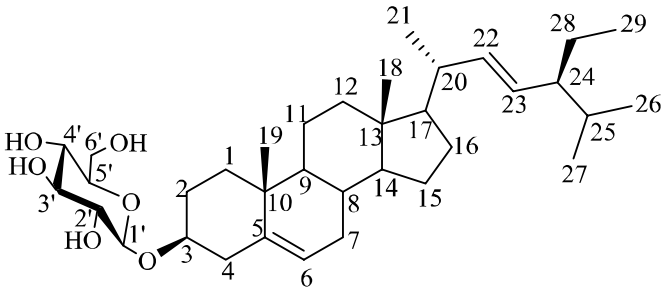

Compound DMG33: **Stigmasterol-3-*O*-*β*-*D*-glucoside (126):** white crystals; m p 274-276 °C; HR-EIMS *m/z*: 574,42334, $C_{35}H_{58}O_6$ [M]$^+$ RMN ^{1}H NMR (500 MHz, Pyridine-d_5) and ^{13}C (125 MHz, Pyridine-d_5) NMR data: see Table 28.

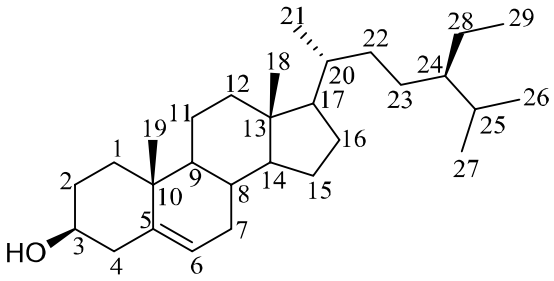

Compound DMG11=DMB11: ***β*-Sitosterol (128):** White powder; mp: 134- 135°C; MS (m/z): 414(M+), 396, 339, 325, 310, 298, 257, 227, 140, 139, 125, 97, 71, 57. ^{1}H NMR ($CDCl_3$, 500 MHz) and ^{13}C ($CDCl_3$, 125 MHz) NMR data: see Table 29.

III.4. CHEMICAL TRANSFORMATIONS AND PRE-FORMULATION OF PHYTO-DRUG.

III.4.1. Methanolysis of microcarpamide DMG32

Microcarpamide DMG32 (1mg) was added to a mixture of HCl (1 ml, 5%) and MeOH (1 ml), and heated at 70 °C for 12 h in a sealed small-volume vial. The reaction mixture was extracted with CH_2Cl_2 and the obtained CH_2Cl_2 layer was concentrated to give Long-Chain-Base (LCB) of sphingosine moiety for LC-MS analysis.

III.4.2. Reduction reaction on Rhinocerotinoic acid DMG12

In a well dried 250 mL ground flask, compound DMG12 (25 mg)(7.86×10^{-5} mol) was added to 25 mL of ethanol (95°). The mixture was heated slowly until the compound dissolved. After cooling the medium at room temperature, 400 mg (0.01 mol) of powdered sodium tetrahydruroborate ($NaBH_4$) was added and the solution was stirred at room temperature for 10 minutes.

a-Hydrolysis

For hydrolysis, 30 mL of distilled water were added to the reactional medium then refluxed for 5 minutes.

b-Isolation of product

The medium was cooled adding ice-cold distilled water (60 mL) to the flask then the content was poured into a cleaned beaker. After crystallization and filtration, the crystals were obtained and dried in an oven at 90°C.

III.4.3. Protocol of pre-formulation of phytomedicine from hydroethanolic root-bark extract

- **Preparation of simple syrup**

Introduce the previously weighed sugar powder into an conical flask with sufficient volume and then add a necessary and sufficient quantity of demineralized water. Heat the mixture to 50°C while stirring for about an hour, until a clear and homogeneous solution is obtained: this is simple syrup.

- **Preparation of the phytomedicine**

Let the simple syrup cool then weigh it and deduce the mass of the active ingredient to be added to it, knowing that 1.3179% of extract corresponds to 97.782% of simple syrup. Introduce a mass of active ingredient, previously weighed, into the simple syrup contained in a flask. Let the active ingredient dissolve until a limpid and homogeneous solution is obtained. Successively and gradually added the aroma, stabilizer and orange essence. The phytomedicine thus prepared is left to stand for 1 hour from time and finally bottled.

III.5. CHARACTERISTIC ANALYTICAL TESTS

III.5.1. Cyanogenic derivative test

Objective: Identification of cyanide function.

Reagents: Distilled water, picric acid

To 15 ml of distilled water we have added 2 g of the powder and then capped immediately and left to macerate for 1 hour. The neck of the conical flask is covered with paper soaked with picric acid and heated for a few minutes. The appearance of a brown color indicates the release of HCN.

III.5.2. Molisch's Test

Objective: Identification of sugars.

Reagents: EtOH, α-naphthol, concentrated H_2SO_4

To the sample to be analyzed, we have introduced into a test tube and dissolved in a solution of 1% ethanol in α-naphthol. A few drops of concentrated H_2SO_4 are added, letting it flow down the side of the tube. The appearance of a purple-red ring at the interface, between the liquids indicates the presence of a sugar or sugars.

III.5.3. Liebermann-Burchard test: identification of terpenes and sterols.

Objective: Identification of triterpenes and sterols.

Reagents: $CHCl_3$, Ac_2O, concentrated H_2SO_4 (50 mL/20 mL/1 mL).

To a $CHCl_3$ solution of the sample to be analyzed, we have added a few drops of acetic anhydride, followed by concentrated H_2SO_4. The presence of triterpenes and their saponins is indicated by a change of color from brick red, through purple, then blue and finally to green. Sterols give a blue color that rapidly changes to green.

III.5.4. Ferric Chloride Test

Objective: Identification of phenols.

Reagents: $FeCl_3$, MeOH

To an alcoholic solution of the sample, we have added a few drops of $FeCl_3$. A color change from yellow to purple indicates the presence of phenols.

III.5.5. Shinoda's Test

Objective: Identification of flavonoids.

Reagents: Mg, MeOH, concentrated HCl

To an alcoholic solution of the sample, we have added a few drops of concentrated HCl and a pinch of Mg fillings. The presence of flavonoids is indicated by effervescence and a deep pink (purplish) color.

REFERENCES

A

Abreu P. M., Rosa V. S., Araùjo E. M., Canda A. B., Kayser O., Bindseil K. U., Siems K. and Seemann A. **1998**. Phytochemical analysis and antimicrobial evaluation of *Detarium microcarpum* bark extracts. *Pharm. Pharmacol. Lett*; **8**, 107-109.

Abhishek K. S. and Vinod K. V. **2012**. Phytochemicals and Pharmacological Potential of *Nyctanthes arbortristis:* A Comprehensive Review. *International Journal of Research in Pharmaceutical and Biomedical Sciences*; **3**, 420-427.

Abhishek S. S., Alok S. W. and Archana R. J. **2008**. Immunomodulatory activity of methanolic extract of Murraya koenigii spreng leaves. *Indian J. Exp. Biol*; **46**, 505-509.

Abreu P. M. and Relva A. **2002**. Carbohydrates from *Detarium microcarpum* bark extract. *Carbohydr. Res* ; **337**, 1663-1666.

Abreu P. M., Rosa V. S., Araùjo E. M., Canda A. B., Kayser O., BindseilK. U., Siems K. and Seemann A., **1998**. Phytochemical analysis and antimicrobial evaluation of *Detarium microcarpum* bark extracts. *Pharm. Pharmacol. Lett*; **8**, 107-109.

Agbenu E., d'Almeida H., Kolou M., Aho M., Agbetiafa K., Padaro E. and David M. **2010**. Evaluation of the Widal-Felix serodiagnostic test in Togo. *Medecine tropicale : revue du Corps de sante colonial* ; **70**, 43-48.

Agbo R. I., Idohou R., Vihotogbé R., Missihoun A. A., Dagba R. A., Assogbadjo A. E. and Agbangla C. **2019**. Spatio-temporal dynamics of suitable habitats for *Detarium microcarpum* Guill. & Perr. (Caesalpiniaceae), a priority food tree species in Benin (West Africa). *Modeling Earth Systems and Environment*; **5**, 595-604.

Agrawal, P. K. (1989). Flavonoid glycosides. *Carbon-13 NMR of flavonoids*.

Aguirre M. C., Delporte C., Backhouse N., Erazo S., Letelier M. E., Cassels B. K. and Negrete R. **2006**. Topical anti-inflammatory activity of 2α-hydroxy pentacyclic triterpene acids from the leaves of *Ugni molinae*. *Bioorganic & medicinal chemistry*; **14**, 5673-5677.

Ahmed A. H., Meyer J. J., Jimeno M. L. and Rodríguez B. **2007**. Bioactive diterpenes from *Orthosiphon labiatus* and *Salvia africana-lutea*. *Journal of natural products*; **70**, 293-295.

Ali M. S., Syed A. I., Shakeel A. and Lobkovsky E. *2007.* A new germacranolide and a new ceramide from Salvia nubicola (Lamiaceae). Zeitschrift fuer Naturforschung; *62b*, 1333-1338.

Antillon M., Joshua L. W., Forrest W. C., Weinberger D., Kurum E., Deok P., Marks F. and Pitzer V. **2017**. The burden of typhoid fever in low- and middle-income countries: A meta-regression approach. *Neglected Tropical Diseases*; **11**, e0005376.

APG II. **2003**. An update of the Angiosperm Phylogeny Group classification for the orders and families of flowering plants: APG II. *Bot. J. Linnean Soc*; **141**, 399-436.

Aquino R., Ciavatta M. L., De Tommasi N. and Gàcs-Baitz E. **1992**. Tetranorditerpènes from *Detarium microcarpum*. *Phytochemistry*; **31**, 1823-1825.

Aquino R., Ciavatta M. L., De Tommasi N., De Simone F. and Pizza C. **1991**. Catechins from *Detarium microcarpum*. *Fitoterapia*; **62**, 455.

Aquino R., De Simone F., De Tommasi N., Piacente S. and Pizza C. **1995**. Structure and biological activity of sesquiterpene and diterpene derivatives from medicinal plants. In: Hostettmann K., Marston M., Maillard M., Hamburger M., (eds.), phytochemistry of Plants used in Traditional Medicine, Proceedings of the Phytochemical Society of Europe n°37, Clarendon Press, Oxford; pp. 268-275.

Aquino R., Ciavatta M. L., De Tommasi N. and Gàcs-Baitz E. **1992**. Tetranorditerpenes from *Detarium microcarpum*. *Phytochemistry*; **31**, 1823-1825.

Aquino R., Ciavatta M. L., De Tommasi N., De Simone F. and Pizza C. **1991**. Catechins from *Detarium microcarpum*. *Fitoterapia;* **62**, 455.

Aquino R., Ciavatta M., De Tommasi N. and Gàcs-Baitz E. **1992**. Phytochemistry ; *31*, 1823-1825.

Arbonnier M. 2000. Arbres, arbustes et lianes des zones sèches d'Afrique de l'Ouest. Cirad. MNHN. UICN. Montpellier. France ; p.541.

Arbonnier M. **2002**. Arbres, Arbustes et Lianes des Zones Sèches d'Afrique de l'Ouest. 2ème Ed., CIRAD - MNHN, Paris; pp. **9**-**18**, 234-235.

Arun S., Anakshi K. and Maheshwari P. K. **1988**. A labdane diterpene and its glycoside from *melodinus monogynus*. *Phytochemistry*; **27**, 2255-2259.

Arvigo R. and Balich M. **1993**. Rainforest remedies: one hundred healing herbs of Belize, *Lotus Press*, Twin lakes, USA.

Aubréville A. **1950**. Flore Forestière Soudano-Guinéenne. Société d'Editions Géographiques Martines et Coloniales, Paris ; pp. 227-231.

Ayafor J. F., Tchuendem M. H., Nyasse B., Tillequin F. and Anke H. **1994**. Novel bioactive diterpenoids from *Aframomum aulacocarpos*. *Journal of natural products*; **57**, 917-923.

B

Balandrin N. F., Kingdom A. D. and Farnsworth N. R. **1993**. Human medicinal agents from biologically active natural products, Pharmaceuticals, Cutler S. J., Cutler H. G. Eds. CRC press: New York, 25-37.

Bankeu K. J. J., Dawe A., Mbiantcha M., Feuya T. G. R., Ali I., Tchuenmogne T. M. A., Mehreen L., Lenta N. B., Ali S. M. and Ngouela A. S. **2017**. Characterization of bioactive compounds from *Ficus vallis-choudae* delile (moraceae). *Trends Phytochem. Res*; **1**, 235-242.

Bastard J., Duc D. K., Fetizon M., Francis M. J., Grant P. K., Weavers R. T. and Wovkulich P. M. **1984**. CMR spectroscopy of labdanic diterpenes and related substances. *Journal of natural products*; **47**, 592-599.

Berhaut J. **1975**. Flore Illustrée du Sénégal-Ficoïdées à Légumineuses. Tome IV. Gouvernement du Sénégal, Ministère de la Protection de la Nature, Ministère du Développement Rural, Direction des Eaux, Dakar, pp. 375-382.

Berk P. A. **2008**. In vitro and in vivo virulence of Salmonella typhimurium DT104: A parallelogram approach. Thesis Wageningen university, Wageningen, The Netherlands; p. 168.

Bhutta Z. A., Khan I. A. and Molla A. M. **1994**. Therapy of multidrug-resistant typhoid fever with oral cefixime, intravenous ceftriaxone. *Pediatric Infectious Disease Journal*, **13**, 990-993.

Bittner M., Schuster A. and Jakupovic J. **1991**. Diterpenes from *Diplostephium meyenii*. *Phytochemistry*; **30**, 1329-1330.

Britto C. D., Wong V. K., Dougan G. and Pollard A. J. **2018**. A systematic review of antimicrobial resistance in Salmonella enterica serovar Typhi, the etiological agent of typhoid. *Neglected tropical diseases*, **12**, e0006779.

Bruneton J. **1993**. Pharmacognosie, Phytochimie, Plantes Médicinales. 3^{e} édition, Techniques et Documents Lavoisier, Paris ; 663-669.

Bruneton J. **1999**. Phytochimie et plantes médicinales. Pharmacognosie, tome III, 3^{e} édition Paris, pp. 266-293.

Bryan F. L. **1977**. Diseases transmitted by foods contaminated by wastewater. *Journal of Food Protection*; **40**, p. 45-56.

Burkill H. M. **1995**. The Useful Plants of West Tropical Africa-Vol. 3 Families J-L. 2nd Ed., White friars Press, London; pp. 101-105.

C

Cao X. T. et al. **1999**. A comparative study of ofloxacin and cefixime for treatment of typhoid fever in children. The Dong Nai Pediatric Center Typhoid Study Group. *Pediatric Infectious Disease Journal*; **18**, p. 245-248.

Cavin A. L. **2007**. Contribution à la connaissance taxonomique et chimique de fruits africains du genre" Detarium"(Fabaceae-Caesalpinioideae) :" *D. microcarpum*" Guill. et Perr. et des formes comestibles et toxiques de" *D. senegalense*" J. F. Gmel. (Doctoral dissertation, University of Geneva.

Chaturvedula V. S. P. and Prakash I. **2012**. Isolation of Stigmasterol and β-Sitosterol from the dichloromethane extract of *Rubus suavissimus*. *Int. Curr. Pharm. J*; **1**, 239-242.

Chen L., Zhu H., Wang R., Zhou K., Jing, Y. and Qiu F. **2008**. ent-Labdane diterpenoid lactone stereoisomers from *Andrographis paniculata*. *Journal of natural products*; **71**, 852-855.

Chen S., Rotaru A. E., Liu F., Philips J., Woodard T. L., Nevin K. P. and Lovley D. R. **2014**. Carbon cloth stimulates direct interspecies electron transfer in syntrophic co-cultures. *Bioresource technology*, **173**, 82-86.

Chingwaru W., Vidmar J. and Kapewangolo P. T. **2015**. The potential of sub-saharan african plants in the management of human immunodeficiency virus infections: A review. *Phytotherapy Research*, **29**, 1452-1487.

Chinou I. **2005**. Labdanes of natural origin-biological activities (1981-2004). *Current medicinal chemistry*; **12**, 1295-1317.

D

Damilola A., Garba J., Wilson I. and Ume U. **2015**. Anti-typhoid and hepatic response in *Salmonella* Typhi infected rats treated with ethanol leaf extract of *Tithonia diversifolia*. *Asian Journal of Plant Science and Research*; **5**, 34-46

Damrong S., Petsom A., Ishikawa T. and Roengsumran S. **2003**. Cytotoxic activity of natural labdanes and their semi-synthetic modified derivatives from Croton oblongifolius. *Planta medica*; **69**, 167-170.

Date K., Shimpi R., Luby S., Haldar P., Katkar A., Wannemuehler K. and Loharikar A. **2020**. Decision Making and Implementation of the First Public Sector Introduction of Typhoid Conjugate Vaccine-Navi Mumbai, India, 2018. *Clinical Infectious Diseases*; **71**, S172-S178.

Date K. A., Bentsi-Enchill A. D., Fox K. K., Abeysinghe N., Mintz E. D., Khan M. I., Sahastrabuddhe S. and Hyde T. B. **2014**. Typhoid fever surveillance and vaccine use-South-East Asia and Western Pacific regions, 2009–2013. MMWR. *Morbidity and mortality weekly report*; **63**, 855.

De Jong P. and Insoo K. B. **2012**. Interviewing for solutions. Nelson Education.

Dekker T. G., Fourie T. G., Elmare´ M., Snyckers F. O. and van der Schyf C. J. **1988**. Studies of South African medicinal plants. Part 7: rhinocerotinoic acid, a labdane diterpene with anti-inflammatory properties from *Elytropappus rhinocerotis*. *S. Afr. J. Chem*; **41**, 33-35

DellaGreca M., Fiorentino A., Monaco P., Previtera L., Temussi F. and Zarrelli A. **2003**. Synthesis of degraded cyanogenic glycosides from Sambucus nigra. *Natural product research;* **17**, 177-181.

Dharani N. **2011**. Field guide to common trees & shrubs of East Africa. *Penguin Random House South Africa*.

Dieudonné N., Mouraba A., Abakar A., Boursou D. and Honore N. T. M. **2017**. In vivo toxicity study and antifilarial activity of four plants from Nord-Cameroon. *European Journal of Medicinal Plants*; 1-12.

Do J. C., Son K. H. and Kang S. S. **1988**. Studies on the constituents of the roots of *Rubus parvifolius* (I)-isolation of (-)-epicatechin. *Korean Journal of Pharmacognosy*; **19**, 170-173.

Dos Santos A. G., Perez C. C., Tininis A. G., Bolzani V. D. S. and Cavalheiro A. J. **2007**. Clerodane diterpenes from leaves of Casearia sylvestris Swartz. *Química Nova,* **30**, 1100-1103.

Dos Santos E. O., Meira M., Vale A. E. D., David J. M., de Queiróz L. P. and David J. P. **2012**. Isolation and characterization of new ceramides from aerial parts of Lepidaploa cotoneaster. *Natural Product Communications*; **7**, 1934578X1200700623.

Doughar J. H., Pukuma M. S. and De N. **2007**. Antibacterial effects of *Balanites aegyptiaca* L. Drel. And *Moringa oleifera* Lam. on *Salmonella Typhi*. *African Journal of Biotechnology*; **6**, 2212-2215.

Dutta P., Mitra U., Dutta S. and De A. **2001**. Ceftriaxone therapy in ciprofloxacin treatment failure typhoid fever in children. *Indian Journal of Medical Research*; **113**, 210.

E

Effa E. E., Lassi Z. S. and Critchley J. A. **2011**. "Fluoroquinolones for treating typhoid and paratyphoid fever (enteric fever)". Cochrane Database System Review; CD004530. doi: 10.1002/14651858.CD004530.pub4. PMID 21975746.

F

Fang X., Chen X., Liu Y., Li Q., Zeng Z., Maiyalagan T. and Mao S. **2019**. Nanocomposites of Zr (IV)-based metal-organic frameworks and reduced graphene oxide for electrochemically sensing ciprofloxacin in water. *ACS Applied Nano Materials*; **2**, 2367-2376.

G

Garg H. S. and Agrawal S. *1995*. A novel sphingosine derivative from the sponge Spirastrella inconstans. Journal of Natural Products, *58*, 442-445.

Giannella R. A. **1996**. Salmonella". Baron's Medical Microbiology (Baron S et al., eds.) (4th ed.). Univ of Texas Medical Branch; Available from: http://www.ncbi.nlm.nih.gov/books/bv.fcgi?rid=mmed.section.1221.

H

Hanson J. R. **1993**. Diterpenoids. Natural Product Reports ; **10**, 159-174.

Hanson J. R. **1998**. Diterpenoids. Natural Product Reports ; **15**, 93-106.

Hanson J. R. **2004**. Diterpenoids. Natural Product Reports ; **21**, 312-320.

Hanson J. R. **2006**. Diterpenoids. Natural Product Reports ; **23**, 875-885.

Hanson J. R. **2007**. Diterpenoids. Natural Product Reports; **24**, 1332-1341.

Harborne J. B. **1994**. Phytochemistry of the Leguminosae.In: Bisby F.A., Buckingham J. and Harborne J. B., (eds.), Phytochemical Dictionary of the Leguminosae-Vol. I Plants and their Constituents.Chapman & Hall, Cambridge.

Hasegawa S. and Hirose Y. **1985**. Diterpenes from the seed of Sciadopitys verticillata. *Phytochemistry*; **24**, 2041-2046.

Hasnah M. S., Hamid A. H. **1993**. Labdane diterpene from *Enicosanthum congregatum*. Pertanika *J. Sci. and Techno*; **1**, 189-193.

Hatake K., Hori K., Takahashi S., Sakamoto K., Mukoyama T. and Tsujimura N. **2006**. Triterpenes and their use as cancer-metastasis inhibitors and health functional foods. Patent number 2006151902. Sakamoto Bio Co. Ltd., Akita Prefecture, Japan.

Havelaar A. H., Garssen J., Takumi K., Koedam M. A., Dufrenne J. B., Van Leusden F. M. and Vos J. G. **2001**. A rat model for dose–response relationships of Salmonella enteritidis infection. *J. Appl. Microbiol;* **91**, 442-452.

Hayashi T., Gotoh K. and Kasahara K. **1996**. Production of scopadulciol by cultured tissues of Scoparia dulcis. *Phytochemistry* ; **41**, 193-196.

Heywood V. H. **1996**. Les Plantes à Fleurs-306 Familles de la Flore Mondiale. Editions Nathan, Paris; pp. 149-152.

Hong-Xi X., Dong H. and Sim K. Y. **1996**. Labdane diterpenes from Alpinia zerumbet. *Phytochemistry*; **42**, 149-151.

Hong-Xi X., Dong H. and Sim K. Y. **1996**. Labdane diterpenes from Alpinia zerumbet. *Phytochemistry*; **42**, 149-151.

Hosoe T., Nozawa K., Lumley T. C., Currah R. S., Fukushima K., Takizawa K., Miyaji M. and Kawai K.I. **1999**. Tetranorditerpene lactones, potent antifungal antibiotics for human pathogenic yeasts, from a unique species of *Oidiodendron*. *Chem. Pharm. Bull* ; **47**, 1591-1597.

Hostettmann K. **1997**. Tout Savoir sur le Pouvoir des Plantes Sources de Médicaments. Editions Favre, Lausanne, pp. 93, 104, 135.

Hostettmann K., Marston A., Ndjoko K. and Wolfender J. L. **2000**. The potential of African plants as a source of drugs. *Current Organic Chemistry*; **4**, 973-1010.

Hutchinson J., Dalziel J. M. and revised by Keay R. W. J. **1958**. Flora of West Tropical Africa.Vol I, part II. 2nd Ed., The Whitefriars Press, London, p. 457.

I

Ikeshiro Y., Hashimoto I., Iwamoto Y., Mase I. and Tomita Y. **1991**. Diterpenoids from Salvia miltiorrhiza. *Phytochemistry*; **30**, 2791-2792.

Ikhiri K. and Ilagouma A. T. **1995**. Constituents of *Detarium microcarpum* bark. *Fitoterapia*; **66**, 274.

Iwagawa T., Yaguchi S., Hase T., Okubo T. and Kim M. **1993**. Diterpene glucosides from *Viburnum suspensum*. *Phytochemistry*; **32**, 1515-1518.

K

Kamperdick C., Adam G., Van N. H. and Van Sung T. **1997**. Chemical constituents of *Madhuca pasquiery*. *Zeitschrift für Naturforschung C*; **52**, 295-300.

Kawasaki M., Hayashi T., Arisawa M., Shimizu M., Horie S., Ueno H. and Tezuka Y. **1987**. Structure of scoparic acid A, a new labdane-type diterpenoid from a Paraguayan crude drug "*Typycha Kuratu*" (*Scoparia dulcis* L.). *Chemical and pharmaceutical bulletin*; **35**, 3963-3966.

Kayser A. F. O., Kiderlen S. L. and Croft. **2003**. Natural products as antiparasitic drugs. *Parasitology Research*; **90**, 55-62.

Keay R. W. J., Phil D., Biol F. T. **1989**. Trees of Nigeria. Oxford University Press, New York. pp. 204-207.

Kerharo J. and Adam J. G. **1962**. Premier inventaire des plantes médicinales et toxiques de la Casamance. *Ann. Pharm. Fr.* ; **20**, 726-727.

Kerharo J. and Adam J. G. 1974. La Pharmacopée Sénégalaise Traditionnelle : Plantes Médicinales et Toxiques. Editions Vigot Frères, Paris; pp. 285-287.

Kiem P. V., Minh C. V., Huong H. T., Lee J. J. and Kim Y. H. **2005**. Analysis of Sterols Analysis of Sterols, 1997. *Chemical & pharmaceutical bulletin*; **53**, 428-430.

Kimbu S. F., Njimi T. K., Sondengam B. L., Akinniyi J. A. and Connolly J. D. **1979**. The structure of a labdane dialdehyde from *Afromomum daniellii* (Zingiberaceae). *Journal of the Chemical Society, Perkin Transactions*; **1**, 1303-1304.

Kouyaté A. M. **2005**. Aspects ethnobotaniques et étude de la variabilité morphologique, biochimique et phénologique de *Detarium microcarpum* Guill. & Perr. au Mali. Thèse de Doctorat. Faculté des Sciences Biologiques Appliquées. Université de Gand. Belgique. 207 p.

Kouyaté A.M. and Van Damme P. **2006**. *Detarium microcarpum* Guill. & Perr. In: Schmelzer, G. H. and Gurib-Fakim, A. (Eds.) Medicinal plants 1 [CD-Rom]. *Wageningen, Netherlands: PROTA Foundation*; **11**.

Kuete V. **2010**. Potential of Cameroonian Plants and Derived Products against Microbial Infections: A Review. *Planta Med Journal* ; **76**, 1479-1491

L

Labayle D. **2001**. Guide Pharmaco, édition lamare, Paris ; 568.

Lajide L., Escoubas P. and Mizutani J. **1995**. Termite antifeedant activity in *Detarium microcarpum*. *Phytochemistry*; **40**, 1101-1104.

Lajide L., Escoubas P. and Mizutani J. **1995**. Termite antifeedant activity in *Detarium microcarpum*. *Phytochemistry*; **40**, 1101-1104.

Lankhorst P. P., Smeets J. W. H. and Haasnoot C. A. G. **1995**. Discrimination of the two diastereoisomeric glycosides heterodendrin and epi-heterodendrin by the combined use of NOE and molecular mechanics. *Carbohydr Res*; **269**, 17-27.

Lechtenberg M., Nahrstedt A. and Fronczek F. R. **1996**. Leucine-derived nitrile glucosides in the Rosaceae and their systematic significance. *Phytochemistry*; **41**, 779-785.

Li T., Horton R. M., Bader D. Liu A. F., Sun Q. and Kinney P. L. **2018**. Long-term projections of temperature-related mortality risks for ischemic stroke, hemorrhagic stroke, and acute ischemic heart disease under changing climate in Beijing, China. *Environ. Intl;* **112**, 1-9.

Lin L. C., Pai Y. F. and Tsai T. H. **2015**. Isolation of luteolin and luteolin-7-O-glucoside from *Dendranthema morifolium* Ramat Tzvel and their pharmacokinetics in rats. *Journal of agricultural and food chemistry*; **63**, 7700-7706.

Luo P., Xia W., Morris-Natschke S. L., Lee K. H., Zhao Y., Gu Q. and Xu J. **2017**. Vitepyrroloids A-D, 2-cyanopyrrole-containing labdane diterpenoid alkaloids from the leaves of *Vitex trifolia*. *Journal of natural products*; **80**, 1679-1683.

M

Ma X., Wu L., Ito Y. and Tian W. **2005**. Application of preparative high-speed counter-current chromatography for separation of methyl gallate from Acer truncatum Bunge. *Journal of Chromatography A*; **1076**, 212-215.

Mabberley D. J. **1981**. The plant-book. Cambridge university press; 321-322.

Mackay Ian M., Katherine E. A. and Andreas N. **2002**. "Real-time PCR in virology." *Nucleic acids research*; **30**, 1292-1305.

Mahato S. B. and Kundu A. P. **1994**. "^{13}C NMR Spectra of Pentacyclic Triterpenoids-a Compilation and some Salient Features", *Phytochemistry*; **37**, 1517-1575.

Malgras D. **1992**. Arbres et Arbustes Guérisseurs des Savanes Maliennes. Editions Karthala et ACCT, Paris; pp. 228-230.

Malongane F., McGaw L. and Mudau F. **2017**. The synergistic potential of various teas, herbs and therapeutic drugs in health improvement: a review. *Journal of the Science of Food and Agriculture*; **97**, 4679–4689

Manitto P. **1981**. *Biosynthesis of natural products* (No. 574.196 M3).

Meier M. A., Branche A., Neeser O. L., Wirz Y., Haubitz S., Bouadma L. and Christ-Crain M. **2019**. Procalcitonin-guided antibiotic treatment in patients with positive blood cultures: a patient-level meta-analysis of randomized trials. *Clinical Infectious Diseases*, **69**, 388-396.

Morita H. and Itokawa H. **1988**. Cytotoxic and antifungal diterpenes from the seeds of Alpinia galanga. *Planta medica;* **54**, 117-120.

N

N'Soki N. S., Cordeiro I. J., dos Santos A. F., Gaspar J. F., Martins C., Rueff J., and de Mendonça D. I. **2010**. 8,15-Epoxylabdane and norlabdane diterpenoids from *Eragrostis viscosa*. *Phytochemistry*; **71**, 798-803.

Naheed R., Sarfraz A. N., Naveen M., Abdul M., Nighat A., Samar A., Shafi U., Pir M. and Choudhary M. I. *2007*. Isolation and enzyme-inhibition studies of the chemical constituents from Ajuga bracteosa. Chemistry and Biodiversity; *4*, 72-83.

Newton S. M., Lau C., Gurcha S. S., Besra G. S., and Wright C. W. **2002**. The evaluation of fortythree plant species for in vitro antimycobacterial activities; isolation of active constituents from Psoralea corylifoliaand Sanguinaria canadensis. *Journal of Ethnopharmacology;* **79**, 57-63.

Nielsen K. A., Olsen C. E., Pontoppidan K. and Moller B. L. **2002**. Leucine-derived cyano glucosides in barley. *Plant Physiol*; **129**, 1066-1075.

Nielsen K. A., Olsen C. E, Pontoppidan K. and Moller B. L. **2002**. Leucine-derived cyano glucosides in barley. *Plant Physiol*.;**129**,1066-1075.

Nyigo V. A., Peter X., Mabiki F., Malebo H. M., Mdegela R. H. and Fouche G. **2016**. Isolation and identification of euphol and β-sitosterol from the dichloromethane extracts of *Synadenium glaucescens*. *The Journal of Phytopharmacology*; **5**, 100-104.

O

Osawa K., Yasuda H., Morita H., Takeya K. and Itokawa H. **1996**. Macrocarpals H, I, and J from the leaves of Eucalyptus globulus. *Journal of natural products*; **59**, 823-827.

Oyewole O. A. and Abalaka, M. E. **2012**. Antimicrobial Activities of *Telfairia occidentalis* (fluted pumpkins) Leaf Extract against Selected Intestinal Pathogens. *Journal of Health Science*; **2**, 1-4

P

Pablo A. G., Alaíde B., Ronan B. **1991**. Occurrence, biological activities and synthesis of Paraguayan crude drug "Typycha Kuratu" (Scoparia dulcis L.). Chemical and mevalonate pathway for terpenoid biosynthesis. Journal of American Chemical miltioriza. *Phytochemistry*; **30**, 4071-4075.

Parry C. M. and Beeching N. J. **2009**. Treatment of enteric fever. *British Medical Journal*; **338**, b1159-b1159.

Parry C. M. **2004**. The treatment of multidrug-resistant and nalidixic acid-resistant typhoid fever in Viet Nam. *Transactions of the Royal Society of Tropical Medicine and Hygiene*; **98**, 413-422.

Pennec Y. L. and Garré M. **2003**. Salmonelloses de l'adulte. Encyclopédie Médico Chirurgical (Maladies infectieuses, 8-018-A-15). Editions Scientifiques et Médicales Elsevier SAS : Paris : p. 9.

Picciarelli P., Piaggesi A., and Alpi A. **1991**. Gibberellins in suspensor, embryo and endosperm of developing seeds of Cytisus laburnum. *Phytochemistry;* **30**, 1789-1792.

Pilly E. B., Kurzon M., Overpeck M. D. and Scheidt P. C. **1992**. Parental alcohol use, problem drinking, and children's injuries. *JAMA*; **267**, 3166-3171.

Pinto V. D. S., Araújo J. S., Silva R. C., da Costa G. V., Cruz J. N., Neto D. A. and Junior M. **2019**. In silico study to identify new antituberculosis molecules from natural sources by hierarchical virtual screening and molecular dynamics simulations. *Pharmaceuticals*; **12**, 36.

Pockrandt D., Ludwig L., Fan A., König G. M. and Li S. M. **2012**. New insights into the biosynthesis of prenylated xanthones: from Aspergillus nidulans catalyses an O-prenylation of xanthones. *Chem. Bio. Chem.*; **13**, 2764-2771.

Pollard M. A., Fischer P. and Windhab E. J. **2011**. Characterization of galactomannans derived from legume endosperms of genus *Sesbania* (Faboideae). *Carbohydrate polymers*; **84**, 550-559.

Pongcharoen S. and Sanguansermsri, P. R. N. D. **2007**. JEG-B Cell Culture Supernatants Cause Reduced Interferon-y and. *Reactions*; **5**, 231.

Preeti G., Divya P. G. and Dipshikha C. **2012**. *Salmonella enterica* serovars Typhimurium and Typhi as model organisms Revealing paradigm of host-pathogen interactions. *Landes Bioscience*; **3**, 377-388.

Q

Qamar F. N., Yousafzai M. T., Khaliq A., Karim S., Junejo A., Baig I. and Sami U. **2020**. Adverse events following immunization with typhoid conjugate vaccine in an outbreak setting in Hyderabad, Pakistan. *Vaccine.*

R

Ragasa C. Y., Hofilena J. G. and Rideout J. A. **2002**. New Furanoid Diterpenes from *Caesalpinia pulcherrima*. *Journal of Natural Products*; **65**, 1107-1110.

Rahman B. A., Wasfy M. O., Maksoud M. A., Hanna N., Dueger E. and House B. **2014**. Multi-drug resistance and reduced susceptibility to ciprofloxacin among *Salmonella enterica* serovar Typhi isolates from the Middle East and Central Asia. *New microbes and new infections*; **2**, 88-92.

Ramkumar M., Ryunju O., Dekai Z., Sung-Gyoo P., Jin S., Alicia K., Mathew S. H. and Sankar G. **2012**. A Mouse Model for *Salmonella Typhi* Infection. *Cell*; **151**, 590-602.

Reagan-Shaw S., Nihal M. and Ahmad N. **2007**. Dose translation from animal to human studies revisited. *The FASEB Journal*; **22**, 659-661.

Reddy P., Rao R. R., Shashidhar J., Sastry B. S., Rao J. M. and Babu K. S. **2009**. Phytochemical investigation of labdane diterpenes from the rhizomes of *Hedychium spicatum* and their cytotoxic activity. *Bio. Org. Med. Chem. Lett*; **19**, 6078-6081.

Rohmer M., Seemann M., Horbach S., Bringer-Meyer S. and Sahm, H. **1996**. Glyceraldehyde 3-phosphate and pyruvate as precursors of isoprenic units in an alternative non-mevalonate pathway for terpenoid biosynthesis. *Journal of the American Chemical Society*; **118**, 2564-2566.

Rowe B., Threlfall E. J. and Ward L. R. **1987**. Does chloramphenicol remain the drug of choice for typhoid? *Epidemiology and Infection*; **98**, 379-383.

Ruzicka L. **1953**. The isoprene rule and the biogenesis of terpenic compounds. *Experientia*; **9**, 357-367.

Ryan K. J. and Ray C. G. **2004**. Sherris Medical Microbiology (4th ed.). McGraw Hill. ISBN 0838585299.

S

Sheng-Jun D., Tao J. Y., Liu K., Jiang Y. T. and Shen L. 2006. Neo-Clerodane diterpenoids from *Scutellaria barbata* with cytotoxic activities. *Phytochemistry*; **67**, 1326-1330.

Shimizu M., Tsuji H., Shogawa H., Fukumura H., Tanaami S., Hayashi T. and Morita, N. **1988**. Anti-inflammatory constituents of topically applied crude drugs. II. Constituents and anti-inflammatory effect of *Cryptomeria japonica* D. Don. *Chemical and pharmaceutical bulletin*; **36**, 3967-3973.

Siddiqui S., Hafeez F., Begum S. and Siddiqui B. S. **1988**. Oleanderol, a new pentacyclic triterpene from the leaves of *Nerium oleander*. *Journal of Natural Products*; **51**, 229-233.

Sob T. V., Tane P., Ngadjui B. T., Connolly J. D. and Dawei M. **1979**. Trypanocidal labdane Sociaty Perkin Trans I; 1303-1304.

Simo, C.C., Kouam, S.F., Poumale, H.M., Simo, I.K., Ngadjui, B.T., Green, I.R., Krohn, K., 2008. Benjaminamide: a new ceramide and other compounds from the twigs of *Ficus benjamina* (Moraceae). Biochem. Systemat. Ecol. 36 (3), 238-243.

Soe G. B. and O. G. D. **1987**. Treatment of typhoid fever and other systemic salmonelloses with cefotaxime, ceftriaxone, cefoperazone, and other newer cephalosporins. Review of Infectious Diseases; **9**, 719-736.

Song J., Willinger T., Rongvaux A., Eynon E. E., Stevens S., Manz M., Flavell R. and Galán, J. **2010**. A mouse model for the human pathogen *Salmonella Typhi. Cell Host Microbe*; **8**, 369-376

Spichiger R-E., Savolainen V. V., Figeat M. and Jeanmonod D., **2002**. Botanique systématique des plantes à fleurs. Une approche phylogénétique nouvelle des Angiospermes des régions tempérées et tropicales. Presses polytechniques et universitaires romandes ; p.413.

Su B. N., Misico R., Park E. J., Santarsiero B. D., Mesecar A. D., Fong H. H. and Kinghorn A. D. **2002**. Isolation and characterization of bioactive principles of the leaves and stems of *Physalis philadelphica*. *Tetrahedron*; **58**, 3453-3466.

Suthari S., Sreeramulu N., Omkar K. and Raju V. S. **2014**. The climbing plants of northern Telangana in India and their ethnomedicinal and economic uses. *Indian J Plant Sci*; **3**, 86-100.

T

Takahashi, J. A., Vieira, H. S., Boaventura, M. A. D., Hanson, J. R., Hitchcock, P. B., & Oliveira, A. B. D. (2001). Mono and diterpenes from seeds of Xylopia sericea. *Quimica Nova*, 24(5), 616-618.

Tolstikova T. G., Sorokina I. V., Tolstikov G. A., Tolstikov A. G. and Flekhter O. B. **2006**. Biological activity and pharmacological prospects of lupine terpenoids: I. Natural lupine derivatives. *Russ. J. Bio org. Chem*.; **32**, 37-49.

Torsell K. B. and Hanson J. R. **1998**. Book review: Natural product chemistry. A mechanistic, biosynthetic and ecological approach. *Natural Product Reports*; **15**, 111.

Tucker S. C. **2002**. Comparative floral ontogeny in Detarieae (Leguminosae: Caealpinioideae). Radially symmetrical taxa lacking organ suppression. Am. J. Bot; **89**, 875-887.

V

Valencia-Chan Lía S., García-Camara I., Torres-Tapia Luis W., Moo-Puc Rosa E. and Peraza-Sanchez Sergio R. **2017**. Lupane-Type Triterpenes of *Phoradendron vernicosum*. *J. Nat. Prod*.; **80**, 3038-3042.

Van Damme P. **1993**. Plantes systematick. Cursus. Universiteit Gent. Faculteit Landbouw kundige en Toegepaste Biologische. Wetens chappen. p.250.

W

W.H.O. **2018**. Typhoid vaccines: WHO position paper March 2018. *Weekly Epidemiological Record*; **93**, 153-172.

Wallace M. R., Yousif A. A., Mahroos G. A., Mapes T., Threlfall E. J., Rowe B. and Hyams K. C. 1993. Ciprofloxacin versus ceftriaxone in the treatment of multiresistant typhoid fever. *European Journal of Clinical Microbiology and Infectious Diseases*; **12**, 907-910.

Wang L. N., Zhang J. Z., Li X., Wang X. N., Xie C. F., Zhou J. C. and Lou H. X. **2012**. Pallambins A and B, unprecedented hexacyclic 19-nor-secolabdane diterpenoids from the Chinese liverwort Pallavicinia ambigua. *Organic letters*; **14**, 1102-1105.

Watson L. and Dallwitz M. J. **1993**. The genera of Leguminosae-Caesalpinioideae and Swartzieae. Information retrieval. Http://www.biodiversity.uno.edu/delta/.

Wilkins E. G. L. and Roberts C. **1988**. Extraintestinal salmonellosis. *Epidemiology and Infection*; **100**, 361-368.

Wink M. **2015**. Modes of Action of Herbal Medicines and Plant Secondary Metabolites. *Medicines*; **2**, 251-286

World Health Organization. **2011**. Guidelines for the Management of Typhoid Fever. WHO, Geneva; 2011.

World Health Organization. **2019**. Typhoid vaccines: WHO position paper, March 2018– Recommendations. *Vaccine*; **37**, 214-216.

Wu S. L., Sung P. J., Su J. H. and Sheu J. H. **2003**. Briaexcavatolides S−V, Four New Briaranes from a Formosan Gorgonian *Briareum excavatum*. *Journal of natural products*; **66**, 1252-1256.

X

Xu C., Zhou W., Wang Y. and Qiao L. **2014**. Hepatitis B virus-induced hepatocellular carcinoma. *Cancer letters;* **345**, 216-222.

Xu H., Song J., Luo H., Zhang Y., Li Q., Zhu Y. and Sun W. **2016**. Analysis of the genome sequence of the medicinal plant *Salvia miltiorrhiza*. *Molecular plant*; **9**, 949-952.

Y

Yang X. D., Xu L. Z. and Yang S. L. **2001**. Xanthones from the stems of *Securidaca inappendiculata*. *Phytochemistry*; **58**, 1245–1249.

Yu S. S., Yu D. Q., Liang X. T. and Cai P. 1999. NMR studies on sugar moieties of some new triterpenoid saponins from *Aralia spinifolia* and *Nothopanax davidii*. *Studies in Plant Science*; 43–51. doi:10.1016/s0928-3420(99)80007-x.

Yu-jie H., Hui L., Xue-lie Y., Shu-wei Z., Wen-qiong W., Lin-yin F. and Li-jiang X. **2014**. Dammmarane-type triterpenoids from *Gentianella azurea*. *J Nat Prod*; **77**, 1201-1209.

Z

Zdero C., Bohlmann F. and Mungai G. M. **1991**. Carvotacetone derivatives and other constituents from representatives of the Sphaeranthus group. *Phytochemistry*; **30**, 3297-3303.

Zorgani A. and Ziglam H. **2014**. Typhoid fever: misuse of Widal test in Libya. *The Journal of Infection in Developing Countries*; **8**, 680-687.

LIST OF PUBLICATIONS

1- William F. Feudjou, Arnaud M. Mbock, Blandine M. O. Wache, Valerie T. Sielinou, Racéline K. Gounoue, Pierre Mkounga, Bruno N. Lenta, Théophile Dimo, Fabrice B. Fekam, Norbert sewald, Augustin E. Nkengfack. An antibacterial isovaleronitrile diglycoside from *Detarium microcarpum.* Guill. Perr. (Fabaceae). *Natural Products Communication*; 2020, 15(6): 1-6.

2- Michel Arnaud Mbock, **William Feudjou Fouatio**, Raceline Gounoue Kamkumo, Patrick Valère Tsouh Fokou, Florence Ngueguim Tsofack, Paul-Keilah Lunga, Jean Justin Essia Ngang, Onana Boyomo, Augustin Ephrem Nkengfack, Bruno Lenta Ndjakou, Norbert Sewald, Fabrice Fekam Boyom, Theophile Dimo. Antisalmonella bioguided investigation of extract and secondary metabolites of Roots of *Detarium microcarpum* Guill. Perr. (Fabaceae). *Journal of Ethnopharmacology*, (2020); DOI: https://doi.org/10.1016/j.jep.2020.113049.

3- William F. Feudjou, Arnaud M. Mbock, Valerie T. Sielinou, Jean J. K. Bankeu, Hugue Fouotsa, Steven C. J. Wouamba, Racéline K. Gounoue, Marcel Freeze, Pierre Mkounga, Bruno N. Lenta, Alembert T. Tchinda, Norbert Sewald and Augustin E. Nkengfack. Antisalmonella activity of secondary metabolites from *Detarium microcarpum* Guill. and Perr. (Fabaceae). *Natural Products Research*, (2021), (**Submitted**).

APPENDICES

Short Communication

An Antibacterial Isovaleronitrile Diglycoside From *Detarium microcarpum* Guill. Perr. (*Fabaceae*)

Natural Product Communications
Volume 15(7): 1–6

DOI: 10.1177/1934578X20936939
journals.sagepub.com/home/npx

SAGE

William F. Feudjou[1,2], Arnaud M. Mbock[3], Marlyse B. W. Ouahouo[1], Valérie T. Sielinou[1], Racéline K. Gounoue[3], Pierre Mkounga[1], Bruno N. Lenta[4], Théophile Dimo[3], Fabrice B. Fekam[5], Norbert Sewald[6], and Augustin E. Nkengfack[1]

Abstract

A new isovaleronitrile diglycoside, named microcarposide (**1**), together with 6 known compounds: lupeol (**2**), betulinic acid (**3**), β-sitosterol glucoside (**4**), methyl gallate (**5**), luteolin (**6**), and epicatechin (**7**), was isolated from the methanolic extract of the fruits of *Detarium microcarpum* Guill. Perr. The structures of the compounds were determined by extensive analysis of 1D- and 2D-^{1}H and ^{13}C NMR spectroscopic data in conjunction with mass spectrometry and by comparison with data reported in the literature. Compound **1** was characterized as (2*R*)-2-[(6"-*O*-β-L-rhamnopyranosyl-β-D-glucopyranosyl)oxy]-3-methylbutanenitrile. Some of the isolated compounds were evaluated for their antibacterial activities against several microorganisms; only compound **1** was active against *Salmonella typhi*, *Salmonella enteritidis*, and *Salmonella typhimurium* with minimum inhibition concentration values of 153.4, 76.7, and 76.7 μM, respectively.

Keywords

Fabaceae, *Detarium microcarpum*, isovaleronitrile diglycoside, microcarposide, antibacterial activity

Received: February 20th, 2020; Accepted: May 18th, 2020.

The genus *Detarium* is a member of the family *Fabaceae*, subdivision *Caesalpinioideae*, and tribe *Detarieae*.[1] Only 2 species of this genus are reported in the literature. The first, *Detarium senegalensis* J.F. Gmel., grows in riparian and dry forests areas, while the second, *D. microcarpum* Guill. and Perr., is a fruit bearing tree growing to a height of about 10 m, which is distributed in dry savannah regions of some western and central Africa countries such as Benin, Burkina Faso, Guinea Bissau, Guinea, Niger, Nigeria, Senegal, Ghana, Togo, Cameroon, and Central African Republic.[2-4] Different parts of this latter plant have been used in traditional medicine for the treatment of several illnesses such as stomach disorders, venereal diseases, and gastrointestinal ailments. The fruit pulp is rich in minerals, such as Ca, P, Fe, K, Na, and Mg, and essential vitamins, such as C, E, B2, and folic acid, which serves as a major food supplement during the dry season.[5] It is worth noting that fruits of plants of the *Fabaceae* family contain cyanogenic glycosides.[6] These are secondary plant metabolites that have been used as chemotaxonomic markers. They are present in more than 2500 plant species of which the most represented botanical families are *Fabaceae*, *Rosaceae*, *Linaceae*, and *Asteraceae*.[6]

Previous phytochemical investigations of the fruit flour of *D. microcarpum* reported about 42% carbohydrates; 36% lipids; and 11% protein, terpenoids, and phenolic compounds, some of which exhibited a wide range of biological properties, including antimicrobial, antimalarial, and cytotoxic effects.[7-9] The seed coat is also reported to possess antimicrobial activity, which could be used in the control of infectious diseases.[10] Although different parts of *D. microcarpum* are used for the treatment of microbial and parasitic diseases, we have found no information regarding their use in the treatment of typhoid

[1]Department of Organic Chemistry, University of Yaoundé I, Cameroon
[2]Laboratory of Phytochemistry, Centre for Research on Medicinal Plants and Traditional Medicine, Institute of Medical Research and Medicinal Plants Studies, Yaounde, Cameroon
[3]Department of Animal Biology and Physiology, University of Yaoundé I, Cameroon
[4]Department of Chemistry, University of Yaoundé I, Higher Teacher Training College, Cameroon
[5]Department of Biochemistry, University of Yaoundé I, Cameroon
[6]Department of Chemistry, Bielefeld University, Germany

Corresponding Author:
Augustin E. Nkengfack, Department of Organic Chemistry, University of Yaoundé I, P.O. Box 812, Yaounde, Cameroon.
Email: ankengf@yahoo.fr

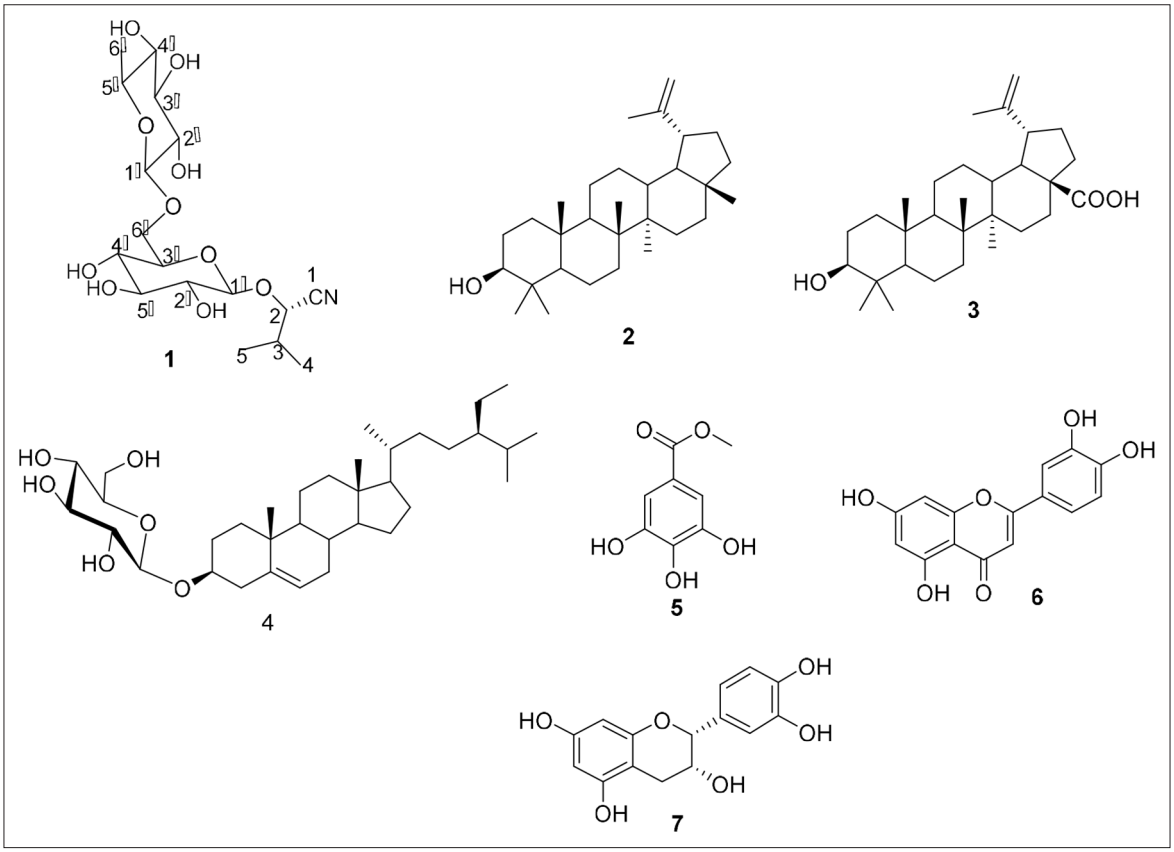

Figure 1. Structures of compounds **1**-**7**.

fever. However, in Cameroon, the local population from where this plant was harvested uses its fruit pulp and root bark decoctions for the treatment of this disease. Thus, in order to either confirm or overturn the ethnobotanical uses of this plant in the treatment of typhoid fever, and as part of our ongoing search for anti-*Salmonella* extracts and secondary metabolites from Cameroonian medicinal plants, we have undertaken the chemical and pharmacological investigation of this plant.

In this paper, we report the structural elucidation of a new isovaleronitrile diglycoside, named microcarposide (**1**), along with 6 known compounds (**2**-**7**), as well as evaluating their antibacterial activity and especially their anti-*Salmonella* activity.

Results and Discussion

Silica gel column chromatography (CC) of the methanol extract of fruits of *D. microcarpum* led to the isolation of a new isovaleronitrile diglycoside, named microcarposide (**1**), along with 6 known compounds lupeol (**2**),[11] betulinic acid (**3**),[12] β-sitosterol glucoside (**4**),[13] methyl gallate (**5**),[14] luteolin (**6**),[15] and epicatechin (**7**).[16] The structures of the known compounds were determined based on the analysis of their spectroscopic data, which showed complete agreement with those reported in the literature (Figure 1).

Compound **1** was obtained as a white powder from the EtOAc/MeOH (9:1) fraction. It reacted positively both with Molisch's and the cyanogenic reagents, suggesting its sugar nature and the presence in its structure of a cyanide moiety. Its molecular formula, $C_{17}H_{29}NO_{10}$, implying 4 degrees of unsaturation, was established from its HR-ESI-TOF-MS (Supplemental Figure S1), which showed, in the positive mode, the protonated molecular ion peak $[M+H]^+$ at m/z 408.1865 (calcd for $C_{17}H_{30}NO_{10}^+$: 408.1864). The presence of the cyanide group in this compound was confirmed by the stretching vibration band observed at υ 2356 cm^{-1} in the IR spectrum. This spectrum also displayed vibration bands characteristic of a hydroxyl group (υ 3363 cm^{-1}) and C_{sp3}-H (υ 2920 cm^{-1}) of aliphatic carbons (Supplemental Figure S2). The 17 carbon atoms of the molecular formula were confirmed by the broad band proton decoupled ^{13}C NMR spectrum (Table 1), which showed 17 signals. These were sorted by DEPT and HMQC techniques into 12 $_{sp3}$ methine carbon signals [among which were 11 oxymethine signals appearing at δ_C 101.9 (C-1'), 101.2 (C-1''), 76.9 (C-5'), 76.1 (C-3'), 73.4 (C-2'), 72.4 (C-4''), 71.9 (C-2), 68.8 (C-3''), 70.9 (C-2''), 70.4 (C-4'), 71.1 (C-5''); and 1 methine signal at δ_C 31.7 (C-3)]; 1 sp^3 oxymethylene signal at δ_C

Table 1. ^{1}H (500 MHz) and ^{13}C (125 MHz) NMR Spectral Data and HMBC Correlations of Compound (**1**) in DMSO.

Position	^{1}H NMR δ_H (nH, m, *J* in Hz)	^{13}C NMR δ_C (m)	HMBC
1	-	118.1	
2	4.51 (1H, d, 5.6)	71.9	$C_{1'}$, C_1, C_3, C_4
3	2.06 (1H, m)	31.7	
4	0.97 (3H, d, 6.8)	18.2	
5	1.11 (3H, d, 6.7)	17.6	
1'	4.34 (1H, d, 7.8)	101.9	C_2, $C_{3'}$, $C_{5'}$
2'	2.99 (1H, dd, 9.9, 6.5)	73.4	
3'	3.32 (1H, s)	76.1	
4'	3.05 (1H, dt, 8.9, 4.5)	70,4	
5'	3.18 (1H, dt, 12.6, 6.5)	76.9	
6a'	3.81 (1H, dd, 11.9, 4.3)	67.0	$C_{1''}$
6b'	3.48 (1H, dd, 11.9, 2.2)		$C_{1''}$
1"	4.59 (1H, d, 5.8)	101.2	$C_{6'}$, $C_{3''}$, $C_{5''}$
2"	3.63 (1H, d, 9.0)	70.9	
3"	3.43 (1H, d, 3.9)	68.8	
4"	3.20 (1H, d, 4.2)	72.4	
5"	3.42 (1H, d, 3.2)	71.1	
6"	1.13 (3H, d, 6.2)	18.4	

67.0 (C-6'), and 3 methyl group signals at δ_C 18.4 (C-6"), 18.2 (C-4), and 17.6 (C-5). Thus, the compound contained 1 quaternary *sp* nitril carbon signal at δ_C 118.1 (C-1).

The combined analysis of the ^{1}H NMR (Table 1) and HMQC (Supplemental Figure S6) spectra of compound **1** showed a set of signals at δ_H 4.51 (1H, d, J = 5.6 Hz, H-2)/δ_C 71.9 (C-2), δ_H 2.06 (1H, m, H-3)/δ_C 31.7 (C-3), δ_H 0.97 (3H, d, J = 6.8 Hz, H-4)/δ_C 18.2 (C-4), and δ_H 1.11 (3H, d, J = 6.7 Hz, H-5)/δ_C 17.6 (C-5), which were assigned to an isovaleronitrile aglycone type moiety (C_5H_9NO).[17] The ^{1}H NMR spectrum of compound **1** also exhibited 2 doublets of 1 proton each at δ_H 4.34 (1H, d, J = 7.8 Hz, H-1') and δ_H 4.59 (1H, d, J = 5.8 Hz, H-1"), which correlated in the HMQC spectrum with the corresponding carbons C-1' at δ_C 101.9 and C-1" at δ_C 101.2, indicative of the presence of 2 sugar moieties. Also observed in these spectra were 2 sets of signals. The first, corresponding to hydroxyl methine and methylene signals at δ_H/δ_C 4.34 (1H, d, J = 7.8 Hz, H-1')/101.9 (C-1'), 2.99 (1H, dd, J = 9.9, 6.5 Hz, H-2')/73.4 (C-2'), 3.32 (1H, s, H-3')/76.1 (C-3'), 3.05 (1H, dt, J = 8.9, 4.5 Hz, H-4')/70.4 (C-4'), 3.18 (1H, dt, J = 12.6, 6.5 Hz, H-5')/76.9 (C-5'), 3.81 (1H, dd, J = 11.9, 4.3 Hz, H-6a')/67.0 (C-6'), and 3.46 (1H, dd, J = 11.9, 2.2 Hz, H-6b')/67.0 (C-6'), was a characteristic of D-glucopyranosyl moiety,[18] whereas the second set, including signals at δ_H/δ_C 4.59 (1H, d, J = 5.8 Hz, H-1")/101.2 (C-1"), 3.63 (1H, d, J = 9.0, H-2")/70.9 (C-2"), 3.43 (1H, d, J = 3.9, H-3")/68.8 (C-3"), 3.20 (1H, d, J = 4.2, H-4")/72.4 (C-4"), 3.42 (1H, d, J = 3.2, H-5")/71.1 (C-5"), and 1.13 (3H, d, J = 6.2, H-6")/18.4 (C-6"), was attributable to an L-rhamnopyranosyl moiety.[18,19] Complete assignment of the protons and carbons of 2 sugar units was achieved by analysis of the COSY, HMQC, and HMBC spectra of this compound.

The linkage between the sugar units and the aglycone and that between 2 sugar units remained to be determined.

The fragment ion observed at m/z 309 (M^+-99) in the HR-ESI-TOF-MS of compound **1**, corresponding to the loss of the aglycone, confirmed that the aglycone was linked to the sugar moieties through an oxygen atom. Furthermore, the HMBC (Supplemental Figure S8) correlations observed between the anomeric proton H-1' of the D-glucose unit at δ_H 4.34 (1H, d, J = 7.8 Hz) and carbons C-3′ (δ_C 76.1), C-5′ (δ_C 76.9), and C-2 (δ_C 71.9) of the aglycone, clearly confirmed its direct attachment to the aglycone (Figure 2). Concerning the linkage between 2 sugar units, the HMBC (Supplemental Figures S8 and S9) correlations were used once again. The HMBC correlation observed between the H-6′ protons of the D-glucose moiety at δ_H 3.81 (1H, dd, J = 11.9, 4.3 Hz, H-6a') and at 3.48 (1H, dd, J = 11.9, 2.2 Hz, H-6b') with the anomeric carbon C-1″ of the L-rhamnose unit at δ_C 101.2 and H-1″ anomeric proton of the L-rhamnose unit at δ_H 4.49 (1H, d, J = 5.8 Hz) and the C-6′ (δ_C 67.0) carbon of the D-glucose unit established the connectivity between 2 sugar units.

The relative stereochemistry of the anomeric protons of 2 sugar units was established to be β from J coupling constant values between H-1'and H-2' ($^{3}J_{H1'\text{-}H2'}$ = 5.0 Hz), and H-1" and H-2" ($^{3}J_{H1''\text{-}H2''}$ = 5.0 Hz), respectively.[18,19]

The absolute configuration of the stereogenic center C-2 of the aglycone was established by comparing the chemical shifts and coupling constants of its proton with those of 2 closely related epimers, heterodendrin and epi-heterodendrin (Supplemental Figure S12).[20] These 2 compounds are glucosides possessing in their structure the same aglycone part directly linked to the same sugar unit as in compound **1**. The

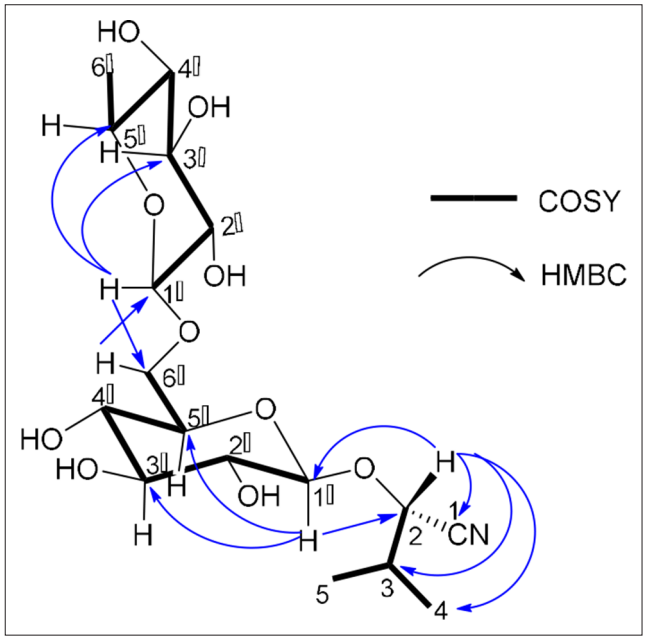

Figure 2. Key 2D NMR correlations of compound **1**.

fact that the ^{1}H NMR data of our compound (chemical shifts and coupling constants) (Table 2) show very close similarities to those of epihetrodendrine let us assign the «***R***» configuration to carbon C-2 as in the epihetrodendrine epimer.[21] Thus, from the above data, compound **1**, to which the trivial name microcarposide was attributed, was assigned to be (2***R***) 3-methyl-2-[β-L-rhamnopyranoside-1(1→6)-β-D-glucopyranosyl] butanenitrile or (2***R***) 2-[β-L-rhamnopyranoside-1(1→6)-β-D-glucopyranosyl]isovaleronitrile or 6′-*O*-rhamnosyl-(*R*)-epiheterodendrine.

Compounds **1** to **5** were assayed for their antibacterial potency against 3 *Salmonella* strains, *Salmonella typhi* (ST), *Salmonella typhimurium* (STM), and *Salmonella enteritidis* (SE). As depicted in Supplemental Table S1, only compound **1** exhibited a moderate activity against 3 strains, with minimum inhibition concentration (MIC) values of 153.4, 76.7, and 76.7 µM on ST, STM, and SE, respectively. However, as compared with the reference drug (RD), ciprofloxacine, compound **1** was much less active. However, the activity of this compound against the microbial strains could justify the use of the fruit pulp of this plant for the treatment of infectious diseases, including typhoid fever.

Experimental

General Experimental Procedures

Melting points were measured on a Buchii melting point apparatus. Optical rotations were recorded on a Perkin-Elmer-241 MC Polarimeter, IR spectra on a Bruker Fourier transform/infrared (ATR) spectrophotometer, mass spectra (ESI-MS) on a Thermo-Finnigan LCQ DECA mass spectrometer, and HR-ESI-MS with a FTHRMS-Orbitrap (Thermo-Finnigan) mass spectrometer. 1D- and 2D-NMR spectra were recorded in deuterated solvents on either a Bruker ARX 500 or an AVANCE DMX 600 NMR spectrometer (proton at 500 MHz and carbon ^{13}C at 125 MHz). All chemical shifts (δ) were measured in parts per million (ppm) using a residual solvent signal as a secondary reference relative to tetramethylsilane as internal standard, while coupling constants (J) are given in Hz. Solvents were distilled prior to use. Analytical grade solvents were used for LCMS. Column chromatography was performed using Merck MN silica gel 60 M (0.04-0.063 nm), and thin layer chromatography (TLC) on aluminum silica gel 60 F_{254} (Merck) precoated plates (0.2 mm layer thickness). Compounds were visualized on TLC either by the use of an UV lamp (254 and 366 nm) or by heating after spraying with 20% H_2SO_4 (v/v) solution. Different mixtures of *n*-hexane (hex), EtOAc, CH_2Cl_2, and MeOH were used as eluting solvents.

Plant Material

The fruits of *D. microcarpum* were harvested in Gamba savanna (Mvina division, Adamaoua region of Cameroon) in March 2018. Identification was made by M. Ngansop Eric, a botanist of the Cameroon National Herbarium, Yaoundé, where a voucher specimen has been deposited under the registration number HNC/57227.

Extraction and Isolation

Air-dried powdered fruit of *D. microcarpum* (1200 g) was extracted 3 times (3 × 10 L) by maceration at room temperature (about 25 °C) in methanol for 48 hours. After filtration,

Table 2. Different Chemical Shift Values for Heterodendrin, Epiheterodendrin,[21] and Compound **1**.

	(*S*)-Heterodendrine		(R)-Epiheterodendrine		Compound **1**	
Position	δ_H (600 MHz, DMSO-d_6)	δ_C (150 MHz, DMSO-d_6)	δ_H (600 MHz, DMSO-d_6)	δ_C (150 MHz, DMSO-d_6)	δ_H (500 MHz, DMSO-d_6)	δ_C (125 MHz, DMSO-d_6)
1	-	117.8	-	118.6	-	118.1
2	4.74 (J = 6.2 Hz)	70.7	4.55 (J = 5.4 Hz)	72.6	4.51 (J = 5.6 Hz)	71.9
1'	4.32 (J = 7.6 Hz)	100.9	4.29 (J = 7.7 Hz)	103.4	4.34 (J = 7.8 Hz)	101.9

the resulting solution was concentrated under reduced pressure to give a dark crude extract (145 g).

Part of this extract (130 g) was fractionated using successively hex (4 × 500 mL) dichloromethane (DCM; 4 × 500 mL), ethyl acetate (EA; 4 × 500 mL), and *n*-butanol (*n*-BuOH; 4 × 500 mL) through flash chromatography over silica gel (200 g), to yield 4 fractions, namely fraction **A** (10 g), **B** (19 g), **C** (30 g), and **D** (57 g), respectively. Fraction **D** (57 g), resulting from *n*-butanol, was subjected to silica gel CC (column dimension: 4.0 × 60 cm), eluting with a gradient of DCM/MeOH (100:0, 1500 mL; 95:5, 1500 mL; 90:10, 1500 mL; 80:20, 1500 mL; 70:30, 1500 mL; 60:40, 1500 mL; and 50:50, 1500 mL) to yield lupeol (**2**) (4 mg), β-sitosterol glucoside (**4**) (3.5 mg), and microcarposide (**1**) (8.3 mg). Fraction **B** (19 g), resulting from dichloromethane, was subjected to silica gel CC (column dimension: 3.0 × 65 cm), eluting with a gradient of hex:EtOAc (100:0, 1500 mL; 90:10, 1500 mL; 80:20, 1500 mL; 70:30, 1500 mL; 60:40, 1500 mL; 50:50, 1500 mL; 40:60, 1500 mL; 30:70, 1500 mL; and 0:100, 1500 mL) to afford betulinic acid (**3**) (7 mg). In a similar manner, fraction **C** (30 g), resulting from EA, was subjected to silica gel CC (column dimension: 3.0 × 65 cm), eluting with a gradient of hex:EtOAc (100:0, 1500 mL; 90:10, 1500 mL; 80:20, 1500 mL; 70:30, 1500 mL; 60:40, 1500 mL; 50:50, 1500 mL; 40:60, 1500 mL; 30:70, 1500 mL; and 0:100, 1500 mL) to yield methyl gallate (**5**) (4.1 mg), luteolin (**6**) (5.3 mg), and epicatechin (**7**) (6.5 mg).

In Vitro Anti-Salmonella *Assays*

The antibacterial activity of compounds **1** to **5** was evaluated using the microdilution method.[22] For determination of MICs and minimal bactericidal concentrations (MBCs) of these compounds, 3 *Salmonella* strains were used: ST, STM, and SE (Supplemental Table S3).

The MIC of compounds **1** to **5** was determined through the broth microdilution method in 96-well microtiter plates. The 96-well plates were prepared by dispensing into each well 50 µL of Mueller Hinton broth. The test substances were initially prepared in DMSO in broth medium at 25 mg/mL. A volume of 100 µL of each test sample was added to the first wells of the microtiter plate. Serial 2-fold dilutions of these test samples were made and 50 µL of inoculum standardized at 10^6 CFU/mL. The last wells (no. 12) served as sterility controls (contained broth only) or negative control (broth plus inoculum). This gave final concentration ranges from 306.80 to 0.29 µM (for compound) and 386.30 to 0.37 µM (for RD: Ciprofloxacin). The plates were incubated at 37 °C for 24 hours. The MICs of the test compounds were determined following the addition of 20 µL of resazurin (alamar blue TM Cell Viability Reagent) solution. Viable bacteria reduced the yellow due to a pink color. The MIC corresponded to the lowest well concentration where no color change was observed, indicating no growth of microorganism. The MBC was determined by adding 50 µL aliquots of the clear wells to 100 µL of freshly prepared broth medium and incubating at 37 °C for 24 hours. The MBC was regarded as the lowest concentration of test sample that did not produce a color change as above. All tests were performed in triplicate on 2 different occasions.

Microcarposide (1)

$C_{17}H_{29}NO_{10}$, white powder (8.3 mg); $-[\alpha]_{589}^{20} = -99$ (c = 0.5, DMSO); – IR ν_{max} cm^{-1} (KBr): 3419(-OH), 2934(-C_{sp3}-H), 2201(-C≡N), 1422-812(-C_{sp3}-O), 665-417(-C_{sp3}-H); **^{1}H NMR (500 MHz, DMSO)**: δ_H 4.59 (1H, s, **H-1"**), 4.51 (1H, d, J = 5.6 Hz; **H-2**), 4.34 (1H, d, J = 7.8 Hz, **H-1'**), 3.81 (1H, dd, J = 11.9, 2.2 Hz, **H-6b'**), 3.63 (1H, d, J = 9.0 Hz, **H-2"**), 3.46 (1H, d, J = 11.9, 4.3 Hz, **H-6a'**), 3.43 (1H, d, J = 3.9 Hz, **H-3"**), 3.42 (1H, d, J = 3.2 Hz, **H-5"**), 3.32 (1H, s, **H-3'**), 3.20 (1H, d, J = 4.2 Hz, **H-4"**), 3.18 (1H, dt, J = 12.6, 6.5 Hz, **H-5'**), 3.05 (1H, dt, J = 8.9, 4.5 Hz, **H-4'**), 2.99 (1H, dd, J = 9.9, 6.5 Hz, **H-2'**), 2.06 (1H, dq, J = 13.3, 6.7 Hz, **H-3**), 1.13 (3H, d, J = 6.2 Hz, **H-6"**), 1.11 (3H, d, J = 6.7 Hz, **H-5**), 0.97 (3H, d, J = 6.8 Hz, **H-4**); **^{13}C NMR (125 MHz, DMSO)**: δ_C 118.1 (**C-1**), 101.9 (**C-1'**), 101.2 (**C-1"**), 76.9 (**C-5'**), 76.1 (**C-3'**), 73.4 (**C-2'**), 72.4 (**C-4"**), 71.9 (**C-2**), 68.8 (**C-3"**), 70.9 (**C-2"**), 70,4 (**C-4'**), 71.1 (**C-5"**), 67.0 (**C-6'**), 31.7 (**C-3**), 18.4 (**C-6"**), 18.2 (**C-4**), 17.6 (**C-5**), see Supplemental Table S1; HR-ESI-TOF-MS: m/z 408.1865 (calcd. for $C_{17}H_{30}NO_{10}^+$: 408.1864).

Acknowledgment

The authors are grateful to the German Academic Exchange Service (DAAD) for the financial support to the Yaoundé-Bielefeld Graduate School of Natural Products with antiparasite and antibacterial activities (YaBiNaPA, Project no. 57316173).

Declaration of Conflicting Interests

The author(s) declared no potential conflicts of interest with respect to the research, authorship, and/or publication of this article.

Funding

The author(s) received no financial support for the research, authorship, and/or publication of this article.

ORCID ID

William F. Feudjou https://orcid.org/0000-0003-1065-6989

Supplemental Material

Supplemental material for this article is available online.

References

1. Watson L, Dallwitz MJ. The families of flowering plants, interactive identification and information retrieval. Australia. Accessed April 23, 2019. https://www.cambridge.org/core/journals/genetics-research/article/families-of-flowering-plants-interactive-identification-and-information-retrieval-by-watson-l-and-dallwitz-m-j-csiro-1993-booklet-40-pages-and-cdrom-available-from-csiro-information-services-po-box-89-east-melbourne-vic-

3002-australia-price-us180-for-customers-outside-australia-new-zealand-10-for-postage-handling-isbn-0-643-05507-x/472189A6980787CD77238CC77A3818E0

2. Tropical Plants Database. Ken Fern. Accessed May 14, 2019. tropical. theferns. info. <tropical. theferns. info/view tropical. php? id=Detarium + macrocarpum
3. Kouyaté AM, Van Damme P. Detarium microcarpum Guill. & Perr. In: Schmelzer GH, Gurib-Fakim A, eds. *Medicinal plants 1 [CD-Rom]*. 11. PROTA Foundation; 2006.
4. Bastide B, Ouédraogo SJ. Feux précoces et production fruitière de *Detarium microcarpum* Guill. et Perr. en zone sud soudanienne du Burkina Faso. *Secheresse*. 2009;20:11-19.
5. Oibiokpa IF, Adoga IG, Saidu AN, et al. Nutritional composition of *Detarium microcarpum* fruit. *Afr J Food Sci*. 2014;8(6):342-350.
6. Jones DA. Why are so many food plants cyanogenic? *Phytochemistry*. 1998;47(2):155-162. doi:10.1016/S0031-9422(97)00425-1
7. Anhwange BA, Ajibola VO, Oniye SJ. Chemical studies of the seeds of *Moringa oleifera* (Lam) and *Detarium microcarpum* (Guill. and Perr.). *Sci J Biol Sci*. 2004;4(6):711-715.
8. Abreu P, Relva A. Carbohydrates from *Detarium microcarpum* bark extract. *Carbohydr Res*. 2002;337(18):1663-1666. doi:10.1016/S0008-6215(02)00025-3
9. Abreu PM, Rosa VS, Araùjo EM, et al. Phytochemical analysis and antimicrobial evaluation of *Detarium microcarpum* bark extracts. *Pharm Pharmacol Lett*. 1998;8:107-109.
10. Ebi GC, Afieroho OE. Phytochemical and antimicrobial studies on *Detarium microcarpum* Guill. and Sperr. (Caesalpinioceae) seeds coat. *Afr J Biotechnol*. 2011;10(3):457-462.
11. Adzu B, Chindo BA, Tarfa FD, et al. Isolation and analgesic property of lupeol from *Diospyros mespiliformis* stem bark. *J Med Plants Res*. 2015;9:813-819.
12. Esposito F, Sanna C, Del Vecchio C, et al. *Hypericum hircinum* L. components as new single-molecule inhibitors of both HIV-1 reverse transcriptase-associated DNA polymerase and ribonuclease H activities. *Pathog Dis*. 2013;68(3):116-124. doi:10.1111/2049-632X.12051
13. Ramiarantsoa H, Attioua BK, Kouamé MA, et al. Le *O-β* -D-glucoside du *β*-sitostérol isolé des feuilles de *Ravenala madagascariensis*. *J So Ouest-Afr Chim*. 2008;26:99-103.
14. Teke GN, Lunga PK, Wabo HK, et al. Antimicrobial and antioxidant properties of methanol extract, fractions and compounds from the stem bark of *Entada abyssinica* Stend ex A. Satabie. *BMC Complement Altern Med*. 2011;11:57 doi:10.1186/1472-6882-11-57
15. Venditti A, Maggi F, Vittori S, et al. Antioxidant and α-glucosidase inhibitory activities of *Achillea tenorii*. *Pharm Biol*. 2015;53(10):1505-1510. doi:10.3109/13880209.2014.991833
16. Jang DS, Lee GY, Lee YM, et al. Flavan-3-Ols having a gamma-lactam from the roots of *Actinidia arguta* inhibit the formation of advanced glycation end products *in vitro*. *Chem Pharm Bull*. 2009;57(4):397-400. doi:10.1248/cpb.57.397
17. Nielsen KA, Olsen CE, Pontoppidan K, Møller BL. Leucine-derived cyano glucosides in barley. *Plant Physiol*. 2002;129(3):1066-1075. doi:10.1104/pp.001263
18. SS Y, DQ Y, Liang XT, et al. NMR studies on sugar moieties of some new triterpenoid saponins from *Aralia spinifolia* and *Nothopanax davidii*. *Studies in Plant Science*. 1999:43-51.
19. Huang Y-jie, Lu H, Yu X-li, et al. Dammarane-type triterpenoids from *Gentianella azurea*. *J Nat Prod*. 2014;77(5):1201-1209. doi:10.1021/np500077z
20. Lechtenberg M, Nahrsted A, Fronczek FR. Leucine-derived nitrile glucosides in the Rosaceae and their systematic significance. *Phytochemistry*. 1996;41(3):779-785. doi:10.1016/0031-9422(95)00661-3
21. Lankhorst PP, Smeets JWH, Haasnoot CAG. Discrimination of the two diastereoisomeric glycosides heterodendrin and epiheterodendrin by the combined use of NOE and molecular mechanics. *Carbohydr Res*. 1995;269(1):17-27. doi:10.1016/0008-6215(94)00345-G
22. Tchakam PD, Lunga PK, Kowa TK, et al. Antimicrobial and antioxidant activities of the extracts and compounds from the leaves of *Psorospermum aurantiacum* Engl. and *Hypericum lanceolatum* Lam. *BMC Complement Altern Med*. 2012;12:136 doi:10.1186/1472-6882-12-136

Journal of Ethnopharmacology 260 (2020) 113049

Contents lists available at ScienceDirect

Journal of Ethnopharmacology

journal homepage: www.elsevier.com/locate/jethpharm

In vitro and *in vivo* anti-salmonella properties of hydroethanolic extract of *Detarium microcarpum* Guill. & Perr. (Leguminosae) root bark and LC-MS-based phytochemical analysis

Michel Arnaud Mbock[a,b,c], William Feudjou Fouatio[d], Raceline Gounoue Kamkumo[b,c], Patrick Valère Tsouh Fokou[c,e], Florence Ngueguim Tsofack[b], Paul-Keilah Lunga[c], Jean Justin Essia Ngang[a], Onana Boyomo[a], Augustin Ephrem Nkengfack[d], Bruno Lenta Ndjakou[f], Norbert Sewald[g], Fabrice Fekam Boyom[c], Theophile Dimo[b,*]

[a] Department of Microbiology, Faculty of Science, University of Yaounde I, P.O. Box, 812, Yaoundé, Cameroon
[b] Department of Animal Biology and Physiology, Faculty of Science University of Yaounde I, P.O. Box, 812, Yaoundé, Cameroon
[c] Department of Biochemistry, Faculty of Science, University of Yaoundé I, P.O. Box, 812, Yaoundé, Cameroon
[d] Department of Chemistry, Faculty of Science, University of Yaoundé I, P.O. Box, 812, Yaoundé, Cameroon
[e] Department of Biochemistry, Faculty of Science, University of Bamenda, P.O. Box 39, Bamenda, Cameroon
[f] Department of Chemistry, Higher Teacher Training College, University of Yaoundé 1, P.O. Box 47, Yaoundé, Cameroon
[g] Department of Chemistry, Bielefeld University, P.O. Box 100131, 33501, Bielefeld, Germany

ARTICLE INFO

Keywords:
Detarium microcarpum
Rhinocerotinoic acid
Salmonella typhimurium
Antisalmonella effects
Typhoid fever

ABSTRACT

Ethnopharmacological relevance: Typhoid fever treatment remains a challenge in endemic countries. *Detarium microcarpum* is traditionally used to manage typhoid.
Aim of the study: The study aims to explore the efficacy of hydroethanolic extract of *Detarium microcarpum* root bark in rats infected with salmonella.
Material and methods: The phytochemical profile of the extract was obtained by UHPLC-MS analysis in an attempt of standardization. The *in vitro* antimicrobial activity was determined using broth dilution method. Salmonella infection was induced by oral administration of *S. thyphimurium* to immunosuppressed rats. Infected rats were then treated 2 h later with the extract (75, 150 and 300 mg/kg), distilled water (normal and salmonella control) and ciprofloxacin (8 mg/kg) for control. Body weight was monitored and stools were cultured to determine the number of colony-forming units. At the end of treatment, animals were sacrificed, blood and organs were collected for hematological, biochemical and histopathological analyses.
Results: Detarium microcarpum extract as well as the isolated compound (rhinocerotinoic acid) exhibited good antimicrobial activity *in vitro* with bacteriostatic effects. The plant extract significantly ($p < 0.05$) inhibited the bacterial development in infected animals with an effective dose (ED_{50}) of 75 mg/kg. In addition, the extract prevented body weight loss, hematological, biochemical and histopathological damages in treated rats.
Conclusion: Detarium microcarpum extract possesses antisalmonella properties justifying its traditional use for the typhoid fever management.

1. Introduction

Typhoid fever is systemic foodborne disease caused by *Salmonella* species such as *Salmonella enterica* serovar typhi (*Salmonella typhi*) and paratyphi (*Salmonella paratyphi*) (Parry et al., 2002) and transmitted via ingestion of contaminated food or water (Aubry et al., 2002). The disease still remains an important global health problem with an estimated 16 million cases leading to 600000 deaths yearly (Date et al., 2014), mainly occurring in developing countries due to poor hygiene (WHO, 2018). *Salmonella* infection begins in the reticulo-endothelial system where intracellular multiplication occurs in macrophages (Aubry et al., 2002). Clinical signs of infection include tiredness, headache, abdominal pain, fever and severe forms leading to cerebral dysfunction, delirium and shock. Occasionally, haemorrhages associated to peritonitis due to the perforation of ulcerated Peyer's patches within the small intestine cause death. Several conventional antimicrobial drugs such as

* Corresponding author.
E-mail address: dimo59@yahoo.com (T. Dimo).

https://doi.org/10.1016/j.jep.2020.113049
Received 29 January 2020; Received in revised form 11 May 2020; Accepted 29 May 2020
Available online 11 June 2020
0378-8741/

beta-lactamines and fluoroquinolones have been developed to control typhoid causative agent, however *Salmonella* has rapidly gained resistance to the most efficient antibiotics (Madhulika et al., 2004). In addition, their expensive cost and side effects raises up an important need to search new accessible antityphoid agents. The use of herbal medicines as complements or alternatives medicines has been on increase due to the cheapness and accessibility. Moreover, about 80% of individuals from developing countries use medicinal plants (WHO, 2018) that seems to be an interesting sources for varieties of new herbal drugs (WHO, 2019). Experimental infection of mice with *Salmonella typhimurium* provides a useful model of human typhoid fever caused by *S. typhi* (Raupach and Kaufmann, 2001). Salmonellosis in rat presents many similarities to the human disease, with the same primary site of colonization, ileum, in both species (Naughton et al., 1996). This offers opportunities to study some antibacterial control strategies.

Detarium microcarpum (Fabaceae) is an African leguminous medicinal plant found in the tropical forests (Mabberley, 2017). Leaves, bark, roots, fruits and seeds of *D. microcarpum* are currently used in Cameroon for the treatment of stomachache, typhoid fever, dysentery, malaria, jaundice, digestive, nutritional and pregnancy disorders (Ebi and Afieroho, 2011). Fruits are rich in vitamin C and are eaten raw or cooked, while leaves and flowers are used as spices and vegetables for the preparation of diets (Kouyaté et al., 2009; Sani et al., 2014). Antimicrobial activities of some parts of *D. microcarpum* have been reported (Akah et al., 2012; Ebi and Afieroho, 2011), but the scientific data of root bark, that are currently used in Central Region in Cameroon are not available yet. The purpose of this work was to investigate the effects of the hydroethanolic extract of *D. microcarpum* root bark on salmonella infection in rat.

2. Material and methods

2.1. Plant material

Fresh parts of leaves, twigs, roots, and root bark of *Detarium microcarpum* Guill. & Perr. were harvested in March 2018 in the savanna of the Gamba village with the geographic coordinates of "8°05′45.0″N 13°36′29.6″E" (Adamaoua Region, Cameroon). The plant was authenticated by a botanist Mr Ngansop Eric, at the Cameroon National Herbarium, in comparison with a voucher specimen deposited under number CNH57227.

2.2. Experimental animals

Six to eight-week old male and female *Wistar* albino rats weighing 160–180 g was used in the study. They were bred in the Animal House of the Laboratory of Animal Physiology, University of Yaounde I. They were maintained in ambient temperature under 12 h light-dark natural cycle. Rats were fed with standard diet and had access to water *ad libitum*. The study was conducted with the approval of the Cameroon National Ethical Committee (Ref n°. FW-IRB00001954).

2.3. Bacterial strains

Different bacterial strains and isolates were used in the study. For the *in vitro* test, *Salmonella typhi* ATCC 19430, *Salmonella enteritidis* ATCC 13076 strains were obtained at ATCC (American Type Culture Collection), whereas *Salmonella typhimurium* isolate was provided by Centre Pasteur of Cameroon, Yaoundé. The purity control of each bacterial strain or isolate was firstly checked by culturing in Salmonella–Shigella agar medium (SS agar) (Liofilchem Italy). Each bacteria was maintained in slants with nutrient agar at 37 °C and subculture in freshly prepared agar plate 24 h prior to the drug susceptibitlity assay.

2.4. Study design

The different plant parts (leaf, twig, root, and root bark) were subjected to preliminary biological screening *in vitro* antibacterial assay. The most active extract was subjected to *in vivo* studies including safety and efficacy on *Salmonella typhimurim*-induced typhoid in rat.

2.5. Extraction and phytochemical analysis

2.5.1. Preparation of plant extract and isolation

The collected materials were dried under shelter at the room temperature and ground into powder. The extract of each plant part (leaves, twigs, roots, and root bark) was obtained through the maceration of 868.0 g powder into ethanol/water (7/3, v/v) (4 L, 48 h x 3) for 48 h. After filtration using Whatman filter paper N°3, the filtrate was then concentrated on a rotary evaporator (Heidolph, Germany) under reduced pressure at 45–55 °C and lyophilized (nema, origin). Afforded extract powders were stored in tightly stoppered bottles at 4 °C in the refrigerator prior to the experiments. Each extract was therefore, submitted to qualitative phytochemical screening to identify some secondary metabolite classes contains such as flavonoids, sterols, triterpenes, alkaloids, glucosides, coumarin, tanins and saponins, using standardized methods (Harbone, 1973). Extracts were subjected to *in vitro* antimicrobial analysis and the most active extract from the root bark was submitted to further bioguided fractionation strategy using the liquid-liquid partition as described by (Zhang et al., 2013). Briefly, the extract (130.0 g) was suspended into distilled water and then subsequently extracted with *n*-hexane, dichloromethane, ethyl acetate and *n*-butanol. Each fraction was evaporated under reduced pressure at 45–55 °C, resulting to four residues named fraction F_1, *n*-hexane [11.0 g, 8.5 % yield], fraction F_2, dichloromethane [20.0 g, 15.4 % yield], fraction F_3, ethyl acetate [34.0 g, 26.1% yield], fraction F_4, *n*-butanol [60.0 g, 46.1% yield] and fraction F_5, the remaining aqueous extract (45.5 g, 32.50 % yield). Each fraction was tested for antibacterial activity and only the active fraction, the ethyl acetate fraction (F_3) (34.0 g), was subjected to silica gel column chromatography. The eluting system consisted of a mixture of *n*-hexane: ethyl acetate in a gradient mode to afford lupeol (**8**) (14.5 mg) (Adzu et al., 2015), unknown compound (**7**) (8.5 mg) whose structure is being elucidated, and compound (**4**) rhinocerotinoic acid (4.0 mg) (Gray et al., 2003). Overall, the fractionation of the ethyl acetate fraction of the hydroethanolic root bark extract led to the isolation of three compounds namely rhinocerotinoic acid, lupeol, and the unknown compound. These compounds were characterized, using one (^{1}H and ^{13}C) and two dimension (DEPT, COSY, HSQC, HMBC) NMR data, in conjunction with the mass spectroscopy.

2.5.2. LC-MS analysis

The phytochemical profile of the extract was obtained by UHPLC-MS analysis in an attempt of standardization. High resolution mass spectra of extract were obtained through a Spectrometer (QTOF Bruker, Germany) equipped with a HESI source. The spectrometer operates in positive mode (mass range: 100–1500, with a scan rate of 1.00 Hz) with automatic gain control to provide high-accuracy mass measurements within 0.40 ppm deviation using Na Formate as calibrant. The following parameters were used for experiments: spray voltage of 4.5 kV, capillary temperature of 200 °C. Nitrogen was used as sheath gas (10 l/min). The spectrometer was attached to an Ultimate 3000 (Thermo Fisher, Germany) UHPLC system consisting of LC-pump, Diode Array Detector (DAD) (λ: 190–600 nm), auto sampler (injection volume 10 µl) and column oven (40 °C). The separations were performed using a Synergi MAX-RP 100 A (50 × 2 mm, 2.5µ particle size) with a H_2O (+0.1 % HCOOH) (A)/acetonitrile (+0.1 % HCOOH) (B) gradient (flow rate 500 µL/min, injection volume 5 µl). Samples were analyzed using a gradient program as follows: 95 % A isocratic for 1.5 min, linear gradient to 100 % B over 6 min, after 100 % B isocratic for 2 min, the

system returned to its initial condition (90 % A) within 1 min, and was equilibrated for 1 min.

2.6. Determination of minimum inhibitory concentrations (MICs) and minimal bactericidal concentrations (MBCs)

The minimum inhibitory concentration (MIC) of the extracts of *Detarium microcarpum* were determined using broth microdilution method in 96-well microtitre sterile plates as previously described (Newton et al., 2002). Briefly, two-fold serial dilutions of the extract, fractions and compound were seeded in a 96 well microtiter plate and inoculated with bacterial inoculum at 10^6 CFU/ml (McFarland) in a final volume of 100 µl of Mueller Hinton broth medium (Oxoid, Thermo Scientific™). The final concentrations ranged from 500 to 0.244 µg/ml (for the plant extract), 250 to 0.122 µg/ml (for extract) and 125 to 0.122 µg /ml (for isolated compound and ciprofloxacin used as the reference drug). The negative control made of broth medium and bacteria inoculum were treated with equivalent amount of DMSO at 0.5% (Loba chemie, India). The sterile control wells containing broth medium was included in the experiment. The plates were incubated at 37 °C for 24 h. The MICs were determined after addition of 20 µL of the yellow rezasurin (alamarblueTMCell Viability Reagent) solution that viable bacteria reduce to pink color after 30 min of incubation at 37 °C (O'brien et al., 2000). The MIC was considered as the lowest concentration that gives no color change, indicating no microorganism growth. The Minimal Bactericidal Concentration (MBC) was determined by sub culturing 50 µl of culture media corresponding to wells without color changes (without rezasurin) into 150 µL of drug-free broth medium. After 24 h incubation at 37 °C the MBCs were revealed by addition of rezasurin as above and define as the lowest concentration of with no color change. Tests were performed in triplicates at three different times. The classification criteria of the antimicrobial activity of extracts, fractions and compounds were based on the MIC threshold reported by (Efferth and Kuete, 2010). The ratio MBC/MIC was calculated to determine the bactericidal (MBC/MIC $\leq$ 4) and bacteriostatic (MBC/MIC $>$ 4) effects.

2.7. Acute oral toxicity study

Eight healthy Wistar rats were used for the acute oral toxicity studies using OECD guideline-423 (OECD, 2001) with slight modifications. Animals were fasted for 12 h, provided only with water. A single dose of 5000 mg/kg of the hydroethanolic extract of *D. microcarpum* root bark were orally administered to four animals while the four others received distilled water at 10 mL/kg. The animals were then, continuously observed for behavioural and autonomic profiles for 2 h to check for any signs of toxicity or mortality up to 14 days.

2.8. In vivo evaluation of the effects of D. microcarpum roots bark extract in rats infected with salmonella

After checking for the purity of the *S. typhimurium* isolate as previously described, the bacteria were maintained in Salmonella–Shigella agar medium (SS agar) (Liofilchem Italy).

The animals were maintained in clean metabolic cages (TECNIPLAST, Germany) (1 rat/cage) during experimental period. Prior to the salmonella infection, they were immunosuppressed by oral administration of cyclophosphamid (30 mg/kg) two day before infection as described by Abhishek et al. (2008). Salmonella infection was carried out according to the method described by Havelaar et al. (2001) with slight modifications. Briefly, 1 mL of bacterial suspension containing 1.5×10^8 CFU of *Salmonella typhimurium* in saline 0.9% NaCl solution was orally administrated to each animal. Two hours later, animals were randomized into seven groups of six animals each (03 males and 03 females) and daily treated for 10 days as follow:

Normal control consisted of healthy rats receiving distilled water (10 ml/kg), immunosuppressed control was uninfected animal treated for two days with cyclophosphamid (30 mg/kg) and received distilled water; salmonella control consisted of immunosuppressed and *Salmonella typhimurium*-infected rats that received distilled water; positive control group was infected animal that received ciprofloxacin (8 mg/kg), and the three test groups consisting in immunosuppressed and infected rats that received *D. microcarpum* root bark extract at the doses of 75, 150, and 300 mg/kg.

During the experimentation, body weight of each animal was recorded daily whereas faecal samples were collected every two days for the determination of the bacterial load.

2.9. Determination of bacterial load

Fecal matter (0.1 g) of each experimental animal collected into sterilized tube was dissolved in 5 ml of saline NaCl 0.9 %. Then, 100 µl of the resulting suspension was spread in a 90 mm Petri dish containing Salmonella–Shigella agar (SS agar) and incubated at 37 °C for 24 h. The bacterial load was recorded by counting the number of *S. typhimurium* colonies forming units (CFU), expressed per gram of fecal matter of each animal.

2.9.1. Animal sacrifice and organs collection

At the end of treatment period, animals were sacrificed under ketamine (30 mg/kg) and diazepam (10 mg/kg). Blood sample were collected into EDTA tubes for haematological analysis and into dry tubes which was centrifugated at 4 °C for 15 min at 3000 g, and supernatant (serum) was collected and kept at -80 °C for biochemical analyses. While some specific organs were removed, weighted, and fixed into 10 % formaldehyde.

2.9.2. Hematological analysis

Hematological parameters analysis included red blood cell (RBC) count, haemoglobin concentration (HGB), haematocrit (Hct), mean corpuscular volume (MCV), platelet (Plt) count, white blood cell (WBC) count, lymphocytes (Lymph), monocytes (Mono), and granulocyte (Gran) which were determined using an automated blood analyzer (XP-300 – Sysmex, Germany).

2.9.3. Biochemical analysis

The biochemical parameters evaluated were alanine aminotransferase (ALT), aspartate aminotransferase (AST), alkaline phosphate (ALP), lipid profile [triglyceride (TG), Total cholesterol (TC), high-density lipoprotein (HDL), and low-density lipoprotein (LDL) and Atherogenic index], creatinine, uric acid, bilirubin and albumin. These analyses were carried out through the procedures described by the commercial kits BIOLABO (France) using spectrophotometer reader (UviLine SI 5000 - SI Analytics®, Germany).

2.9.4. Histopathological analysis

The cross sections of tissues of each organ were prepared and analyzed using conventional techniques (Treuting et al., 2017). Sections of liver, stomach, kidney, and intestine (jujenum) fixed into 10% formalin were dehydrated in ascending grades of alcohol and cleared in xylene. The fixed tissue was embedded in paraffin wax and sectioned into 5 µm thick with the rotary microtome, then stained with hematoxylin and eosin. The sections were examined with light microscope and photographed using a microscopic camera (Axioshop, Germany).

2.10. Statistical analysis

Data were expressed as mean ± SEM (standard error of mean). Statistical analysis was performed by one-way ANOVA (analysis of variance) followed by the Bonferroni post-test using GraphPad 7 software. Difference was considered as significant at $p < 0.05$.

Table 1
Phytochemical analysis of the hydroethanolic extracts of *Detarium microcarpum*.

	Extract			
Metabolites	Root	Root bark	Leaf	Twig
Flavonoids	+	+	+	+
Sterols	+	+	+	+
Triterpenes	+	+	+	+
Glucosides	+	+	+	+
Coumarins	+	+	+	+
Saponins	+	+	+	+
Alkaloids	–	–	–	–
Tannins	–	–	–	–

+ = present, - = absent.

3. Results and discussion

3.1. Phytochemical analyses and LC/MS chemical profile

The phytochemical analysis of *D. microcarpum* roots, roots bark, leaves and twigs extracts revealed in all of them, the presence of phenolic compounds, flavonoids, sterols, triterpenes, glucosides, coumarins, and saponins, whereas alkaloids and tannins were absent (Table 1).

Fig. 1 and Table 2 summarize the major peaks in the chemical profile of the hydroethanolic extract of *D. microcarpum* root bark. Eight compounds were detected by UPLC-DAD-MS (Fig. 1a) among which, 2 were isolated.

Compound **4** (rhinocerotinoic acid): white crystal, mp. 187–189 °C , $[\alpha]_D^{18}$ +38.9° (c 0.236, $CHCl_3$). (+)HRESI-MS (Fig. 1b) [M+H]+ at m/z 319.2156 (calcd for $C_{20}H_{31}O_3$, 319.2268). ^{1}H NMR (DMSO, 500 MHz): δ 5.68 (1H, d, H-14), 2.37 (2H, dd, H-11), 2.33 (2H, dd, H-12), 2.22 (2H, m, H-1), 2.14 (3H, d, H-16), 1.92 (1H, d, H-6a), 1.68 (3H, s, H-19), 1.64 (1H, dd, H-5), 1.52 (2H, m, H-2), 1.41 (1H, dd, H-3a), 1.35 (1H, dd, H-6b), 1.22 (1H, dd, H-3b), 1.06 (3H, s, H-17), 0.89 (3H, s, H-18), 0.85 (3H, s, H-20); ^{13}C NMR (DMSO, 125 MHz): δ 198.9(C-7), 167.8(C-15), 167.0(C-9), 158.3(C-13), 129.7(C-8), 116.6(C-14), 50.2(C-5), 41.2(C-3), 41.0(C-10), 39.1(C-1), 35.4(C-6), 35.2(C-12), 33.2(C-4), 32.7(C-11), 27.7(C-20), 21.5(C-18), 18.6(C-2), 18.6(C-16), 18.1(C-17), 11.4(C-19) (Dekker et al., 1988; Gray et al., 2003).

Compound **8** (Lupeol) ^{1}H NMR($CDCl_3$, 500 MHz): δ 4.70, 4.60 (2H, s, H-29a, 29 b), 3.22 (1H, m, H-3), 0.79, 0.81, 0.85, 0.97, 0.99, 1.06, 1.71 (each 3H, s); ^{13}C NMR ($CDCl_3$, 125 MHz): δ 151.0(C-20), 109.3(C-29), 79.0(C-3), 55.3(C-5), 50.4(C-9), 48.3(C-18), 48.0(C-19), 43.0(C-17), 42.9(C-14), 40.8(C-8), 40.0(C-22), 38.9(C-4), 38.7(C-1), 38.1(C-13), 37.2(C-10), 35.6(C-16), 34.3(C-7), 29.9(C-21), 28.0(C-23), 27.5(C-2), 27.4(C-15), 25.1(C-12), 20.9(C-11), 19.3(C-30), 18.3(C-6), 18.0(C-28), 16.1(C-25), 15.9(C-26), 15.5(C-24), 14.6(C-27) (Adzu et al., 2015).

Table 2
Main signals exhibited in the LC-MS spectra of compounds detected in *D. microcarpum* and proposed attribution.

N°	Tr (min)	[M+H]$^+$		Molecular Formular	Name of Compound
		Exp.	Calcl.		
1	0.3	203.0523	203.26	$C_6H_{12}O_6$	Glucose
2	3.3	147.0435	147.0417	$C_7H_8O_2$	Not Identified
3	4.6	319.2275	319.2268	$C_{20}H_{30}O_3$	Not Identified
4	4.7	319.2156	319.2268	$C_{20}H_{30}O_3$	Rhinocerotinoic acid (**4**)
5	4.9	319.2226	343.2268	$C_{20}H_{30}O_3$	Not Identified
6	5.6	303.2326	303.2319	$C_{20}H_{31}O_2$	Not Identified
7	5.9	305.2485	271.2195	$C_{20}H_{32}O_2$	Not Identified (**7**)
8	6.9	227.3424	227.3432	$C_{30}H_{50}O$	Lupeol (**8**)

The compounds 4 showed antisalmonella activity wheras the compound 8 was not active.

3.2. In vitro antibacterial activities of extracts and compound

The *in vitro* antibacterial effects (MIC, MBC and MIC/MBC parameters) of extracts, fractions, and isolated compounds from *D. microcarpum* are illustrated in Table 3. The crude extracts, fractions and isolated compounds showed variable inhibitory activities against microbial strains. Root bark extract displayed good antibacterial activities against all microorganisms tested with MIC ranging from 4.55 ± 1.72 to 208.30 ± 41.67 µg/mL, while root, leaves and twigs extracts only inhibited the growth of some tested bacterial strains. Moreover, among the fractions, only ethyl acetate fraction (F_3) expressed moderate antibacterial activity (MIC: 250-125 µg/ml) (Table 3). The compound 4 (rhinocerotinoic acid) exhibited good activity against all salmonella strains tested with MIC values ranging of 31.25–62.50 µg/mL. The other fractions (F_1, F_2, F_4 and F_5) and other isolated compounds showed no antisalmonella activity.

3.3. Acute oral toxicity studies

No toxicity signs or death were recorded with the plant extract administration, indicating that the oral lethal dose-50 (LD_{50}) of the hydroethanolic extract of *Detarium microcarpum* root bark was greater than 5000 mg/kg.

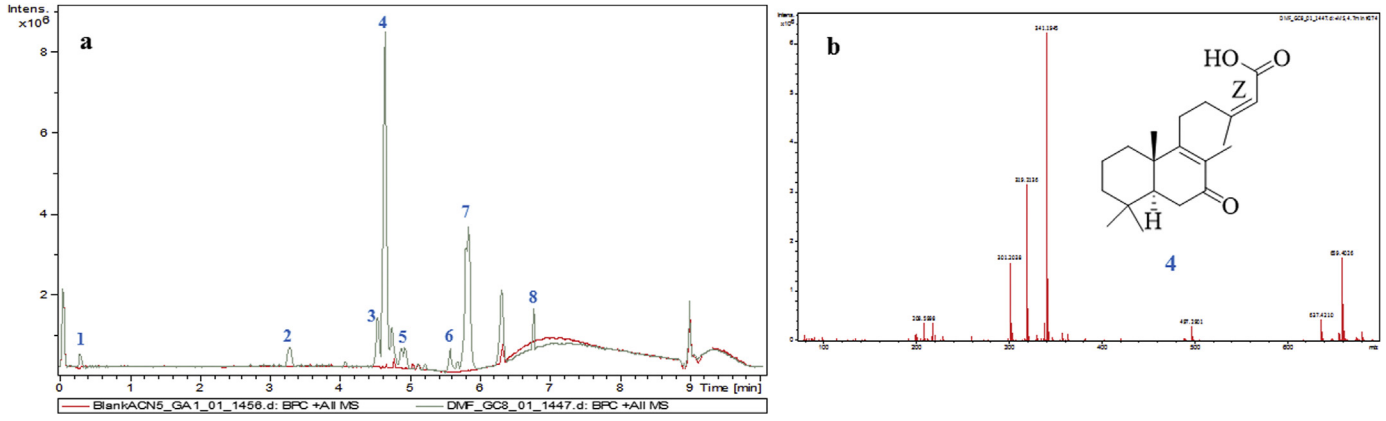

Fig. 1. a: LC-MS chromatogram coupled with mass spectrometry of the roots bark hydroethanolic extract of *Detarium microcarpum*. Peak1 to peak 8 represent the different compounds observed in the extract. (**1b**): Mass spectrum of major compound. (4) = Labdane-type diterpene class: Rhinocerotinoic acid.

Table 3
Inhibition parameters (MIC, MBC) of *D. microcarpum* extracts against different salmonella.

Extracts	Parameters	Bacteria strains		
		St	**Stm**	**Se**
Roots	MIC (µg/mL)	13.02 ± 2.60	4.55 ± 1.72	> 500
	MBC(µg/mL)	208.30 ± 41.67	52.08 ± 10.42	ND
	MBC/MIC	15.99	16.02	ND
Roots Bark	MIC (µg/mL)	9.11 ± 2.44	4.55 ± 1.72	208.30 ± 41.67
	MBC (µg/mL)	208.30 ± 41.67	83.33 ± 20.83	333.30 ± 166.70
	MBC/MIC	22.86	18.31	1.60
Leaves	MIC (µg/mL)	> 500	333.30 ± 83.33	> 500
	MBC (µg/mL)	ND	> 500	ND
	MBC/MIC	ND	ND	ND
Twigs	MIC (µg/mL)	> 500	72.92 ± 27.56	> 500
	MBC (µg/mL)	ND	416.70 ± 83.33	ND
	MBC/MIC	ND	5.71	ND
Fractions				
F_1	MIC (µg/mL)	> 250	> 250	> 250
	MBC (µg/mL)	ND	ND	ND
	MBC/MIC	ND	ND	ND
F_2	MIC (µg/mL)	> 250	> 250	> 250
	MBC (µg/mL)	ND	ND	ND
	MBC/MIC	ND	ND	ND
F_3	MIC (µg/mL)	250.00	250.00	250.00
	MBC (µg/mL)	500	500	500
	MBC/MIC	2	2	2
F_4	MIC (µg/mL)	> 250	> 250	> 250
	MBC (µg/mL)	ND	ND	ND
	MBC/MIC	ND	ND	ND
F_5	MIC (µg/mL)	> 250	> 250	> 250
	MBC (µg/mL)	ND	ND	ND
	MBC/MIC	ND	ND	ND
Compounds				
(4)	MIC (µg/mL)	62.50	31.25	31.25
	MBC (µg/mL)	125	125	62.5
	MBC/MIC	2	4	2
(8)	MIC (µg/mL)	> 125	> 125	> 125
	MBC (µg/mL)	ND	ND	ND
	MBC/MIC	ND	ND	ND
Ciprofloxacin	MIC (µg/mL)	0.5	0.5	1
	MBC (µg/mL)	2	2	4
	MBC/MIC	4	4	4

Values represent mean ± SEM, n = 3, St: *Salmonella typhi* ATCC 19430; Stm: *Salmonella typhimurium*; Se: *Salmonella enteritidis* ATCC 13076. MIC = Minimum inhibitory concentration; MBC = Minimum bactericidal concentration. F_1 = *n*-hexane fraction; F_2 = dichloromethane fraction; F_3 = ethyl acetate fraction; F_4 = *n*-butanol fraction; F_5 = aqueous fraction.

3.4. Effects of hydroethanolic extract of D. microcarpum root bark on the bacterial load in salmonella-infected rat

The inoculation of 1 ml of NaCl 0.9 % suspension containing 1.5×10^8 CFU of *Salmonella typhimurium* to immunosuppressed rat induced salmonella infection with gradual increase of bacterial load up to 600 ± 41.67 CFU/g of feces after 10 days of experiment (Fig. 2).

The daily administration of single dose of *D. microcarpum* extract starting 2 h post inoculation significantly decreased the bacterial load ($p < 0.001$) at the dose 150 and 300 mg/kg/bw compared to the salmonella control. At the end of treatment, the extract induced complete clearance (100%, $p < 0.001$) of bacteria load at all the tested doses compared to salmonella control. No significant change in the bacterial load was observed between the tested doses of the extract and ciprofloxacin (8 mg/kg.bw).

3.5. Effect of the hydroethanolic extract of D. microcarpum root bark on body weight and relative weight of organs

Fig. 3 summarizes the effect of the *D. microcarpum* root bark extract on body weight evolution. The salmonella infection induced significant decrease in body weight ($p < 0.001$) by 12.38 % and 36.36 % from day 3 (d4) to day 9 (d10) respectively, in untreated group compared to the normal group (Fig. 3A). It was also observed from day 4 (d5) to the day 9 (d10), a significant decrease in body weight ($p < 0.001$) of *Salmonella* control compared to immunosuppressed control. Meanwhile, the plant extract administration 2 h post inoculation significantly increased the body weight ($p < 0.001$) of infected animals as compared to the *Salmonella* control.

Inoculation of 1 mL of *S. typhimurium* suspension (1.5×10^8 CFU) to immunosuppressed rat resulted after ten days to significant increase ($p < 0.001$) in relative weight of liver, kidney and spleen as compared to normal control and immunosuppressed control (Fig. 3B). However,

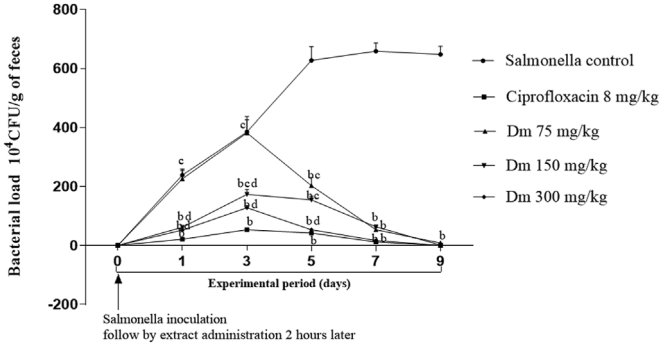

Fig. 2. Kinetic effects of extract on the bacterial load in salmonella-infected rats. Values are expressed as mean ± SEM. n = 6. [b]p < 0.001: significant difference compared to salmonella control; [c] p < 0.001: significant difference compared to ciprofloxacin (8 mg/kg.bw) control; [d] p < 0.001: significant difference between the test groups.

ten days administration of *D. microcarpum* extract led to a significant decrease (p < 0.001) in relative weight of these organs. No significant change was observed in weight of liver, kidney and spleen of the test groups compared to the ciprofloxacin control. Likewise, no change was recorded in weight of stomach and intestine of the experimental animals.

3.6. Effects of hydroethanolic extract of D. microcarpum root bark on some haematological parameters

Table 4 presents the effects of treatment on some haematological parameters in infected rats. The induction of salmonella infection resulted in significant reduction (p < 0.001) of erythrocytes, hemoglobin, hematocrit, and leucocytes while thrombocytes increased in salmonella control as compared to the normal control and the immunosuppressed control. The daily administration of the extract significantly increased (p < 0.001) the red blood cells (RBC) count, haemoglobin (Hb) concentration, haematocrit (Hct) and mean corpuscular volume (MCV) in treated animals compared to salmonella control. It was also recorded, a significant increase (p < 0.001) in white blood cells (WBC), lymphocytes, monocytes and granulocytes count in the infected animals treated with the plant extract compared to salmonella control. However, no significant change pattern was observed between treated groups.

3.7. Effects of the hydroethanolic extract of D. microcarpum root bark on some serum biochemical parameters

The effects of *D. microcarpum* extract on some biochemical parameters are summarized in Table 5. Salmonella infection provoked significant increase (p < 0.001) in ALAT, ASAT, APL, albumin, bilirubin, creatinine, and uric acid levels compared to normal control and to immunosuppressed control. However, the daily administration of plant extract to infected animals significantly decreased (p < 0.001) these parameters by 65.46%, 43.93% and 65.45% in ALAT, by 34.41%, 31.81% and 40.25% in ASAT, by 44.85%, 40.68% and 37.99% in APL activities, by 19.38%, 11.77% and 13.82% in albumin, by 31.42%, 34.28% and 28.57% in total bilirubin levels at the respective doses of 75, 150 and 300 mg/kg, compared to salmonella control (Table 5). The plant extract also induced significant decrease (p < 0.001) in creatinine level by 38.05% and 42.53% and in uric acid concentration by 32.57%, 45.71% and 44% at the same doses. It was observed an increase in uric acid by 39.83% (p < 0.001) in animal treated with plant extract at 75 mg/kg compared to immunosuppressed control. Moreover, no significant change was observed in these parameters between normal and immunosuppressed control, as well among the treated groups.

It results that, *Salmonella typhimurium* infection induced significant increase (p < 0.001) in the total Cholesterol (T-Cho) by 34.61%, triglycerides by 33.33%, LDL Cholesterol (LDL-Cho) levels by 44.00% and atherogenic index by 50.00% compared to normal control and immunosuppressed control. Meanwhile, *Salmonella typhimurium* infection induced significant decrease (p < 0.001) in HDL Cholesterol (HDL-Cho) by 40% in salmonella control. The administration of the plant extract to infected animal significantly protected (p < 0.001) from the increase in T-Cho, triglycerides, LDL-Cho and atherogenic index and from the decrease of HDL-Cho level, whatever the dose, compared to salmonella control. No significant change was noted neither in lipid profile parameters between normal control and immunosuppressed control, nor between treated groups.

3.8. Effects of D. microcarpum root bark extract on the histopathology of some organs

The histological analysis of liver, intestine (jujenum), and kidney of salmonella-infected animals, treated with the *D. microcarpum* hydro-alcoholic root bark extract is illustrated in Figs. 4–6. The liver section of normal control revealed normal parenchyma in which centrolobular vein, hepatocytes and sinusoids are well identified (Fig. 4A) while some sinusoids clarification was observed in the immunosuppressed control (Fig. 4B). It appears that typhoid fever provokes in liver section of salmonella control, some damages including inflammation with leukocyte infiltration, hepatocyte cytolysis (Fig. 4C) which disappeared in treated groups (Fig. 4 D, E, F and G).

The intestine section of normal and immunosuppressed controls presented normal architecture with from the internal to external distinct intestinal lumen, mucous, submucosa, muscular and serous

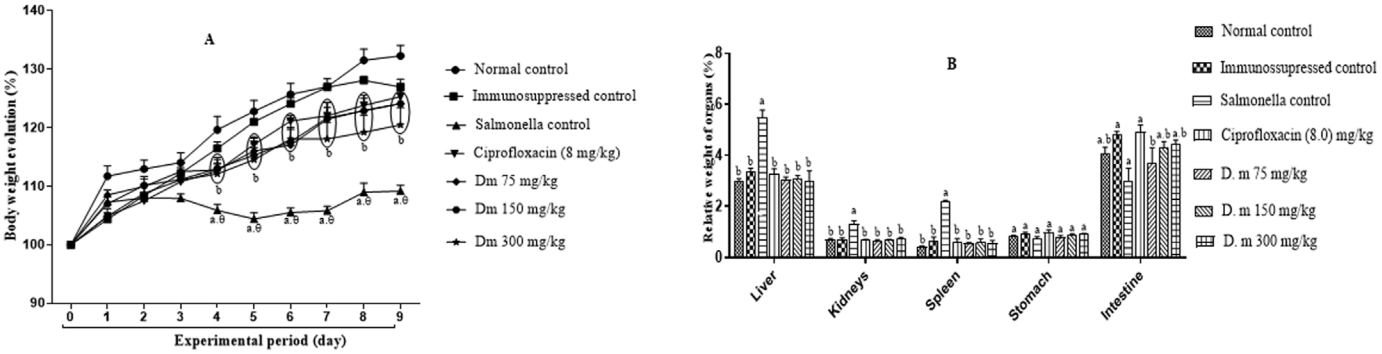

Fig. 3. Effects of extract on body weight evolution (A) and relative weight of organs (B) in *S. typhimurium* infected in rat. Values are expressed as mean ± SEM. n = 6. [a]p < 0.001: significant different compared to normal control; [e] p < 0.001: significantly different compared to immunosuppressed control [b] p < 0.001: significant different compared to salmonella control.

Table 4
Effects of *D. microcarpum* on some haematological parameters in infected animals.

Blood parameter	RBC (10^6/µL)	HGB (g/dL)	Hct (%)	MCV (fL)	Plt (10^3/µL)	WBC (10^3/µL)	Lymph (%)	Mono (%)	Gran (%)
Normal control	7.50 ± 0.20	13.00 ± 0.28	45.00 ± 0.99	57 ± 2.60	666 ± 66	4.90 ± 0.36	56.00 ± 4.60	31.00 ± 3.50	46.24 ± 3.52
Immunosuppressed control	7.40 ± 0.26	12.00 ± 0.44	43.00 ± 1.90	55.00 ± 2.20	751 ± 47	4.10 ± 0.26	50.00 ± 2.20	34.00 ± 2.30	39.49 ± 3.46
Salmonella control	5.10 ± 0.4[a. e]	8.50 ± 0.49 [a. e]	35.00 ± 1.10[a. e]	45.00 ± 2.9[a]	1035 ± 100[a]	2.40 ± 0.31[a. e]	33.00 ± 1.70 [a. e]	19.00 ± 1.60 [a. e]	21.35.00 ± 5.79[a]
Ciprofloxacin (8.0) mg/kg	7.20 ± 0.29[b]	12.00 ± 0.54[b]	43.00 ± 2.10[b]	59.00 ± 1.30[b]	873 ± 124	3.60 ± 0.13[b]	53.00 ± 5.00[b]	41.00 ± 7.00[b]	48.12 ± 3.08[b]
D.m 75 mg/kg	7.00 ± 0.23[b]	12.00 ± 0.30[b]	42.00 ± 1.60[b]	61.00 ± 2.70[b]	850 ± 166[b]	4.00 ± 0.30[b]	58.00 ± 6.00[b]	46.00 ± 4.80[b]	35.17 ± 6.72
D.m 150 mg/kg	7.00 ± 0.35[b]	12.00 ± 0.62[b]	42.00 ± 2.10[b]	61.00 ± 2.40 [b]	768 ± 800[b]	5.60 ± 0.51[b. c]	56.00 ± 4.50[b]	46.00 ± 5.10[b]	41.10 ± 7.06[b]
D.m 300 mg/kg	7.40 ± 0.39[b]	13.00 ± 0.64[b]	42.00 ± 2.40[b]	57.00 ± 1.60[b]	828 ± 204[b]	4.20 ± 0.47[b]	57.00 ± 2.10[b]	44.00 ± 4.90[b]	43.79 ± 5.26[b]

Values are expressed as mean ± SEM. n = 6. [a]p < 0.001: significant difference compared to normal control; [e]p < 0.001: significant difference compared to immunosuppressed control; [b]p < 0.001: significant difference compared to salmonella control; [c]p < 0.001: significant difference compared to ciprofloxacin (8 mg/kg) control.

Table 5
Effects of hydroethanolic extract of *D. microcarpum* root bark on some biochemical parameters.

Experimental group of animals	Normal control	immunosuppressed control	Salmonella control	Ciprofloxacin (8.0 mg/kg)	D.m 75 mg/kg	D.m 150 mg/kg	D.m 300 mg/kg
ALAT(IU/L)	36.00 ± 0.88	36.00 ± 1.80	66.00 ± 5.80[a. e]	36.00 ± 0.74[b]	35.00 ± 4.40[b]	37.00 ± 2.2[b]	36.00 ± 1.80[b]
ASAT(IU/L)	106.00 ± 2.30	108.00 ± 4.80	154.00 ± 4.60[a. e]	103.00 ± 2.50[b]	101.00 ± 3.80[b]	105.00 ± 1.70[b]	92.00 ± 1.30[b]
ALP (IU/L)	238.00 ± 18.00	234.00 ± 18.00	408.00 ± 29.00 [a. e]	242.00 ± 17.00[b]	225.00 ± 26.00[b]	242.00 ± 14.00[b]	253.00 ± 8.90[b]
Albumin (µg/mL)	437.00 ± 9.90	433.00 ± 8.80	557.00 ± 11.00[a. e]	471.00 ± 9.40[b]	449.00 ± 10.00[b]	458.00 ± 7.90[b]	480.00 ± 16.00[b]
Bilirubin (µg/mL)	2.30 ± 0.08	2.50 ± 0.13	3.50 ± 0.09[a. e]	2.50 ± 0.11[b]	2.40 ± 0.09[b]	2.30 ± 0.14[b]	2.50 ± 0.14[b]
Total CHO (mmol/L)	1.70 ± 0.03	1.60 ± 0.03	2.60 ± 0.12[a. e]	1.80 ± 1.70[b]	1.60 ± 0.08[b]	1.60 ± 0.11[b]	1.80 ± 0.22[b]
Trigycerides (mmol/L)	0.80 ± 0.03	0.83 ± 0.05	1.2 ± 0.08[a. e]	0.86 ± 0.08[b]	0.82 ± 0.09[b]	0.68 ± 0.04 [b]	0.62 ± 0.04 [b]
HDL CHO (mmol/L)	1.30 ± 0.03	1.10 ± 0.05	0.78 ± 0.02[a. e]	1.30 ± 0.06[b]	1.20 ± 0.05[b]	1.10 ± 0.02[b]	1.20 ± 0.06[b]
LDL CHO (mmol/L)	1.40 ± 0.11	1.50 ± 0.04	2.50 ± 0.09[a. e]	1.30 ± 0.07[b]	1.60 ± 0.09[b]	1.50 ± 0.10[b]	1.30 ± 0.04[b]
Atherogenic index	0.14 ± 0.00	0.18 ± 0.01	0.28 ± 0.01[a. e]	0.12 ± 0.00[b]	0.16 ± 0.01[b]	0.13 ± 0.00[b]	0.13 ± 0.01[b]
Creatinine (µmol/L)	83.00 ± 1.90	81.00 ± 3.60	134.00 ± 8.60[a. e]	81.00 ± 1.60[b]	83.00 ± 1.80[b]	77.00 ± 3.90[b]	77.00 ± 3.10[b]
Uric acid (µmol/L)	64.00 ± 4.20	71.00 ± 2.90	175.00 ± 3.10[a. e]	96.00 ± 13.00[b]	118.00 ± 11.00[a. e. b]	95.00 ± 15.00[b]	98.00 ± 17.00[b]

Values are expressed as mean ± SEM. n = 6. [a] p < 0.001: significant difference compared to normal control; [e] p < 0.001: significant difference compared to immunosuppressed control; [b] p < 0.001: significant difference compared to salmonella control.

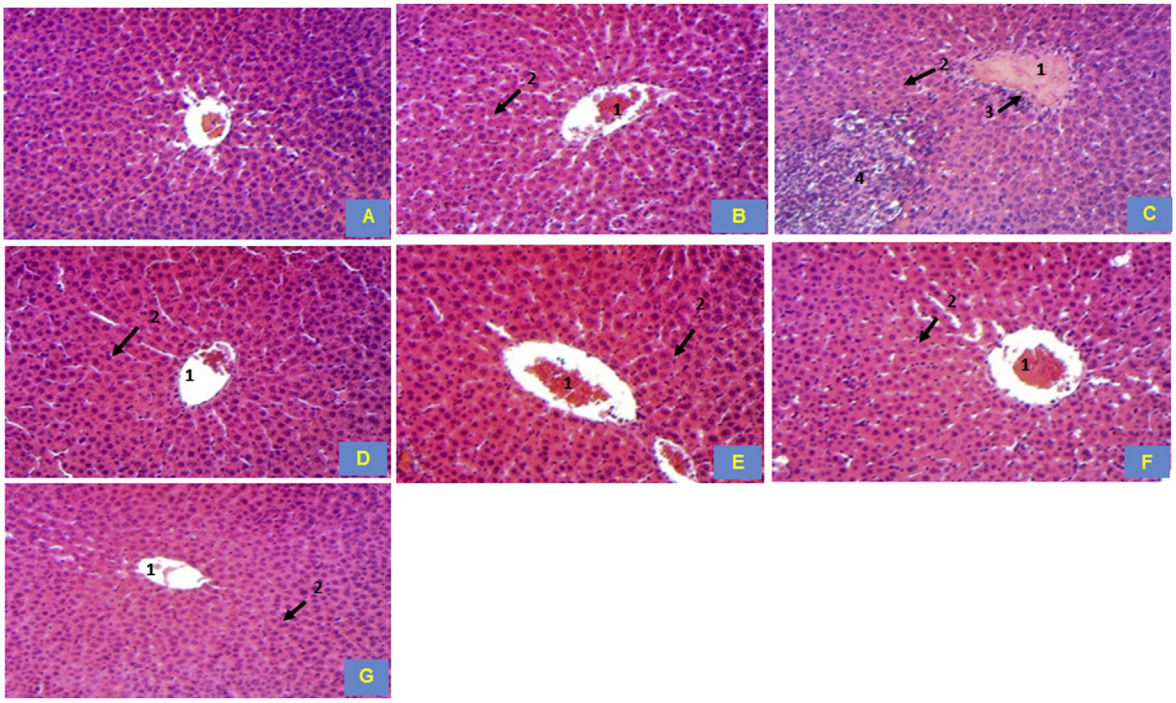

Fig. 4. Effects of *D. microcarpum* hydroethanolic extract on the micrography of liver section in salmonella-infected rats (HE x 400). 1: Centro-lobular vein, 2: Hepatocytes, 3: leukocyte inflammation, 4: hepatocyte cytolysis. A–G: A: Normal control, B: Immunosuppressed control, C: Salmonella control, D: ciprofloxacin control, E: Rats treated at 75 mg/kg of the extract; F: Rats treated at 150 mg/kg of the extract, G: Rats treated at 300 mg/kg of the extract.

(Fig. 5A and B). The intestine section of salmonella control shows some major damages such as no diffuse infiltration with predominantly polymorphonuclear leukocytes, destruction of intestinal epithelium, and fibrinopurulent exudate in the intestinal lumen (Fig. 5C). The plant extract administration and ciprofloxacin protected the intestine of infected animals from damages with a general aspect similar to the normal control (Fig. 5 D, E, F and D).

The normal control and immunosuppressed control groups

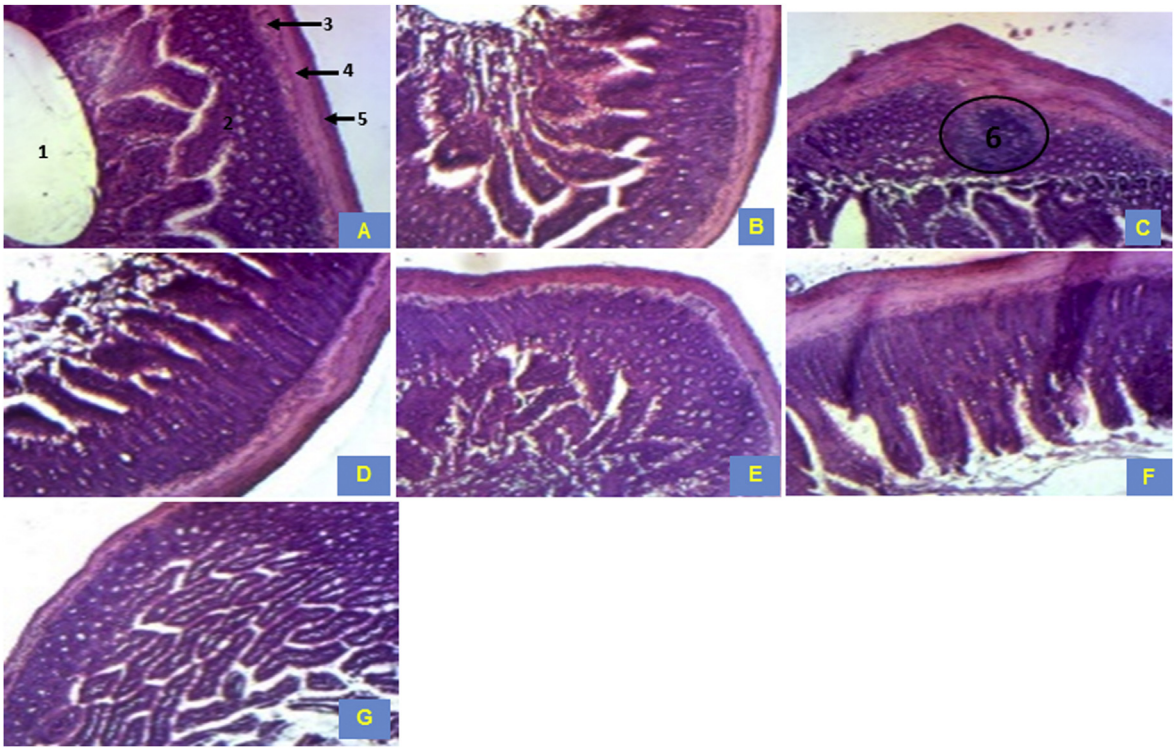

Fig. 5. Effects of *D. microcarpum* hydroethanolic extract on the micrography of intestine (jujenum) section in salmonella-infected rats (HE x 400); 1: intestinal lumen, 2: Mucous, 3: Submucosa, 4: muscular, 5: Serous, 6: No diffuse infiltration with predominantly polymorphonuclear leukocytes, destruction of intestinal epithelium, and fibrinopurulent exudate in the intestinal lumen. A–G: A: Normal control, B: Immunosuppressed control, C: Salmonella control, D: ciprofloxacin control, E: Rats treated at 75 mg/kg of the extract; F: Rats treated at 150 mg/kg of the extract, G: Rats treated at 300 mg/kg of the extract.

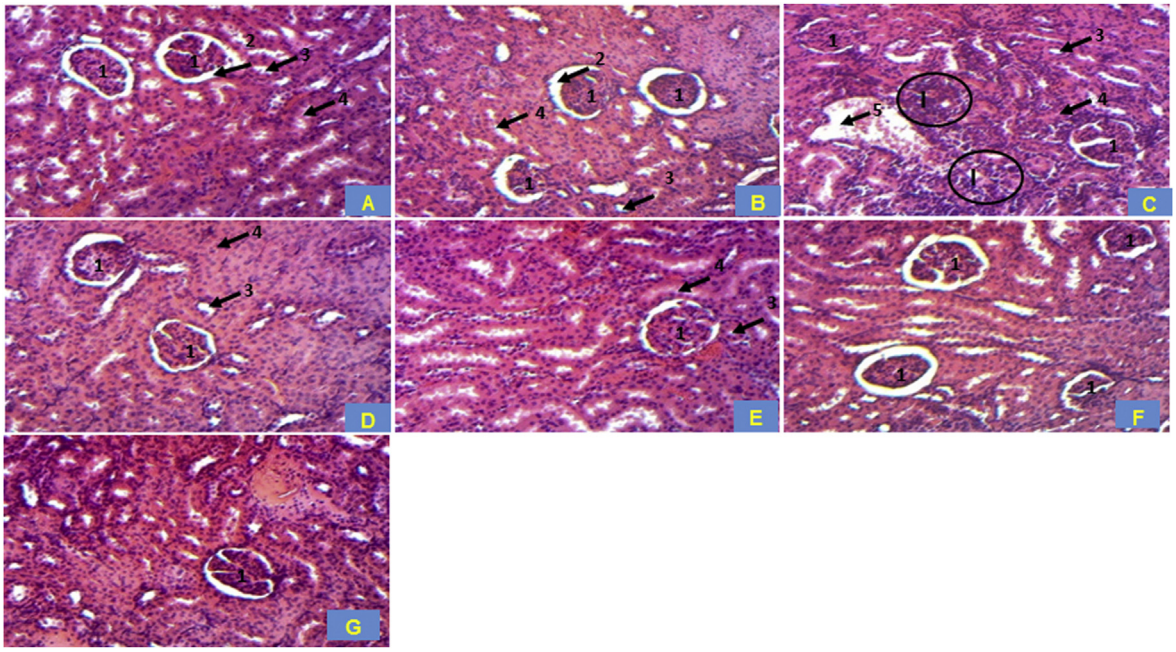

Fig. 6. Effects of *D. microcarpum* hydroethanolic extract on the micrography of kidney section in salmonella-infected rats (HE x 400); 1: glomerulus, 2: urinary space, 3: distal convoluted tubule, 4: proximal convoluted tubule, 5: glomerulosclerosis, 6: mesangial expansion, I: inflamation. A–G: A: Normal control, B: Immunosuppressed control, C: Salmonella control, D: Ciprofloxacin control (8.0 mg/kg), E: Rats treated at 75 mg/kg of the extract; F: Rats treated at 150 mg/kg of the extract, G: Rats treated at 300 mg/kg of the extract.

presented normal kidney anatomy with proximal and distal convoluted tubules and glomerular (Fig. 6A and B). The kidney of the untreated rats exhibits glomerulosclerosis, mesangial expansion and inflammation (Fig. 6C). Those of animals treated with ciprofloxacin or *D. microcarpum* hydro-alcoholic root bark extract showed inconsiderable injuries pattern (Fig. 6 D, E, F, G).

4. Discussion

The present study aimed to evaluate the *in vitro* and *in vivo* anti-salmonella activity of hydro-ethanolic of *Detarium microcarpum* extracts. *Detarium microcarpum* uses are reported in communities for treatment of different diseases including typhoid fever (Sodipo and Wannang, 2015). The extracts from different parts of *D. microcarpum* were *in vitro* tested on microbial agents and, the most active extract was further evaluated for its *in vivo* anti-salmonella effects.

The *D. microcarpum* hydro-ethanolic extracts of leaf and twig exhibited poor inhibition on *Salmonella* strains and isolate while the root and root bark extracts showed strong antibacterial potencies, with the root bark extract exerting the more prominent effect. Although, the antisalmonella activity increased from extract to fractions, the resulting compound (rhinocerotinoic acid) was less active than the parent extract and fractions. Therefore, it is likely that compound (**4**) might not contribute alone to the observed activity and could probably act in synergy with other compounds present in the fraction/extract. The phytochemical analysis of the extract revealed its complexity in terms of bioactive compounds of which, most are well known for their biological activities such as antibacterial agents. Antimicrobial mechanisms involved in the observed activity might include disruption of pathogen membrane by phenolic, sterol and terpene compounds in which belong the isolated compound (rhinocerotinoic acid), interruption of DNA/RNA synthesis and function provoked by coumarins, interference with intermediary metabolism or the interruption of normal communication (Quorum sensing, QS) caused by flavonoids (Cowan, 1999). It has been also reported that compounds of the labdane-type diterpene class possess antimicrobial, antifungal, antiviral, anticancer and antioxidant activities (Papaefthimiou et al., 2014).

In the present study, the orally inoculation of *Salmonella enterica* serovar *typhimurium* isolate to healthy rats resulted to an establishment of infection, which is the classical transmission pathway of salmonellosis. The *S. enterica* serovar *typhimurium* infection begins with the invasion of intestinal epithelial cells and requires the activation of Spi1 (Salmonella pathogenicity island 1), a finely regulated type III secretion system (TTSS or type three secretion system) in response to environmental signal variations (Ellermeier and Slauch, 2007; Que et al., 2013). As in many bacteria, Fe–S proteins are involved in many essential pathways, and the assembly of these metal centers involves biogenetic pathways; ISC (iron-sulfur cluster) and SUF (sulfur assimilation), which are activated only under stress conditions (Py and Barras, 2014). This infection was accompanied by some physiological changes in the animals as the excretion of watery stool, the presence of blood and mucus in the stool, the reduction of its mobility, the loss of body weight and the increase of bacterial load in the feces (Fig. 1). This observation suggests that bacteria has proliferated into the organs after invading the digestive system, and challenging the non-specific defense mechanism of animal (Fodouop SPC et al., 2014). The *Detarium microcarpum* root bark administration, 2 h post inoculation significantly decreased the bacterial load in treated animal, proving its effective antibacterial activity as observed in the *in vitro* assay. This anti-salmonella activity of the extract may be ascribed both to the presence of metabolites groups identified in the extract, acting by activation of immune system cells as observed through the proliferation of WBCs in the present study (Suresh et al., 2018) or by iron chelation due to phenolic compounds, including labdane-type diterpene which is required for bacteria survival (Kortman et al., 2012; Papuc et al., 2017). A synchronization in the complete bacterial clearance noted between the *D. microcarpum* extract and Ciprofloxacin (8 mg/kg) treatment, used as reference drug in this study, suggesting effective anti-salmonella activity of the extract.

Salmonella typhimurium infection in rat is an example of bacterium which invades the bloodstream, spreads throughout the body, invades organs (liver, kidney, intestine, stomach and other organs), and secretes endotoxins after escaping from macrophage cells (Nwankpa et al., 2012). Classically, the general form of disease includes the passage of

Salmonella through the lymphatic system of the intestine into the blood which are carried to various organs (liver, spleen, kidneys) and can cause organ damage and dysfunction as seen in the study. These physiological changes are manifested by an increase in transaminases (ALT and AST), APL, albumin, bilirubin and lipid profile disturbance which express a hepatic function failure, and damage in the liver section of salmonella control (Fig. 5). It has been reported that salmonella infection provokes disturbance in membrane permeability, structure or fluidity, causes translocation of the liver transaminases to blood. The release of endotoxin induce a cascade of transduction signal leading to the translocation of NK– KB factors in the nucleus (Rietschel et al., 1991). These factors induced the production of inflammatory factors such as cytokine (TNF and interferon) and multiple metabolite of arachidonic acid which can stimulate the production of free radicals as NO and impair liver function (Bradham et al., 1998; Charpin, 2007).

It was also reported a reduced pyruvate levels and down-expression of the genes regulating lipid metabolism in the chicken liver after infection with salmonella that result in a lipid metabolism disturbance (Coble et al., 2013). The increase in total cholesterol and LDL cholesterol recorded in salmonella control suggests that salmonella infection favour the accumulation of fatty acids in blood capillaries and predisposes to possible risk of atherosclerosis and cardiovascular diseases (Kapur NK et al., 2008). This lipid profile alteration recorded in our study was alleviated by the extract administration, demonstrating its protective role in the liver function.

The increase of creatinine and uric acid levels recorded in infected rats are signs of kidneys failure which is well described in salmonella infection and could be due to local or systemic effects of circulating *Salmonella* endotoxin (Khan et al., 1998). Salmonella infection involves Angiotensin II in the production of pyrogenic cytokines, such as IL-1, (Watanabe et al., 2000). Thus, Salmonella toxin effects in concert with activation of the renin angiotensin axis and release of proinflammatory cytokines produce renal perfusion disorders that impair renal function (Janssen van Doorn et al., 2006). In fact, the decrease of serum creatinine and uric acid levels in this study reveals repair effect of the kidneys after the administration of *Detarium microcarpum* root bark extract, indicating the benefit role of the extract in the reestablishment of kidney integrity. The extract also protected from intestine damages induced by salmonella infection.

5. Conclusion

The *D. microcarpum* hydroethanolic extracts expressed inhibitory effects on some microorganisms agents with the best *in vitro* anti-salmonella activity observed with the *D. microcarpum* root bark. This extract expresses effective anti-salmonella activity in infected rat. It has also protected infected animal from the decrease in body weight, disturbances in transaminases, alkaline phosphatase, albumin, bilirubin, lipid profile, creatinine, uric acid compared to the untreated infected rats. No acute toxicity side effects was observed with the plant extract. The overall results obtained in the present work provide, the baseline information for the possible use of the hydroethanolic extract of *D. microcarpum* as alternative treatment to salmonellosis or typhoid fever. This anti-salmonella property observed in the extract justify its use in the traditionally healing to salmonellosis. Further safety and clinical study are needs to confirm it efficacy.

Authors' contributions

MAM and WFF carried out the study. WFF and BLN collected plant and prepared the extract, contributed to the phytochemical studies and isolated compound. MAM and RGK drafted the manuscript. RGK, AEN and TD designed and supervised the study. PVTF, FNT and PKL performed the biological analysis and data calculation. FFB, JJEN, OB, BLN, TD and NS critical revised the manuscript. All the authors contributed to the final version of the manuscript.

Declaration of competing interest

The authors declare that they have no competing interests.

Acknowledgements

This work was supported by the Yaoundé-Bielefeld Bilateral School Natural Products with Antiparasitic and Antibacterial Activity (YaBINaPA) project, financially supported by Deutscher Akademischer Austauschdienst (DAAD) [grant number 57316173].

References

Abhishek, S.S., Alok, S.W., Archana, R.J., 2008. Immunomodulatory activity of methanolic extract of Murraya koenigii spreng leaves. Indian J. Exp. Biol. 46, 505–509.
Adzu, B., Chindo, B.A., Tarfa, F.D., Salawu, O.A., Igoli, O.J., 2015. Isolation and analgesic property of lupeol from Diospyros mespiliformis stem bark. J. Med. Plants Res. 9, 813–819.
Akah, P.A., Nworu, C.S., Mbaoji, F.N., Nwabunike, I.A., Onyeto, C.A., 2012. Genus Detarium: ethnomedicinal, phytochemical and pharmacological profile. Phytopharmacology 3 (2), 367–375.
Aubry, P., Niyongabo, T.H., Nizigiye, J., Muhirwa, G., Kamanfu, G., Ndahiragije, A., 2002. Non-typhus salmonella bacteria during human immunodeficiency virus (HIV) infection in African adults. Trop. Med. 52, 447–450.
Bradham, C.A., Plümpe, J., Manns, M.P., Brenner, D.A., Trautwein, C., 1998. Mechanisms of hepatic toxicity. I. TNF-induced liver injury. Am. J. Physiol. 275, 387–392.
Charpin, D., 2007. Maladies allergiques, maladies environnementales. Rev. Prat. 57, 1297–1303.
Coble, D.J., Sandford, E.E., Ji, T., Abernathy, J., Fleming, D., Zhao, H., Lamont, S.J., 2013. Impacts of Salmonella enteritidis infection on liver transcriptome in broilers. Genesis 51 (5), 357–364.
Cowan, M.M., 1999. Plant products as antimicrobial agents. Clin. Microbiol. Rev. 12 (4), 564–582.
Date, K.A., Bentsi-Enchill, A.D., Fox, K.K., Abeysinghe, N., Mintz, E.D., Khan, M.I., Sahastrabuddhe, S., Hyde, T.B., 2014. Typhoid fever surveillance and vaccine use—south-East Asia and Western Pacific regions, 2009–2013. MMWR Morb. Mortal. Week. Rep. 63 (39), 855.
Dekker, T.G., Fourie, T., Matthee, E., Snyckers, F.O., Van der Schyf, C., Boeyens, J., Denner, L., 1988. Studies of South African medicinal plants: Pt. 7. S. Afr. J. Chem. 41 (1), 33–35.
Ebi, G., Afieroho, O., 2011. Phytochemical and antimicrobial studies on Detarium microcarpum Guill and Sperr (Caesalpinioceae) seeds coat. Afr. J. Biotechnol. 10 (3), 457–462.
Efferth, T., Kuete, V., 2010. Cameroonian medicinal plants. Pharmacol. Deriv. Nat. Prod. 1 (123).
Ellermeier, J.R., Slauch, J.M., 2007. Adaptation to the host environment: regulation of the SPI1 type III secretion system in Salmonella enterica serovar Typhimurium. Curr. Opin. Microbiol. 10 (1), 24–29.
Fodouop, S.P.C., Gatsing, D., Tangue, B.T., Tagne, R.S., Tala, S.D., Tchoumboué, J., Kuiate, J.R., 2014. Effect of Salmonella typhimurium infection on rat's cell oxidation and in vivo antioxidant activity of Vitellaria paradoxa and Ludwiguia abyssinica aqueous extract. Asian Pac. J. Trop. Dis. 4 (1), 931–937.
Gray, C.A., Davies-Coleman, M.T., Rivett, D.E., 2003. An improved synthesis of rhinocerotinoic acid. Tetrahedron 59 (2), 165–173.
Harbone, J.B., 1973. Phytochemical Methods. Chapman and Hall, New York, USA, pp. 1–150.
Havelaar, A.H., Garssen, J., Takumi, K., Koedam, M.A., Dufrenne, J.B., Van Leusden, F.M., De La Fonteyne, L., Bousema, J.T., Vos, J.G., 2001. A rat model for dose–response relationships of Salmonella enteritidis infection. J. Appl. Microbiol. 91, 442–452.
Janssen van Doorn, K., Pierard, D., Spapen, H., 2006. Acute renal dysfunction in Salmonella gastroenteritis. J. Clin. Gastroenterol. 40, 910–912.
Kapur, N.K., Ashen, D., Blumenthal, R.S., 2008. High density lipoprotein cholesterol: an evolving target of therapy in the management of cardiovascular disease. Vasc. Health Risk Manag. 4 (1), 39–57.
Khan, M., Coovadia, Y., Sturm, A.W., 1998. Typhoid fever complicated by acute renal failure and hepatitis: case reports and review. Am. J. Gastroenterol. 93 (6), 1001–1003.
Kortman, G.A.M., Boleij, A., Swinkels, D.W., Tjalsma, H., 2012. Iron availability increases the pathogenic potential of Salmonella typhimurium and other enteric pathogens at the intestinal epithelial interface. PloS One 7 (1) e29968-e29968.
Kouyaté, A.M., Van Damme, P., De Meulenaer, B., Diawara, H., 2009. Contribution des produits decueillette dans l'alimentation humaine. Cas de Detarium microcarpum. Afr. Focus 22 (1), 77–88.
Mabberley, David J., 2017. Mabberley's Plant-Book: a Portable Dictionary of Plants, Their Classification and Uses. Cambridge University Press.
Madhulika, U., Harish, B.N., Parija, S.C., 2004. Current pattern in antimicrobial susceptibility of Salmonella Typhi isolates in Pondicherry. Indian J. Med. Res. 120, 111–114.
Naughton, P.J., Grant, G., Spencer, R.J., Bardocz, S., Pusztai, A., 1996. A rat model of infection by Salmonella typhimurium or Salmonella enteritidis. J. Appl. Bacteriol. 81,

651–656.
Newton, S.M., Lau, C., Gurcha, S.S., Besra, G.S., Wright, C.W., 2002. The evaluation of forty-three plant species for in vitro antimycobacterial activities; isolation of active constituents from Psoralea corylifolia and Sanguinaria canadensis. J. Ethnopharmacol. 79 (1), 57–67.
Nwankpa, P., Eteng, M.U., Oze, G., Nwanjo, H.U., Ezekwe, S., 2012. Effect of Chromolaena odorata on serum lipid profile and oxidative stress status in Salmonellae typhi infested wistar rats. Ann. Biol. Res. 3 (10), 4696–4700.
O'brien, J., Wilson, I., Orton, T., Pognan, F., 2000. Investigation of the Alamar Blue (resazurin) fluorescent dye for the assessment of mammalian cell cytotoxicity. Eur. J. Biochem. 267 (17), 5421–5426.
OECD, 2001. 423: acute oral toxicity-acute toxic class method. OECD Guidel. Test. Chem. 1, 14.
Papaefthimiou, D., Papanikolaou, A., Falara, V., Givanoudi, S., Kostas, S., Kanellis, A.K., 2014. Genus Cistus: a model for exploring labdane-type diterpenes' biosynthesis and a natural source of high value products with biological, aromatic, and pharmacological properties. Front. chem. 2 35-35.
Papuc, C., Goran, G.V., Predescu, C.N., Nicorescu, V., Stefan, G., 2017. Plant polyphenols as antioxidant and antibacterial agents for shelf-life extension of meat and meat products: classification, structures, sources, and action mechanisms. Compr. Rev. Food Sci. Food Saf. 16, 1243–1268.
Parry, C.M., Hien, T.T., Dougan, G., White, N.J., Farrar, J.J., 2002. Typhoid fever. N. Engl. J. Med. 347, 177–1782.
Py, B., Barras, F., 2014. Du fer et du soufre dans les protéines. Comment la cellule construit-elle les cofacteurs fer-soufre essentiels à son fonctionnement ? Med. Sci. 30 (12), 1110–1122.
Que, F., Wu, S., Huang, R., 2013. Salmonella pathogenicity island 1(SPI-1) at work. Curr. Microbiol. 66 (6), 582–587.
Raupach, B., Kaufmann, S.H., 2001. Immune responses to intracellular bacteria. Curr. Opin. Immunol. 13, 417–428.
Rietschel, E.T., Seydel, U., Zahringer, U., Schade, U.F., 1991. Bacterial endotoxins: molecular relationships between structure and activity. Infect. Dis. Clin. 5, 753–779.
Sani, Agunu, A., Danmalam, U.H., Ibrahim, H., 2014. Pharmacognostic studies of the stem bark of detarium microcarpum Guill. And Perr. (Fabaceae). Nat. Prod. Chem. Res. 1 (4).
Sodipo, O., Wannang, N., 2015. Ethnopharmacological survey of plants used by tradomedical practitioners (TMPs) in the treatment of typhoid fever in Gomari Airport Ward, Jere local government area, Borno State, Nigeria. Am. J. Ethnomed. 2 (4), 2348–9502.
Suresh, G., Das, R.K., Kaur Brar, S., Rouissi, T., Avalos Ramirez, A., Chorfi, Y., Godbout, S., 2018. Alternatives to antibiotics in poultry feed: molecular perspectives. Crit. Rev. Microbiol. 44 (3), 318–335.
Treuting, P.M., Dintzis, S.M., Montine, K.S., 2017. Comparative Anatomy and Histology: a Mouse, Rat, and Human Atlas. Academic Press.
Watanabe, T., Hashimoto, M., Wada, M., Imoto, T., Miyoshi, M., Sadamitsu, D., Maekawa, T., 2000. Angiotensin-converting enzyme inhibitor inhibits dehydration-enhanced fever induced by endotoxin in rats. Am. J. Physiol. Regul. Integr. Comp. Physiol. 279 (4), R1512–R1516.
W.H.O, 2018. Typhoid vaccines: WHO position paper March 2018. Wkly. Epidemiol. Rec. 93 (13), 153–172.
W.H.O, 2019. Fifty-third Report of the WHO Expert Committee on Specifications for Pharmaceutical Preparations. WHO Expert Committee on Specifications for Pharmaceutical Preparations WHO Technical Report Series No. 1019.
Zhang, C., Huang, K., Yu, P., Liu, H., 2013. Ionic liquid based three-liquid-phase partitioning and one-step separation of Pt (IV), Pd (II) and Rh (III). Separ. Purif. Technol. 108, 166–173.

Glossary

ALP: alkaline phosphate
ALT: alanine aminotransferase
AST: aspartate aminotransferase
ATCC: American Type Culture Collection
CFU: Colony Forming Unit
DMSO: dimethylsulfoxyd
HDL:: high-density lipoprotein
LDL:: low-density lipoprotein
MIC: minimum inhibitory concentration
MBC: minimal bactericidal concentration
MCV: mean corpuscular volume
OECD: Organization for Economic Co-operation and Development
TG: triglycerides
TC: Total cholesterol
UHPLC-MS: Ultra-high-performance liquid chromatography mass spectrometry
WHO: world health organization